C APPENDICES – FIELD VALIDATION CASES

APPENDIX 1 - FIELD CASE 1: SCHIERMONNIKOOG (NL) [HYDRO]

Case description

Hydrodynamic data were obtained along a cross-shore transect at the tail of the Dutch barrier island 'Schiermonnikoog' in the Wadden Sea during a measurement campaign of the department Physical Geography of Utrecht University (UU) in the winter of 2014-2015. The campaign was part of the PhD research of Anita Engelstad and Daan Wesselman. The measurements are used for the validation of the hydrodynamics in the BOI-version of the dune erosion model XBeach, with a focus on the validation of simulated infragravity waves.

The location of the measurements is indicated in Figure C-1. The beach and nearshore morphology near the transect are almost uniform in the alongshore direction. The cross-shore profile is a typical Wadden Sea profile, with a mildly sloping shoreface (about 1:700) and three offshore bars. The slope of the beach up to NAP - 3 m is about 1:200. In the intertidal zone, two to three bars are present, which are also visible in the aerial photograph (Figure C-1) and in Figure C-2. The highest point along the transect – the beach crest – is at less than NAP + 1.8 m: no dunes are present at the tail and the tail is completely inundated several times per year. At the landward side of the beach crest, the profile gently slopes towards the Wadden Sea. The elevation along the intertidal and subtidal part of the transect has been measured with an RTK-GPS system at the beginning and the end of the field campaign. For the subtidal part, open-source yearly Jarkus transects and 'Vaklodingen' data of RWS are available.

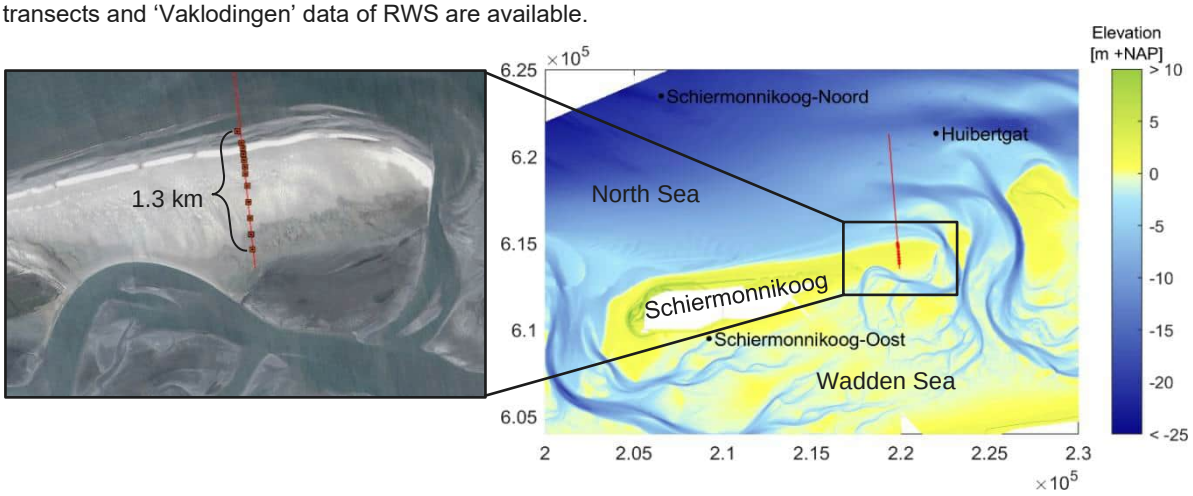

Figure C-1 Overview of the study area. Right: bed level near/at Schiermonnikoog ('Vaklodingen' 2012-2015), the location of the (offshore) hydraulic stations of RWS (black dots) and the transect (red line) with measurement equipment locations (red dots). Left: aerial photograph of the tail of Schiermonnikoog at 04-20-2014 (Google Earth). The coordinates in RD-coordinates.

The conditions at the case site are mesotidal, mixed-energy and tide-dominated. Generally, the offshore high water levels are about NAP + 0.7 m during neap tide and NAP + 1.2 m during spring tide (Wesselman et al., 2017). The mean offshore significant wave height ranges from 0.5 - 1 m in summer to 1 - 2 m in winter and can increase to 8 - 11 m during (north-western) storm events. The highest recorded water level setup during storm surges at this location is approximately 3.5 – 4 m (Engelstad et al., 2017).

During the observation period, the island tail was flooded 11 times during high water due to storm setup. The highest water levels and wave heights were observed during the storm on 10 and 11-01-2015, with local wind speeds of about 19 m/s from the west and waves from the northwest. This storm is used for the XBeach simulation with BOI-settings for the hydrodynamic validation. The offshore conditions are based on RWS data shared by the UU: offshore water level data at the North Sea ('Huibertgat' station) and in the Wadden Sea ('Schiermonnikoog-Oost' station), and wave height, period and directional spreading at the North Sea ('Schiermonnikoog-Noord' wave buoy) with a 10-min data interval.

The storm peak is defined as the moment with highest water levels (WL = NAP + 2.7 m at the North Sea at Huibertgat and NAP + 2.9 m in the Wadden Sea at Schiermonnikoog-Oost) and coincides with high tide. At this moment, the offshore significant wave height (H_s) was about 6.0 m, and the significant wave period (T_s or $T_{1/3}$) was 12 s. The hydraulic conditions during the storm are shown in Figure C-3. The highest H_s at the station Schiermonnikoog-Noord was 7.1 m and occurred during the low tide (about NAP - 0.3 m) in advance of the storm peak. The corresponding T_s was 13 s. The wave heights remained higher than 5 m for a full day. During the storm, the waves were more focused: the directional wave spreading

decreased from more than 35° to about 23° during the storm peak and about 29° afterwards. Based on the water level, the return period of this storm is about 10 years.
During the field campaign, measurements along the transect from the North Sea to the Wadden Sea (red dots in Figure C-1) were performed using among others ten stand-alone pressure transducers (PT's) from 04-11-2014 to 31-01-2015. The PT's recorded the water level continuously at 10 Hz with an accuracy of ~1 mbar (approximately 1 cm). Short and infragravity wave heights were determined for 15 min blocks by multiplying the standard deviation of the second-order detrended sea surface elevation by four, using a highpass filter (0.05-1 Hz) for short waves and a lowpass filter (0.005-0.05 Hz) for infragravity waves. The water depth was determined by adding the distance between the sensor and the bed level to the measured water depth above the sensor. This bed level was measured in at the begin of November 2014 and the end of January 2015 and has been linearly interpolated in between. More information on the data can be found in Wesselman et al. (2017) and Engelstad et al. (2017). The processed data were made available by the UU in order to compare this with the XBeach model output.

Model setup

A hydrodynamic XBeach 1D simulation (without sediment transport and morphology) is set up for the transect through the pressure transducers based on the method described in the main report and the data as described in the section above. The grain size is based on the values measured along the transect during the field campaign: the D_{50} is set to 200 µm and D_{90} to 300 µm (Engelstad et al., 2017; Wesselman et al., 2017).

Grid and bathymetry

Figure C-2 shows the cross-section and grid cell size of the XBeach transect. The RTK-GPS measurements of 31 January 2015 of the field campaign are used as basis for the cross-shore profile. This transect is extended into the North Sea with the Jarkus transect at RSP 18.40 in 2014, which aligns with the transect. Further offshore, the local 'Vaklodingen' data of 2013 are used to extend the profile about 4 km in offshore direction. The elevation offset at the connection point of the Vaklodingen and Jarkus data due to morphological changes between the moments of data collection has been removed. Finally, the offshore end of the profile is extended manually to deep water (NAP - 23.5 m) with an artificial slope of 1:50 according to the BOI guidelines. The cross-shore grid was set-up using the standard BOI procedure, resulting in 1599 grid points and a spatial resolution that varies from 7.9 m offshore to at least 2.5 m at the beach crest.

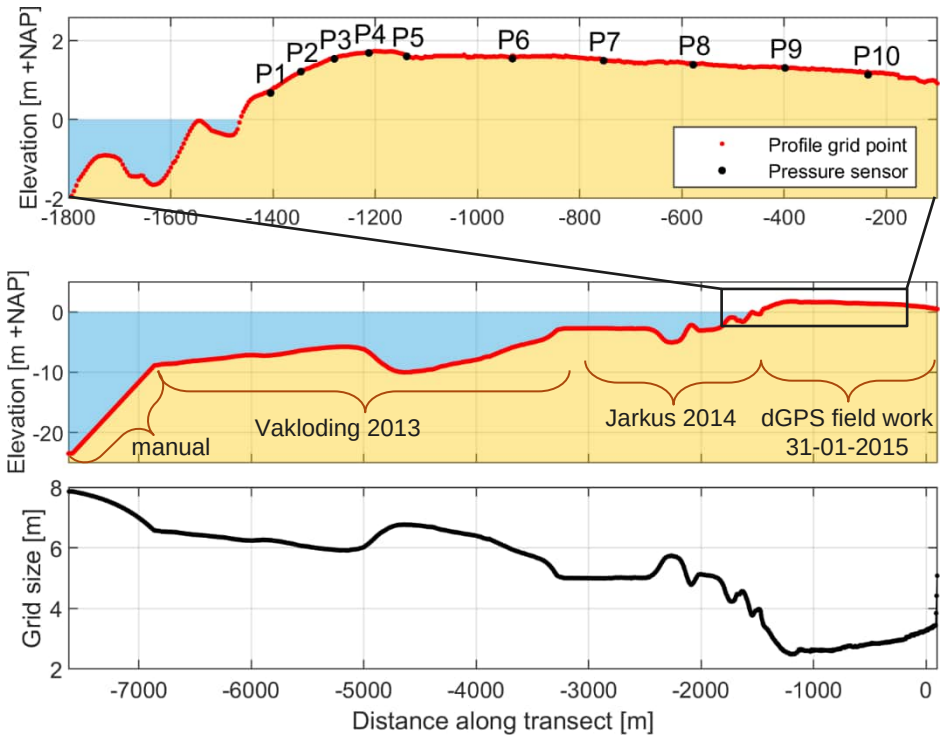

Figure C-2 Overview of the initial bed level including data source (middle panel) and grid cell size (bottom panel) along the XBeach transect at Schiermonnikoog. The upper panel zooms in on the beach where the pressure sensors (P#) were deployed.

Hydraulic boundary conditions

Figure C-3 shows the imposed hydraulic boundary conditions in the XBeach simulation for the storm period from 10-01-2015 7h AM to 11-01-2015 8h PM. At the offshore model boundary (North Sea), the water level time series recorded at the Huibertgat station during the storm period is imposed. At the landward end – i.e. the Wadden Sea side – the water level time series recorded at the Schiermonnikoog-Oost station is imposed. Furthermore, the spectral significant wave height H_{m0}, average wave period of the longest 1/3rd of the waves $T_{1/3}$ and the directional wave spreading σ at the Schiermonnikoog-Noord station are converted to average values per hour. σ (in rad) is converted to a directional wave spreading coefficient using $s = 2/\sigma^2 - 1$, resulting in s-values ranging between 3 and 12. These wave characteristics are imposed on the offshore boundary as H_{m0}, T_p and σ of a time-varying JONSWAP spectrum with a mean wave direction perpendicular to the coast.

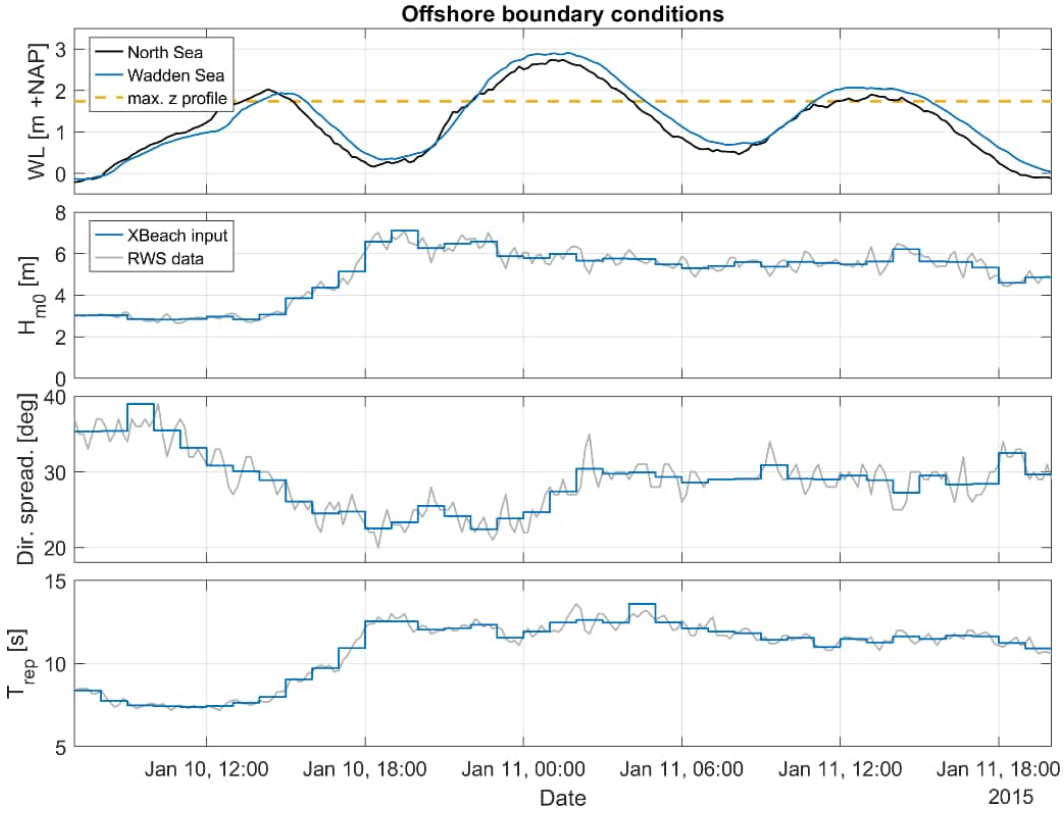

Figure C-3 Time series of the XBeach offshore hydraulic boundary conditions for the Schiermonnikoog case (blue and black lines) based on recorded data at the Huibertgat (water level North Sea), Schiermonnikoog-Oost (water level Wadden Sea) and Schiermonnikoog-Noord (wave characteristics) station (grey lines).

Model output settings and post-processing

At the location of the pressure transducers, the water level (zs), bed level (zb) and rms-wave height (H_{rms}) are saved as model output with a frequency of 10 Hz, similar to the measured data. The spectral significant wave height (H_{m0}) of the short waves (0.05-1 Hz, referred to with 'hf': high frequency or 'g': gravity) is calculated as $\sqrt{2} * H_{rms}$ and root-mean-square-averaged over the same 15-min blocks as the measured data. The H_{m0} of the infragravity waves (0.005-0.05 Hz, referred to with 'ig') is determined from the spectral integration (using Hann filter and Welch method) of the detrended water level signal in the 0.005-0.05 Hz domain (based on fast Fourier transformation) for the same 15-min blocks. These wave characteristics are compared with the measured data.

Besides, time-averaged output is saved for each 0.5 hour for all grid points to create a cross-shore profile of the water level (mean, min and max), bed level, short wave height (mean, min and max H_{rms}) and low frequency wave height ($4 * \sqrt{\text{zs1\_var}}$). In this case, the low frequency wave height (referred to with 'lf') is based on the entire frequency domain present in the water level and hence includes very low frequency waves (VLF's), instead of only the infragravity wave domain (0.005-0.05 Hz). This results in higher wave heights than for the point locations.

Results

In this section, the hydrodynamic XBeach validation results are presented and compared to the measured data. First, an overview of the modelled hydrodynamics is given along the cross-section during the storm peak (Figure C-4), followed by a comparison of the data over time at the measurement locations at the beach (e.g. Figure C-5). Lastly, the goodness of fit (GoF) between the model and measured data is presented (Figure C-6; Table C-1). Discussion on the causes of differences between modelled and measured values and the link between the water depth and wave heights follows in the next section.

Overview of spatial patterns

Figure C-4 shows the spatial patterns in the water level and wave heights (H_{m0}) along the cross-section during the storm peak. At this moment, the water level is about NAP + 3 m and the island tail is inundated. The short wave height significantly reduces above the submerged intertidal bars and at the beach due to wave breaking. This pattern is also visible in the measured short wave heights at the beach. At P1, the modelled short wave height has already been significantly reduced to about 1.2 m. At the Wadden Sea side of the beach crest (P4), the remaining modelled short waves show little decay during the storm peak, while there is a slight increase in wave height in the measurements (as will be explained in the discussion). The modelled low frequency wave height (IG+VLF) increases offshore of the cross-section in Figure C-4, and gradually decreases over the intertidal bars, the beach and – in case of total submergence – the island tail towards the Wadden Sea. This pattern is also observed in the measured infragravity wave heights (note that the H_{m0} is lower in this case because VLF's are excluded). The wave height of the low frequency waves relative to the short wave height increases towards the beach crest.

Overall, the patterns along the cross-section in the measured and modelled water level and wave heights are similar. Some absolute differences between the model and the measurements are observed, as will be discussed in the next section.

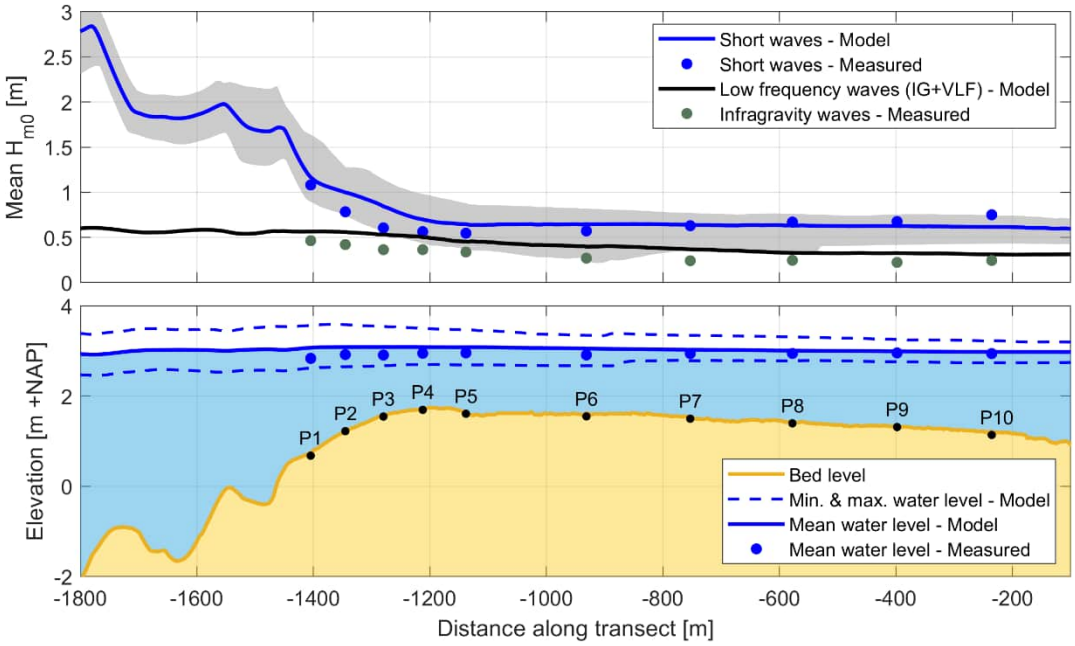

Figure C-4 Cross-section with the modelled and measured water level and spectral significant wave height (Hm0) of high and low frequency waves during the storm peak (11-01-2015 00:30-02:00). The grey zone around the modelled Hm0 hf indicates the minimum and maximum Hm0 hf. Note the difference between the modelled low frequency Hm0 (no frequency domain filter) (black line) and the measured infragravity Hm0 (0.005 and 0.05 Hz) at the point locations (grey-green dots).

Time series

Figure C-5 shows an example time series of the water depth and wave heights during the three tidal cycles just before and during the storm for the first measurement location at the beach (P1; see section "Additional figures" for the time series for P2-P10). The dots represent the measured values and the blue line the modelled values. In the time series, both measured and XBeach long wave heights represent infragravity waves in the 0.005-0.05 Hz domain.

Only during flood, water levels were high enough for the pressure sensors to measure. At P1, the bed level is lower than at the other locations, resulting in a longer inundation period and larger water depths up to about 2.3 m during the storm peak. At the moment of the highest waves, between the first and second high tide, the water level was too low to measure the water depth and wave heights at the beach.

The modelled water depth and wave heights are close to the measured values and show a similar and consistent pattern over time, modulated by the tides. The short wave height is delimited by breaking and independent of the offshore conditions: during the first high tide (before the storm), the wave height is similar to those during the third high tide (during the storm) with similar water depths. On the contrary, the infragravity waves are higher during the storm (2nd and 3rd high tide) than before the storm (1st high tide). The scatter in the infragravity wave height is relatively large in both the measurements and the model, which is largely related to the way the infragravity wave height is calculated. At the beach (P1-P4), the infragravity wave height seems to be overestimated by the model during the first tidal cycle before the storm. However, during the storm peak (highest water levels) and the following high tide the model matches the measurements well, which is most relevant for the intended application of the BOI XBeach model for dune erosion during (extreme) storms.

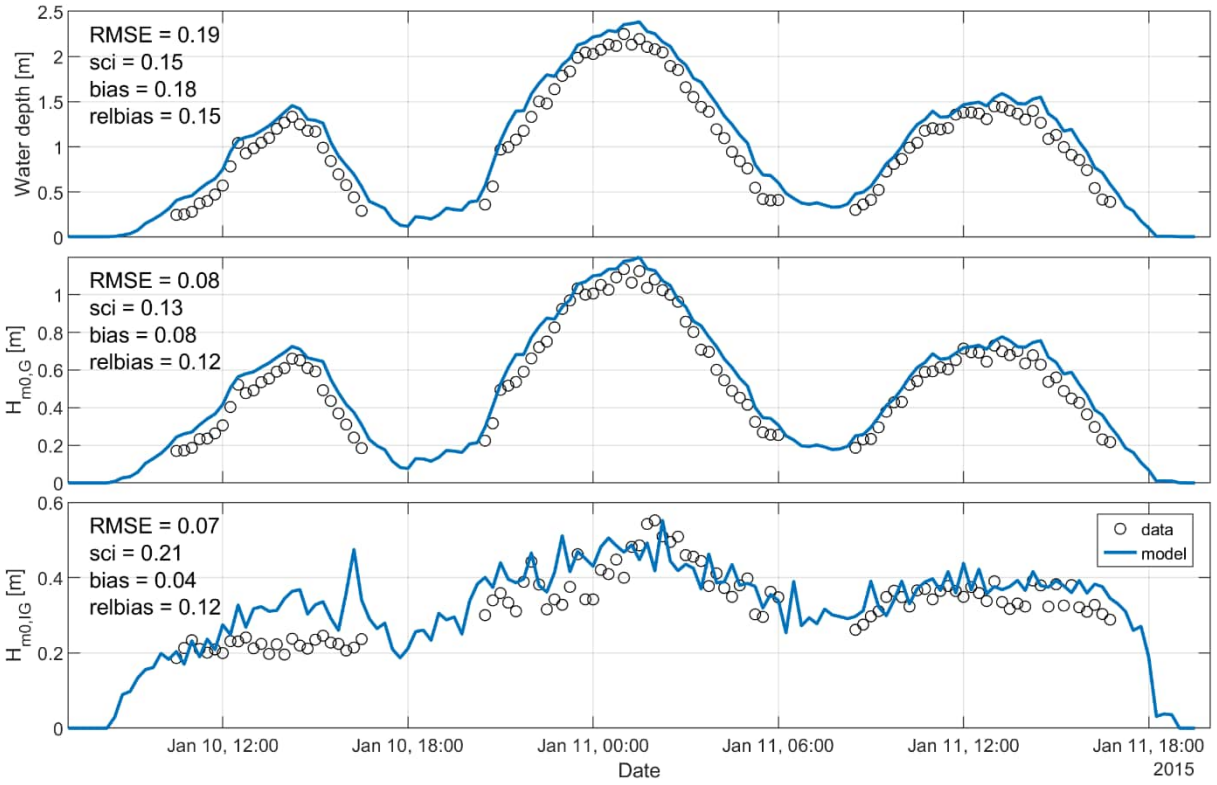

Figure C-5 Time series of measured and modelled water depth, short and infragravity spectral significant wave height including goodness-of-fit indicators for measurement location P1.

Goodness of fit (GoF)

Figure C-6 shows the measured versus the modelled water depth and wave height of the short and infragravity waves for the entire model period. In general, the point clouds are close to the 1:1 line, indicating a good fit. This is confirmed by the overall goodness-of-fit (GoF) indicators in Table C-1 and in the subplots of the time series: for example, the RMSE is 13 cm, 12 cm and 7 cm for respectively the water depth, $H_{m0\,g}$ and $H_{m0\,ig}$ for the entire model period for all locations together. The scatter is smallest for the water depth. However, there is an overall bias (overestimation by the model) of 7 cm, 5 cm and 4 cm in respectively the water depth, $H_{m0\,g}$ and $H_{m0\,ig}$ for the entire model period for all locations together.

The goodness of fit varies between the measurement locations. At the North Sea side (blue colours in Figure C-6), the water depths and both wave heights are slightly overestimated by the model, which gradually shifts to a slight underestimation at the Wadden Sea side (green to orange colours), especially for the water depth and short wave height. This is also reflected by the linear fit in Figure C-6 and the bias and relative bias of the different locations in Table C-1. Based on the time series, these trends are similar for all three tidal cycles. In general, the best fit for the water depth as well as the wave heights is found on the gentle slope in the profile towards the Wadden Sea (P6-P9) and least good fit at P3 (and to a lesser extent P2 and P4) high at the beach.

If only the tidal cycle with the storm peak is considered (second modelled tidal cycle) - which is most relevant for dune erosion -, the GoF indicators for all locations together have a slightly better scatter index but a slightly less good RMSE, bias and relative bias for the water depth and short wave height. The GoF for the storm peak is however better for the infragravity wave height, which is most important for dune erosion. Moreover, if only the measurement locations on the beach are considered (excluding the overwash zone that is less relevant for dune erosion), the overall GoF is less good for both the entire period as the storm peak (as will be explained in the discussion). Though again, the GoF of the infragravity wave heights at the beach during the storm compared to the entire model period is slightly better.

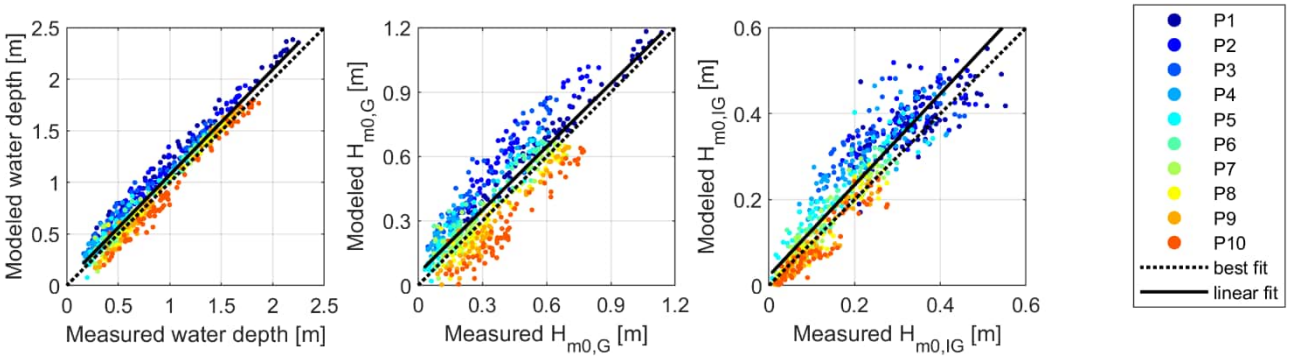

Figure C-6 Scatter plot of the modelled versus measured water depth (left), spectral significant wave height (H_{m0}) of short waves (G) (middle) and infragravity waves (IG) (right) for all measurement locations at Schiermonnikoog. The dashed line indicates a perfect 1:1 relationship, the continuous line represents a linear data fit.

Table C-1 Goodness-of-fit (GoF) indicators for the modelled water depth and the spectral significant wave height for high frequency and infragravity waves compared to the measurements. For the overall performance, the indicators are shown for all locations together and for the entire model period, while for the performance most relevant for dune erosion, also the indicators for the beach only (P1-P5) and during only the second tide with the storm peak are shown. Colours per indicator indicate relative GoF between the locations of all hydrodynamic cases (greener = better fit).

		Water depth [m]				$H_{mo\,hf}$ [m]				$H_{mo\,ig}$ [m]			
		RMSE	sci	bias	rel.bias	RMSE	sci	bias	rel.bias	RMSE	sci	bias	rel.bias
Individual locations, entire period	P1	0.19	0.15	0.18	0.15	0.08	0.13	0.08	0.12	0.07	0.21	0.04	0.12
	P2	0.19	0.19	0.18	0.18	0.21	0.43	0.20	0.41	0.09	0.27	0.07	0.21
	P3	0.18	0.23	0.17	0.21	0.19	0.57	0.18	0.55	0.11	0.40	0.09	0.34
	P4	0.12	0.17	0.10	0.15	0.13	0.42	0.12	0.40	0.09	0.37	0.08	0.31
	P5	0.09	0.12	0.07	0.09	0.08	0.29	0.07	0.24	0.06	0.31	0.05	0.25
	P6	0.07	0.08	0.04	0.05	0.08	0.24	0.07	0.19	0.04	0.26	0.04	0.21
	P7	0.07	0.08	0.01	0.02	0.05	0.13	0.01	0.03	0.03	0.20	0.02	0.12
	P8	0.06	0.07	-0.01	-0.01	0.06	0.15	-0.04	-0.10	0.02	0.17	0.00	-0.01
	P9	0.07	0.07	-0.03	-0.03	0.08	0.20	-0.07	-0.18	0.03	0.20	-0.01	-0.09
	P10	0.12	0.11	-0.10	-0.09	0.15	0.33	-0.14	-0.31	0.04	0.26	-0.02	-0.18
All locations	Entire period	0.13	0.14	0.07	0.07	0.12	0.29	0.05	0.11	0.07	0.28	0.04	0.15
	Only 2nd tide	0.14	0.12	0.09	0.08	0.13	0.25	0.06	0.12	0.07	0.25	0.04	0.13
Beach (P1-P5)	Entire period	0.16	0.17	0.14	0.15	0.14	0.31	0.13	0.27	0.08	0.29	0.06	0.22
	Only 2nd tide	0.18	0.15	0.17	0.14	0.17	0.29	0.15	0.25	0.09	0.26	0.06	0.17

Discussion

In general, the validation results showed a good fit between the measured and modelled water depths and wave heights at the tail of Schiermonnikoog. This is the case for not only the zone up to the beach crest, but also across the island tail during the storm overwash conditions. The newly implemented αE parameter seems to work fine, even for the directional spread of less than 30° during the storm peak. However, some spatial variation in the goodness of the fit is observed, which can be at least partly explained by the following factors.

Morphological changes
The performance was best inland of the beach crest, which could be related to the smaller morphological changes in this part of the profile. Over the 2 months of the field campaign, largest bed level changes were observed in the intertidal beach part of the cross-shore profile and directly onshore of the beach crest (Engelstad et al., 2017) and limited changes at the rest of the island tail. In the measured data, the water depth is determined from the water level by using a linear interpolation of the bed level at the begin and end of the field campaign, while in XBeach only the final bed level is used for the beach and island tail. This could have resulted in differences in water depth, which also affect the wave breaking process and herewith the wave heights: a larger water depth results in less short wave breaking and more energy transfer to longer wave lengths and hence higher high frequency and infragravity waves. Moreover, bar migration further offshore in the zone where the up to ~2 year older 'Vaklodingen' and Jarkus data has been used could also have resulted in some deviations in water level and wave heights.

Delayed short wave breaking in relation to breaking parameter *gamma*
The small overestimation of the water depth and wave heights by the model at the beach and just behind the beach crest might (also) be related to somewhat delayed short wave breaking due to a slightly too high breaking parameter *gamma* for this case. A *gamma* of 0.46 was used as part of the default BOI settings, which is slightly higher than the *gamma* of 0.45 used in the 1D XBeach model of Wesselman et al. (2017) for the same location. In general, a lower *gamma* (at least smaller than the default 0.55) is more appropriate for gentle shoreface slopes like this Wadden profile compared to steeper profiles such as along the Holland coast (Wesselman et al., 2017). This would suggest that a lower gamma value for specific areas or profile shapes might improve the model results, but this requires further research and calibration (but little additional validation and calibration data is available). Even so, since the hydrodynamic offsets in this case are relatively small and can also be related to e.g. morphological changes, this case alone gives no direct need to adjust the *gamma* value.

Boundary conditions at Wadden Sea side
In the XBeach model, waves only approach from the offshore (North Sea) boundary. So, no waves reach the profile from the Wadden Sea side, while in reality they do (Engelstad et al., 2017). Consequently, the wave heights - especially of the high frequency waves - are slightly underestimated during overwash conditions, resulting in the negative bias at the locations closest to the Wadden Sea.

Conclusion

The hydrodynamics in the BOI-version of dune erosion model XBeach have been validated by comparing the model results for a cross-section at the tail of Schiermonnikoog with measurements during storm conditions. Overall, the default 1D BOI XBeach model set-up was well capable of simulating the hydrodynamic conditions (both water levels and (short and long) waves) at the gently sloping profile during the storm with overwash conditions. The newly implemented αE parameter seems to work fine, even for the directional spread of less than 30° during the storm peak. Some small deviations could largely be explained by case-specific issues related to the model input.

Additional figures

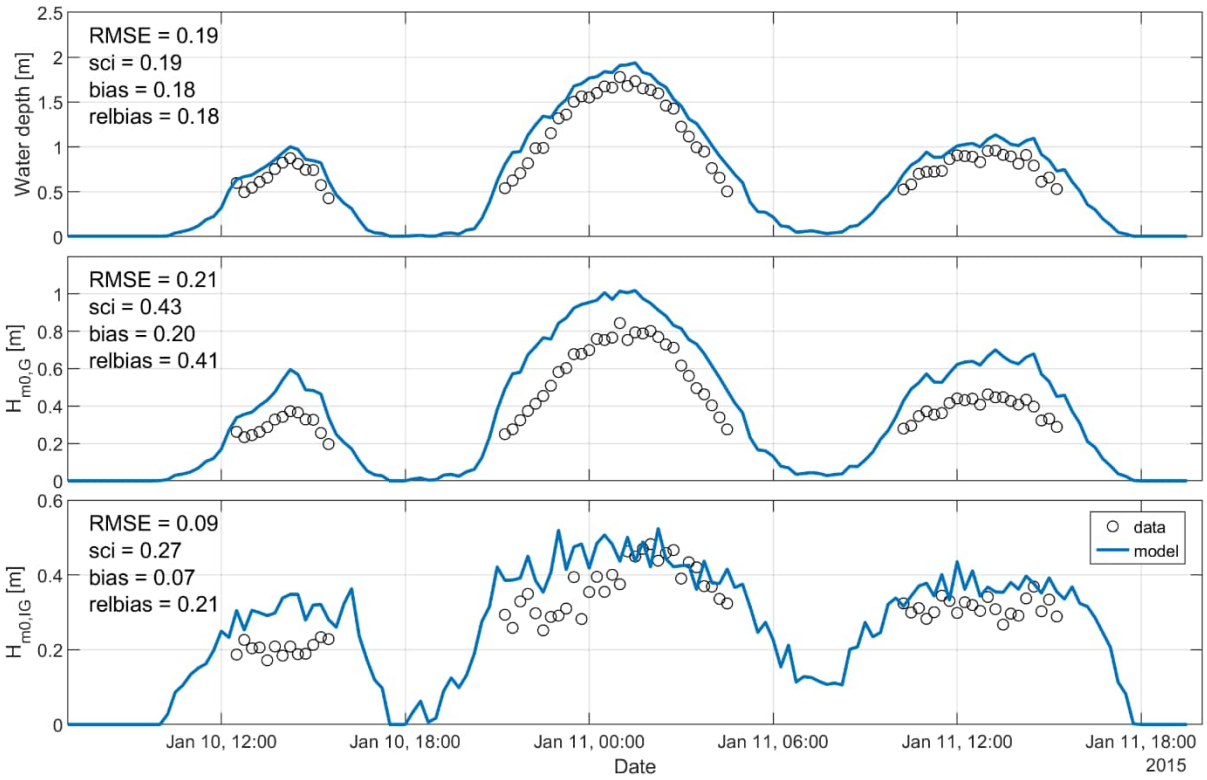

Figure C-7 Time series of measured and modelled water depth, spectral significant wave height of short and infragravity waves including goodness-of-fit indicators for measurement location P2.

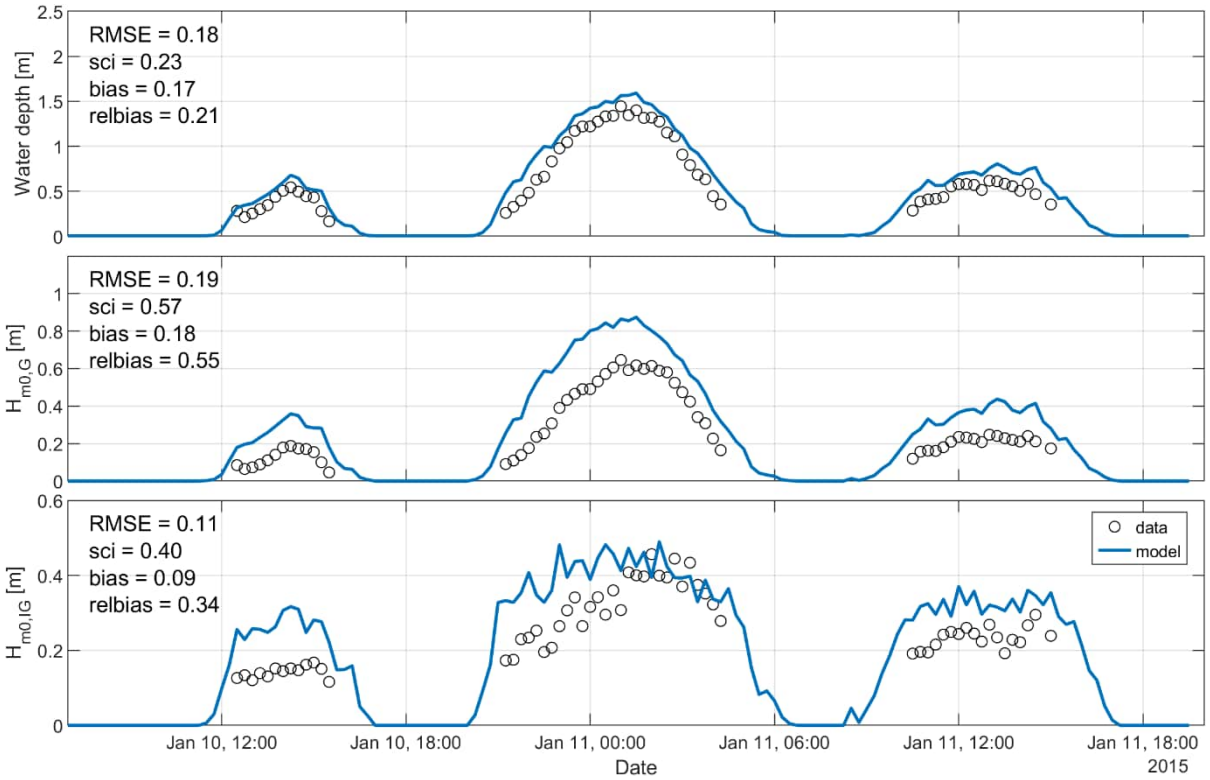

Figure C-8 Time series of measured and modelled water depth, spectral significant wave height of short and infragravity waves including goodness-of-fit indicators for measurement location P3.

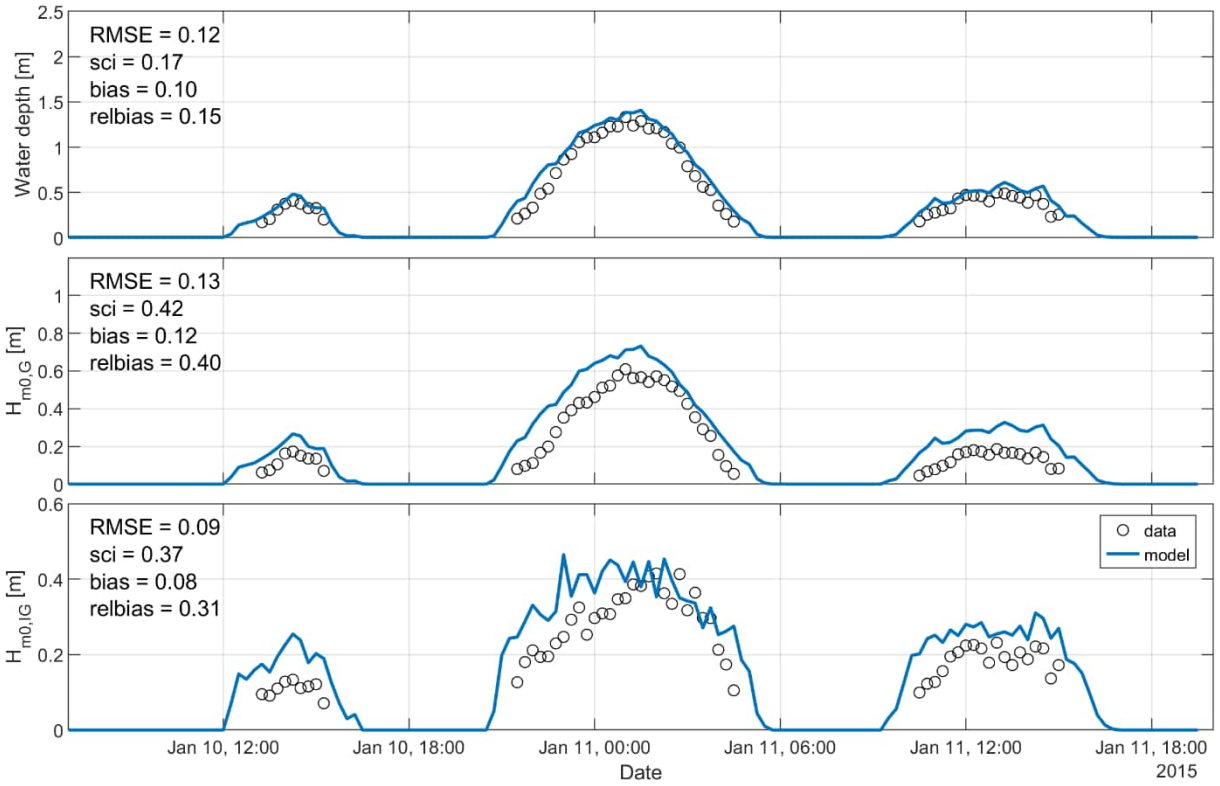

Figure C-9 Time series of measured and modelled water depth, spectral significant wave height of short and infragravity waves including goodness-of-fit indicators for measurement location P4.

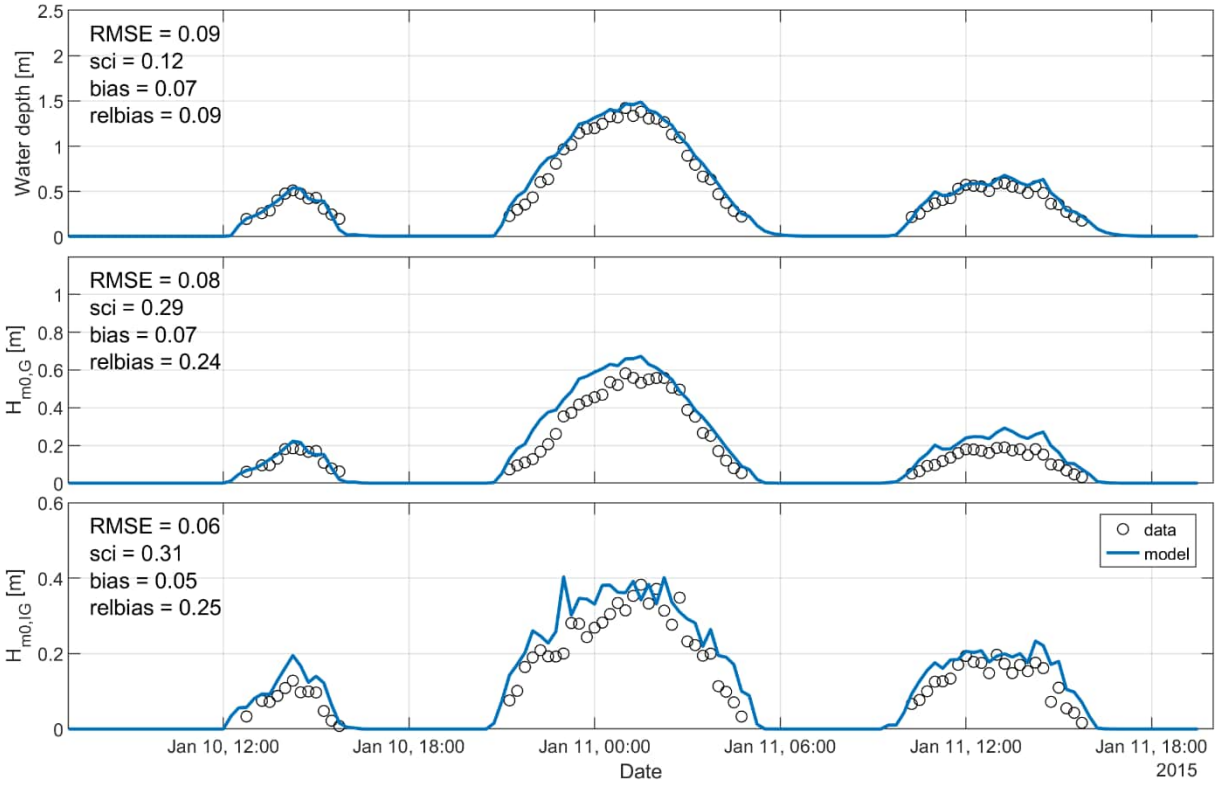

Figure C-10 Time series of measured and modelled water depth, spectral significant wave height of short and infragravity waves including goodness-of-fit indicators for measurement location P5.

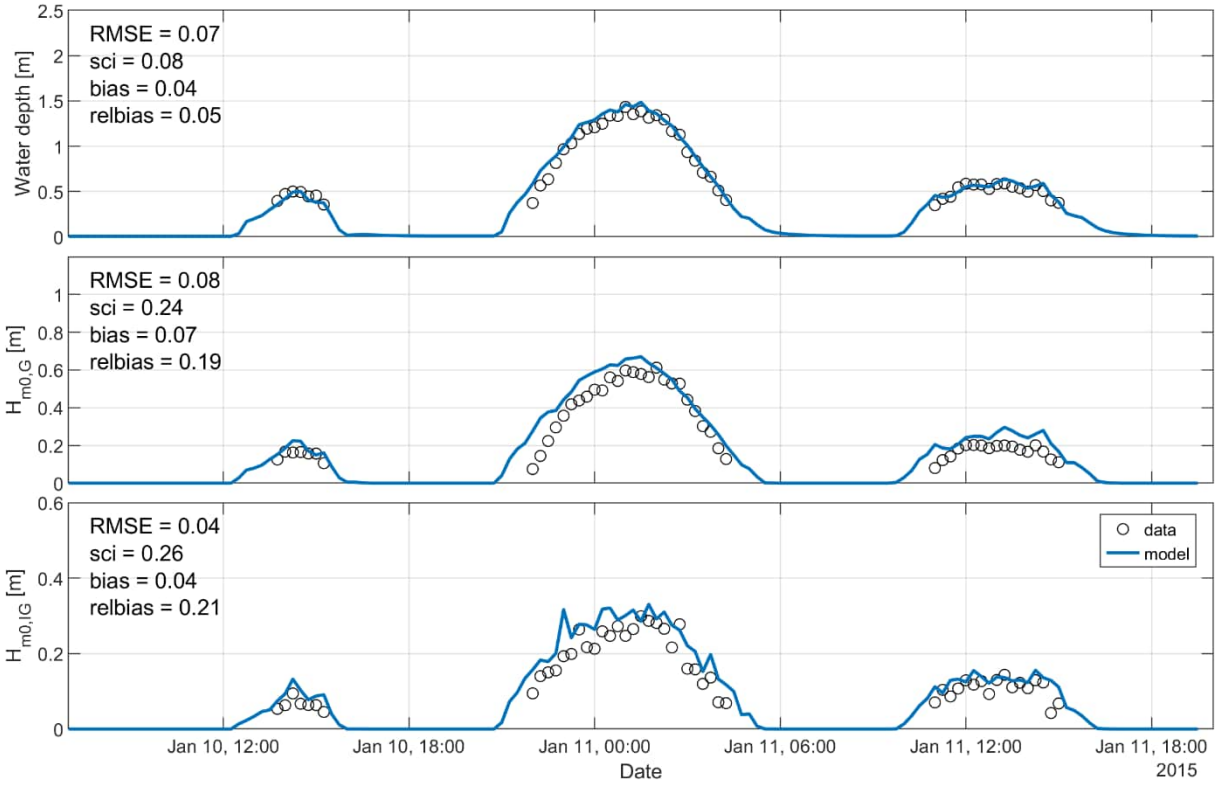

Figure C-11 Time series of measured and modelled water depth, spectral significant wave height of short and infragravity waves including goodness-of-fit indicators for measurement location P6.

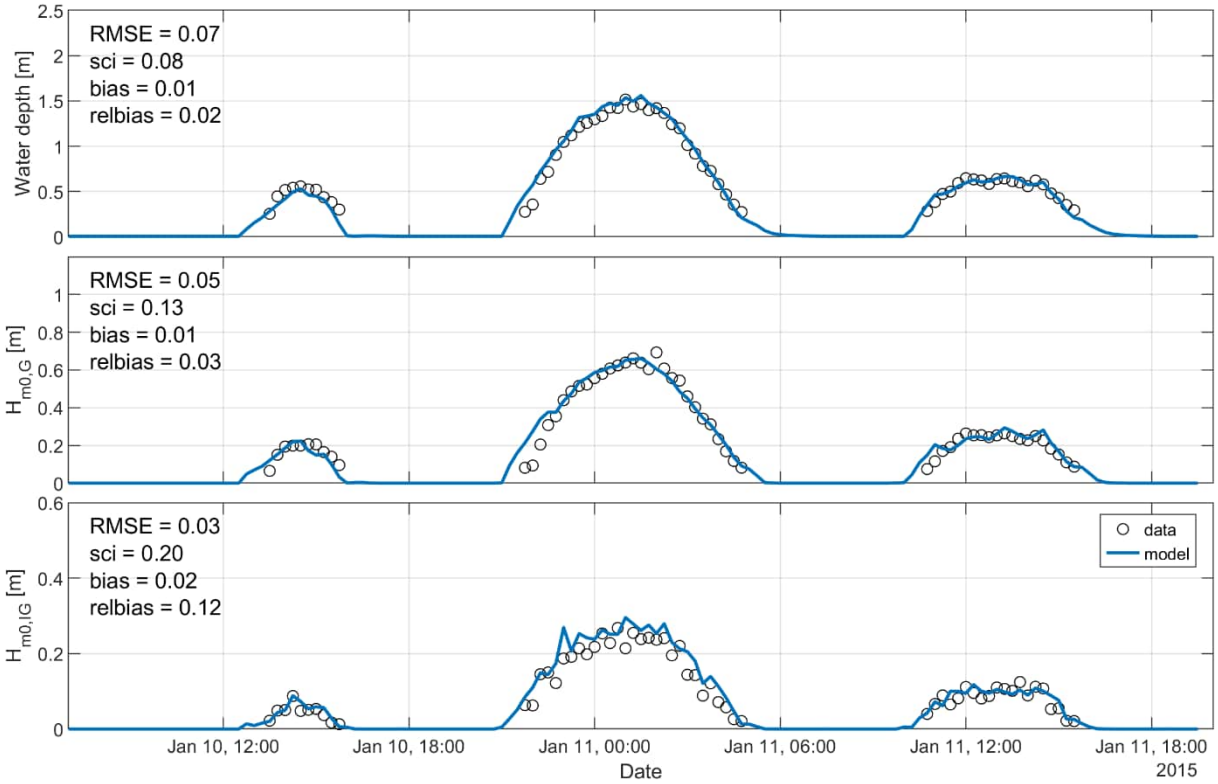

Figure C-12 Time series of measured and modelled water depth, spectral significant wave height of short and infragravity waves including goodness-of-fit indicators for measurement location P7.

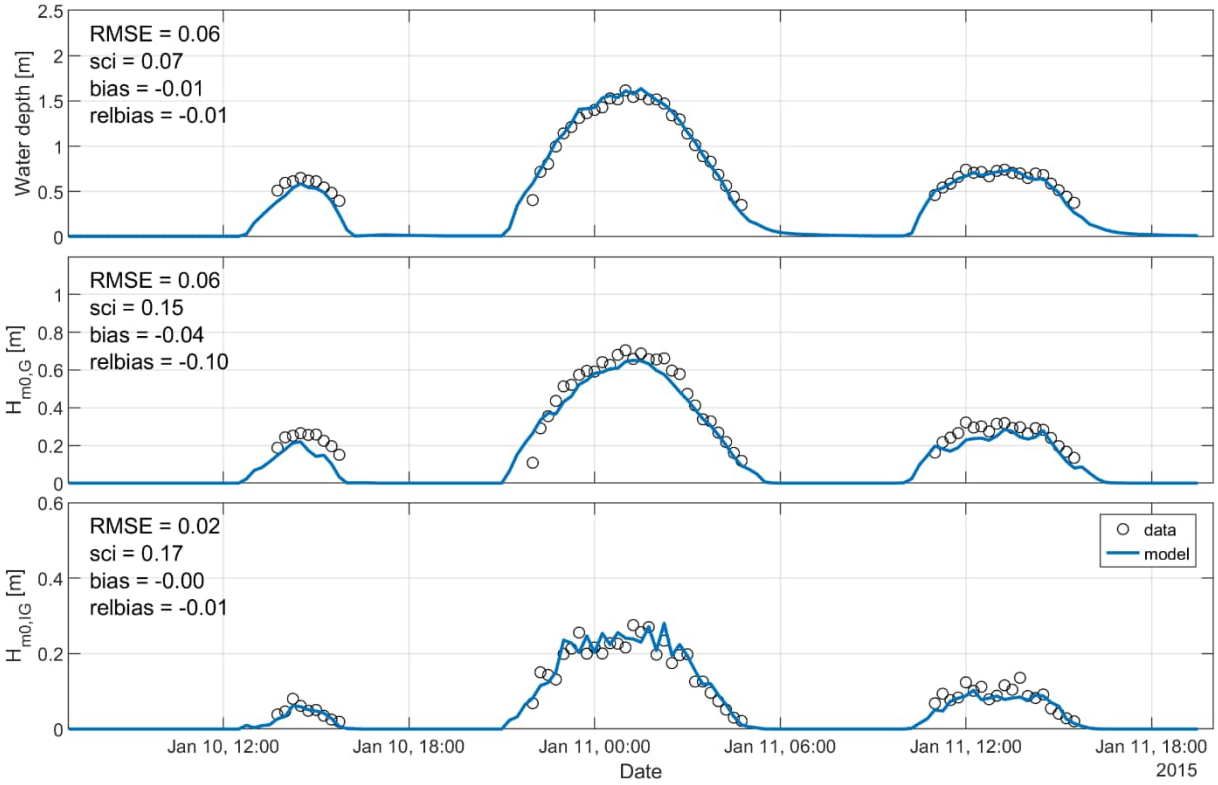

Figure C-13 Time series of measured and modelled water depth, spectral significant wave height of short and infragravity waves including goodness-of-fit indicators for measurement location P8.

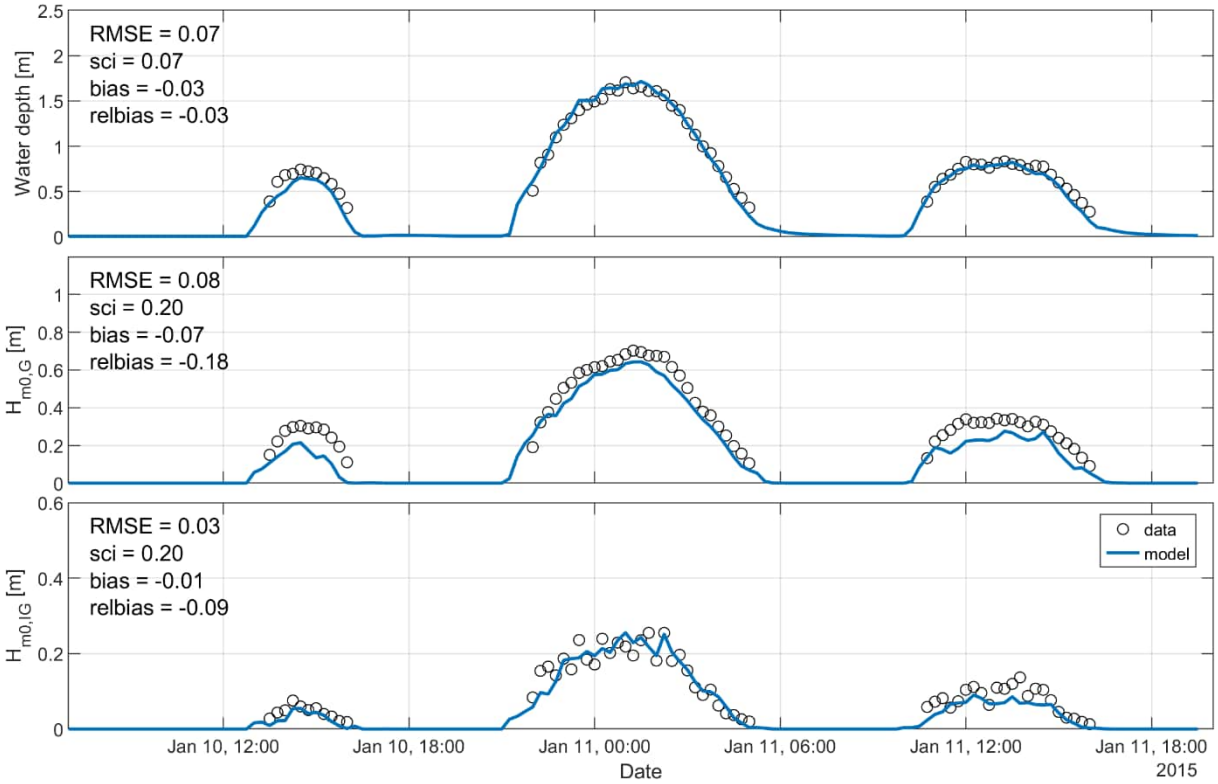

Figure C-14 Time series of measured and modelled water depth, spectral significant wave height of short and infragravity waves including goodness-of-fit indicators for measurement location P9.

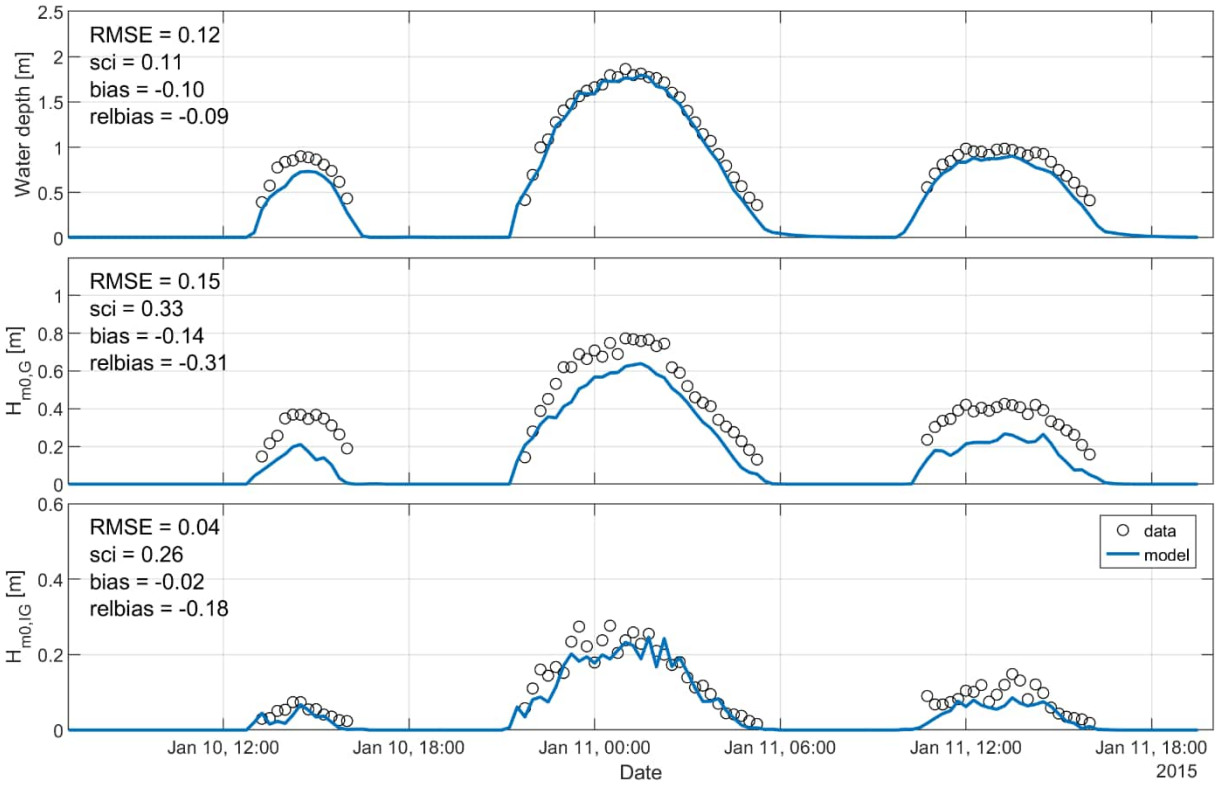

Figure C-15 Time series of measured and modelled water depth, spectral significant wave height of short and infragravity waves including goodness-of-fit indicators for measurement location P10.

APPENDIX 2 - FIELD CASE 2: SAINT TROJAN (FRANCE) [HYDRO]

Case description

The field dataset of Saint Trojan in France is used for hydrodynamic validation of the BOI-version of dune erosion model XBeach, in particular regarding the infragravity-wave behaviour. The field campaign took place in February 2017 on the gently sloping Saint-Trojan Beach during an energetic storm. Bertin et al. (2020) compared observations to a 2DH XBeach model and presented detailed analysis on infragravity-wave behaviour.

The field site is a dissipative sandy beach located in the central part of the French Atlantic coast (Figure C-16), along the southwestern coast of Oléron Island. The continental shelf in front of the study area is about 150 km wide, with a very gently sloping shoreface, the 20 m isobath being some 10 km away from the shoreline. The beach slope typically ranges from about 0.0015 at the shoreface to 0.015 in the intertidal area, and the beach is mainly composed of fine and well-sorted sands (D_{50} = 0.18–0.22 mm). The tidal regime in this region is semidiurnal and macrotidal, with a tidal range varying between about 1.5 m during neap tides and 5.5 m during spring tides. Tidal currents are weak at the studied beach, and the impact of tides on short waves remains mostly restricted to water level variations.

The storm Kurt generated very long swell waves that reached the coast between the 2nd and 3rd of February 2017. At the deep-water buoy of Biscay (Figure C-16a), the mean wave period increased from 8.0 to 13.0 s, and H_s rapidly increased from 3.0 m to almost 10.0 m, which corresponds to a return period on the order of 1 year (Nicolae-Lerma et al., 2015). The wave hindcast described in Guérin et al. (2018) suggests that the peak wave period T_p exceeded 20 s.

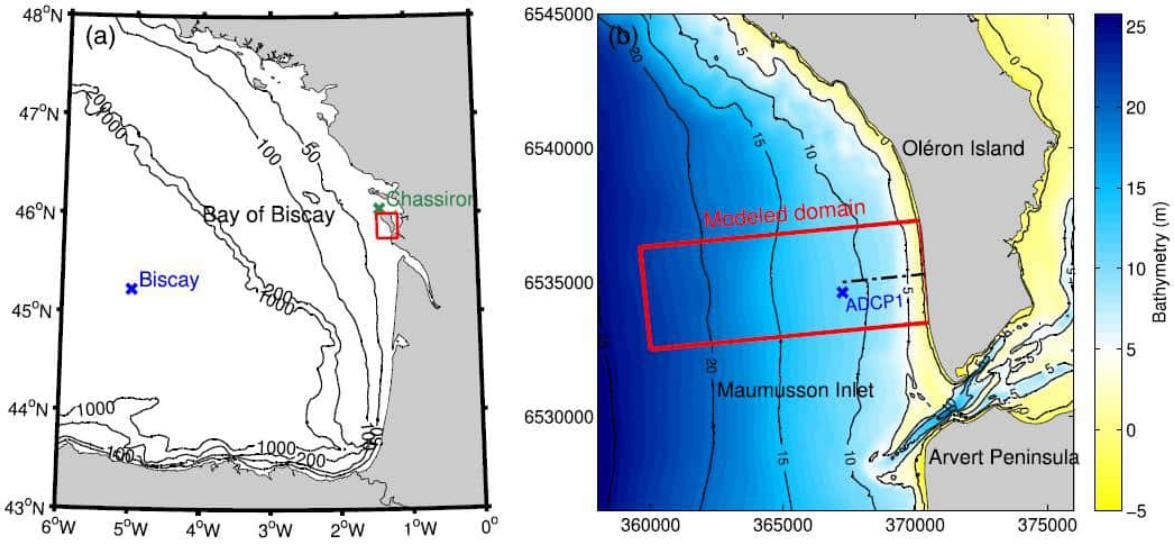

Figure C-16 Location of the Saint Trojan area in the Bay of Biscay, with the Biscay buoy (×) and Chassiron Meteorological station (×). (b) Detailed bathymetry of the study area (m relative to mean sea level), incl. location of offshore ADCP1 (×) and the instrumented cross-shore profile (dashed line). The coordinates are in meter (Lambert-93 projection). Source: Bertin et al. (2020).

The measurement period of the field campaign encompassed four tidal cycles, from the 1st of February 2017 to the 3rd of February 2017, and is characterized by a tidal range of 3.5 to 4 m. An Acoustic Doppler Current Profiler (ADCP1) equipped with a pressure sensor was deployed about 3 km offshore (Figure C-16b). In the intertidal zone, nine pressure transducers (PT) sampling at 4 Hz were deployed (Figure C-17), as well as a second ADCP at the location of PT3. For each sensor, bottom pressure measurements were first corrected for sea level atmospheric pressure measured at the nearby meteorological station of Chassiron (Figure C-16a). The entire record was then split into consecutive bursts of 30 min, and only the bursts in which the sensor was continuously submerged were considered. PT9 was never continuously submerged for more than 30 min and data from this PT was therefore discarded. Bottom pressure power density spectra $E_p(f)$ were computed using Fast Fourier Transforms, with 10 Hanning windows, 50% overlapping segments (20 degrees of freedom). These pressure spectra were subsequently converted into elevation spectra considering linear wave theory.

The spectral significant wave height (H_{m0}) was computed as $H_{m0} = 4\sqrt{m0}$ where the upper threshold frequency was set to 0.4 Hz. The threshold frequency between the high-frequency waves and the lower infragravity waves is time-varying and defined following Roelvink and Stive (1989) and Hamm and Peronnard (1997) as half the continuous peak frequency f_p. It is important to note that in processing of the observations the infragravity-wave frequency band was not delimited by a lower threshold, and therefore also covers the VLF (very low frequency) waves. For more information on the field campaign and data processing please refer to Bertin et al. (2020).

Model setup

A 1D XBeach model has been set-up, loosely based on the 2DH XBeach model described by Bertin et al. (2020) while at the same time respecting the BOI model set-up and settings as described in the main report.

Grid and bathymetry

From this 2DH XBeach model, the cross-shore transect closest to the observation stations was used as a starting point for the 1D model. This transect lies some 10 m away from the 9 pressure transducers, and about 400 m from the ADCP1. While considering the offshore conditions presented in Figure C-18 as the governing conditions (H_s = 7.5 m, $T_{m-1,0}$ = 16.5 s), the profile has been extended seaward according to BOI guidelines with a 1:10 slope to a depth of over 30 m. A cross-shore grid was set-up following standard BOI procedure, resulting in 1018 grid cells and a spatial resolution that varies from 15 m (offshore) to 1 m at the coast. The initial bed level across the 1D transect as well as the cross-shore distribution of grid sizes are presented in Figure C-17.

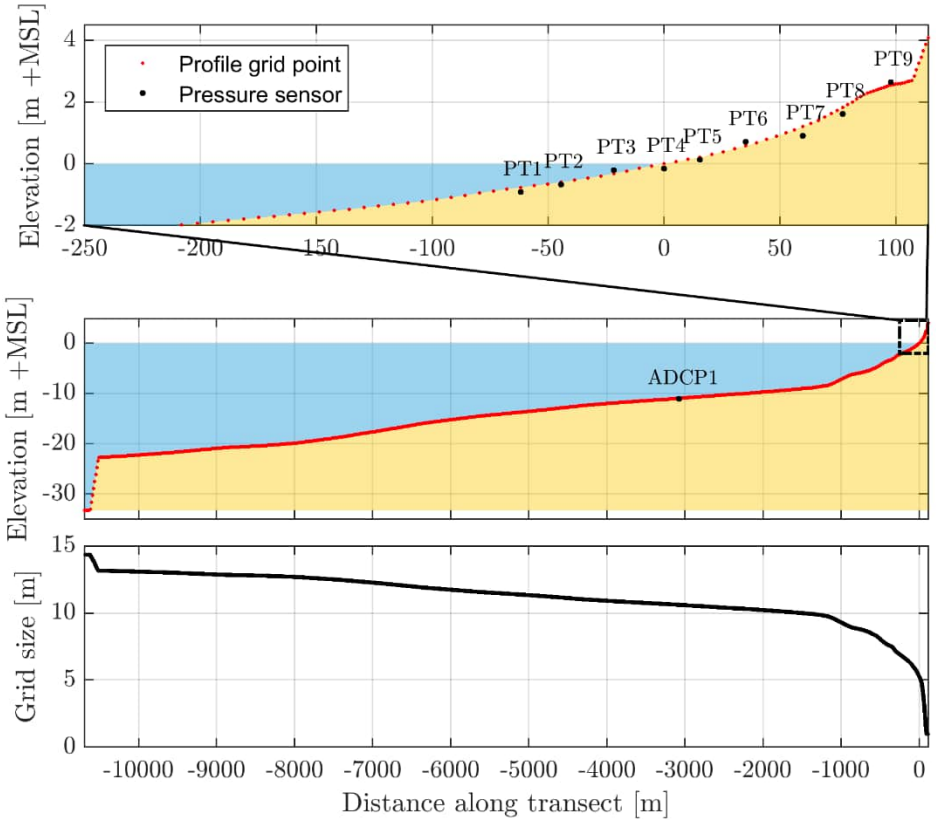

Figure C-17 Overview of the initial bed level (middle panel, in which the red dots represent the bed level per grid point) and the grid cell size (bottom panel) along the 1D XBeach transect at Saint Trojan Beach. The upper panel zooms in on the most onshore section of the profile where most measurement instruments were deployed.

Hydraulic boundary conditions

An overview of the hydrodynamic forcing conditions that were used to force the XBeach model is presented in Figure C-18. In analogy to Bertin et al. (2020), the model was forced with water level time series that were obtained at the ADCP1. Furthermore, wave conditions are imposed through directional wave spectra that were obtained within a regional application of the WaveWatchIII model (Tolman, 2009) forced by wind fields that followed from the climate forecast system reanalysis of Saha et al. (2010).

The available wave spectra that were used to force the model contain time-varying mean wave directions which differ from the shore-normal direction. This is in contrast with the standard BOI procedure. In this particular case, to make sure that all wave energy propagates towards the coast, a single directional bin has been used that captures all wave energy (*thetamin* = -180*, thetamax* = 180*, dtheta* = 360*)*, and all wave energy was set to the shore-normal direction (*snell* = 0).

In analogy with the observations, during the post-processing of the model results, no separation was made between infragravity waves (IG) and very low frequency (VLF) waves: the entire low-frequency range was considered (VLF + IG).

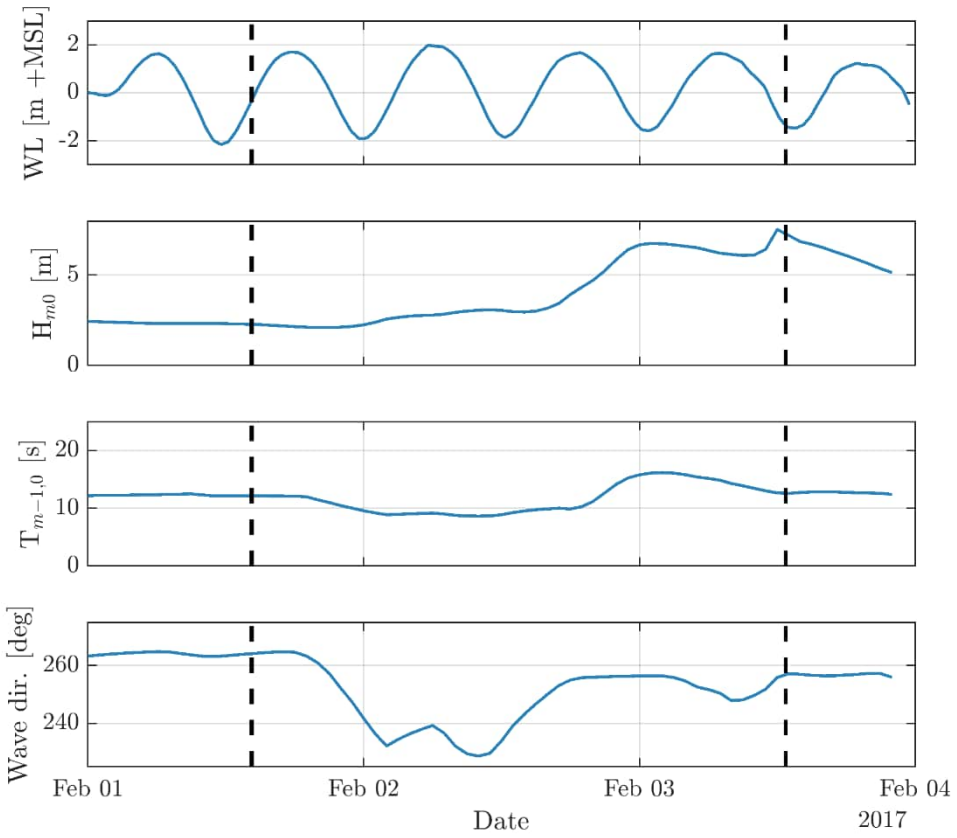

Figure C-18 Time series of the offshore hydraulic boundary conditions for the Saint Trojan case. The water level time series were recorded at the ADCP1, whereas the H_s, $T_{m-1,0}$ and wave direction are obtained from directional wave spectra that originate from a regional implementation of the WaveWatch III model (see Bertin et al. 2020 for more information). The vertical dashed black lines indicate the start and end of the measurement period of the pressure transducers in the intertidal zone.

Results

In this section, the hydrodynamic XBeach validation results are presented and compared to the measured data. First, an overview of the spatial patterns in the modelled hydrodynamics is given along the cross-section during the storm peak (Figure C-19), followed by a comparison of the data over time at ADCP1 offshore (Figure C-20) and at the measurement locations on the beach (e.g. Figure C-21, Figure C-22). Finally, the goodness of fit (GoF) between the model and measured data is presented (Figure C-23; Table C-2). Discussion on the causes of differences between modelled and measured values and the link between the water depth and wave heights follows in the Discussion section.

Overview of spatial patterns

The observed and predicted water level, short- and long-wave heights during the peak of the storm are presented in Figure C-19. The observations show that the water level during the peak of the storm is some 2 m above mean sea level (MSL). The short waves are breaking towards the shore and are only some 1.5 m in height at the seaward side of the transect (sensor PT1). Over a stretch of 150 m, they dissipate their energy completely. The low frequency waves (VLF + IG) are of similar magnitude as the short-waves at PT1. While the short waves continue to dissipate their energy during shoreward propagation, the low frequency waves increase in height up to 2 m at some 50 m of the shoreline. From that moment on, they rapidly decrease in height. For more information on the infragravity-wave behaviour we refer to Bertin et al. (2020).
Overall, the XBeach model predictions with default settings follow both the water level variations and wave height transformation closely. However, the short-wave height is consistently slightly overestimated, as will be discussed later on.

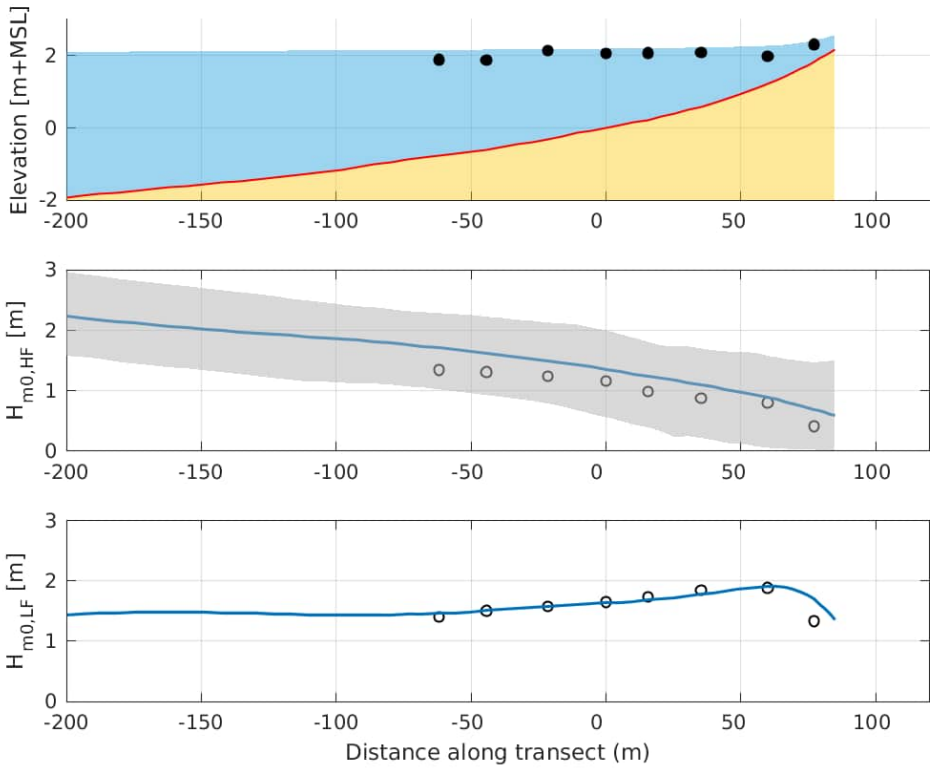

Figure C-19 Cross-section at the transect location during storm peak (3rd of February 2017 at 8 AM) of the water level (upper panel), short-wave height (middle panel) and low-frequency (IG and VLF) wave height (middle panel). In blue the model results, and the observations are represented by circles. In grey the predicted minimum and maximum short-wave heights during the half hour around the peak of the storm.

Time series at ADCP1

A time series of the observed and modelled water depth and wave characteristics at ADCP1 is presented in Figure C-20. The dashed vertical lines delimit the period that instruments were deployed on the beach itself. The water depth variations show a tidal amplitude variation of some three to four meter during the measurement period. The short-wave height increases from 2 to 6 meters during the storm and is depth limited. The tidal amplitude variations modulate short wave breaking at this location, and dictate the maximum attained short-wave height. The low-frequency wave height (VLF + IG) increases from several tens of centimetres before the storm to over 1 m during the peak of the storm. Like the short waves, the low-frequency wave-height signal is modulated by the tide. We refer to Bertin et al. (2020) for a detailed analysis and interpretation.

As mentioned above, in general the model predictions follow the observations closely, although the short-wave height is consistently overestimated. In turn, this affects the infragravity-wave behaviour, which is overestimated as well during the peak of the storm. During the second high-tide, there is however an underestimation of the infragravity-wave height.

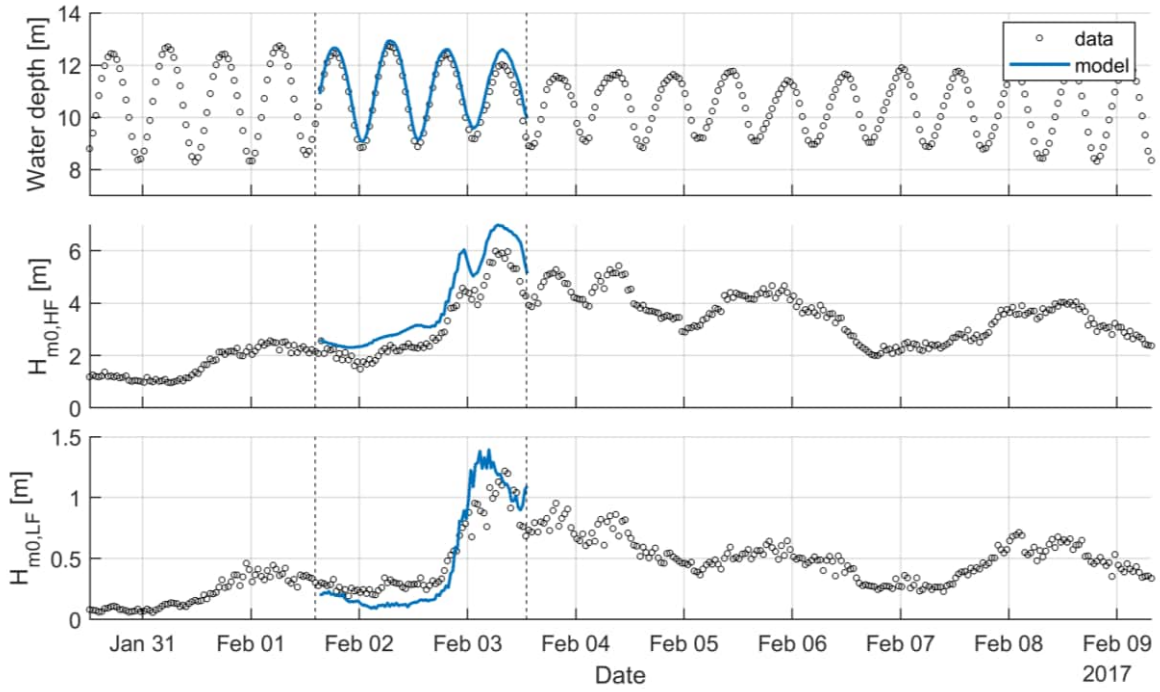

Figure C-20 Time series of observed (circles) and modelled (solid lines) bulk parameters at the location of ADCP1 (Figure C-17) at ~11 m water depth. (a) Water depth, (b) short-wave height and (c) low-frequency wave height . The dashed vertical lines indicate the measurement period of the instruments installed on the beach.

Time series at the beach and goodness of fit (GoF)

The local time series of observed and modelled water depth and wave-height variations of measurement locations PT3 and PT7 are depicted in Figure C-21 and Figure C-22 respectively. Figures of the other locations are presented in section “Additional figures”. The sensors are exposed at low-tide and measuring during high tide. At PT3, the maximum water depth is some 2 m. The short-wave heights are modulated by the tidal water depth variations and attain a maximum of 1.2 m during high tide. Their maximum height is irrespective of the offshore wave conditions, as their maximum height is limited by breaking, and is almost similar before and during the storm. On the contrary, long wave heights increase substantially during the storm, of some 0.5 m before the storm, to up to 1.5 m during the peak of the storm – and of the same height or slightly larger than as short waves. In shallower water, at PT8, the same trends are visible. Short-wave heights decrease further over the transect, and long waves are now dominant, especially during storm conditions, but also before the storm they are larger than the short waves.

In line with the previous figures, the model predictions follow the observations closely on the whole, while a consistent overestimation of the short-wave height is visible. Again, an underestimation of the low-frequency-wave height during the second high tide is observed.

The goodness-of-fit indicators are presented in each subplot, and additionally assembled in Table C-2. To give an example, the short-wave height overestimation during the whole measurement period of the XBeach model predictions is reflected in an average bias of 0.22 m over the whole transect, while the average water depth bias is smaller with 0.11 m and the low-frequency wave-height bias is 0.04 m. During the storm peak the average bias in water depth and short-wave height decreases slightly to 0.09 m and 0.22 m respectively. The infragravity-wave height bias increases to 0.18 m, which is discussed further in the next section.

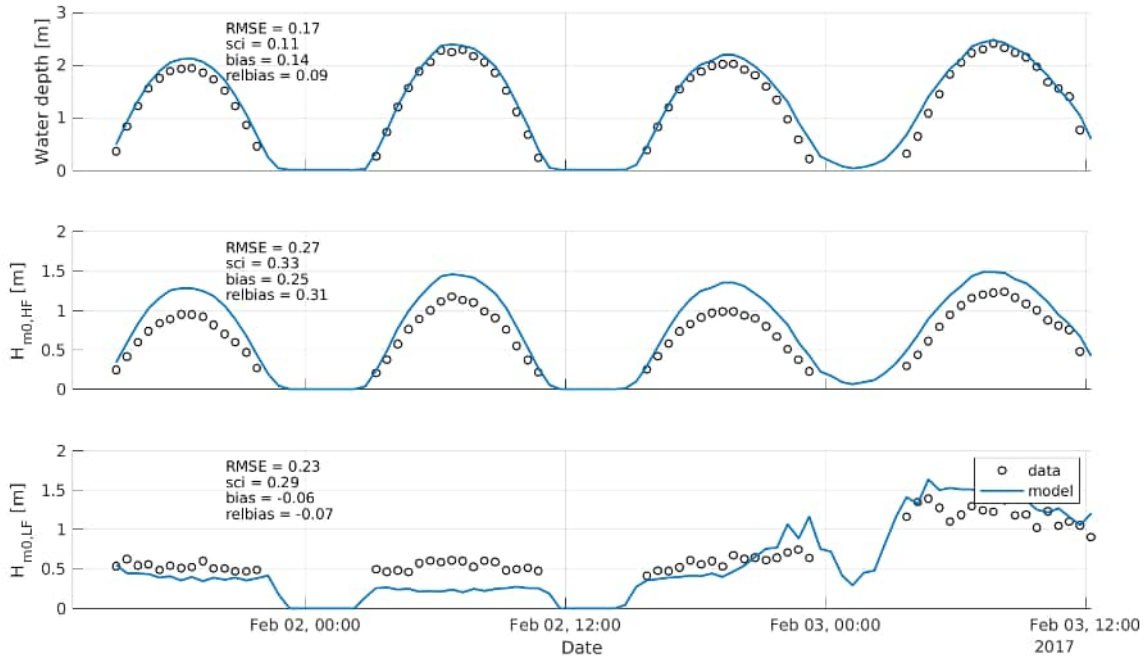

Figure C-21 Modelled (blue line) against observed (circles) water depth (top), short-wave height (middle) and low-frequency wave height (bottom) at PT3.

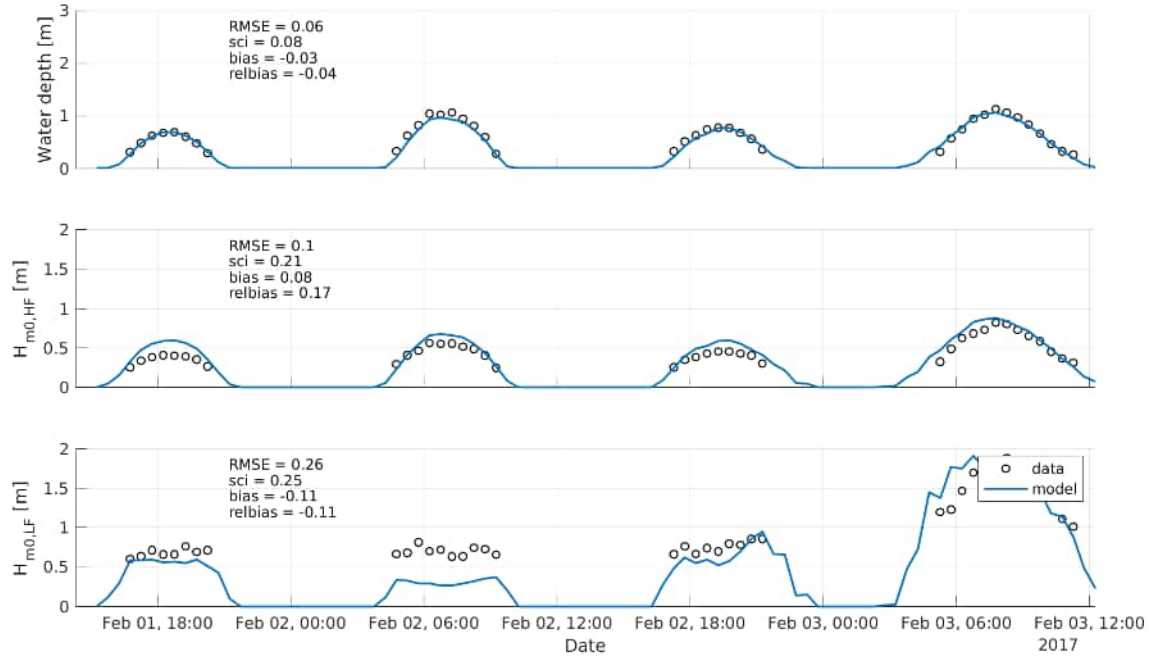

Figure C-22 Modelled (blue line) against observed (circles) water depth (top), short-wave height (middle) and low-frequency wave height (bottom) at PT7.

Table C-2 Goodness-of-fit (GoF) indicators for the modelled water depth and the high- and low frequency wave heights compared to the measurements at the PT1 to PT8 (seaward to landward side of measurement transect). Colours per indicator indicate relative GoF between the locations of all hydrodynamic cases (greener = better fit). For the performance most relevant for dune erosion, also the indicators for the storm peak only are shown. The GoF for the storm peak is taken between the 3rd of February 2017 at 3 AM to 11 PM.

Pressure sensor nr.	Water depth [m]				$H_{mo\,hf}$ [m]				$H_{mo\,lf}$ [m]			
	RMSE	sci	bias	rel.bias	RMSE	sci	bias	rel.bias	RMSE	sci	bias	rel.bias
P1	0.12	0.06	0.07	0.04	0.21	0.21	0.19	0.19	0.23	0.32	-0.01	-0.01
P2	0.25	0.14	0.23	0.13	0.34	0.41	0.32	0.39	0.22	0.29	0.01	0.01
P3	0.17	0.11	0.14	0.09	0.27	0.33	0.25	0.31	0.23	0.29	-0.06	-0.07
P4	0.10	0.07	0.04	0.03	0.23	0.32	0.21	0.29	0.22	0.26	-0.05	-0.06
P5	0.21	0.17	0.18	0.14	0.28	0.45	0.27	0.43	0.23	0.26	-0.05	-0.05
P6	0.21	0.22	0.19	0.20	0.18	0.32	0.18	0.30	0.27	0.28	-0.07	-0.08
P7	0.06	0.08	-0.03	-0.04	0.10	0.21	0.08	0.17	0.26	0.25	-0.11	-0.11
P8	0.15	0.33	-0.13	-0.30	0.18	0.73	0.16	0.64	0.26	0.33	0.03	0.03
Overall	0.17	0.12	0.11	0.07	0.24	0.33	0.22	0.29	0.24	0.28	-0.04	-0.04
Overall, *storm peak only*	0.18	0.11	0.09	0.06	0.24	0.28	0.22	0.26	0.29	0.23	0.18	0.14

Modelled versus observed water depths **and wave heights**

An aggregated scatter plot of observed versus modelled water depths and wave heights is presented in Figure C-23. As seen in the above presented analyses, the overall trends are well captured by the model – over the whole measurement transect. The consistent overestimation in short-wave height of on average 22 cm is clearly visible. In addition, a constant offset is also visible in the water depths.

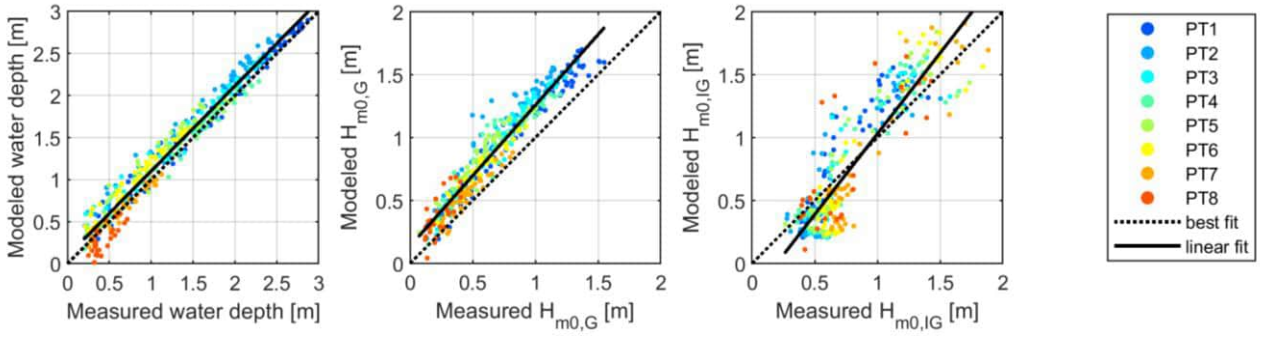

Figure C-23 Scatter plot of the modelled (predicted) versus observed water depths (left), short-wave height $H_{m0,HF}$ (middle) and low-frequency wave-height $H_{m0,LF}$ (right) for all measurement locations at Saint Trojan. The dashed line indicates a perfect 1:1 relationship, the continuous line represents a linear data fit.

Discussion

In general, the validation results showed a good fit between the measured and modelled water depths and wave heights at the Saint Trojan Beach. However, there are some offsets between the model and observations. The three most important offsets are further discussed in this section.

Short-wave height overestimation

An overestimation of the short-wave height was observed for all locations (Figure C-23). Bertin at al. (2020) already pointed out that as a consequence of the very mild sloping beach, a breaking parameter *gamma* value of 0.38 was necessary to well capture the short-wave breaking. Therefore, it is not a surprise that the short-wave height was overestimated with the BOI settings. Additional model runs confirm that by only changing the gamma parameter to the value proposed by Bertin et al. (2020), a 1D XBeach model approach was able to reproduce this wave breaking as well (example given in Figure C-24). For instrument location PT3 the RMSE reduces from 0.27 m to 0.1 m by reducing the gamma parameter to 0.38, and the relative bias from 0.31 to 0.11 (compare Figure C-21 to Figure C-24). Nevertheless, such a very mild slope is not representative for the Dutch coast and hence not desirable to further calibrate the gamma parameter on.

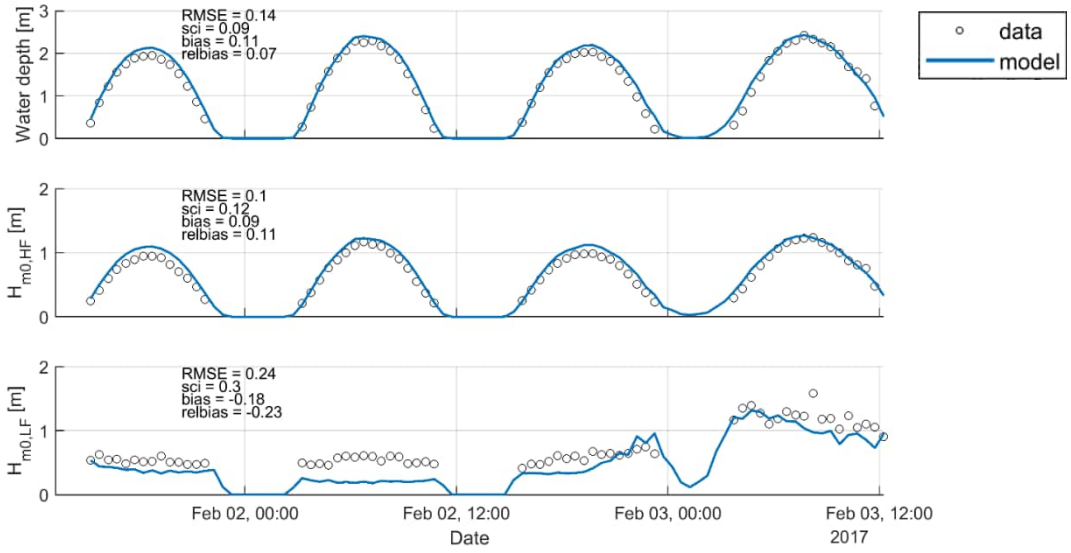

Figure C-24 Modelled (blue line) against observed (circles) water depth (top), short-wave height (middle) and low-frequency wave height (bottom) at PT3 with the gamma parameter at 0.38 – like in Bertin et al. (2020).

Water-depth offset

The aggregated scatter plot (Figure C-23) which compares the observed and modelled water depths shows a consistent, though minimal, overestimation of the water depths by the XBeach model. This is partly caused by the fact that in the original 2DH model set-up a somewhat smoothened version of the observed bed levels was used (by Bertin et al. (2020)). This 2D bed level was used in the current study as the initial bed. Figure C-17 shows however that the actual elevation for most of these pressure transducers is somewhat scattered around the profile used in the model. A second source of water depth offset is the delayed onset of short-wave breaking. For the simulation with the *gamma* breaking parameter set to 0.38 (as in Bertin et al. (2020) the water depth offset reduces shoreward, to almost zero for the instrument locations close to the dune foot.

Infragravity wave height offsets

Overall, the infragravity wave height in the XBeach results corresponds well with the measured values. Hence, the newly implemented αE parameter seems to work fine. However, some relatively small offsets were observed. The infragravity wave height overestimations during in particular the fourth tidal cycle – the peak of the storm – find their source in the short-wave height overestimation discussed here above (compare Figure C-21 to Figure C-24). The delayed breaking of the short waves results in a longer time for energy transfer to the low frequency waves, which consequently grow too high. The low infragravity wave height in the model during the second tidal cycle is related to the large directional spread of the short-wave field (> 35 degrees). These wave heights are an underestimation of the observations. This underestimation is unlikely to be related to the use of a 1D model (and the newly implemented αE parameter), as the infragravity wave height was also considerably underestimated in the 2DH XBeach model of Bertin et al. (2020). While the underestimation may be due to missing physics in both the 1D and 2DH versions of the XBeach model, it is also highly likely that the directional spread in the XBeach model boundary conditions are not fully correct for this tidal cycle, as these are based on a wave hindcast (Bertin et al., 2019) rather than observations. An overestimation of wave spreading in the wave hindcast would lead to an underestimation of the infragravity-wave height in XBeach.

Conclusion

The hydrodynamics in the BOI-version of the XBeach model have been validated with field measurements of storm conditions at the very gently sloping Saint Trojan Beach (France). Based on this validation is concluded that the newly updated and calibrated XBeach model is well capable of simulating hydrodynamic characteristics as water depths and short- and long-wave behaviour during extreme storm conditions. The observed offsets between the model and the measurements can be well explained and, except for the *gamma* parameter choice, are not related to the XBeach model set-up. The newly introduced αE parameter (to mimic the effect of directional spread while simulating in 1D profile mode) seems to capture long-wave heights very well.

Additional figures

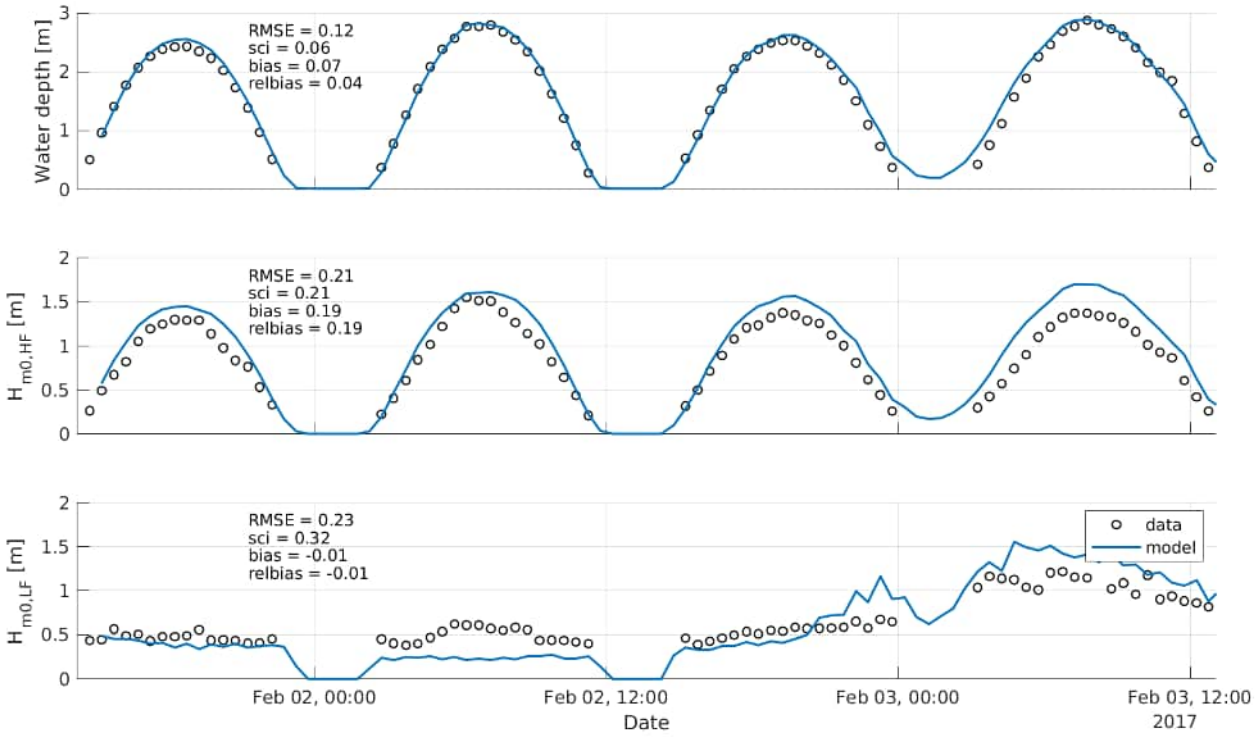

Figure C-25 Modelled (blue line) against observed (circles) water depth (top), short-wave height (middle) and low-frequency wave height (bottom) at PT1.

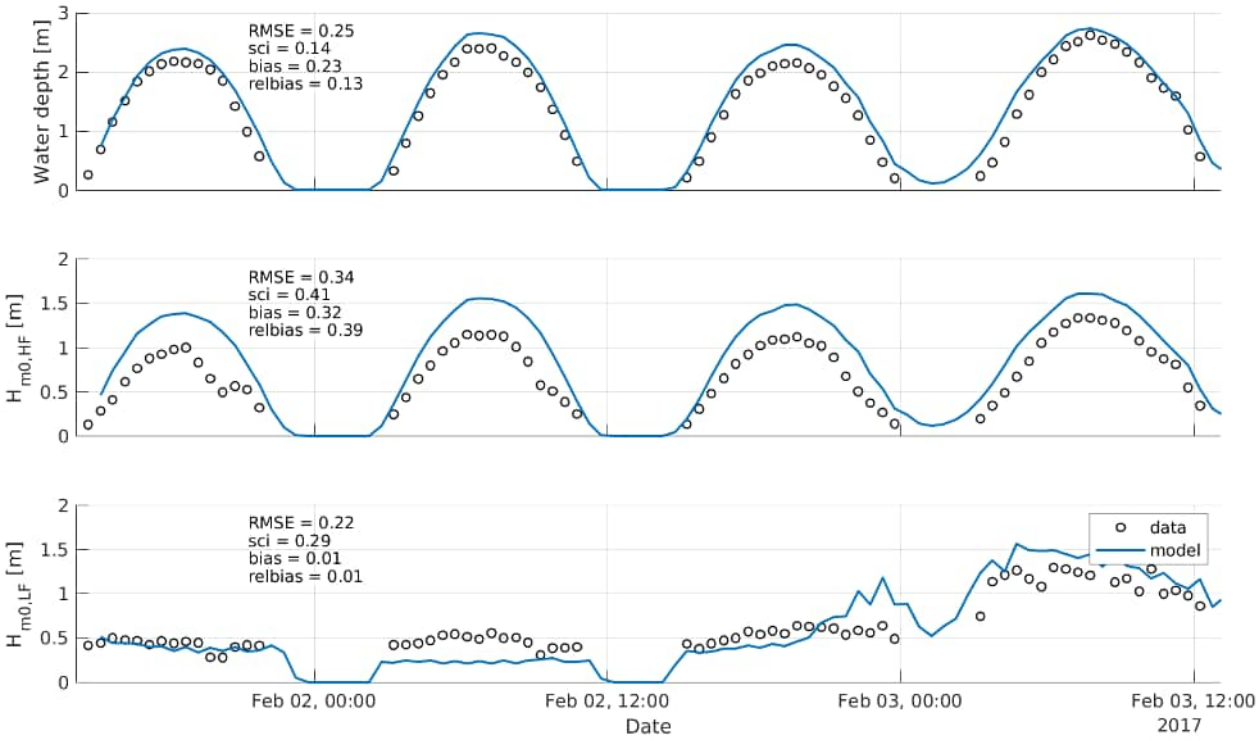

Figure C-26 Modelled (blue line) against observed (circles) water depth (top), short-wave height (middle) and low-frequency wave height (bottom) at PT2.

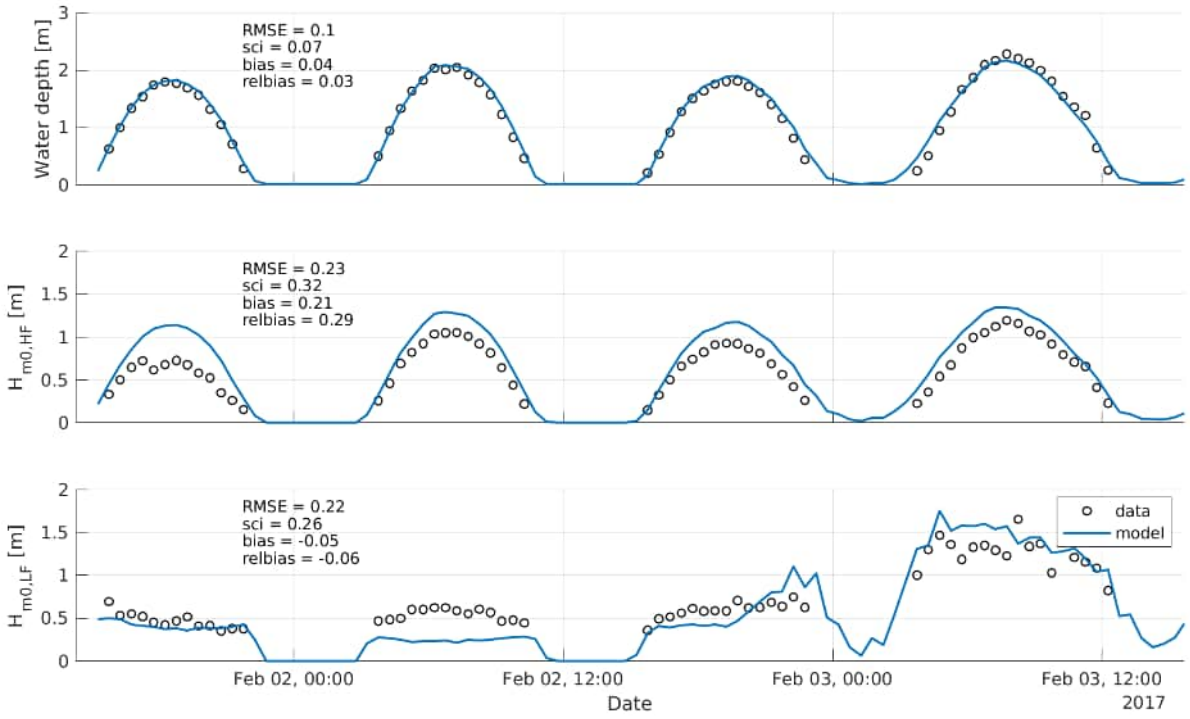

Figure C-27 Modelled (line) against observed (circles) water depth (top), short-wave height (middle) and low-frequency wave height (bottom) at PT4.

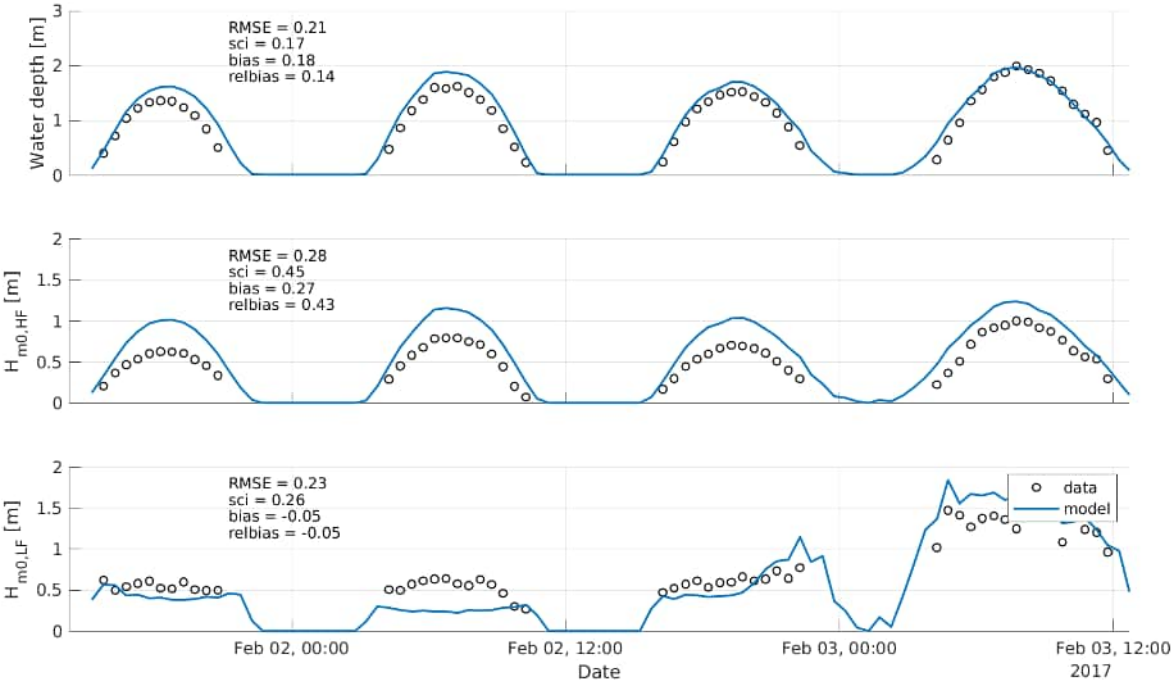

Figure C-28 Modelled (line) against observed (circles) water depth (top), short-wave height (middle) and low-frequency wave height (bottom) at PT5.

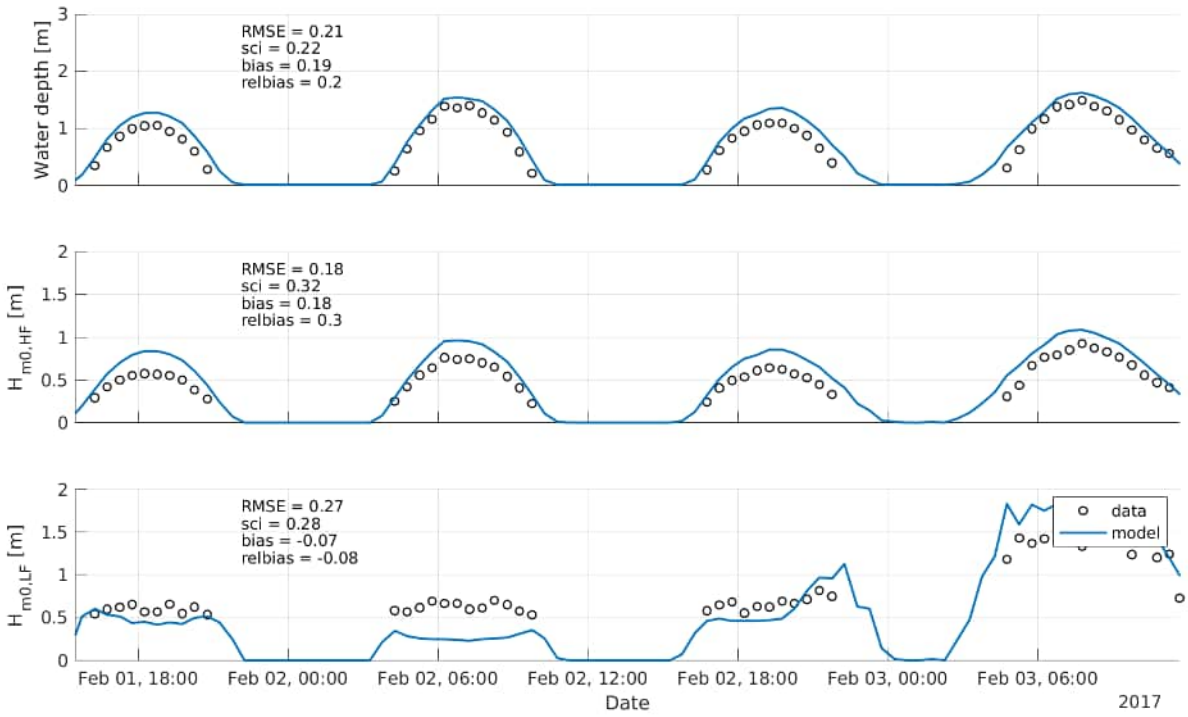

Figure C-29 Modelled (line) against observed (circles) water depth (top), short-wave height (middle) and low-frequency wave height (bottom) at PT6.

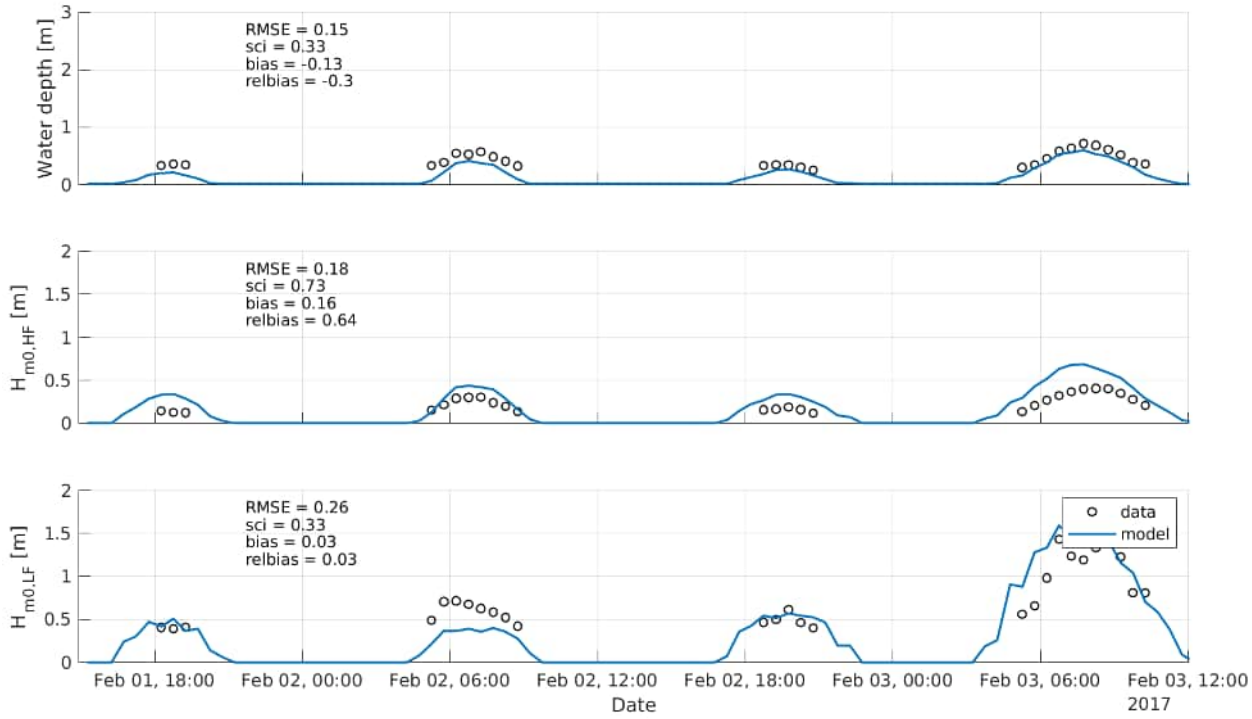

Figure C-30 Modelled (line) against observed (circles) water depth (top), short-wave height (middle) and low-frequency wave height (bottom) at PT8.

APPENDIX 3 - FIELD CASE 3: FLEMISH COAST (BELGIUM) [MORPHO]

Case description

On 5-6 December 2013, the north-western storm in the North Sea called 'Storm Xaver' or the 'Sint Nicholas storm (Sinterklaasstorm)' with relatively low wind speeds and a long fetch resulted in high surge levels in combination with moderately high waves (Trouw et al., 2015). This resulted in beach and dune erosion along among others the Belgian coast on the order of 8 m^3/m (Lanckriet et al., 2015). The Coastal Division of the Flemish Government collected 122 cross-shore profiles of the beach and (first) dune row during a dGPS survey 2-4 days before this storm and based on an airborne lidar survey 4 days after this storm (Trouw et al., 2015). A selection of these pre- and post-storm profiles (Figure C-31) is used for the validation of the morphodynamics in the BOI-version of the dune erosion model XBeach, focusing on dune erosion volumes and retreat distances.

Figure C-31 Overview of the Belgian coastline with the location of the analysed cross-shore profiles measured before and after the Sint Nicholas storm and the water level (WL) and wave measurement locations used for this case.

Based on the data of the Vlaamse Banken, the offshore storm surge levels reached up to TAW + 6.0 m[8] (5 min average) during the Sint Nicholas storm at measurement pole 'A2' and 'Scheur Wielingen' in front of the Belgian coast (bottom depth respectively about -7 m LAT[9] and -10 m LAT) (Figure C-3). This was the result of a combined high storm setup and spring tide. At the harbour of Ostend, storm surge levels reached TAW + 6.19 m (Trouw et al.; 2015). The observed water levels were the highest since 1953 and were estimated to have a return period of about 40 years in Belgium (IMDC, 2005). Furthermore, significant wave heights reached up to 3.8 m (20 min average) at the offshore wave buoy 'ZW-Akkaert' at LAT - 20 m (Figure C-3). The highest peak occurred during rising tide; at the peak water level, the wave height was already about 0.5 m lower. The peak wave period during the storm was about 8 s with a peak to 15 s at the end of the storm at the same location. This corresponds to a return period in the order of 1 year along the Belgian coast (IMDC, 2005). The waves approached approximately shore-normal from the northwest. After more than one day of high waves, the wave height gradually reduced, together with the storm surge.

[8] *TAW = 'Tweede Algemene Waterpassing'. This is the local reference level for elevations in Belgium, corresponding with the average sea level in Oostende during low tide. Compared to the Dutch reference level (and MSL), TAW = -2.33 m NAP. Hence, 5.33 m +TAW corresponds to the average dune foot elevation at 3 m +NAP in the Netherlands.*

[9] *LAT = 'Lowest Astronomical Tide'. At Zeebrugge, LAT ≈ TAW - 0.23 m.*

The Belgian coast has gently sloping, dissipative beaches that are slightly steeper towards the east. They are mainly composed of fine to medium sand (Degraer et al., 2003). The tidal regime along the Belgian coast is semidiurnal and macrotidal, with a of 3.7-3.9 m neap tidal range and 4.5-5 m spring tidal range which slightly decrease from west to east (Degraer et al., 2003). To prevent the beaches from erosion by the strong tidal currents, a large part of the coastline is protected by groynes. Moreover, a concrete dike along much of the coastline protects the inland from flooding (Degraer et al., 2003). 15 profiles in the areas with natural beach-dune transitions between Ostend and the Dutch-Belgian border are selected for this case study (Figure C-31). The selection is based on:

- The setting: only profiles with dunes without dune toe protection or hard structures like boulevards up until the dune erosion zone during the storm are selected. The profiles should also be away from harbour jetties to limit 2D effects on dune erosion;
- The elevation of the landward end of the pre-storm profiles: only the profiles with measurement data reaching above TAW + 9 m are included, to ensure that all bed level changes occur well within the model's grid extent.;
- The reliability of the post-storm profiles: dune erosion scarps in profiles up to nr. 39 might have been flattened by bulldozers before the post-storm survey and hence are excluded.

The beaches in the selected profiles have a slope of on average 1:45 to 1:65 from the dune toe to the relatively flat zone at TAW - 5 m (westernmost profiles) to TAW - 7 m (easternmost profiles) (Figure C-35). Just below mean sea level, 2-4 bars are present in all profiles except the easternmost profiles (117-121). The relatively flat plateau extends more than 10 km into the sea and contains some sand banks (Figure C-32). Further offshore, seaward of the profiles, the bathymetry is characterized by large sand banks at intermediate to deep water.

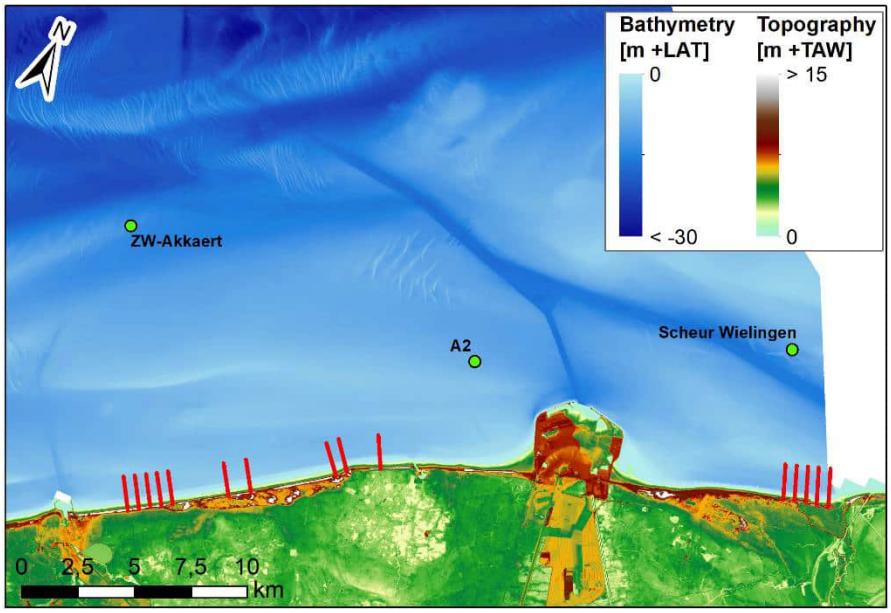

Figure C-32 Overview of the elevation surrounding the selected cross-shore profiles and the hydraulic measurement locations used in the Belgian coast validation case. Bathymetry data ('DTM Belgisch Continentaal Plat 20 m') of the Coastal Division of the Flemish Government, topography data ('Digitaal Hoogtemodel Vlaanderen II 1 m raster') of 'Geopunt Vlaanderen'.

Model setup

A morphodynamic XBeach 1D simulation (including sediment transport and morphology) is set up for the 15 transects based on the method as described in the main report and the data as described in the section above. The median grain size (D_{50}) for each profile (Table C-3) is adopted from Lanckriet et al. (2015), who used these in their XBeach model for the same profiles. The values are based on the Belgian guidelines for the 2007 coastal safety assessment. For profile 79 and 80, where the beach was nourished after 2008, the D_{50} of the design grain size (about 300 μm) has been used (Lanckriet et al., 2015). The D_{90} is set to 1.5 times the D_{50}.

Table C-3 Median grain size (D_{50}) for the XBeach 1D profiles along the Flemish coast based on Lanckriet et al. (2015).

Profile nr.	60	61	62	63	64	69	71	79	80	83	117	118	119	120	121
D_{50} [μm]	215.6	215.6	215.6	215.6	308.1	308.1	308.1	300	300	218	257	257	271	271	271

Grid and bathymetry

Figure C-33 and Figure C-2 show the initial cross-section and grid cell size of the XBeach transect for profile nr. 79 and 119 as an example. The initial cross-section of the other profiles is visible in Figure C-35 and in the figures in the Additional Figures section. All profiles start at the landward side with the pre-storm dGPS measurements of the first dune and the beach up to approximately the low-tide shoreline (≈ TAW + 0 m), with a cross-shore resolution of 2-15 m. Note that in most profiles, not the entire first dune is included, and sometimes higher dunes are present behind the first dune.

Each profile is extended with singlebeam survey data of June-July 2013 of the nearshore up to about TAW - 5 m. The dGPS and singlebeam data are described by Trouw et al. (2015). The offshore end of the profile is extended manually to deep water with an artificial slope of 1:50 at the most offshore point of the singlebeam data on the profile, following the BOI guidelines. The cross-shore grid was also set-up using the standard BOI procedure, resulting in 822 to 1008 grid points depending on the profile and a spatial resolution that varies from 2.7 m offshore to 1.0 m in the dunes.

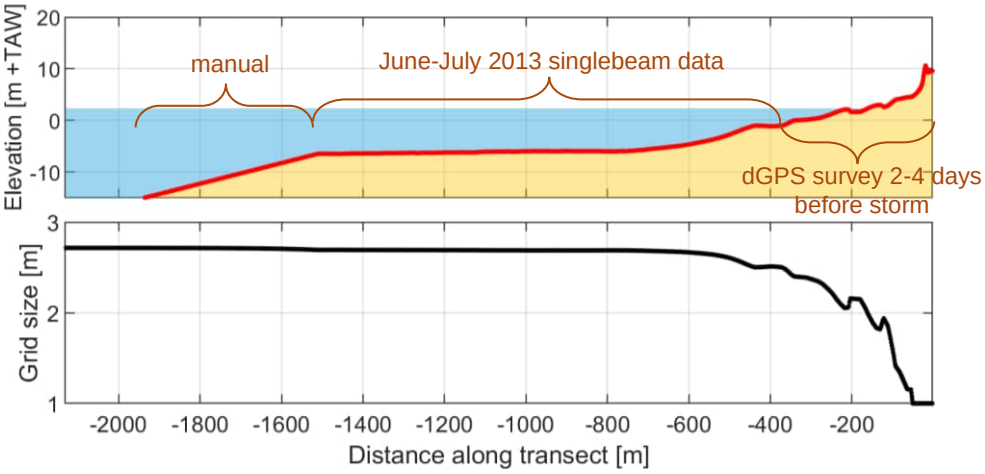

Figure C-33 Overview of the initial bed level including data source (top panel) and grid cell size (bottom panel) along the XBeach transect nr.79 along the Belgian coast: a profile with bars around mean water level (blue).

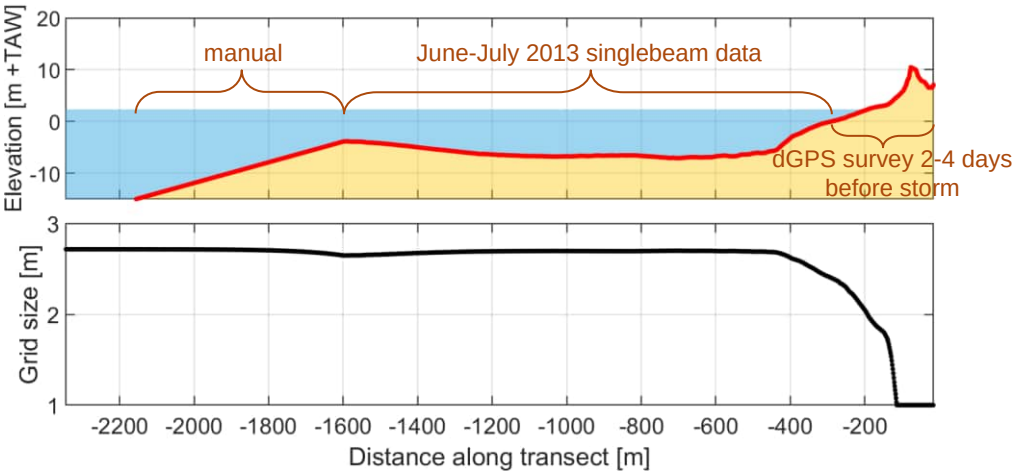

Figure C-34 Overview of the initial bed level including data source (top panel) and grid cell size (bottom panel) along the XBeach transect nr.119 along the Belgian coast: a profile without bars around mean water level (blue), and a large sand bank offshore.

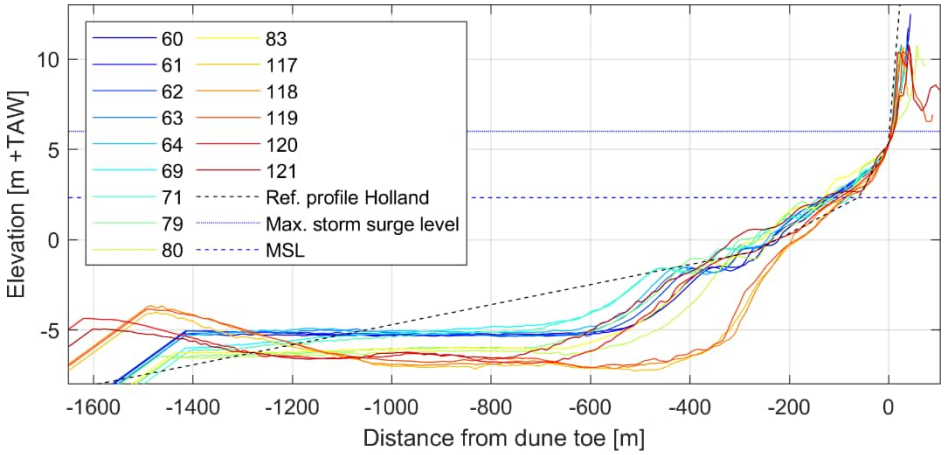

Figure C-35 Overview of the XBeach cross-shore profiles of all 15 selected profiles along the Belgian coast up to the point of the manual extension of the profile at the seaward end.

Hydraulic boundary conditions

Figure C-3 shows the imposed hydraulic boundary conditions in the XBeach simulation for the modelled storm period of 6 tidal cycles (04-12-2013 7:30h PM to 07-12-2013 11:30h PM), similar to the XBeach simulations in Lanckriet et al. (2015). At the offshore model boundary (North Sea), the water level time series recorded at the 'A2' station during the storm period is imposed for profiles west of the harbour of Zeebrugge (profile nr. ≤99). Water levels measured at the 'Scheur Wielingen' station are used for profiles east of this harbour (profile nr. > 99). Furthermore, the spectral significant wave height H_{m0}, peak wave period T_p and the directional wave spreading σ at the 'ZW-Akkaert' station are converted to average values per hour. σ (in rad) is converted to a directional wave spreading coefficient using $s = 2/\sigma^2 - 1$, resulting in s-values ranging between 2 and 16. These wave characteristics are imposed on the offshore boundary as a time-varying JONSWAP spectrum directed perpendicular to the coast. The peak wave period is relatively low during the storm and shows a peak at the end of the storm, while the mean wave period (not shown and used) showed a pattern more similar to that of the wave height.

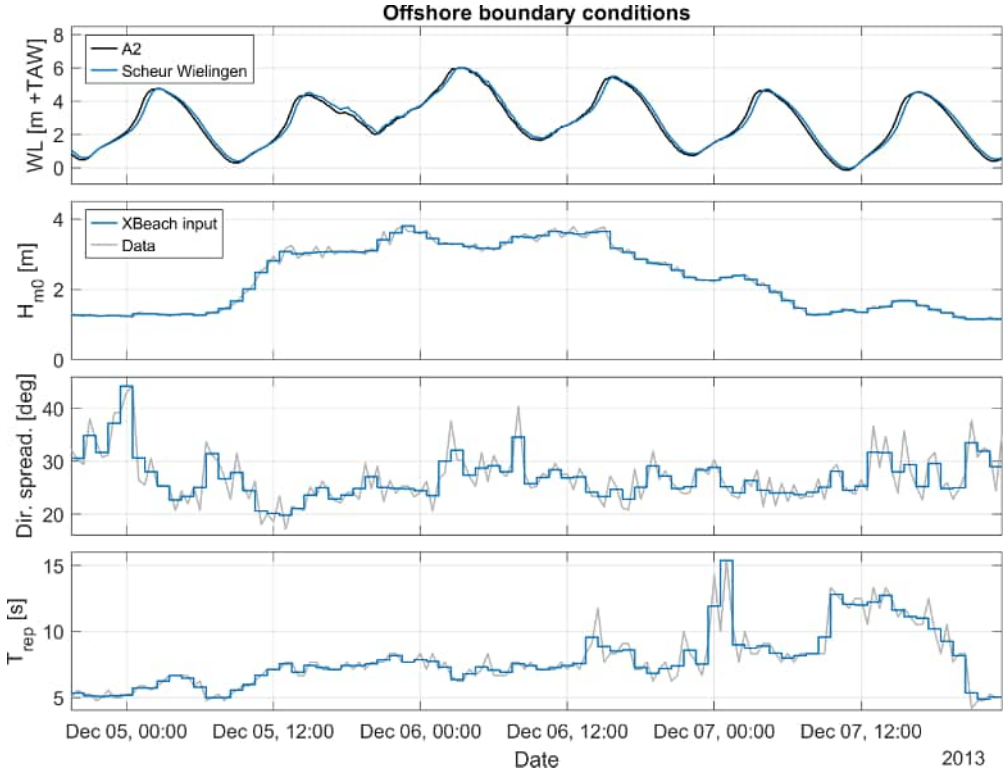

Figure C-36 Time series (CET) of the XBeach offshore hydraulic boundary conditions for the Belgian coast case based on recorded data at the A2 (water level, profile nr. ≤99), Scheur Wielingen (water level, profile nr. > 99) and ZW-Akkaert station (waves).

Model output settings and post-processing

The XBeach profile at the last timestep is compared with the first time step. The XBeach dune erosion volume is calculated as the negative volume difference between these profiles above the highest storm surge level (TAW + 6.0 m). The measured dune erosion volume is calculated in the same way using the initial profile and the post-storm profile based in the airborne LiDAR measurements at 10 December 2013. In the measurements, some volume changes occurred behind the first dune top, which is not related to wave action. Hence, only the dune erosion volume that starts at the dune toe of the first dune has been included. The dune retreat distance is measured at TAW + 7.0 m, 1 m above the highest storm surge level, at the lower part of the dune where most erosion occurred.

Results

Changes in morphology in the cross-shore profiles

Figure C-51 shows the pre- and post-storm profile for profile nr. 62 based on the measurements and on the XBeach simulation. A similar figure for all other profiles is shown in the Additional figures section. Note that the dune top in some profiles (e.g. 119) is not very accurate in the measured post-storm profile, but this does not affect the analyses. Profile 62 is shown here because it has dune erosion volumes and retreat distances closest to the average of all profiles (Table C-4).

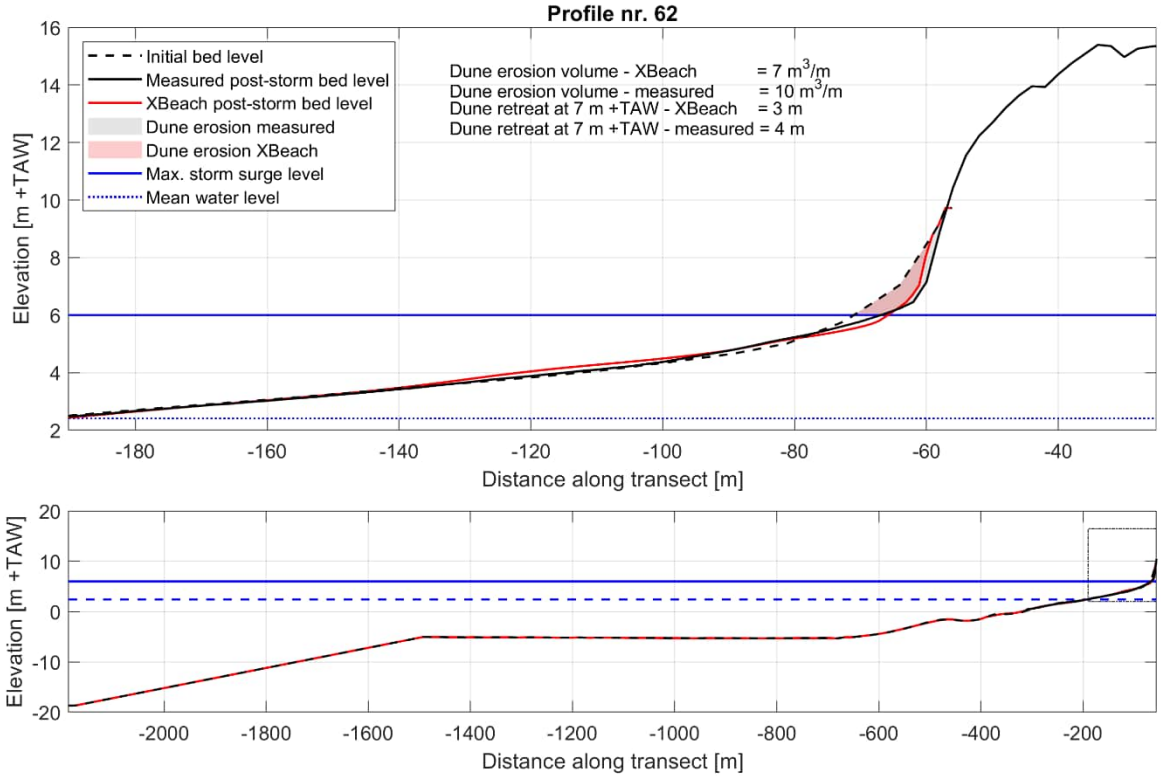

Figure C-37 Cross-section profile nr. 62 before and after the Sint Nicholas storm based on the measurements and XBeach, including dune erosion volumes and retreat distances. Bottom: entire XBeach profile, top: zoom of beach and dune profile.

At all locations, the dune toe has been eroded during the Sint Nicholas storm in both the measurements and XBeach. Erosion generally took place up to about TAW + 8 m, which is 2 m above the storm surge level. An exception is profile 69, 79 and 120, where dune erosion up to the dune top at about TAW + 10 m seems to have occurred based on the measurements, while the highest dune erosion level in XBeach was somewhat lower. This seems related to the steeper dune front in XBeach. The dune erosion starts below the maximum storm surge level, generally around TAW + 5.5 m, in both the measured and XBeach profiles.

In the XBeach simulations, a small deposition berm below the eroded dune is present with a volume up to the dune erosion volume. However, in the measured profiles, this deposition berm is often smaller or even absent, resulting in a slight difference in the profile slope with the XBeach post-storm profile. The clearest deposition berm in the XBeach simulation as well as measured profiles is visible in profile nr.118-121. The shape of these deposition berms in the XBeach post-storm profile is very similar to that in the measurements. Below the deposition berm, the XBeach profiles remain quite stable: the bars do not show strong migration and no clear unexpected profile shape changes occur. As far as the measured profiles reach, this is in line with the measurements.

Dune erosion volumes and dune toe retreat distances

The dune erosion volumes and retreat distances based on the measured pre- and post-storm profiles and the XBeach simulations for all 15 profiles are tabulated in Table C-4 and plotted against each other in Figure C-38. Overall, the dune erosion volumes are small: on average 10 m^3/m (min. 4 m^3/m, max. 19 m^3/m) based on the measured profiles. The dune retreat rate was on average 4.3 m (min. 1.2 m, max. 8.4 m) at one meter above storm surge level. The differences between the measured and XBeach dune erosion are also included in the table. The XBeach simulations structurally slightly underestimate the dune erosion volume by about 3 m^3/m, and retreat distance by about 0.9 m. Note that the difference of 0.9 m in the retreat distance is smaller than the horizontal model resolution of 1 m. As the observed erosion is small, the relative difference between observed and modelled erosion volumes and retreat distance is on average 27% and 22% respectively.

It should be noted that only dune erosion above maximum storm surge level was accounted for in Table C-4, while also some dune erosion below this level occurs. In most profiles, XBeach calculated more erosion than in the measurements below this level, which compensates for the underestimation above maximum storm surge level. Hence, overall, dune erosion is well reproduced by XBeach.

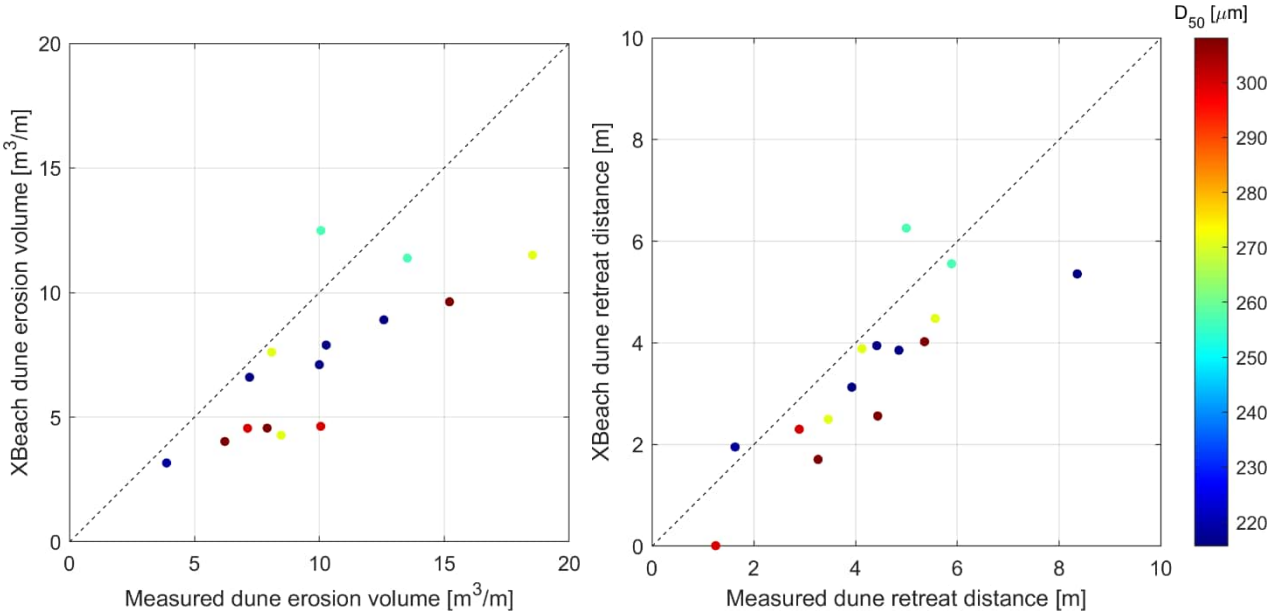

Figure C-38 Modelled versus measured dune erosion volumes and dune retreat distances for the Sint Nicholas storm along the Flemish coast. The dashed line indicates a perfect fit; colours indicate the grain size used for each profile.

Table C-4 Dune erosion volume and retreat distance for the Sint Nicholas storm in the XBeach simulation and the measured profiles for the 15 selected profiles along the Flemish coast. Negative differences mean underestimation of the measured values in the XBeach simulation. Colours per column indicate the degree of similarity between the simulations and observations based on all morphological cases (greener = better fit).

Profile nr.	Erosion volume				Retreat distance at TAW + 7 m			
	XBeach [m^3/m]	Measured [m^3/m]	Difference [m^3/m]	Difference [%]	XBeach [m]	Measured [m]	Difference [m]	Difference [%]
60	9	13	-4	-29%	5.4	8.4	-3.0	-36%
61	7	7	-1	-8%	3.9	4.9	-1.0	-21%
62	7	10	-3	-29%	3.1	3.9	-0.8	-20%
63	8	10	-2	-23%	3.9	4.4	-0.5	-11%
64	5	8	-3	-42%	2.6	4.4	-1.9	-42%
69	10	15	-6	-37%	4.0	5.4	-1.3	-25%
71	4	6	-2	-35%	1.7	3.3	-1.6	-48%
79	5	10	-5	-54%	2.3	2.9	-0.6	-20%
80	5	7	-3	-36%	0.0	1.2	-1.2	-99%
83	3	4	-1	-19%	2.0	1.6	0.3	20%
117	11	14	-2	-16%	5.6	5.9	-0.3	-6%
118	12	10	2	24%	6.3	5.0	1.3	25%
119	8	8	0	-6%	3.9	4.1	-0.2	-6%
120	12	19	-7	-38%	4.5	5.6	-1.1	-19%
121	4	8	-4	-50%	2.5	3.5	-1.0	-28%
Average	**7**	**10**	**-3**	**-27%**	**3.4**	**4.3**	**-0.9**	**-22%**

Discussion

In general, the small dune erosion volumes and retreat distances for the 15 profiles were simulated well by XBeach, especially regarding the absolute differences and taking the dune erosion below maximum storm surge level into account as well. The dune erosion volume and retreat distances varied somewhat alongshore between the profiles in both the measurements as the XBeach simulations. This can be related to among others variation in the initial profiles (elevation as well as shape, e.g. beach steepness) and grain size variation. Moreover, the post-storm storm profile shape produced by XBeach seems realistic.

Alongshore processes

A difference between the measurements and the XBeach simulations is the absence of a clear deposition zone in 9 of the 15 measured profiles, while it generally is present in XBeach. This might be related to 2D-processes such as alongshore sediment transport related to oblique waves, which is not incorporated in the 1D XBeach model with BOI-settings with perpendicular waves. 2D-processes due to alongshore variation could also explain the relatively large difference between measured and modelled dune erosion for among others profile 79-80 (located in a bend in the coastline, a local erosional hotspot (Lanckriet et al., 2015)), 71 (located close to De Haan where the beach and dune characteristics abruptly change) and 120-121 (in a slightly bended coastline, close to the channel 'Zwin').

Reliability of measured profiles

Also the reliability of the measured (post-storm) profile could play a role in differences between the measured and modelled profiles. Trouw et al. (2015) indicate that along the entire coast, dune erosion cliffs have been smoothened with machinery in the days after the storm, before the post-storm profile measurements. Along the western section of the coast, the exact location and extent of the adjustment of the post-storm profile was unknown, and hence, these profiles were excluded in this analysis. Along the middle and eastern section, the Coastal Division of the Flemish Government adjusted the profiles, but the displacement of sand was assumed to be small (max. about 10 m; Trouw et al., 2015). Hence, the effect on the erosion volumes should be limited, but it might have resulted in an error in the retreat distances and explain the relatively gentle dune erosion slopes in some of the post-storm measured profiles.

Grain size dependency and αD_{50}

Figure C-39 shows the grainsize dependency of the measured and modelled dune erosion for all profiles together. The measured dune erosion volumes seem to be largely independent of the D_{50} (on average a slight increase for larger grainsizes), although the scatter is large. The XBeach simulations also show no strong correlation with the D_{50} (on average a slight decrease for larger grainsizes). This suggests that an expected increase in the erosion volume for smaller grains is compensated by a gentler beach slope. The dune retreat distances decrease with increasing D_{50}, as expected. In the XBeach simulations, a similar trend is observed. For both the dune erosion volumes and retreat distances as function of the D_{50}, the main difference with the measurements is the bias: the slight underestimation of the dune erosion by XBeach above maximum storm surge level. Overall, this indicates that the current grain size dependence (with $\alpha D_{50} = 0.4$) is fine for this field case.

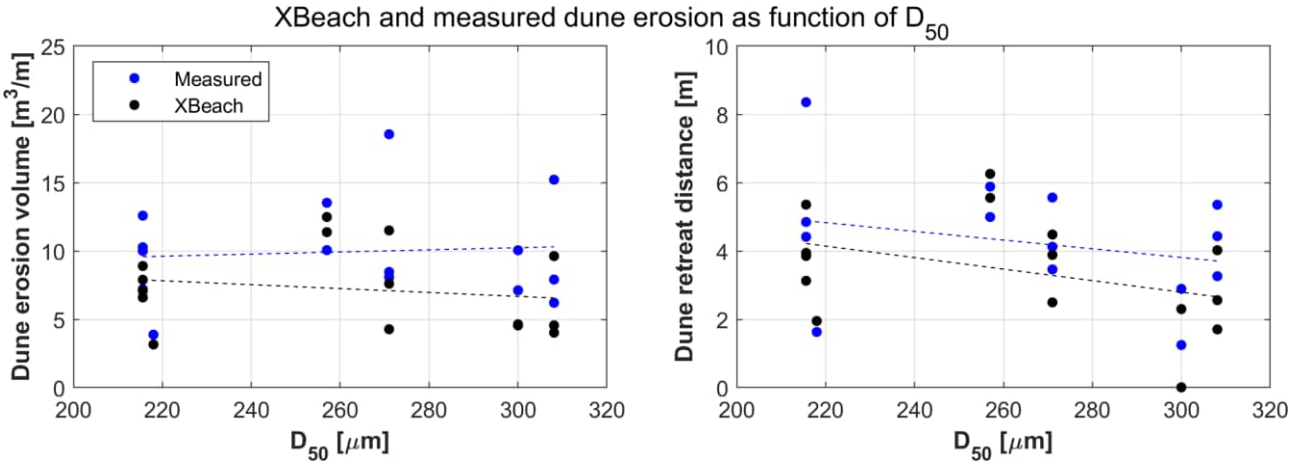

Figure C-39 Modelled XBeach (black dots) and measured (blue dots) dune erosion volumes (left) and retreat distances (right) as function of the $D_{50}$of each profile in the Flemish coast case . The dashed lines are linear trendlines through the data.

Conclusion

The morphodynamics in the BOI-version of the XBeach model have been assessed with 15 measured profiles just before and after the Sint Nicholas storm in 2013 along the shallow and gently sloping Belgian coast. Based on this study, it is concluded that the newly updated and calibrated XBeach model is capable of simulating dune erosion during storm conditions with an error of only a few m^3/m in the dune erosion volume and maximal a few m in dune toe retreat distance. The error between measured and modelled is consistently negative (underestimation by XBeach), although this is partly compensated if dune erosion below the maximum storm surge level is also taken into account. The post-storm storm profile shape produced by XBeach seems realistic. Moreover, the sensitivity of XBeach to the grain size ($\alpha D_{50} = 0.4$) seems appropriate for this field case since the relation between measured and modelled dune erosion as function of the D_{50} is similar.

Additional figures

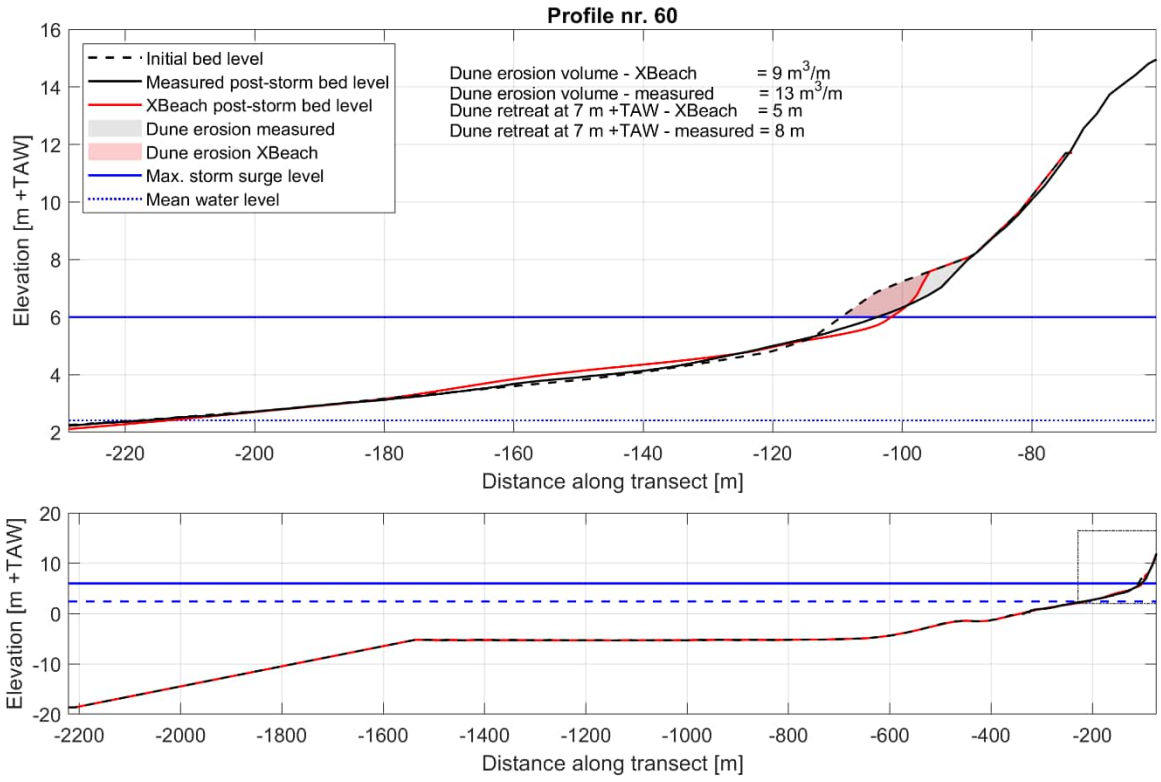

Figure C-40 Cross-section profile nr. 60 before and after the Sint Nicholas storm based on the measurements and XBeach, including dune erosion volumes and retreat distances. Bottom: entire XBeach profile, top: zoom of beach and dune profile.

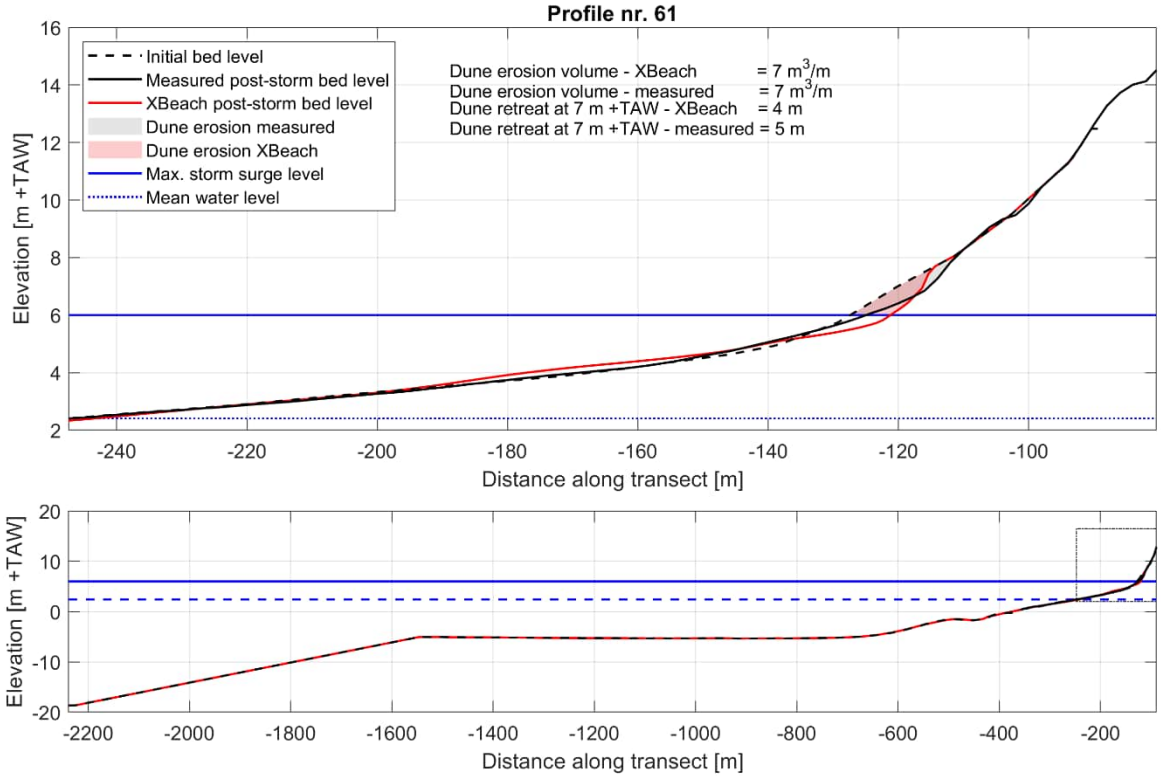

Figure C-41 Cross-section profile nr. 61 before and after the Sint Nicholas storm based on the measurements and XBeach, including dune erosion volumes and retreat distances. Bottom: entire XBeach profile, top: zoom of beach and dune profile.

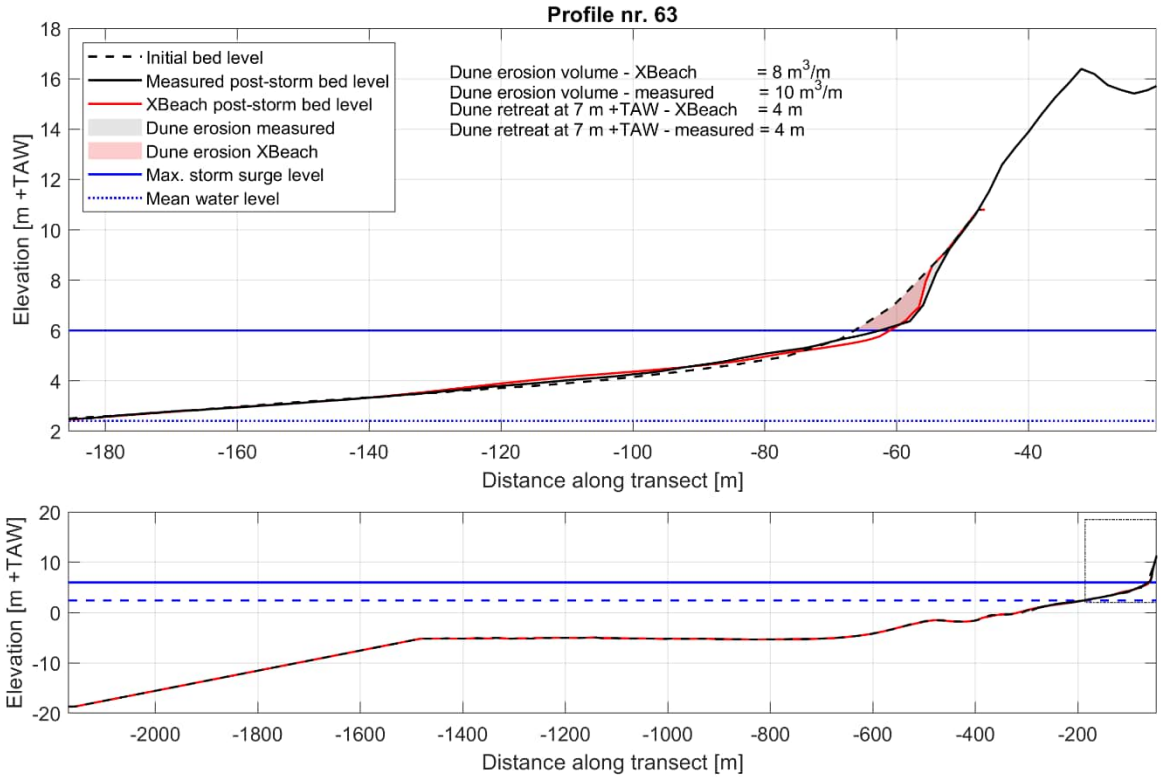

Figure C-42 Cross-section profile nr. 63 before and after the Sint Nicholas storm based on the measurements and XBeach, including dune erosion volumes and retreat distances. Bottom: entire XBeach profile, top: zoom of beach and dune profile.

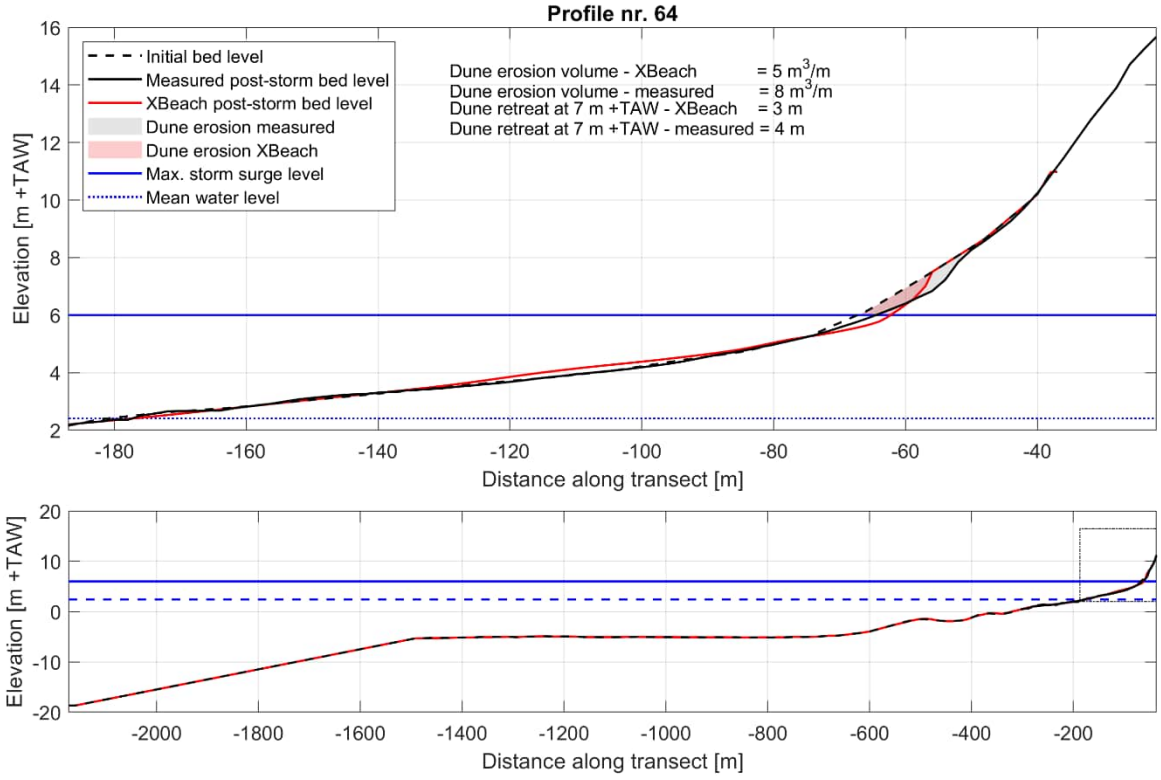

Figure C-43 Cross-section profile nr. 64 before and after the Sint Nicholas storm based on the measurements and XBeach, including dune erosion volumes and retreat distances. Bottom: entire XBeach profile, top: zoom of beach and dune profile.

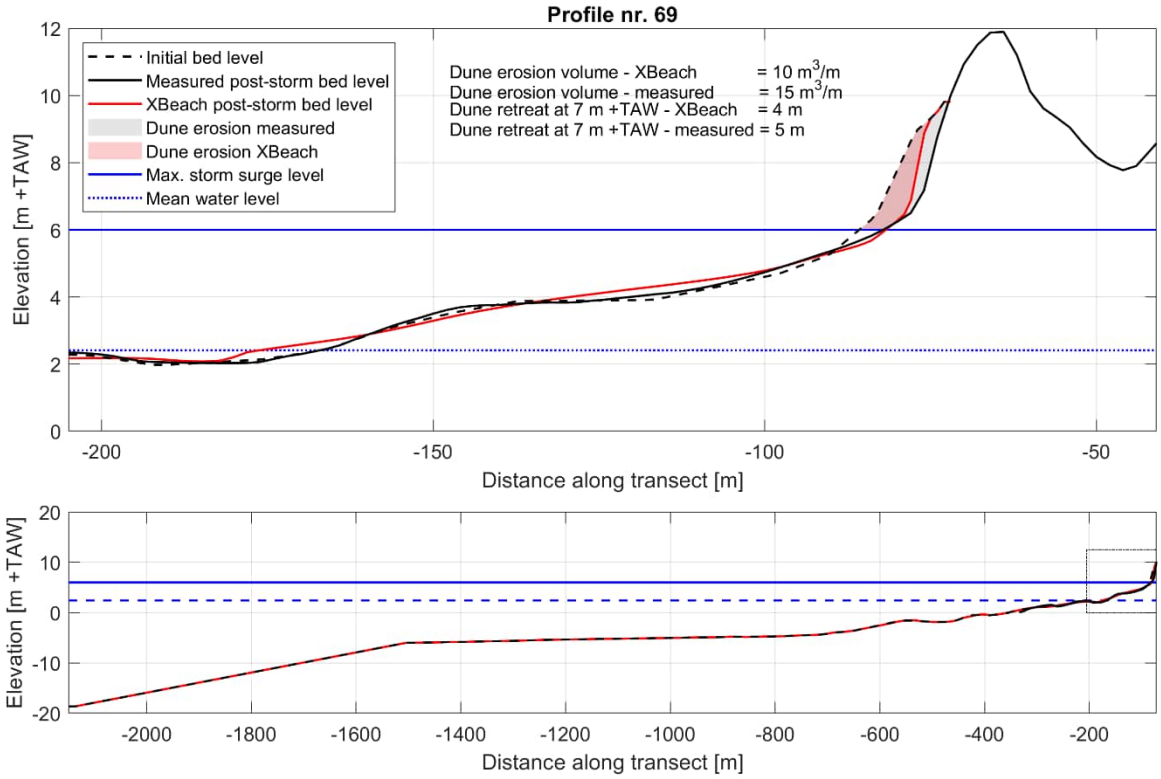

Figure C-44 Cross-section profile nr. 69 before and after the Sint Nicholas storm based on the measurements and XBeach, including dune erosion volumes and retreat distances. Bottom: entire XBeach profile, top: zoom of beach and dune profile.

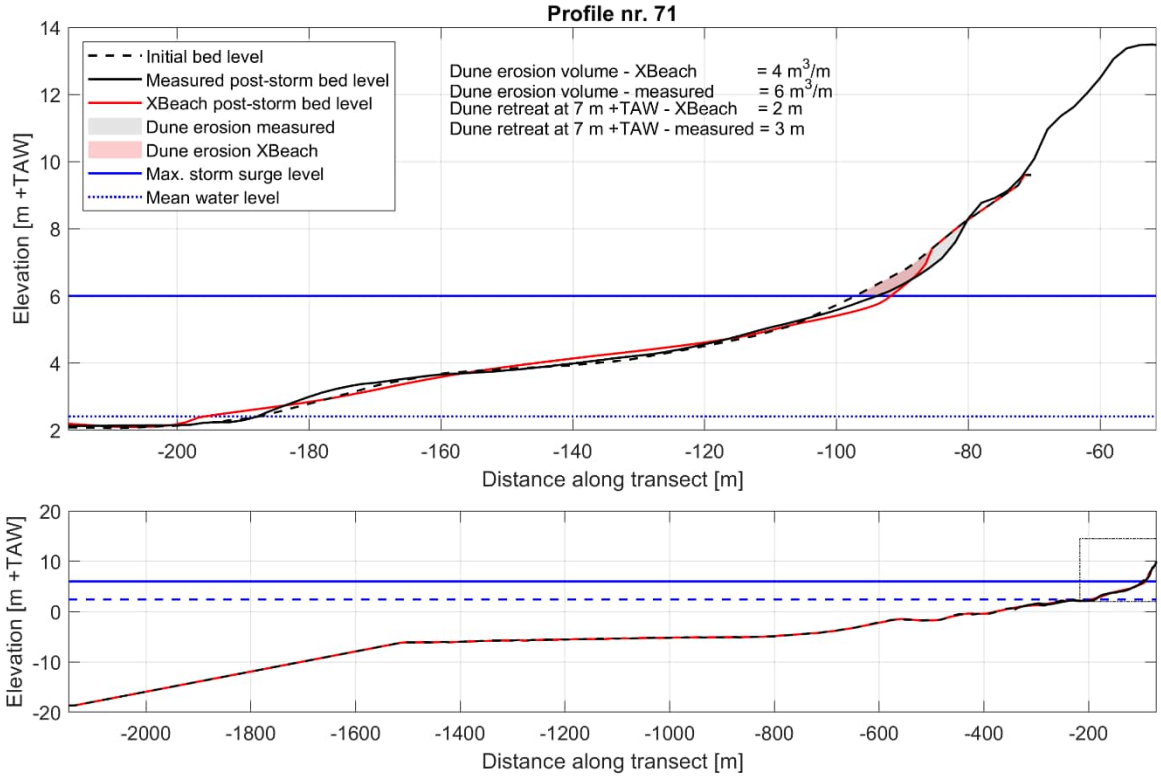

Figure C-45 Cross-section profile nr. 71 before and after the Sint Nicholas storm based on the measurements and XBeach, including dune erosion volumes and retreat distances. Bottom: entire XBeach profile, top: zoom of beach and dune profile.

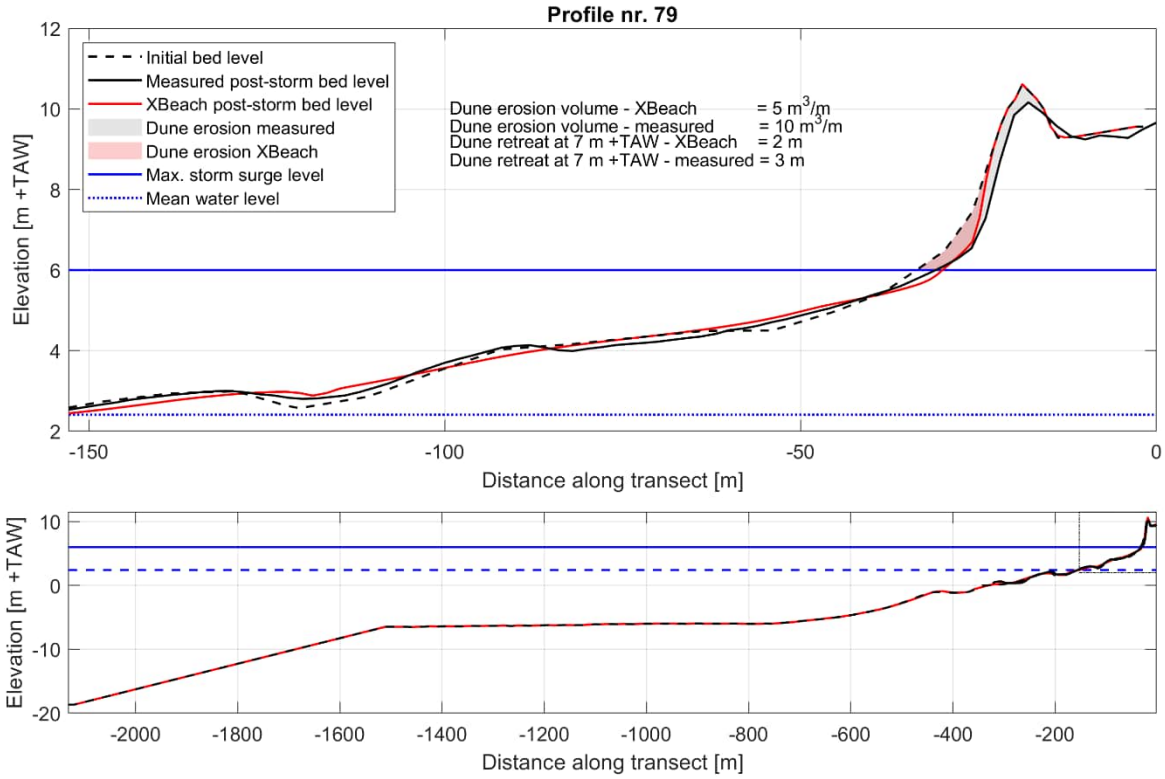

Figure C-46 Cross-section profile nr. 79 before and after the Sint Nicholas storm based on the measurements and XBeach, including dune erosion volumes and retreat distances. Bottom: entire XBeach profile, top: zoom of beach and dune profile.

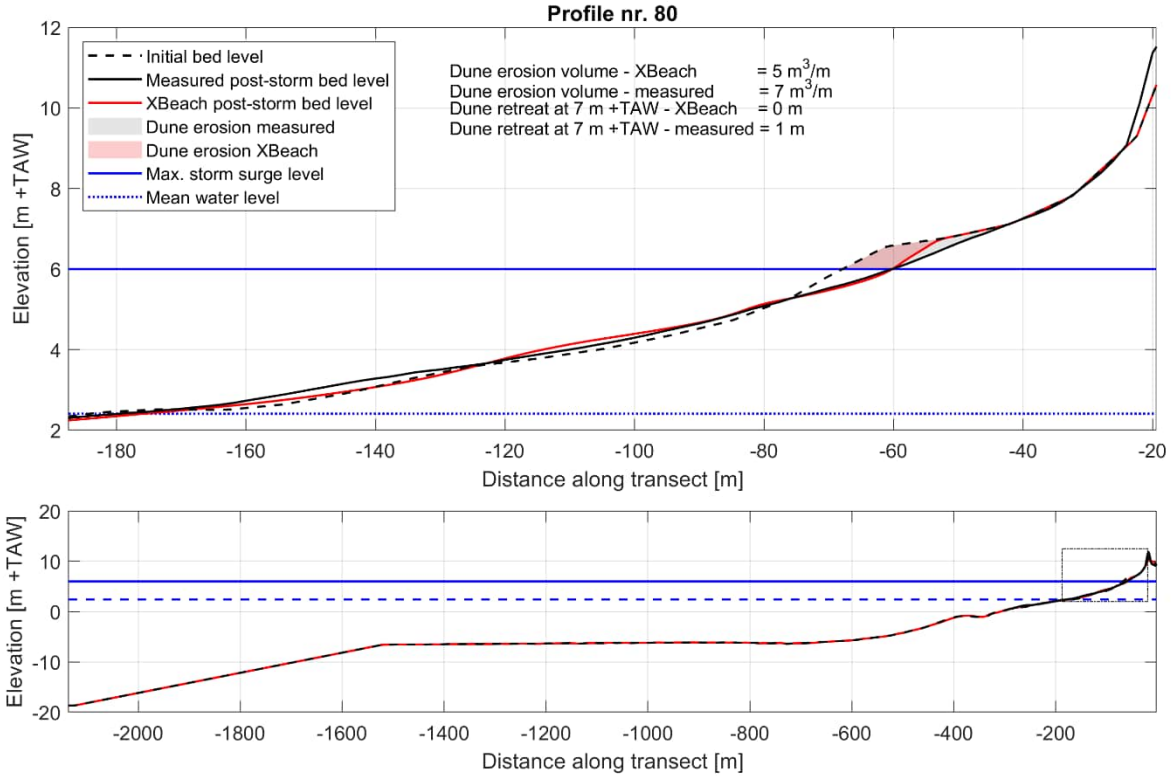

Figure C-47 Cross-section profile nr. 80 before and after the Sint Nicholas storm based on the measurements and XBeach, including dune erosion volumes and retreat distances. Bottom: entire XBeach profile, top: zoom of beach and dune profile.

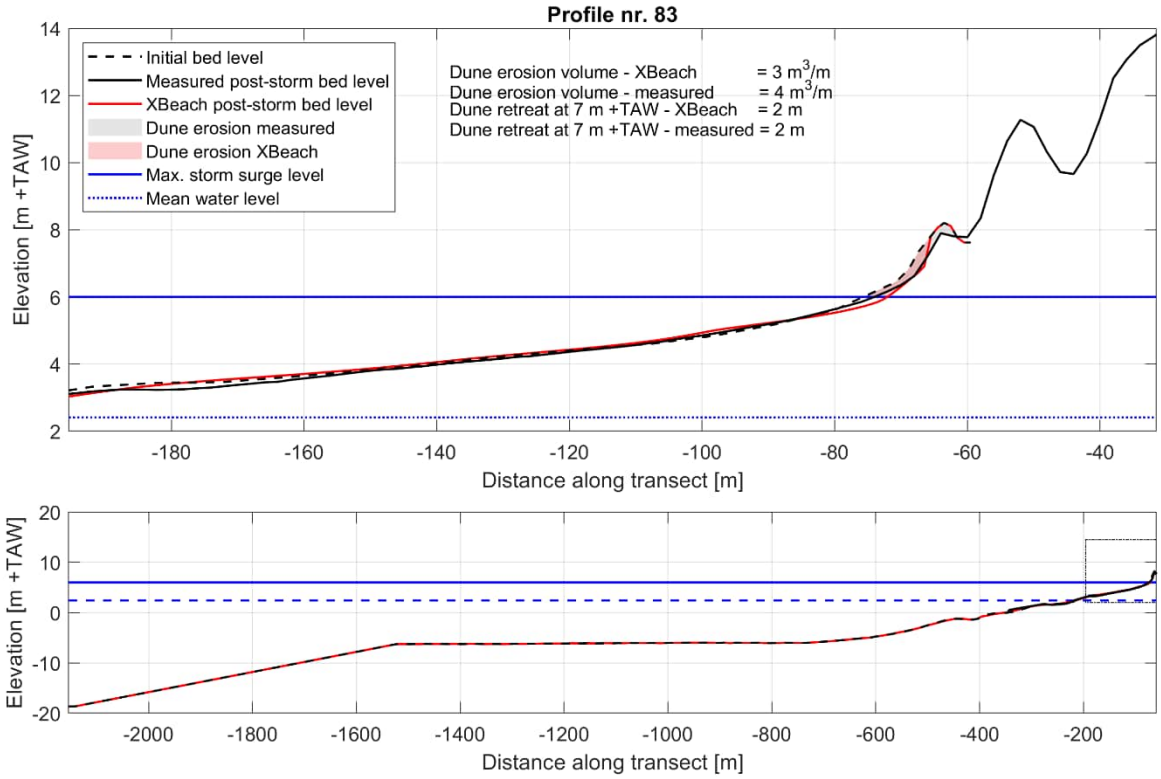

Figure C-48 Cross-section profile nr. 83 before and after the Sint Nicholas storm based on the measurements and XBeach, including dune erosion volumes and retreat distances. Bottom: entire XBeach profile, top: zoom of beach and dune profile.

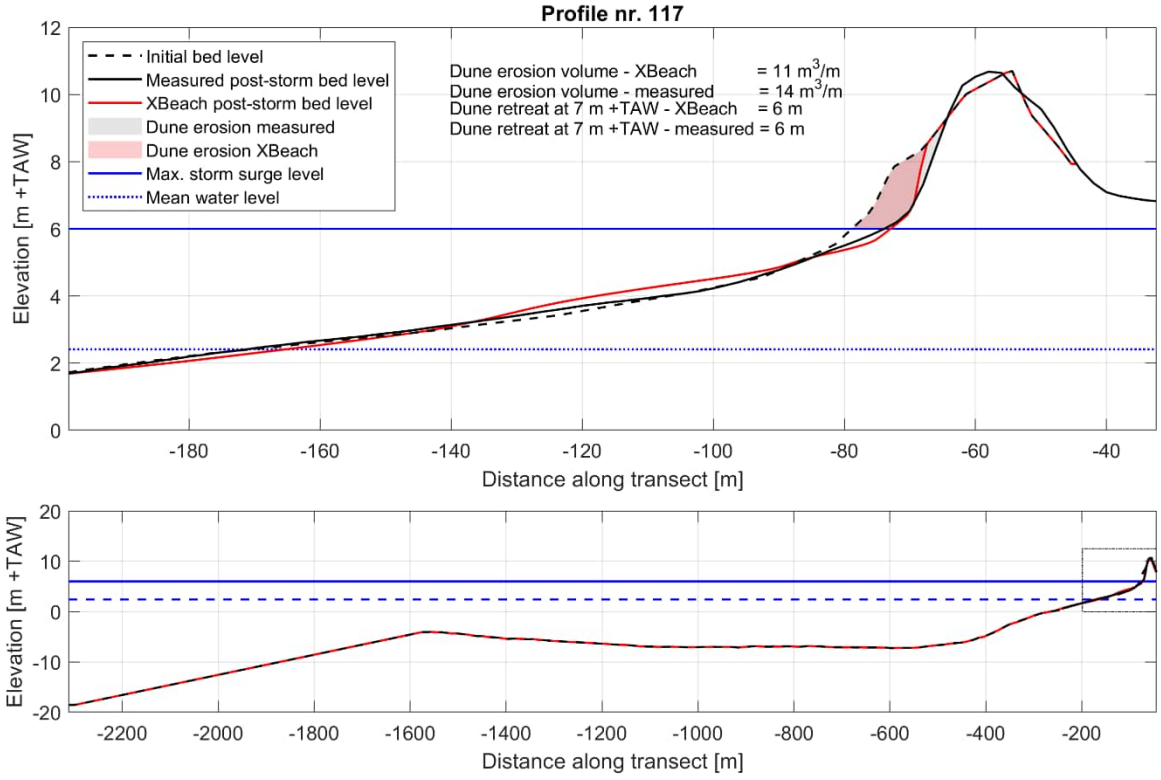

Figure C-49 Cross-section profile nr. 117 before and after the Sint Nicholas storm based on the measurements and XBeach, including dune erosion volumes and retreat distances. Bottom: entire XBeach profile, top: zoom of beach and dune profile.

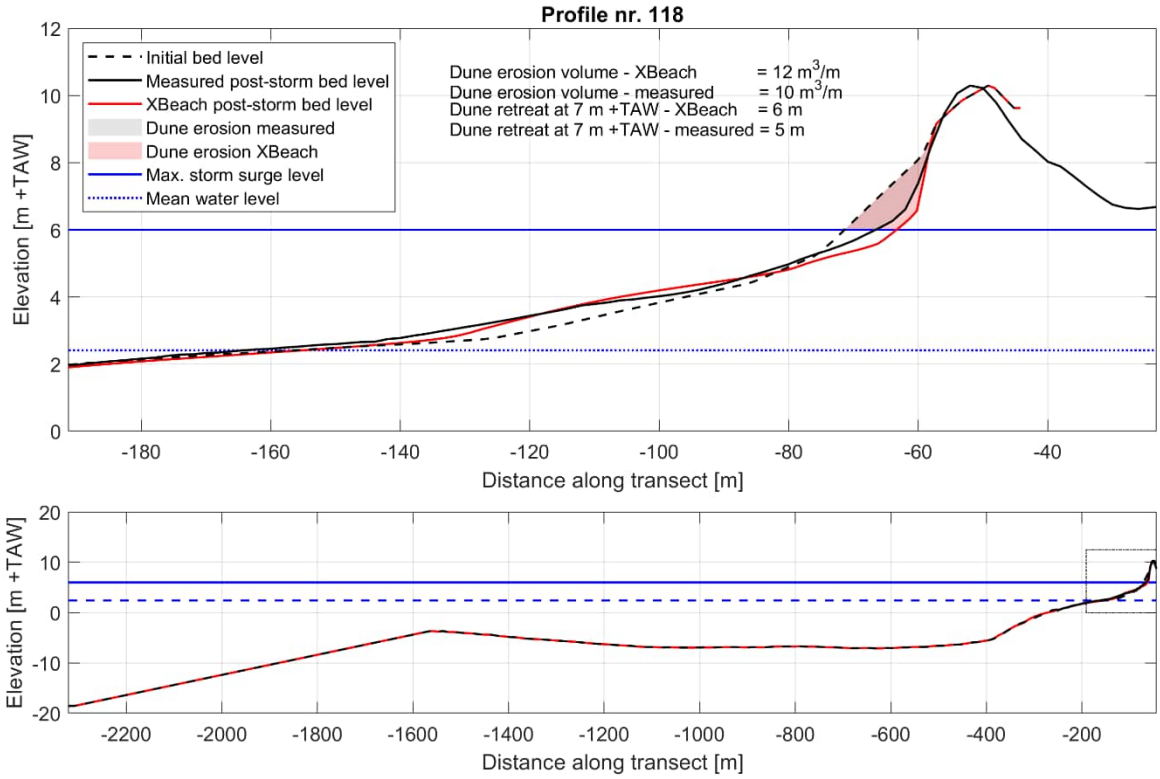

Figure C-50 Cross-section profile nr. 118 before and after the Sint Nicholas storm based on the measurements and XBeach, including dune erosion volumes and retreat distances. Bottom: entire XBeach profile, top: zoom of beach and dune profile.

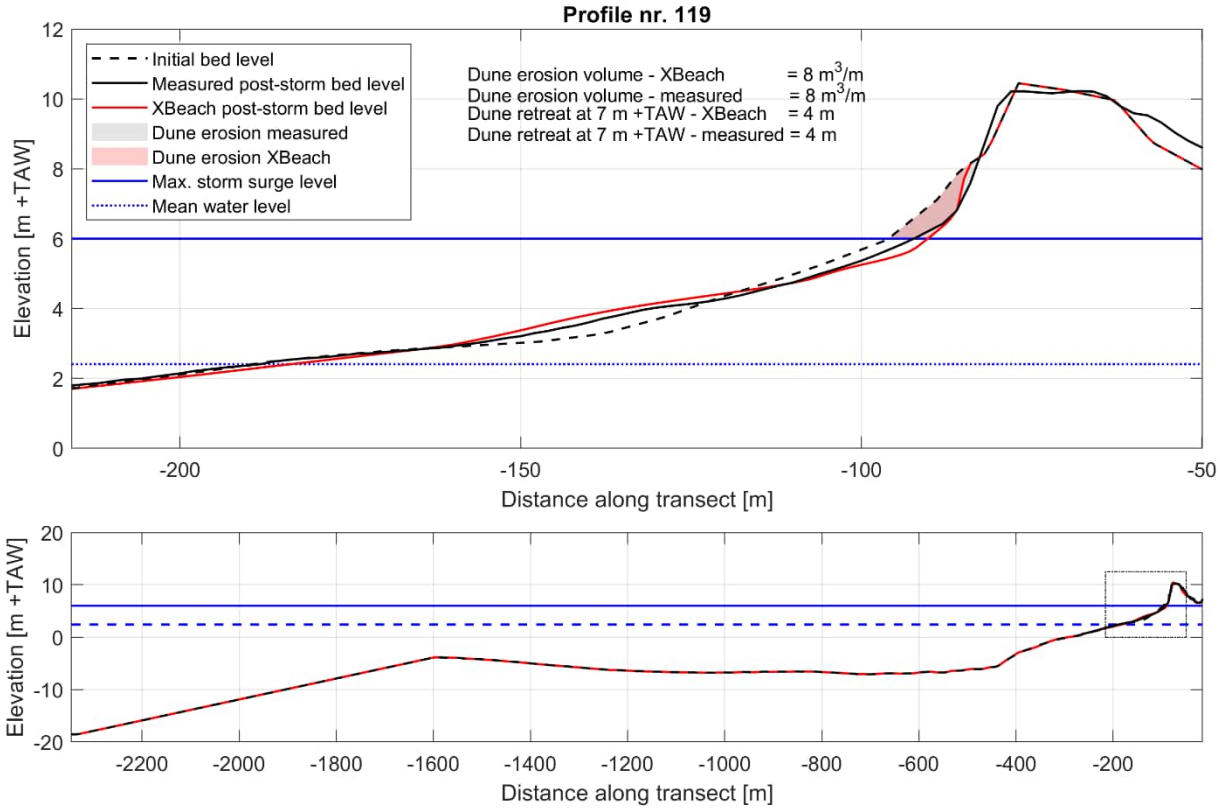

Figure C-51 Cross-section profile nr. 119 before and after the Sint Nicholas storm based on the measurements and XBeach, including dune erosion volumes and retreat distances. Bottom: entire XBeach profile, top: zoom of beach and dune profile.

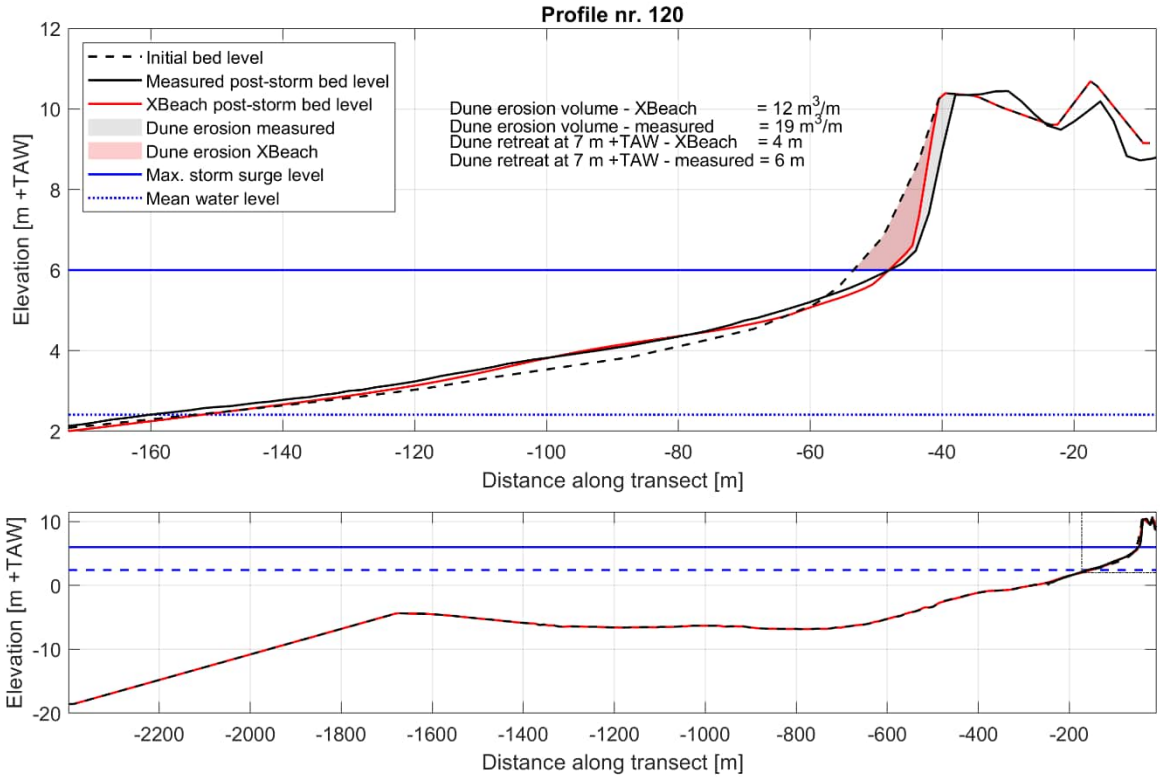

Figure C-52 Cross-section profile nr. 120 before and after the Sint Nicholas storm based on the measurements and XBeach, including dune erosion volumes and retreat distances. Bottom: entire XBeach profile, top: zoom of beach and dune profile.

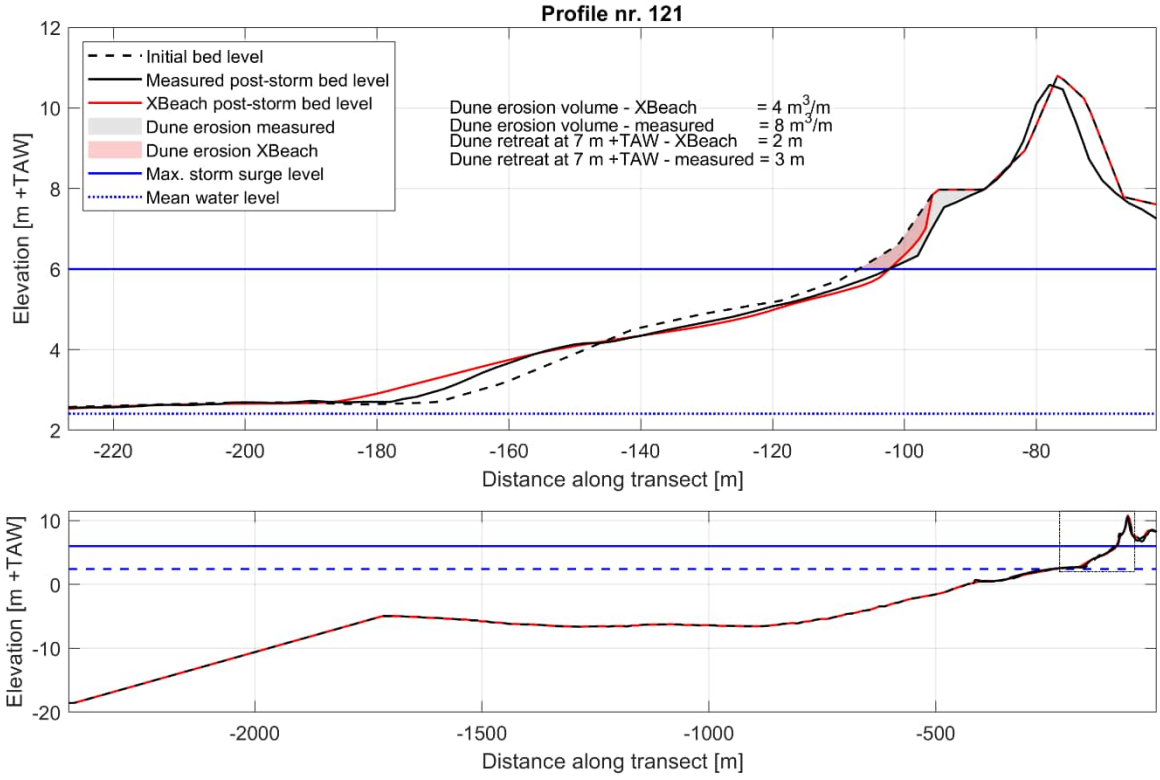

Figure C-53 Cross-section profile nr. 121 before and after the Sint Nicholas storm based on the measurements and XBeach, including dune erosion volumes and retreat distances. Bottom: entire XBeach profile, top: zoom of beach and dune profile.

APPENDIX 4 - FIELD CASE 4: FIRE ISLAND, NY (USA) [MORPHO]

Case description

Hurricane Sandy made landfall as a Category 1 post-tropical storm on the New Jersey Coast on October 29, 2012. The storm severely impacted Fire Island barrier island off the Long Island, New York, coast, where profile volume loss along the entire barrier island varied from 25% to 75% (Hapke et al., 2013). Off the coast of Bellport (NY, Figure C-54), an uninhabited section of the barrier island, Wilderness Area, breached during Sandy. Dune crests were lowered, and large wash-over fans developed in the area around the breach. Prior to the storm, the area was covered by dune grass, wetland and woody vegetation. The sea floor offshore of Fire Island shows shoreface-connected sand ridges in the western part and smaller, sorted bedforms along the eastern part of the island that includes the Wilderness area (Schwab et al., 2013). The cross-shore profiles are characterized by a steeply sloped beach (1:20 slope), a pronounced alongshore-uniform breaker bar, and a shoreface slope that gradually becomes less steep (1:85 slope) up to the wide continental shelf at a depth of ~25 m.

During Sandy, maximum water levels (surge and tide) ranged from NAVD88[10] + 1.8 m (Montauk) to + 3.5 m (The Battery) along the barrier island and offshore significant wave heights reached 10 m with periods up to 14 s. LiDAR surveys of the island were flown pre-Sandy in May 2012 (Fredericks et al., 2016) and post-Sandy on November 5, 2012. An average median grain size of 400 µm was reported based on samples at the beach at Wilderness (Bernier et al., 2018) with a grading of D_{90}/D_{50} = 1.5.

Comparison of pre- and post-storm observations of bed elevations (Figure C-54) shows that the initial dune crest heights ranged from 2 to 6 m above MSL, much lower than generally found in the Netherlands. The observed cumulative erosion-sedimentation patterns show that the dune front eroded several meters along the entire stretch of coast. A breach developed between kilometre marks (KM) 1 and 1.2 where originally a high dune was located. Large overwash deposits were observed east of the breach (KM 1.2–2). West of the breach the dune crests were initially higher, and impact remained in the collision regime with few washover deposits.

Van der Lugt et al. (2019) setup a 2DH morphodynamic XBeach model with hydrodynamic forcing extracted from a regional coupled D-Flow FM/SWAN model, and showed that the model predicted erosion volumes, dune-crest lowering and breach-formation well. The model bathymetry and boundary conditions of this 2DH model are used to set-up 1D transects and validate the BOI-XBeach settings for morphological storm impact.

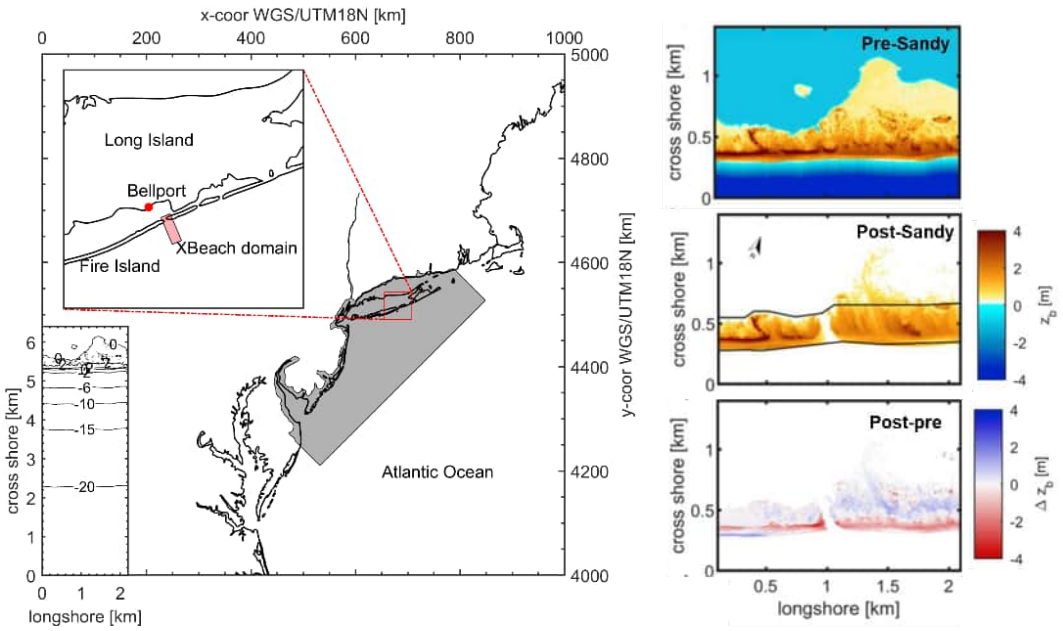

Figure C-54 Left: Model domain extent of the nested regional D-Flow FM/SWAN model (in grey) and the XBeach model (in red): Wilderness breach. Right: observed pre- (top) and post-(middle) bathymetry and sedimentation/erosion (bottom).

[10] *NAVD88 = North American Vertical Datum of 1988. MSL corresponds to -0.073 m NAVD88 at Sandy Hook NJ (NOAA).*

Model setup

Grid and bathymetry

The bathymetry for the Fire Island case was constructed from pre-storm LiDAR Surveys (Fredericks et al., 2016; Wright et al., 2014) reaching up to 8 m water depth with a resolution of 1 m, supplemented with NGDC Coastal Relief Map data (NGDC, 1999) for deeper waters. As the subaqueous back bay was only partially covered by LiDAR surveys, the entire back bay bed level was schematized and extrapolated from the LiDAR surveys to a constant level of NAVD88 + 1 m (Van der Lugt et al., 2019). Six 1D XBeach models (Figure C-57) have been set-up to validate the XBeach model for the various morphodynamic responses observed at Wilderness:

- Two profiles (transects 365 and 405) include an initial dune height of ~6 m and resulted in erosion of the dune face (i.e. collision regime);
- Three (transects 005, 105 and 205) profiles with an initial dune height of ~3 - 4 m were completely eroded due to Hurricane Sandy (i.e. inundation regime);
- One profile (transect 305) for which overwash occurred, but was not entirely eroded.

Each of the profiles has been extended seaward according to BOI guidelines with a 1:50 slope to a depth of 30 m. Cross-shore grids were set-up following standard BOI procedure resulting in approximately 1500 ± 100 grid cells per profile and spatial resolution that varies from 9 m (offshore) to 1 m at the coast. Initial bed levels across the 1D transect as well as the cross-shore distribution of grid size are shown for two profiles; observed collision regime (Figure C-55) and inundation regime (Figure C-56). An overview of initial bed levels for all 6 profiles combined, is presented in Figure C-58. The shoreface of the profiles is similar for all profiles. A D_{50} of 400 µm is applied.

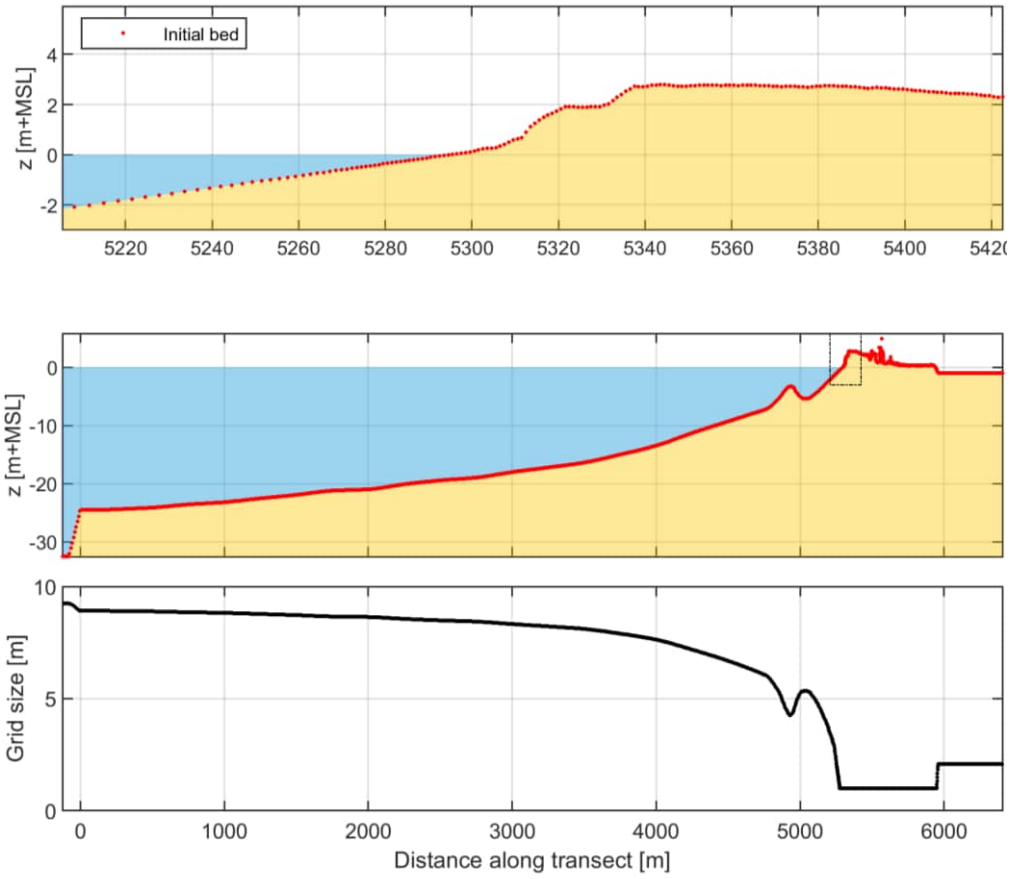

Figure C-55 Overview of the pre-storm bed level along the 1D XBeach transect representing breaching of the dune profile (middle panel), and cross-shore distribution of the grid size (lower plot). Besides that, the upper plot presents a zoom on the last part of the profile where most erosion is to be expected.

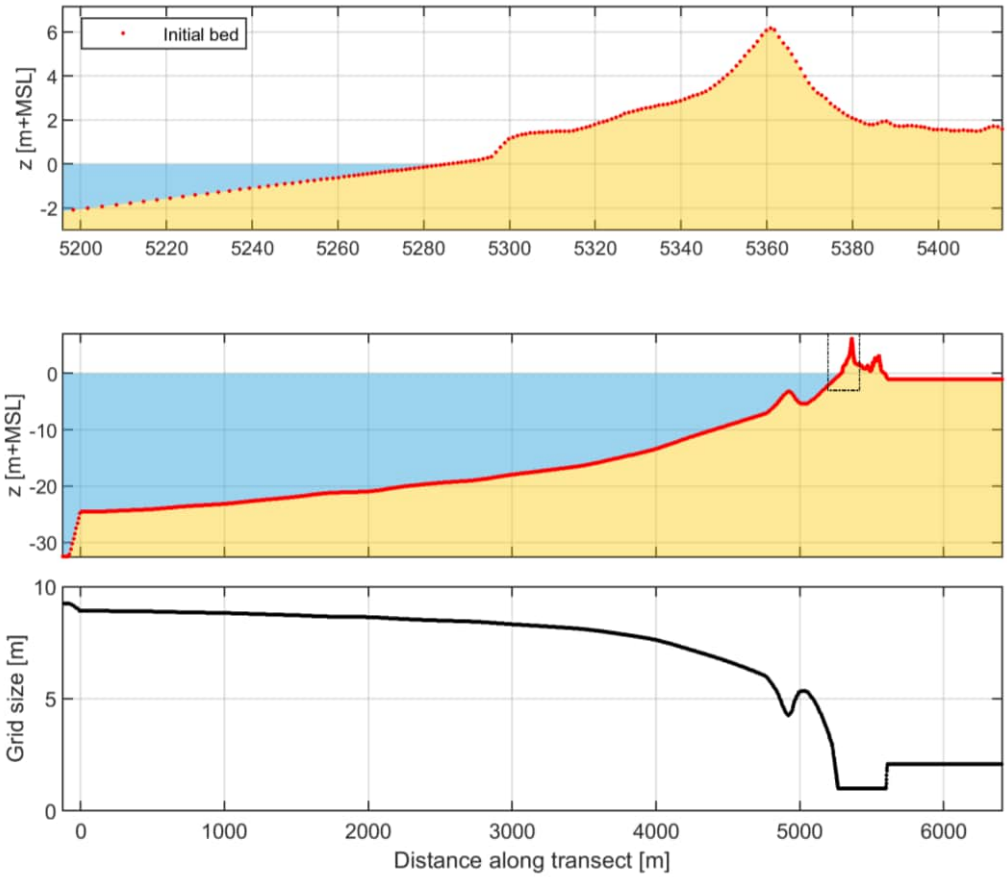

Figure C-56 Overview of the pre-storm bed level along the 1D XBeach transect representing a profile in collision regime (middle panel), and cross-shore distribution of the grid size (lower plot). Besides that, the upper plot presents a zoom on the last part of the profile where most erosion is to be expected.

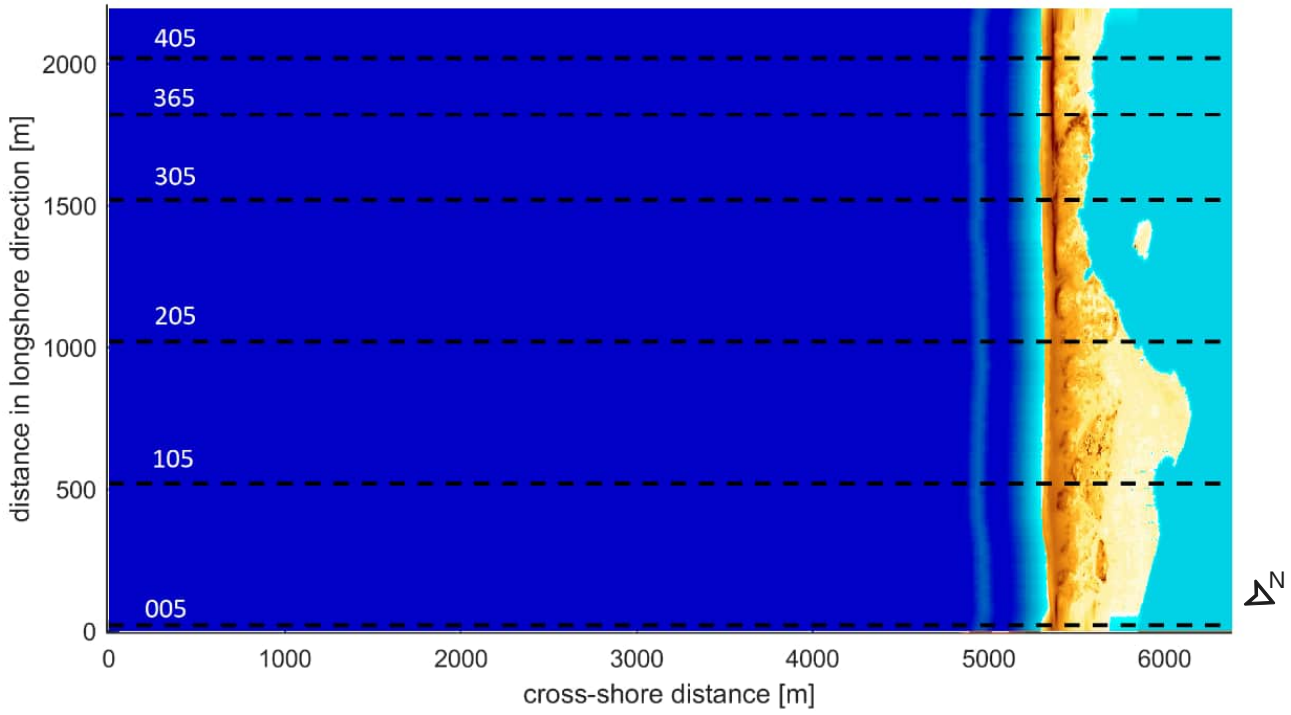

Figure C-57 Overview of the location of the six transects in the Wilderness domain.

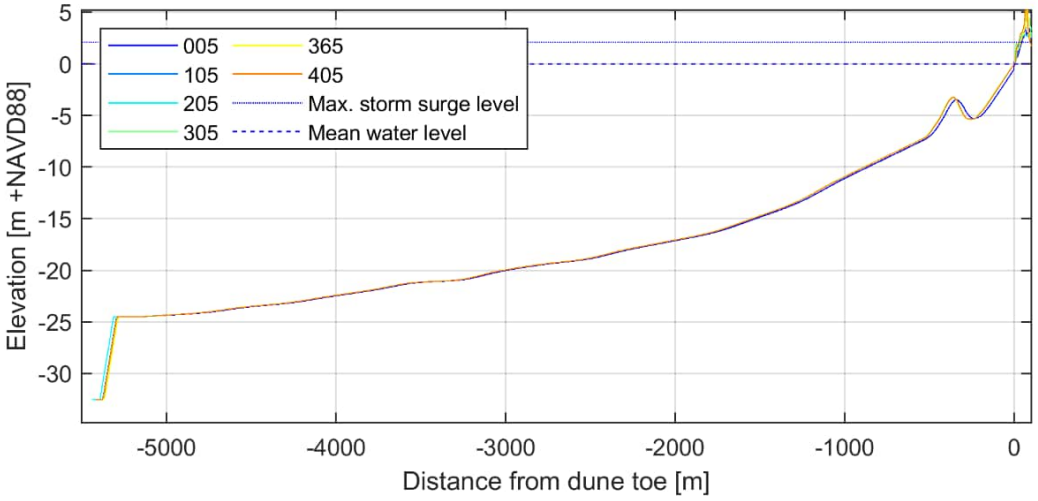

Figure C-58 Overview of initial bed levels for all six 1D transects combined into one figure.

Hydraulic boundary conditions

Hydrodynamic boundary conditions (combined tide-surge water levels, and 2D wave spectra) for the morphodynamic models were generated by a series of coupled D-Flow FM/SWAN models (Van der Lugt et al., 2019). The offshore significant wave height (H_{m0}) varied between 3 and 10 m, with a peak period (T_p) between 9 and 16 s (Figure C-59). During Sandy, the offshore waves were coming from the east during the lead up to the storm and turned to the southeast at the peak of the storm. The maximum surge level on the offshore boundary of the XBeach grid was 2.2 m. Furthermore, a water level boundary condition is imposed in the back-barrier bay (landside of the profiles) to be able to capture the observed ebb-surge after the peak of the storm. The model simulation time was chosen to range one day before the peak of the storm to half a day after the peak of the storm to allow for the back flow between bay and ocean to occur.

The 2D wave spectra that were used to force the model contain time-varying mean wave directions which differ from the shore-normal direction (157 °N). This is in contrast with the standard BOI procedure. In this particular case, to make sure that all wave energy propagates towards the coast, a single directional bin has been used (defined following nautical convention) that captures all wave energy (*thetamin = 67, thetamax = 247, dtheta = 180)*, and all wave energy was set to the shore-normal direction (*snells = 0)*.

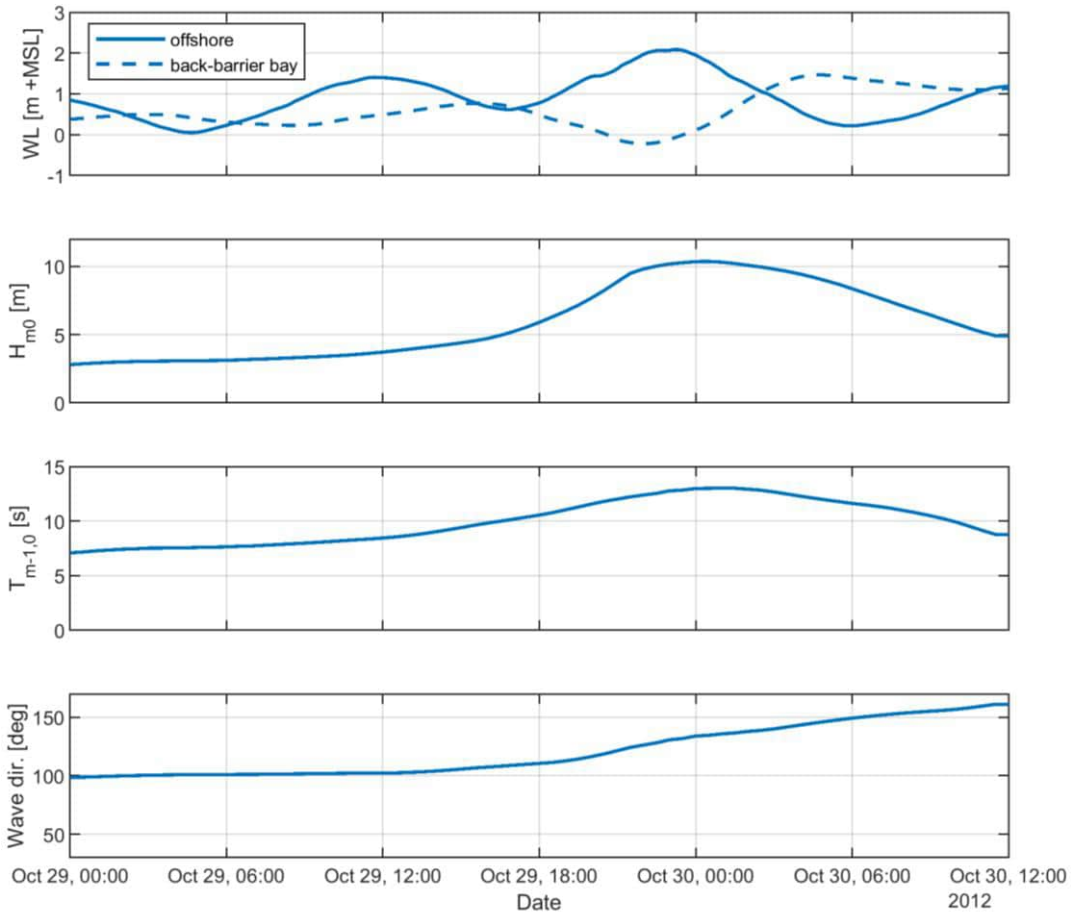

Figure C-59 Time series of the offshore hydraulic boundary. The water level time series and wave heights, periods and mean direction are extracted from a series of coupled D-Flow FM/SWAN models. Mean wave directions are defined with respect to the North. Total duration of the simulation is 36 hours.

Results

The XBeach model results are validated using the post-Sandy LiDAR data obtained on November 5, 2012.

Inundation regime profiles
For transects 005, 105 and 205 measurements show that the dune is completely eroded by the storm (Figure C-60, Figure C-63 and Figure C-64), which is also predicted by the model. The modelled post-storm shape of the profile differs from the observations, resulting in some differences in erosion volumes (Table C-5) as far as this difference is above maximum storm surge level, but overall breaching of the dunes is achieved in the model. Retreat distances could not be determined for these profiles since the dunes are completely eroded.

Overwash profile
In transect 305, a combination of erosion of the dune face and lowering of the dune crest is observed in the measurements (Figure C-61). Although the lowering of the dune crest is well captured by the model, the post-storm profile shape differs from the observations. This is mainly expressed by the modelled dune retreat which is approximately half of the measured dune retreat.

Collision regime profiles
For the transects 365 and 405 with higher initial dunes than the other profiles, the dunes were not completely eroded, but erosion of the dune face was observed (Figure C-65 and Figure C-62). For profile 405, XBeach underestimates the erosion volume almost by a factor two. Nonetheless, the post-storm profile shape shows good resemblance with the observations. For profile 365, the modelled erosion volume is spot on and the deviation between modelled and measured dune retreat is less than 1 m (less than model resolution).

The model results show that the sand eroded from the dunes is deposited between NAVD88 -1 m and + 1 m for the cases characterised by the collision regime. Since no post-storm under water measurements were obtained, these finding cannot be validated.

Table C-5 Modelled and measured erosion volumes and retreat distances in absolute values, difference in absolute values and relative difference for all Fire Island profiles. NaN means that no dune retreat could be determined, i.e. the dune has breached. Negative differences mean underestimation of the measured values in the XBeach simulation. Colours per column indicate the degree of similarity between the simulations and observations based on all morphological cases (greener = better fit).

Profile nr.	Erosion volume				Retreat distance [m] at NAVD88 + 3 m			
	XBeach [m^3/m]	Measured [m^3/m]	Difference [m^3/m]	Difference [%]	XBeach [m]	Measured [m]	Difference [m]	Difference [%]
5	51	51	0	0%	NaN	NaN	NaN	NaN
105	54	45	9	21%	NaN	NaN	NaN	NaN
205	75	75	0	0%	NaN	NaN	NaN	NaN
305	54	68	-14	-20%	13.6	28.6	-15.0	-52%
365	25	25	0	2%	5.0	5.9	-0.8	-14%
405	32	56	-24	-43%	13.5	23.1	-9.6	-41%
Average	**49**	**53**	**-5**	**-7%**	**10.7**	**19.2**	**-8.5**	**-36%**

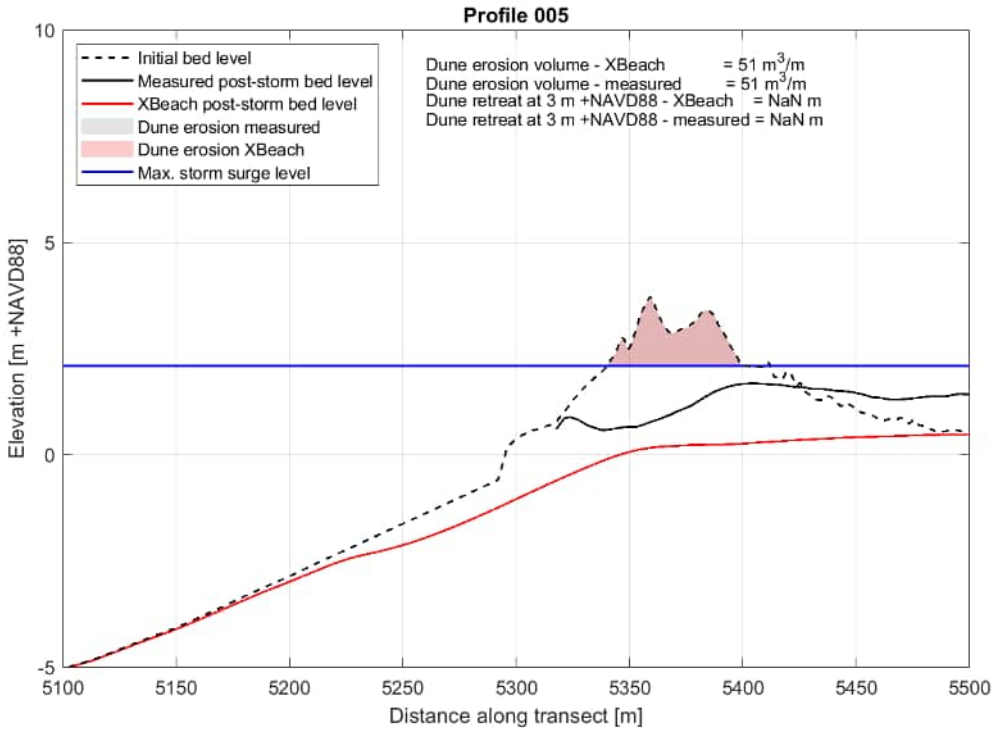

Figure C-60 XBeach results for cross-shore transect 005 at Fire Island: a profile in the inundation regime. Initial bed levels are depicted by the black dotted line, observed post-storm bed levels by the black solid line and XBeach model results are presented in red. The modelled dune erosion is shown by the red shaded area.

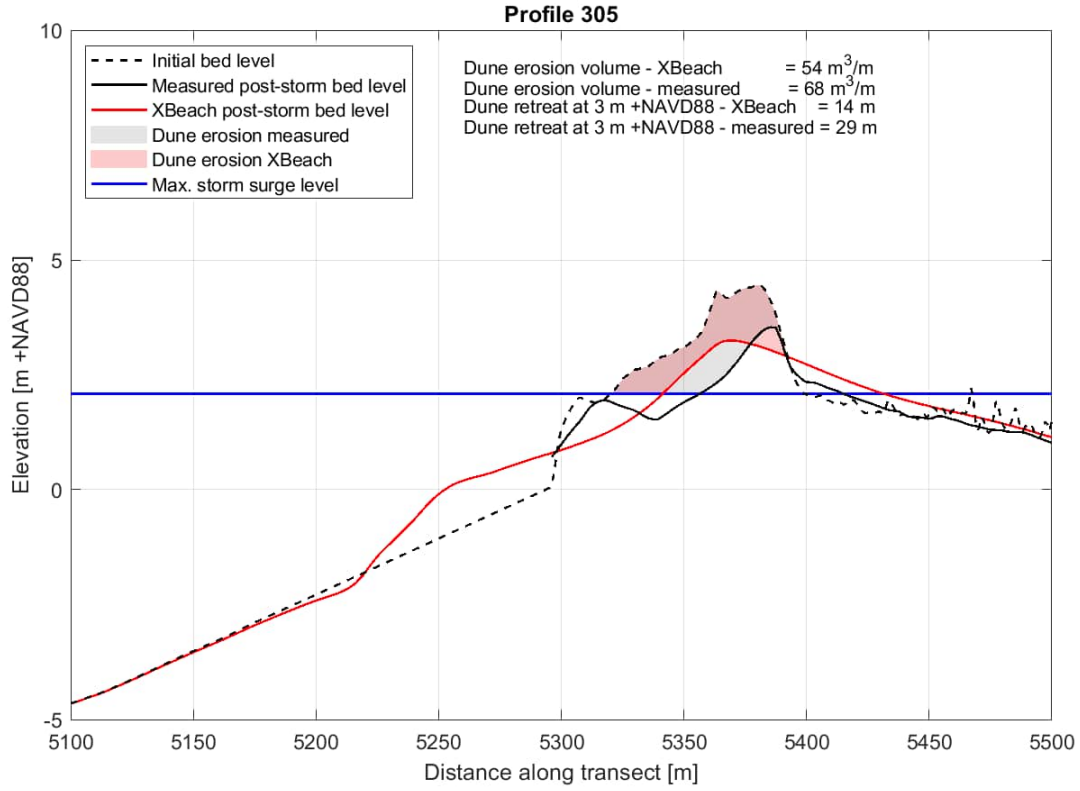

Figure C-61 XBeach results for cross-shore transect 305 at Fire Island: a profile with overwash. Initial bed levels are depicted by the black dotted line, observed post-storm bed levels by the black solid line and XBeach model results are presented in red. The modelled dune erosion is shown by the red shaded area.

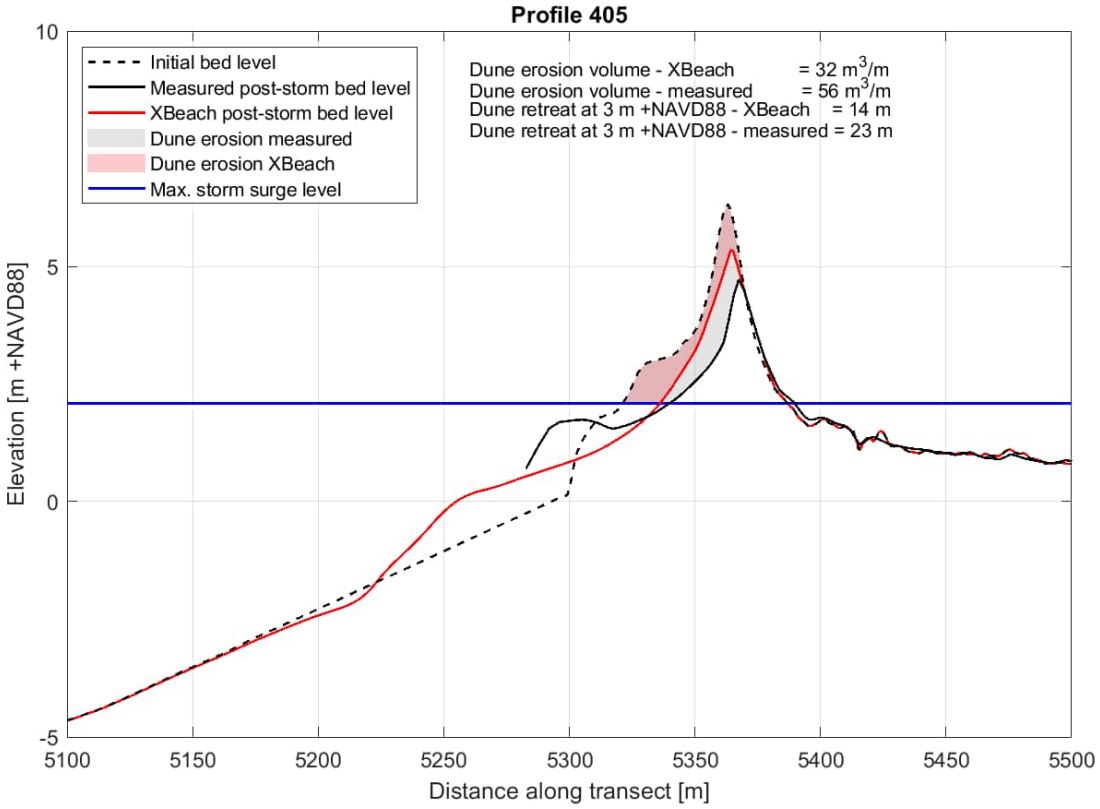

Figure C-62 XBeach results for cross-shore transect 405 at Fire Island: a profile in the collision regime. Initial bed levels are depicted by the black dotted line, observed post-storm bed levels by the black solid line and XBeach model results are presented in red. The modelled dune erosion is shown by the red shaded area.

Discussion

For the Fire Island case, XBeach predicts the occurrence of breaching of dunes with low initial crest levels (profile 005, 205 and 205) well and as a consequence, the dune erosion volume above maximum storm surge level is also accurately predicted.

For profile 305, overwash is observed and also modelled, though the modelled post-storm profile shape deviates from the measured profile. In general, slight differences in the boundary conditions (e.g. due to different randomizations of the timeseries) can significantly affect the modelled erosion volumes for profiles that are subject to overwash but without the occurrence of a breach (Deltares (2021b), not shown here). Taking that into account, the model prediction of profile 305 is good.

The profiles in the collision regime at Fire Island (profile 365 and 405) have a very similar pre-storm profile, and also their offshore forcing conditions in the XBeach model are almost equal. As a consequence, the model results for these profiles are also similar. However, the measured erosion of profile 405 is almost twice the measured erosion of profile 365. The reason for this difference is not clear, but could be related to local geotechnical variations in dune strength (e.g. differences in sediment composition or rooting), uncertainties in the initial profile (the profiles might have changed between the date of the pre-storm survey and the landfall of the hurricane) or alongshore processes that are not captured within the 1D XBeach models.

Conclusion

Hurricane Sandy impacted Fire Island, NY on October 29, 2012, and resulted in erosion and breaching of the dunes on the barrier islands. The six 1D profiles of this case are characterized by a relatively steep beach/shoreface and coarse grain size (D_{50} of 0.4mm), compared to typical Dutch coastal profiles. XBeach showed that it is able to reproduce the (occurrence of) breaching and overwash of the low dunes well. In addition, XBeach showed that it is also able to capture the erosion of the coarse-grained profiles with higher initial dunes, though absolute erosion volumes are sometimes underestimated.

Additional figures

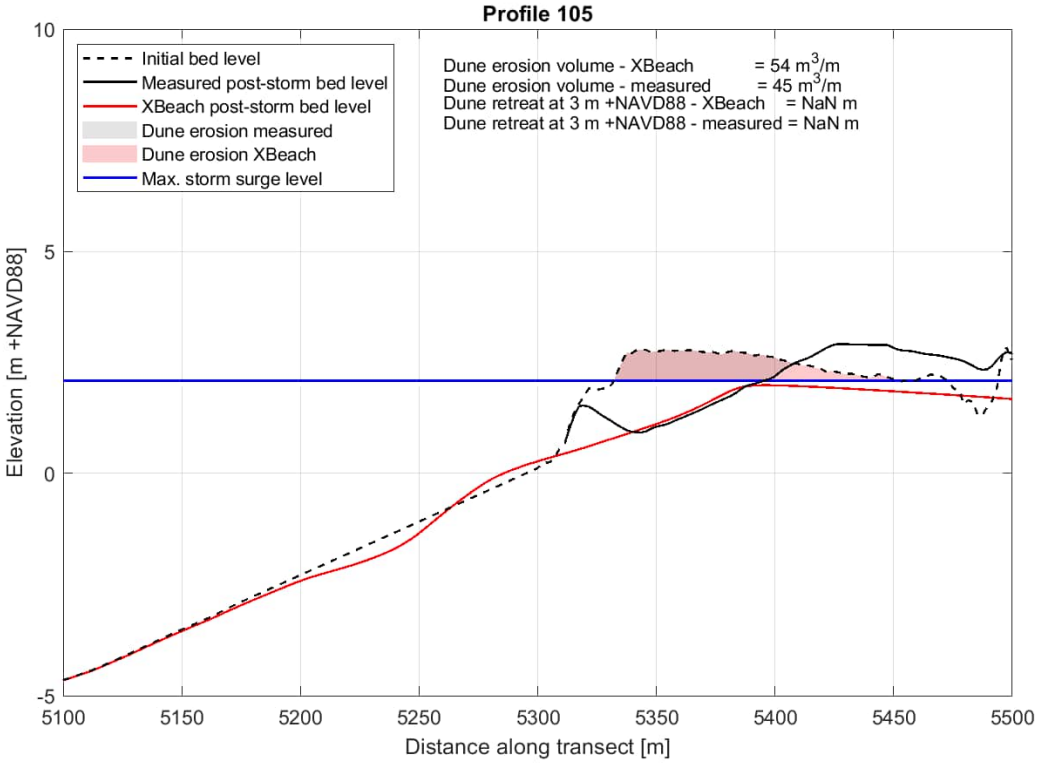

Figure C-63 XBeach results for cross-shore transect 105 at Fire Island. Initial bed levels are depicted by the black dotted line, observed post-storm bed levels by the black solid line and XBeach model results are presented in red. The modelled dune erosion is shown by the red shaded area.

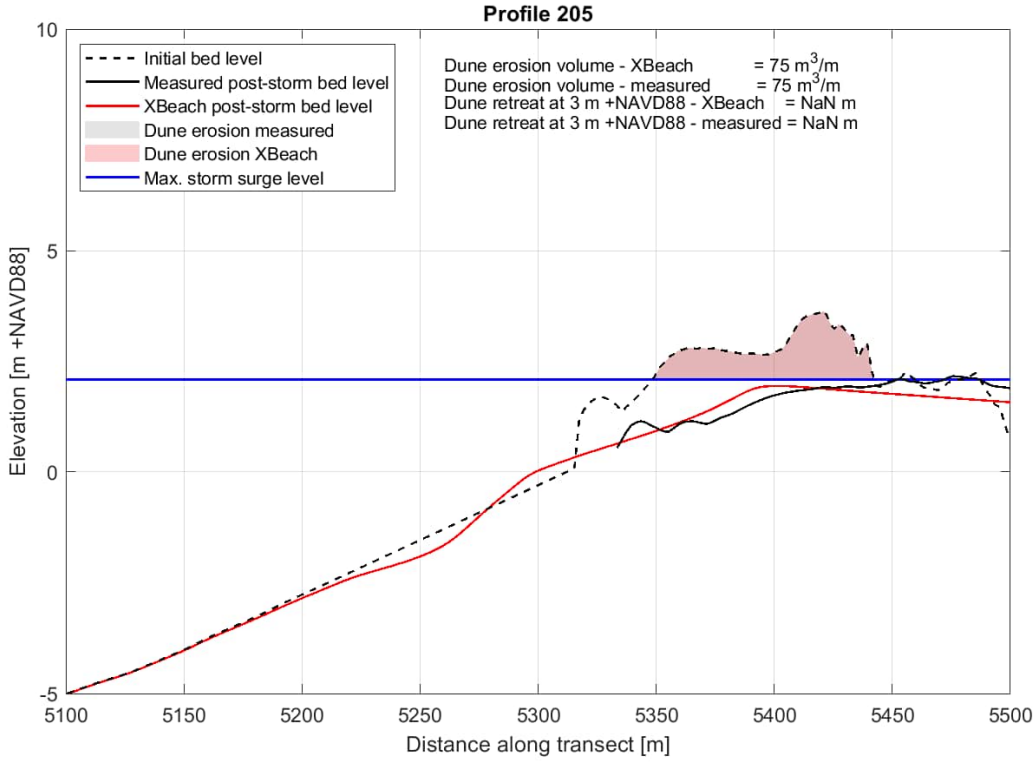

Figure C-64 XBeach results for cross-shore transect 205 at Fire Island. Initial bed levels are depicted by the black dotted line, observed post-storm bed levels by the black solid line and XBeach model results are presented in red. The modelled dune erosion is shown by the red shaded area.

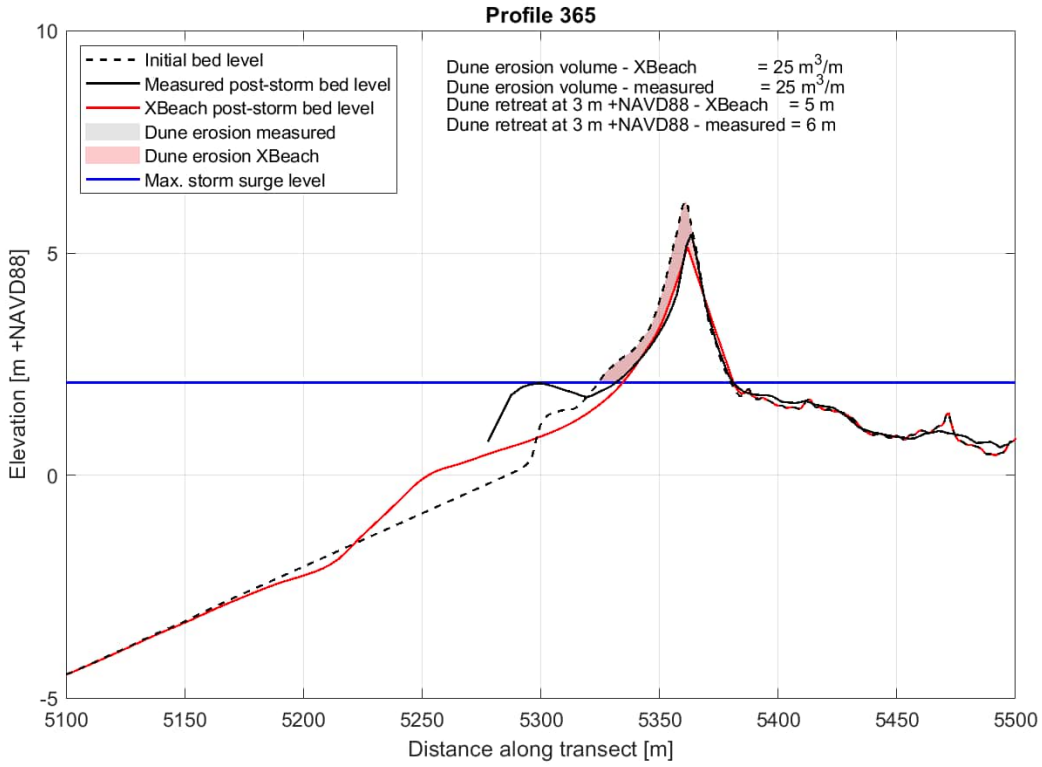

Figure C-65 XBeach results for cross-shore transect 365 at Fire Island. Initial bed levels are depicted by the black dotted line, observed post-storm bed levels by the black solid line and XBeach model results are presented in red. The modelled dune erosion is shown by the red shaded area.

APPENDIX 5 - FIELD CASE 5: VEDERSOE (DENMARK) [MORPHO]

Case description

Vedersoe is located on the Danish North Sea coast. Coastal measurements along multiple transects were obtained before and after a severe storm in January 2005 and reported by the Danish Coastal Authority. The observed dune retreats and erosion volumes show a high variability in alongshore direction. A study by the Danish Coastal Authority (DCA), as a part of the larger EU-InterReg project Building with Nature, considered two 1D transects close to each other (< 500 m) for which the observed dune retreat ranges from 4 to 14 meter, see Figure C-66 (Kystdirektoratet, 2021). Though the profiles show large similarity, the different erosive behaviour is likely due to the presence of a berm (above storm surge level) which reduces the erosion for one of the profiles. The two transects at Vedersoe are used to validate the BOI-XBeach model and settings for morphological changes due to storm impact. Compared to the Dutch coast, the Danish profiles have a similar slope in the lower shoreface, but a steeper surf zone.

According to Saye and Pye (2006) the Danish Southwest coast has a strong alongshore variation in grain size, with grain sizes *up to* 0.4 mm. Clemmensen et al. (2006) show that dunes in the southwest of Denmark are mainly formed by aeolian transport of fine-grained sand with a D_{50} of around 0.2 mm. They also note that the 'inland' dunes are more coarse-grained than the coastal dunes. Hence, the D_{50} of the dunes near Vedersoe are in the range 200-400 µm.

The wave climate during the storm in 2005 is measured by wave buoys located outside Nymindegab (~50 km southward of Vedersoe at 17.5 m depth). At the deep-water wave buoy, the peak wave period T_p increased from 9.0 to 13.3 s, and H_s rapidly increased from 2.9 to 6.6 m. Water levels during the storm are obtained at a tidal gauge on one of the headlands of Ferring (~30 km to the North from Vedersoe) and reached up to MSL + 3 m during the 2005 storm.

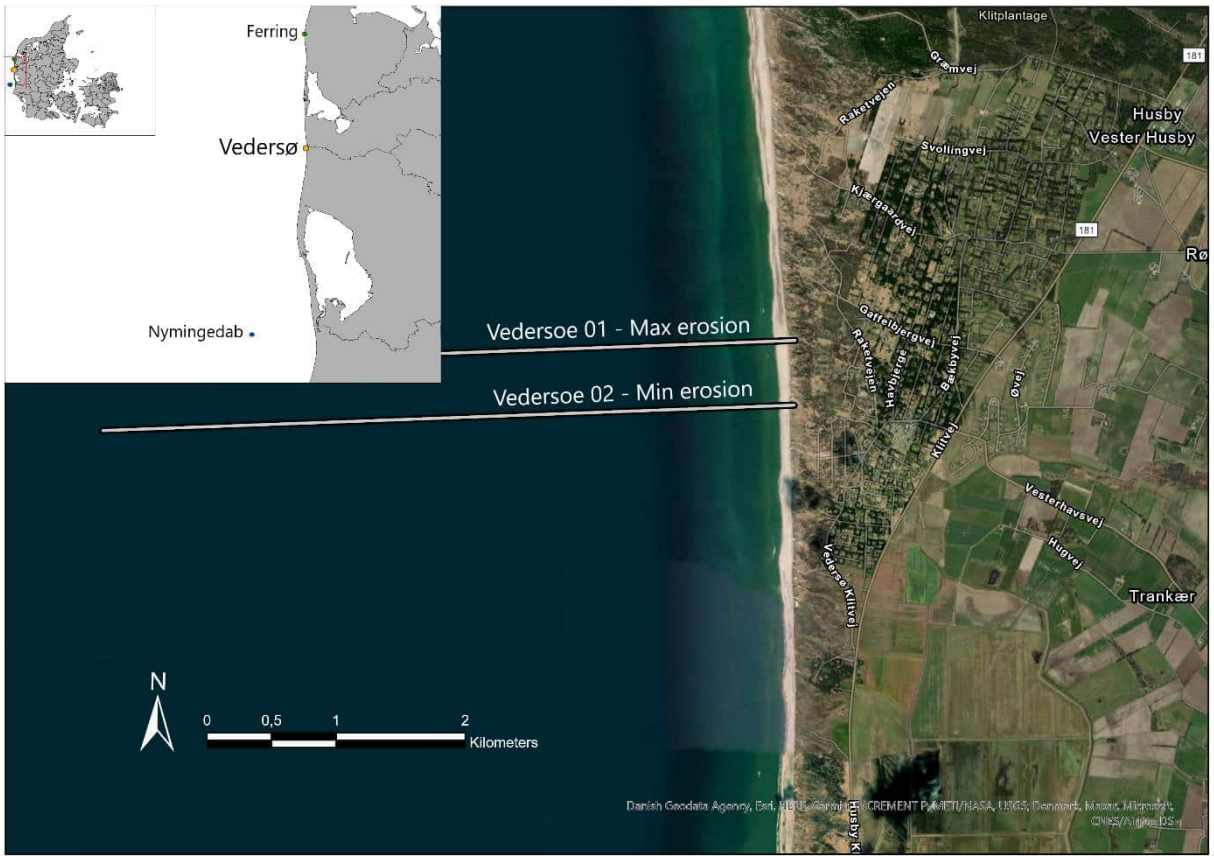

Figure C-66 Location of the study area near Vedersoe (Denmark). The two different transects considered in this study are located close to each other, but different morphological behaviour is observed. Source: Kystdirektoratet (2021).

Model setup

The two profiles obtained from the Danish Coastal Authority are used to set-up two 1D XBeach models (Vedersoe 01 and Vedersoe 02), combined with the default BOI model set-up and settings.

Grid and bathymetry

Pre-storm dune measurements were only collected up to MSL + 5 m, whereas the post-storm measured dune crests are much higher. For the initial XBeach model bathymetry, the missing part of the dune profile in the pre-storm profiles is approximated by a seaward shift of the post-storm observed dune front (see grey dashed lines in Figure C-67 and Figure C-68). While considering the offshore conditions presented in Figure C-59 as the governing conditions (H_s = 6.6 m, $T_{m-1,0}$ = 13.3 s) for both profiles, the profiles have been extended seaward according to BOI guidelines with 1:50 slopes to depths of over 20 m. Cross-shore grids were set-up following standard BOI procedure, resulting in 999 and 1032 grid cells for the transects Vedersoe 01 and Vedersoe 02 respectively. Spatial resolutions vary from 10 m (offshore) to 1 m at the coast. The (estimated) pre- and post-storm bed levels across the 1D transects as well as the cross-shore distribution of grid sizes are presented in Figure C-67 and Figure C-68. The main difference between the two profiles is the presence of a berm above storm surge level in transect Vedersoe 02.

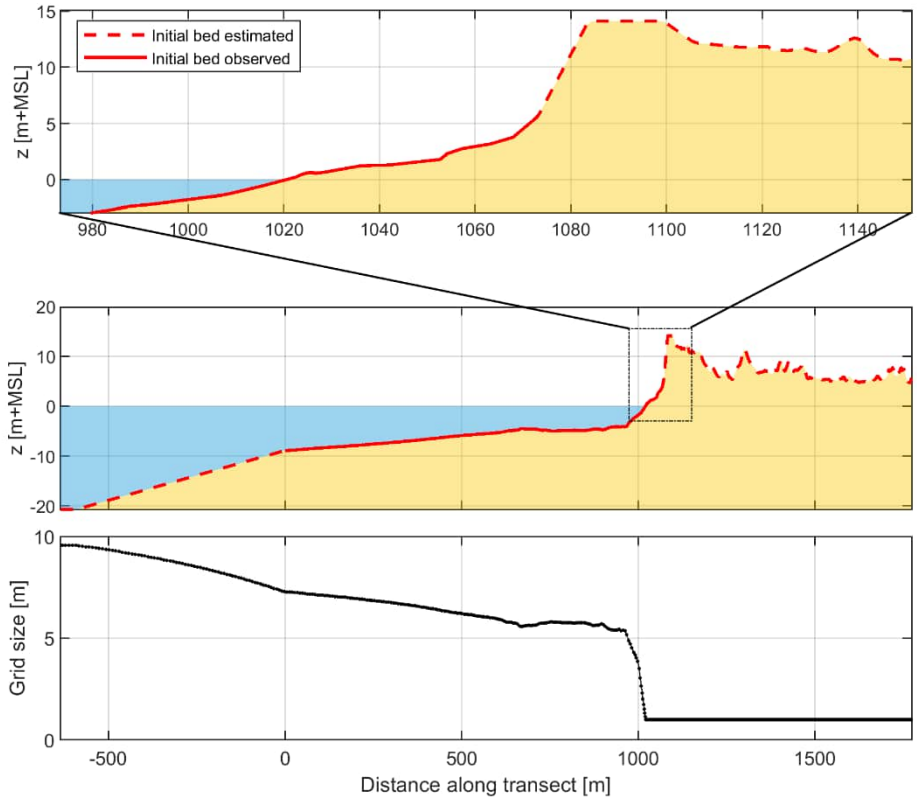

Figure C-67 Overview of the (estimated) pre- and post-storm bed level along the 1D XBeach transect describing the Vedersoe 01 profile (middle panel), and cross-shore distribution of the grid size (lower plot). Besides that, the upper plot presents a zoom on the last part of the profile where most erosion is to be expected.

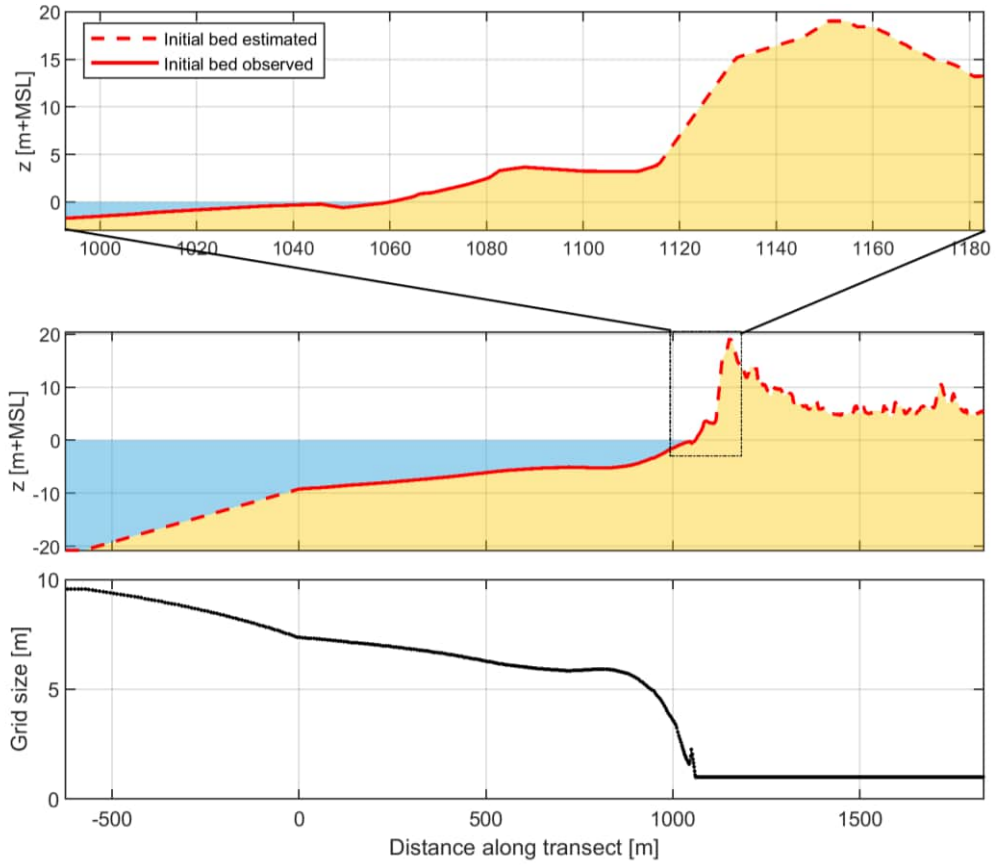

Figure C-68 Overview of the (estimated) pre- and post-storm bed level along the 1D XBeach transect describing the Vedersoe 02 profile (middle panel), and cross-shore distribution of the grid size (lower plot). Besides that, the upper plot presents a zoom on the last part of the profile where most erosion is to be expected.

Hydraulic boundary conditions

The model was forced with water level time series that were obtained at Ferring. Furthermore, wave conditions are imposed through JONSWAP wave spectra that are based on the observations at the wave buoy at Nymindegab. Although observed mean wave directions during the 2005 storm vary over the duration of the storm, the mean wave direction of the JONSWAP wave spectra is defined perpendicular to the coast. In addition, a directional spreading of approximately 30° (s = 6) is used (in analogy with BOI procedure). An overview of the hydrodynamic forcing conditions that were used to force the XBeach models (equal forcing is used for both transects) is provided in Figure C-59. The models are run for a total simulation period of 95 h, which was in analogy by the forcing conditions used in the study of Kystdirektoratet (2021).

Grain size

The representative grain size of the beach and dunes at Vedersoe is uncertain. Based on the Saye and Pye (2006) and Clemmensen et al. (2006), the D_{50} is in the range of 200 μm to 400 μm. 400 μm is quite coarse and most likely corresponds to more inland dunes, so the grain size of the first dune row probably is between 200 and about 300 μm. Therefore, an average D_{50} of 250 μm is used in the main set of simulations. To provide insight in the consequences of this uncertainty about the actual grain size, simulations with a minimum and maximum D_{50} of 0.2 and 0.4 mm will be discussed in the discussion section.

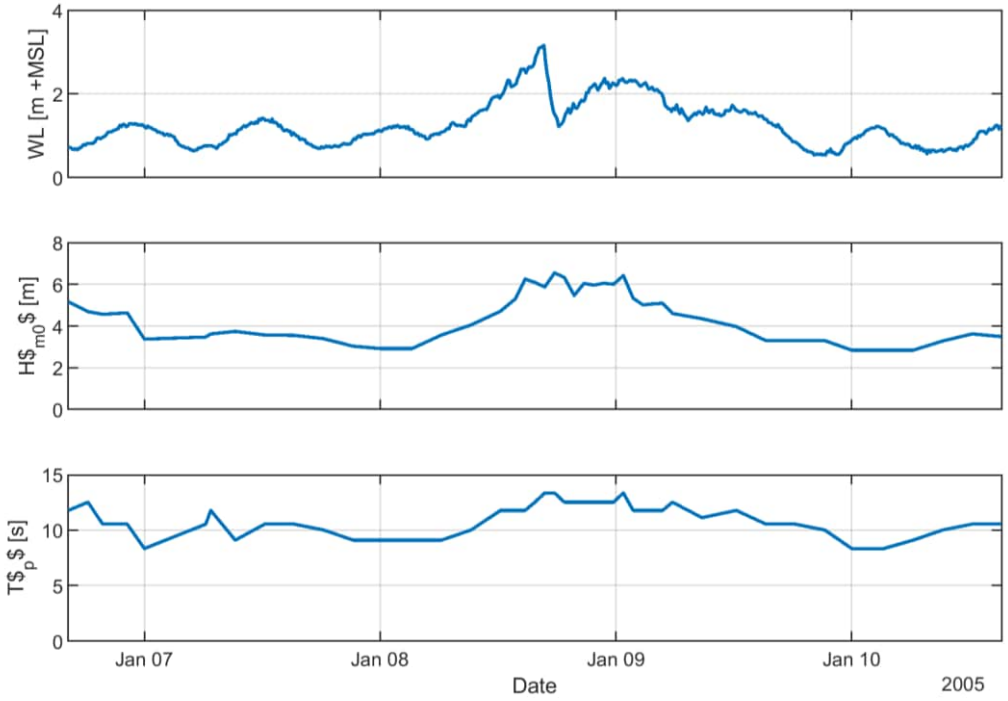

Figure C-69 Time series of the offshore hydraulic boundary. The water level time series were recorded at Ferring, whereas the wave heights and wave periods are recorded by a wave buoy outside Nymingedab. Total duration of simulation is ~4 days.

Results

Although the two transects are located within ~500 m of each other and were exposed to the same hydrodynamic forcing, their morphological response differs significantly. The results for Vedersoe 01 are presented in Figure C-70 and the results for Vedersoe 02 are presented in Figure C-71. In general, comparing the observed post-storm profiles with the XBeach results shows a good match for the dune retreat (see Table C-6) whereas the modelled dunes remain somewhat steeper than observed. Since a large part of the initial bed levels are approximated, it should be noted that both observed and measured erosion volumes are a reasonable estimation rather than real observations. Therefore, also the retreat of the dune front at MSL + 5 m is quantified, as this is the highest level that included actual observed bed levels.

An overview of the modelled and observed erosion volumes and dune retreats of the transect are provided in Table C-6. Focusing on the Vederoe 01 transect (Figure C-70), the XBeach model results show a similar dune erosion volume as in the measurements, with a 6% overprediction of the dune retreat distance at MSL + 5 m due to the steeper dune face in the XBeach post-storm profile.

The Vedersoe 02 transect is characterized by considerably less erosion. Modelled dune retreat at MSL + 5 m exceeds the observed dune retreat by approximately 1.7 m (36% overestimation). The observed and modelled dune erosion volumes in Table C-6 show a 15% underestimation of the erosion volume by the XBeach model. However, the graphical comparison provided in Figure 6 shows that this difference is mainly found in the upper part of the profile for which no measurements were available for the pre-storm bed levels.

For both profiles, eroded sand is deposited between MSL + 0 and -5 m. Though the slope of this area of deposition corresponds to the observed slope, modelled depositions exceed the observed depositions, presumably due to the absence of alongshore transport processes in the 1D model.

Table C-6 Quantitative comparison of modelled and observed erosion volumes and dune retreat for both Vedersoe profiles; both absolute and relative differences are presented. Negative differences = underestimation by XBeach (and vice versa). Colours indicate the degree of similarity between the simulations and observations (greener = better fit).

Profile nr.	Erosion volume				Retreat distance at MSL + 5 m			
	XBeach [m^3/m]	Measured [m^3/m]	Difference [m^3/m]	Difference [%]	XBeach [m]	Measured [m]	Difference [m]	Difference [%]
1	178	178	0	0%	17.7	16.7	1.0	6%
2	66	78	-12	-15%	6.3	4.7	1.7	36%

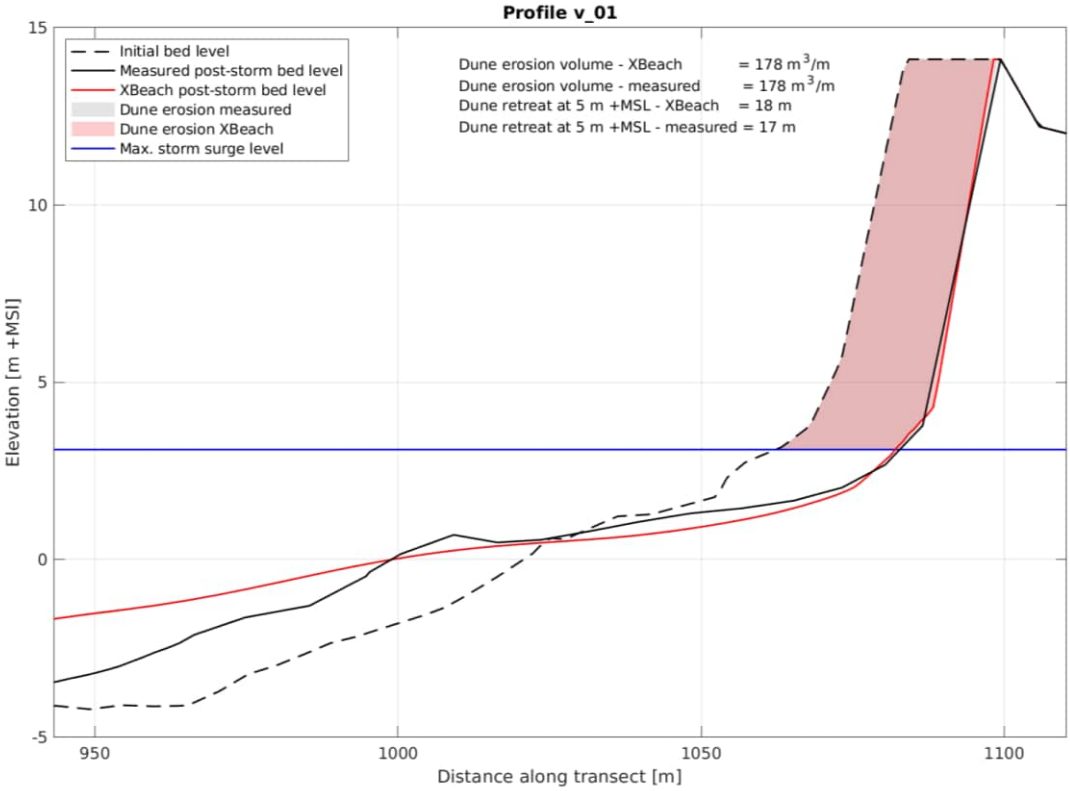

Figure C-70 XBeach results for cross-shore transect Vedersoe 01 Initial bed levels are depicted by the black dashed line, observed post-storm bed levels by the black solid line and XBeach model results are presented in red. The modelled dune erosion is shown by the red shaded area, whereas the observed dune erosion is depicted with the grey shaded area.

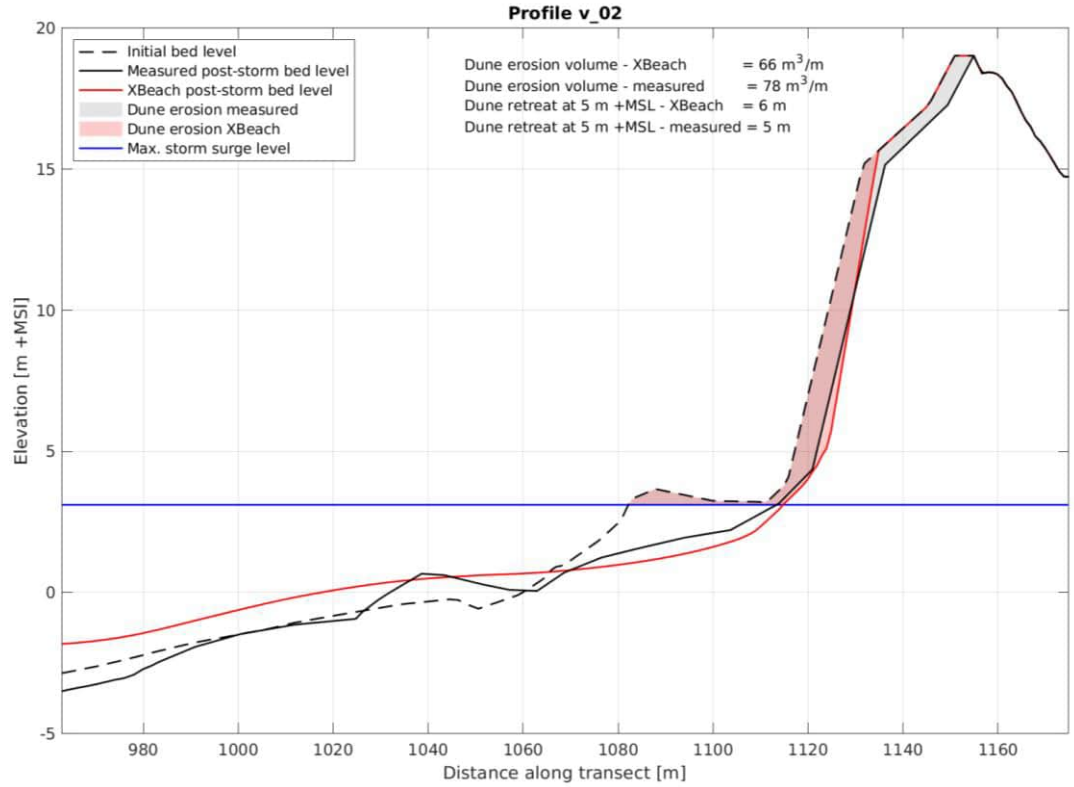

Figure C-71 XBeach results for cross-shore transect Vedersoe 02. Initial bed levels are depicted by the black dashed line, observed post-storm bed levels by the black solid line and XBeach model results are presented in red. The modelled dune erosion is shown by the red shaded area, whereas the observed dune erosion is depicted with the grey shaded area.

Discussion

XBeach is able to reproduce the alongshore variation in observed dune erosion volumes and retreat distances for the two different Vedersoe transects (with and without beach berm). The dune retreat distances are slightly overestimated, as the modelled post-storm slope of the dune face remains somewhat steeper than observed.

Uncertainty due to extrapolation of pre-storm profiles
Pre-storm observed bed levels were collected only up to MSL + 5 m, and the remaining dune profile was approximated by a seaward shift of the post-storm profiles. This introduces an uncertainty in the initial bed level that is used as input for the model, which may affect the modelled post-storm dune face slope. Especially for the Vedersoe 02 case, this introduced significant uncertainty in the relative erosion volume error due to the low observed erosion volume.

Uncertainty in representative grain size
Another source of uncertainty is the selected grain size (D_{50}) for the Vedersoe case. As mentioned in the model setup, the minimum D_{50} probably is 0.2 mm and the maximum 0.4 mm. Therefore, to provide insight into the impact of the grain size uncertainty on the model results, the model is also run for a minimum D_{50} of 0.2 mm and a maximum of 0.4 mm. Figure C-72 shows that a higher D_{50} of 0.4 mm significantly changes the morphological change due to the storm for the Vedersoe 01 profile. Dune retreat and erosion volume is reduced to a minimum (14 m and 135 m^3 respectively, see Table C-7), and significantly reduces model skill. In addition, the model result with a D_{50} of 0.2 mm show that the dune erosion volume increases to 200 m^3 for the Vedersoe 01 profile (see Table C-7) and as such, the predicted erosion is overestimated compared to the measurements. This is also the case for the modelled dune retreat which increases to 19.7 m for the Vedersoe 01 profile. Since 200 µm is closer to 250 µm than 400 µm, the differences for this change in grain size are smaller compared to the main simulation. Overall, the best-estimate of the grain size of 250 µm resulted in dune erosion volumes closest to the measurements.

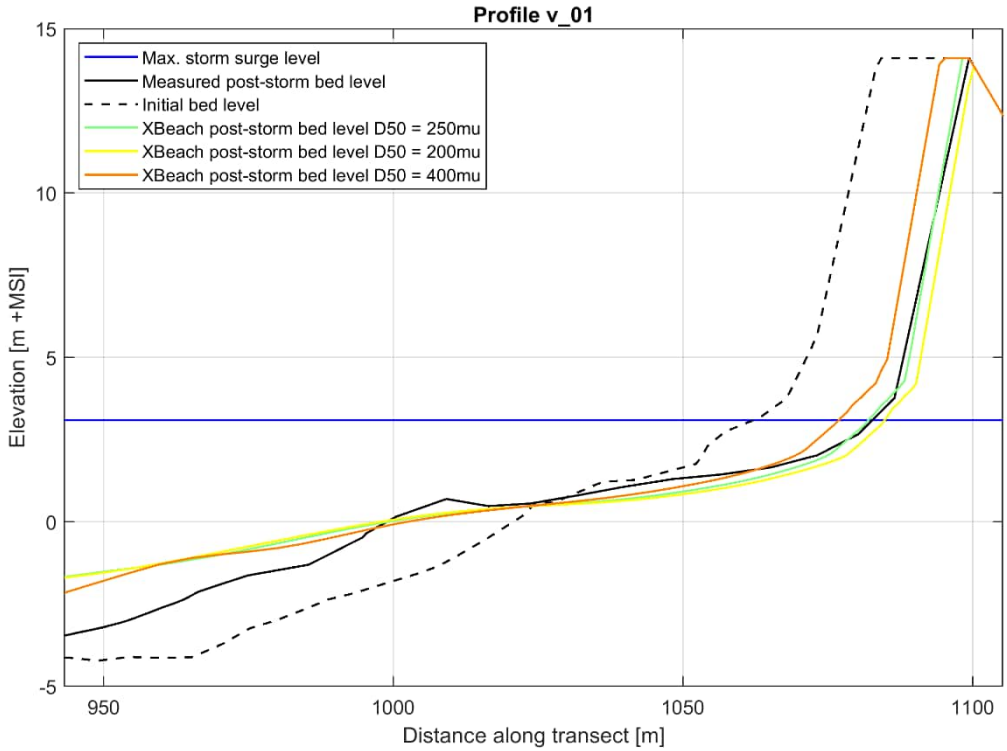

Figure C-72 Additional XBeach results for cross-shore transect Vedersoe 01 with different values of D_{50}. Initial bed levels are depicted by the black dashed line, observed post-storm bed levels by the black solid line and XBeach model results are presented in green, yellow and orange.

Table C-7 Quantitative comparison of observed and modelled erosion volumes and retreat distances for a range of grain sizes for both Vedersoe profiles. A D_{50} of 250 µm is the best-estimate for this case, 200 µm the minimum and 400 µm the maximum based on Saye and Pye (2006) and Clemmensen (2006).

Profile nr.	Erosion volume [m^3/m]				Retreat distance [m] at MSL + 5 m			
	XBeach			Measured	XBeach			Measured
	D_{50} = 250 µm	D_{50} = 200 µm	D_{50} = 400 µm		D_{50} = 250 µm	D_{50} = 200 µm	D_{50} = 400 µm	
1	178	200	135	178	17.7	19.7	14.0	16.7
2	66	81	42	78	6.3	7.5	4.3	4.7

Conclusion

Measurements of the 2005 storm impact at Vedersoe, Denmark are used for morphological validation. Two transects with a different morphological response to the storm were run. The observed post-storm profiles are well predicted by XBeach, with dune retreat distances overpredicted by 6 and 36% respectively. Modelled dune erosion volumes show a smaller difference with the observations, but since the data describing the initial dune profiles was incomplete, this should be treated with care.

These results are based on the application of a best-estimate D_{50} of 250 µm, but literature indicates that grain sizes at the Danish West coast dunes is in the range of 200 µm to 400 µm. Overall, the D_{50} of 250 µm results in dune erosion values closest to the measured volumes. The maximum D_{50} of 400 µm results in underestimation of dune erosion (up to 43 m^3/m), while the minimum D_{50} of 200 µm results in overestimation of dune erosion (up to 22 m^3/m). Hence, the uncertainty in dune erosion volume related to the grain size is up to a few tens of percentages.

APPENDIX 6 - FIELD CASE 6: LANGEOOG (GERMANY) [MORPHO]

Case description

The island of Langeoog is one of seven inhabited barrier islands situated along the East Frisian German North Sea coast (Figure 1). The shoreface of Langeoog can be characterized by migrating sand shoals through the ebb-tidal delta and a breaker bar system that migrates in eastern direction, comparable to the morphological configuration for the Dutch Wadden Sea Islands. The mildly sloping and shallow shoreface extents to deeper water with a slope of ~1:300. On Langeoog approximately 3.9 million m³ of sand have been nourished since 1971 to protect the inhabited areas landwards of the dunes. This coastal area can be classified as mesotidal with semidiurnal tides with a mean tidal range of about 2.7 m at the Langeoog gauge. The mean grain size (D_{50}) for Langeoog northern beaches is in the order of 0.25 mm (Interreg, 2021). The upper beach and dune foot area has a mean grain size of 0.20 mm, whereas in the surf zone it is in the order of 0.30 mm.

Storm Xaver passed Langeoog from 5 to 7 December 2013, in the Netherlands referred to as 'Sinterklaasstorm', and led to an extreme maximum storm surge level of NHN[11] +3.95 m at Langeoog gauge station. Offshore of Langeoog a maximum wave height of H_s = 7 m and period T_p = 15 s was observed. The storm caused significant dune erosion at the Northern side of the island. Two months prior to the storm, October 2013, a beach nourishment was deployed on the North-Western part of the island (Figure 1). A large part of the beach nourishment was eroded due to the storm, and the observed dune erosion landwards of the nourishment was considerably less compared to the adjacent dunes.

Topographic measurements of the beach/dunes were collected after the beach nourishment placement, on October 18th, 2013, 2 months prior to Storm Xaver. Post-storm topography was collected on December 13th, 2013 for the area around the beach nourishment and April 30th, 2014 for the Eastern part of the island. Bathymetric data of the shoreface was collected in August 2013.

In the Interreg VB North Sea Region Building with Nature project a 2D XBeach model of Langeoog was set-up and validated for the 2013 storm (Hillman et al., 2021). The 2D model domain is 4 km in longshore and 4.5 km in cross-shore direction, and covers the area where the beach nourishment was located (Figure 1). The initial model bathymetry was constructed by combining the August 2013 shoreface measurements and October 18th, 2013 topographic measurements. From this 2D model bathymetry and accompanying forcing conditions, six transects were extracted to use for the morphological validation of the BOI-XBeach model and settings.

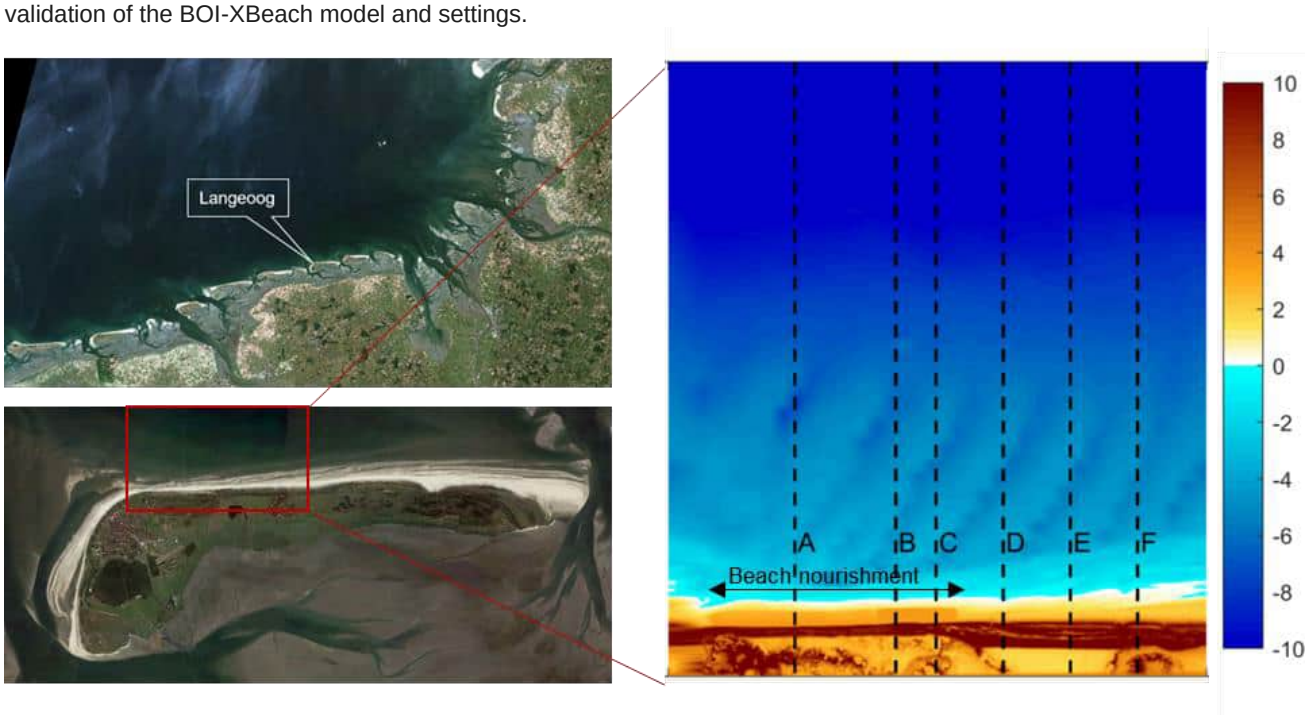

Figure C-73 Location of the study site in Langeoog, Germany and locatation of the XBeach model. Model input bathymetry (right panel) with the location of the beach nourishment and the six transects A to F (Hillman et al., 2021).

[11] *Normalhöhennull, vertical datum in Germany. MSL = NHN 0 +/- 0.1 m (Interreg, 2021)*

Model setup

Grid and bathymetry

Six 1D XBeach models have been set-up, based on the 2DH XBeach initial model bathymetry as developed by Hillman et al. (2021). Transect A to C are located at the beach nourishment and transect D to F are located at the Eastern side of the nourishment (see Figure C-73). Each of the profiles has been extended seaward according to BOI guidelines with a 1:50 slope to a depth of 23 m. Cross-shore grids were set-up following standard BOI procedure resulting in approximately 1100 ± 50 grid cells per profile and spatial resolution that varies from 8 m (offshore) to 1 m at the coast. The profiles can be divided into two groups with similar initial beach profiles: 3 profiles with- and 3 without beach nourishment. Because of the large correspondence within the group, initial bed levels across the 1D transect as well as the cross-shore distribution of grid size are presented for just one profile per group (see Figure C-74 for transect B (with nourishment) and Figure C-75 for transect E). In addition, the initial bed levels of all six profiles are depicted together in Figure C-76. A D_{50} of 0.25mm is applied, based on the observed mean grain size at the Langeoog beaches.

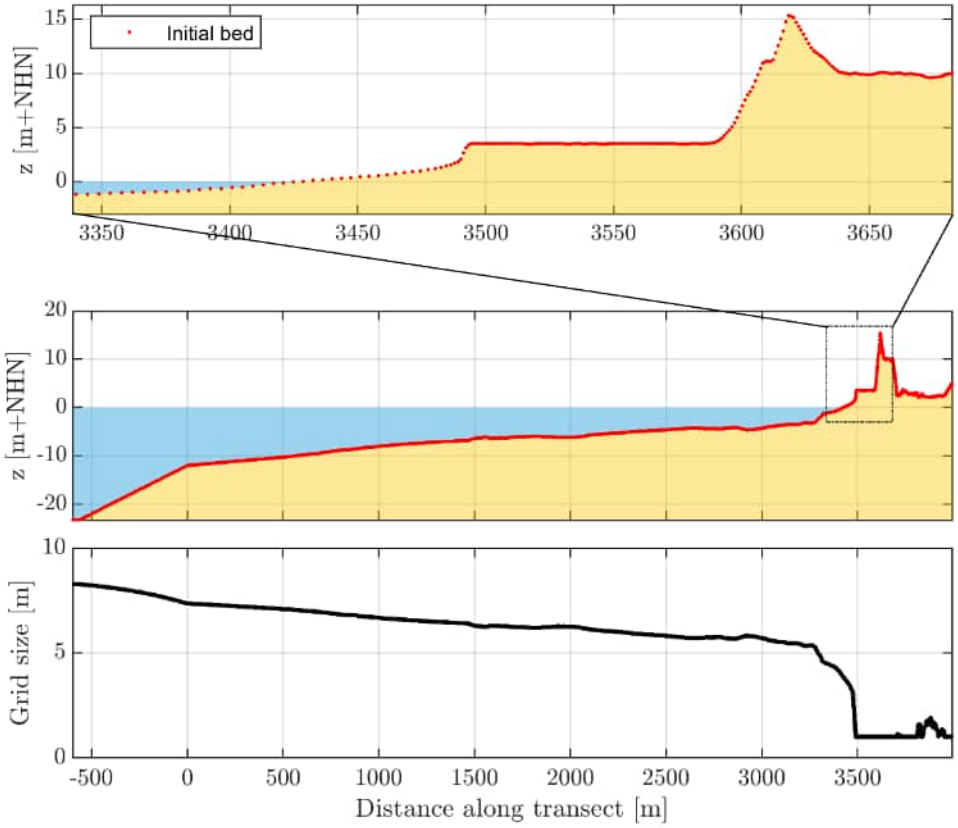

Figure C-74 Overview of the initial bed level along the 1D XBeach transect B (middle panel, in which the red dots represent the bed level per grid point), and cross-shore distribution of the grid size (lower plot). Besides that, the upper plot presents a zoom on the last part of the profile where the beach nourishment was placed.

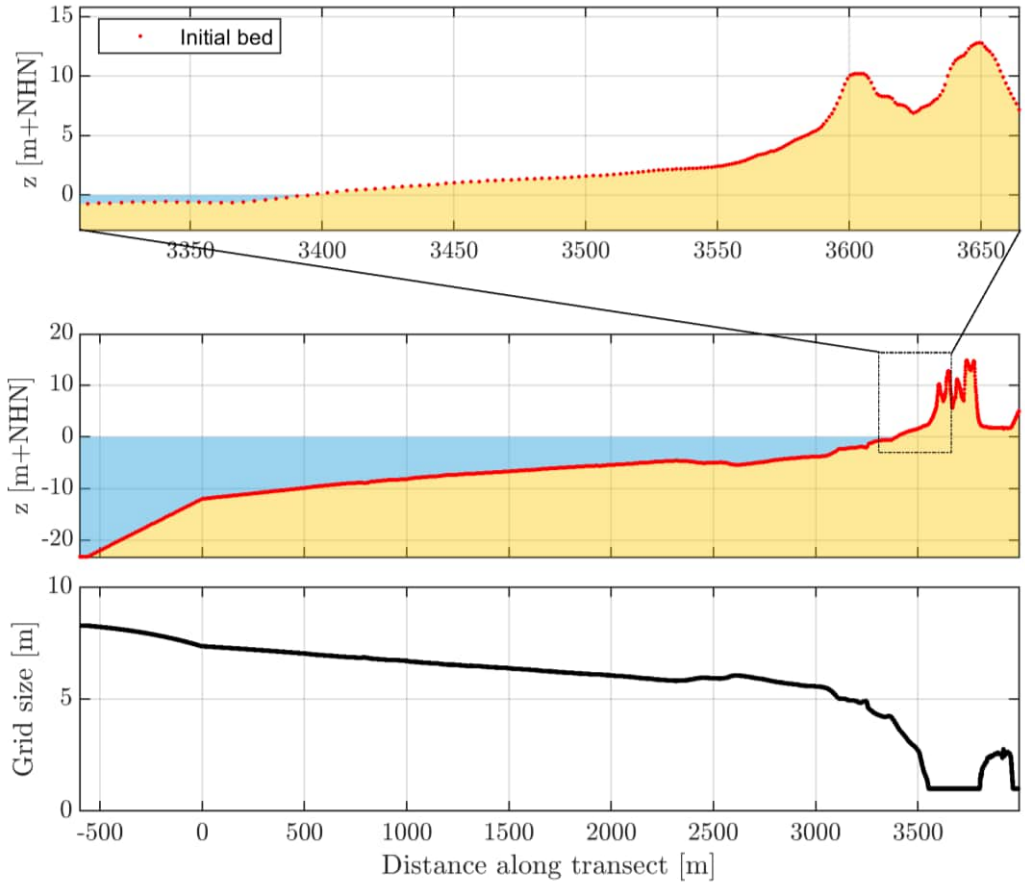

Figure C-75 Overview of the initial bed level along the 1D XBeach transect E (middle panel, in which the red dots represent the bed level per grid point), and cross-shore distribution of the grid size (lower plot). Besides that, the upper plot presents a zoom on the last part of the profile where no beach nourishment is present (in contrast to transect B).

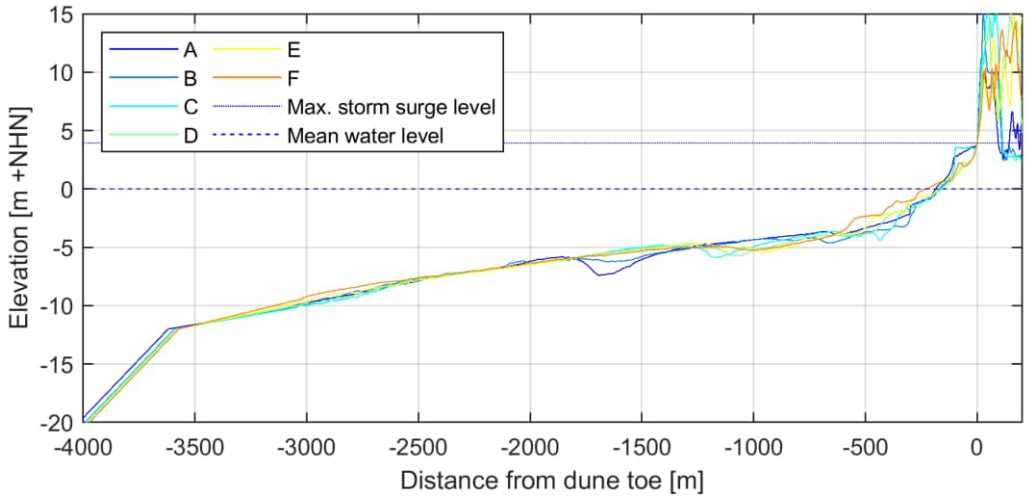

Figure C-76 Overview of the initial bed levels for the six different transects. Dune toe for this specific case is defined at the maximum storm surge level.

Hydraulic boundary conditions

Forcing conditions are based on observations (tidal and surge elevation from WSA EMS-NORDSEE) and SWAN model simulations as developed within the EasyGSH project (Plüß et al., 2020 - EasyGSH-DB (baw.de)). From the SWAN-model, wave conditions are extracted at approximately 10 km distance from the island (~20 m water depth), and provided significant wave heights, peak wave periods and mean wave directions. These wave characteristics are used to force the model with a sequence of half hourly-varying JONSWAP spectra (Van Dongeren et al., 2003). Instead of using the time-varying mean wave directions, the mean wave direction of the JONSWAP wave spectra is defined perpendicular to the coast and a directional spreading of approximately 30° (s = 6) is used (in analogy with BOI procedure). An overview of the hydrodynamic forcing conditions that were used to force the XBeach model is presented in Figure C-77. The models are run for a total simulation period of 56 h, which captures the entire period where elevated water levels and increased wave heights were observed during the December 2013 storm.

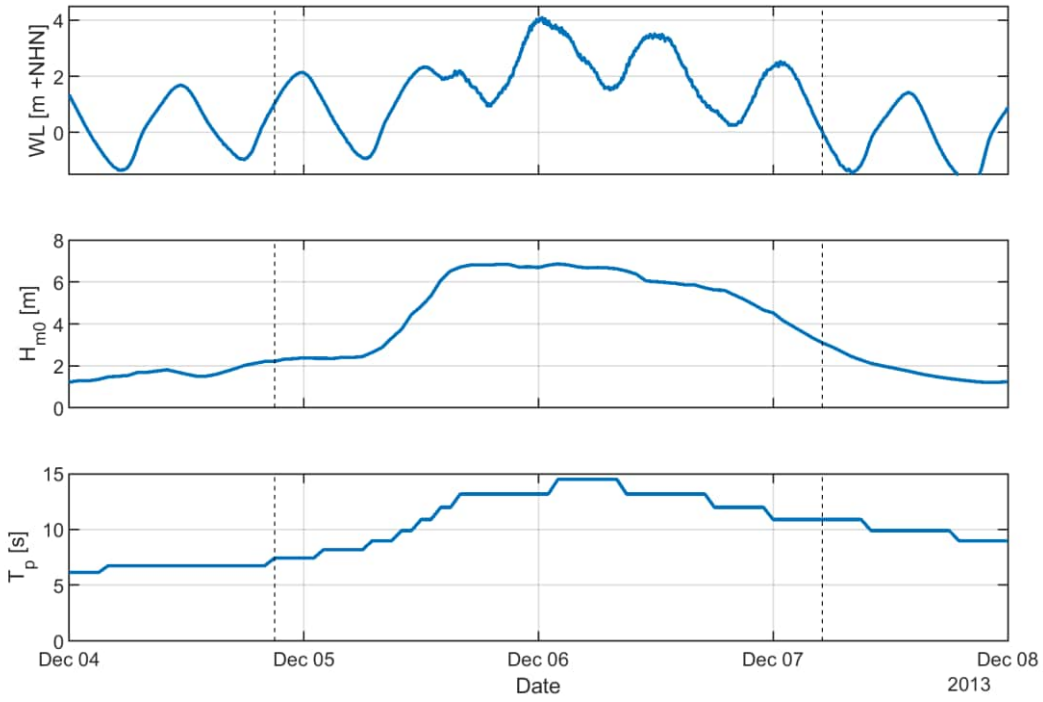

Figure C-77 Time series of the offshore forcing conditions for the XBeach model with the black dashed lines indicating the start and end of the simulation period. The water level time series are based on observations (Hillamn et al., 2021), and H_s, T_p and wave direction are obtained from a SWAN model (Plüß et al., 2020).

Results

The model results are validated using the topography measurements of the beach and dunes, collected on December 13th 2013, for the area around the beach nourishment and April 30th, 2014 for the Eastern part of the island. The vertical reference level of maximum dune retreat is determined at NHN + 5 m, based on the observed pre- and post-storm data.

Transects A to C are located at the beach nourishment and the results of the XBeach simulations are presented in Figure C-78 for transect A (Figure C-80 and Figure C-81 for B and C). The results show that XBeach underestimates the erosion of the beach nourishment. The shape of the beach looks similar (but elevated). The underestimation of the eroded sand from the nourishment in combination with the deposition of eroded dune sand results in an increase in bed level at the dune foot. In contrast to the measurements, dune erosion is found higher up in the dune profile (from NHN + 6 m to NHN + 10 m, rather than from NHN + 4 m to NHN + 8 m), which affects the quantitative comparison (see Table C-8) for the dune retreat distance. At the NHN + 5 m reference level, the observed profiles show a retreat of the dune face whereas XBeach predicts a seaward displacement of the dune face. Based on a qualitative comparison in profile shapes, XBeach overestimates the dune retreat and the retreat is located higher up in the profile. However, although the erosion is higher in the dune profile, the dune erosion volumes of transect B and C are quite similar to the observed volumes.

The results for transects D to F (the profiles without a beach nourishment) are presented in Figure C-79 for transect D (Figure C-82 and Figure C-83 for E and F). Similar to the profiles with beach nourishment, the modelled dune erosion is located higher up in the profile, the dune toe is elevated (due to the deposition of eroded dune sand) and the erosion volumes are larger than in the observations (see Table C-8). However, modelled dune retreat values at NHN + 5 m correspond better with the observations.

Table C-8 Quantitative comparison of modelled and observed erosion volumes and dune retreat for all 6 Langeoog profiles. In addition, both absolute and relative differences are presented. Negative differences mean underestimation of the measured values in the XBeach simulation. Colours per column indicate the degree of similarity between the simulations and observations based on all morphological cases (greener = better fit).

Profile nr.	Erosion volume				Retreat distance [m] at NHN + 5 m			
	XBeach [m^3/m]	Measured [m^3/m]	Difference [m^3/m]	Difference [%]	XBeach [m]	Measured [m]	Difference [m]	Difference [%]
A	16	1	15	1540%	-2.9	0.5	-3.4	-658%
B	15	13	2	17%	-2.7	3.5	-6.2	-176%
C	10	10	0	3%	-2.3	4.0	-6.3	-157%
D	31	18	13	74%	5.1	6.5	-1.4	-21%
E	28	14	14	100%	5.7	7.0	-1.4	-19%
F	27	11	16	146%	7.1	4.5	2.5	56%
Average	**21**	**11**	**10**	**313%**	**1.7**	**4.3**	**-2.7**	**-163%**

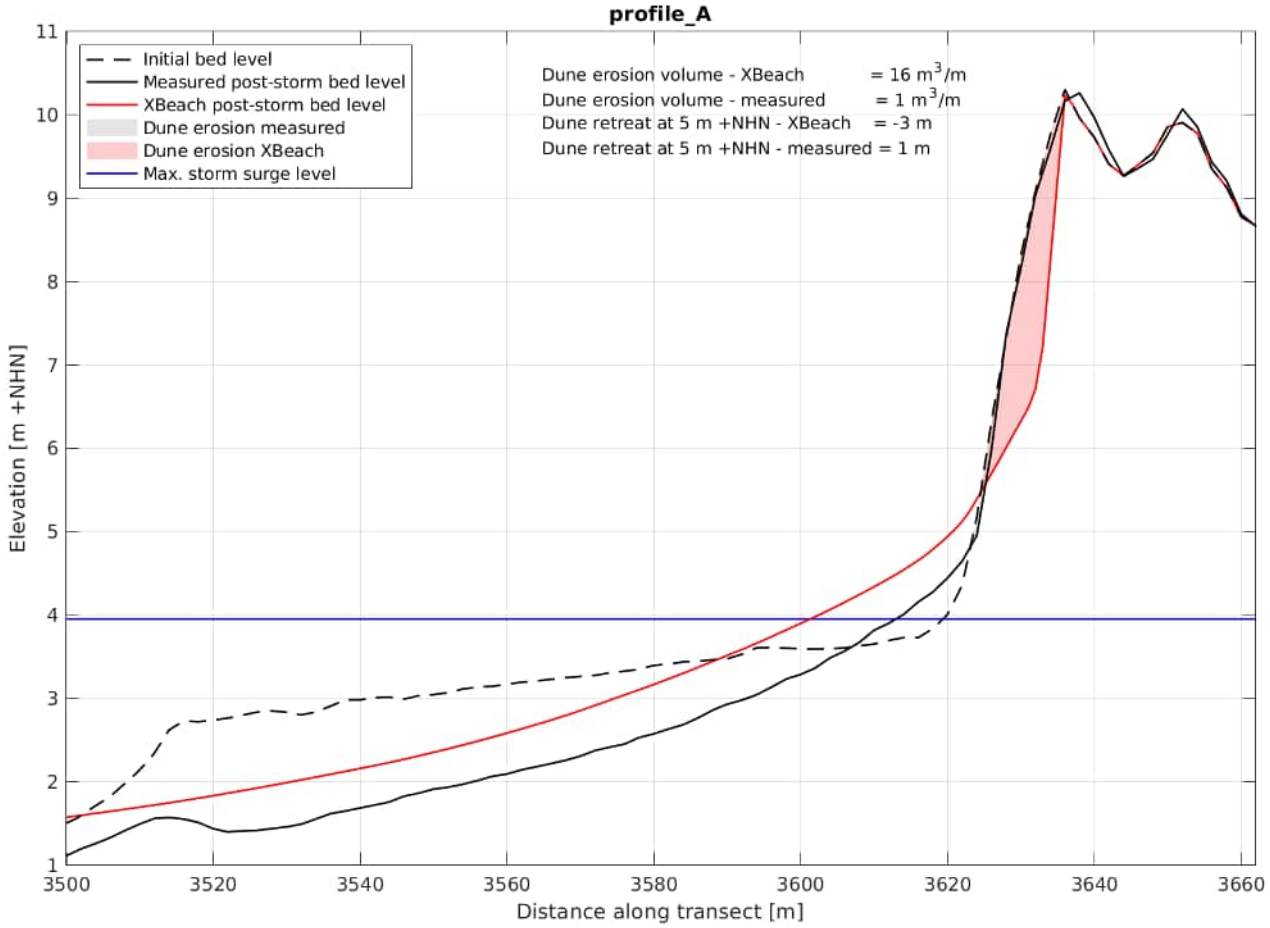

Figure C-78 XBeach results for cross-shore transect A at Langeoog. Initial bed levels are depicted by the black dotted line, observed post-storm bed levels by the black solid line and XBeach model results are presented in red. The modelled dune erosion is shown by the red shaded area.

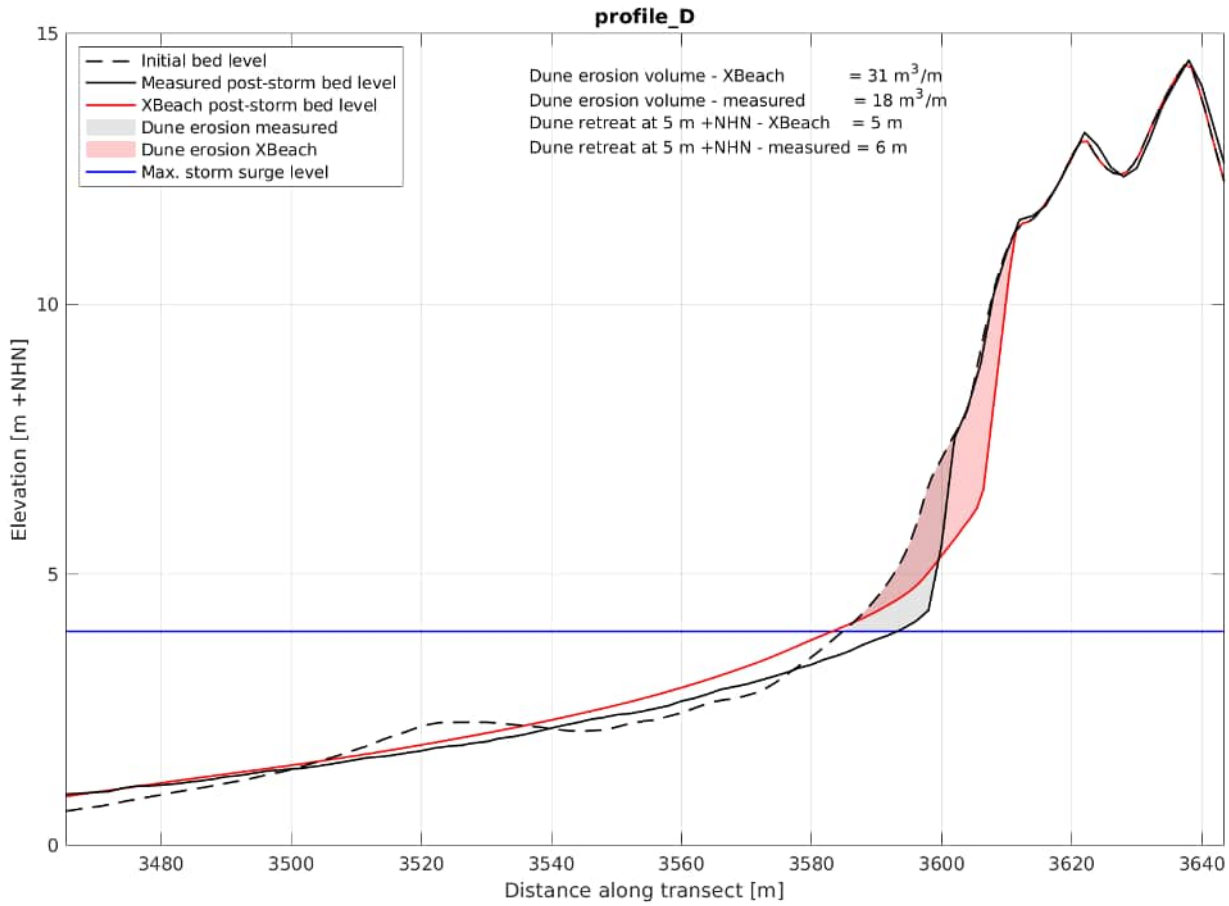

Figure C-79 XBeach results for cross-shore transect D at Langeoog. Initial bed levels are depicted by the black dotted line, observed post-storm bed levels by the black solid line and XBeach model results are presented in red. The modelled dune erosion is shown by the red shaded area.

Discussion

Erosion higher in the dune

For all six profiles in the Langeoog case, the dune erosion modelled by XBeach occurs higher up in the profile compared to the observations. The deposited volume of sand on the beach is therefore also at a higher elevation compared to observations. This affects the quantification of the morphological changes as these are determined based on fixed vertical reference levels (i.e. maximum storm surge level for erosion volumes and NHN + 5 m for retreat distances). The dune erosion volumes in Table C-8 correspond to the volume change above the maximum storm surge level only: if the erosion of the dune foot would be incorporated in the observed erosion volumes, the difference between measured and modelled dune erosion would be significantly smaller for especially transect D to F.

During the update of the BOI settings as described in Deltares (2021a), profile B and E of the Langeoog case were included in the set of profiles for selecting appropriate values for the *facAs* and *wetslp* parameter. It was noticed that, for unknown reasons, the optimal settings for this specific case were a relatively high *wetslp* and a low *facAs* compared to the other calibration profiles. These settings improved the erosion volumes and resulted in dune erosion somewhat lower in the profile, but could not explain the difference between modelled and measured entirely. Hence, although a slightly different combination for *facAs* and *wetslp* could improve the results for this specific case slightly compared to the chosen, overall best combination of *facAs* and *wetslp*, other factors do play a role.

Uncertain initial bed level
A probable explanation for the underestimation of the erosion of the beach nourishment is that the pre-storm observations were collected on the day the beach nourishment was placed, October 18th 2013, almost two months prior to the storm event on December 6th. In that period the shape of the beach nourishment may have changed due to natural processes (e.g. aeolian- or wave-induced). Therefore, the underprediction of the erosion of the beach nourishment and the higher elevated dune foot may be due to the initial shape of the beach nourishment in the input model bathymetry that may have been different (less steep/lower) in reality, causing offsets in the hydrodynamics and in turn morphodynamics.

Alongshore processes
In addition, longshore processes may have had an effect on the alongshore distribution of the beach nourishment during the storm. Waves were predominately originating from the Northwest during the storm, and may have induced sediment transport in easterly direction. This sediment would have been deposited on the beach and/or shoreface, influencing the post-storm topography observations. Such alongshore processes are not captured with a 1D model approach and could therefore explain the differences between the modelled and observed.

Conclusion

The island of Langeoog is located along the East Frisian German North Sea coast and was impacted by Storm Xaver from 5 to 7 December 2013. The storm caused significant dune erosion at the Northern side of the island, where two months prior to the storm a beach nourishment was placed. For six profiles with and without a beach nourishment, XBeach predicts dune erosion higher up in the dune profile compared to observations and generally dune erosion volumes are overestimated. This is among others related to alongshore processes could not be simulated in 1D and uncertainties in the initial bed level.

Additional figures

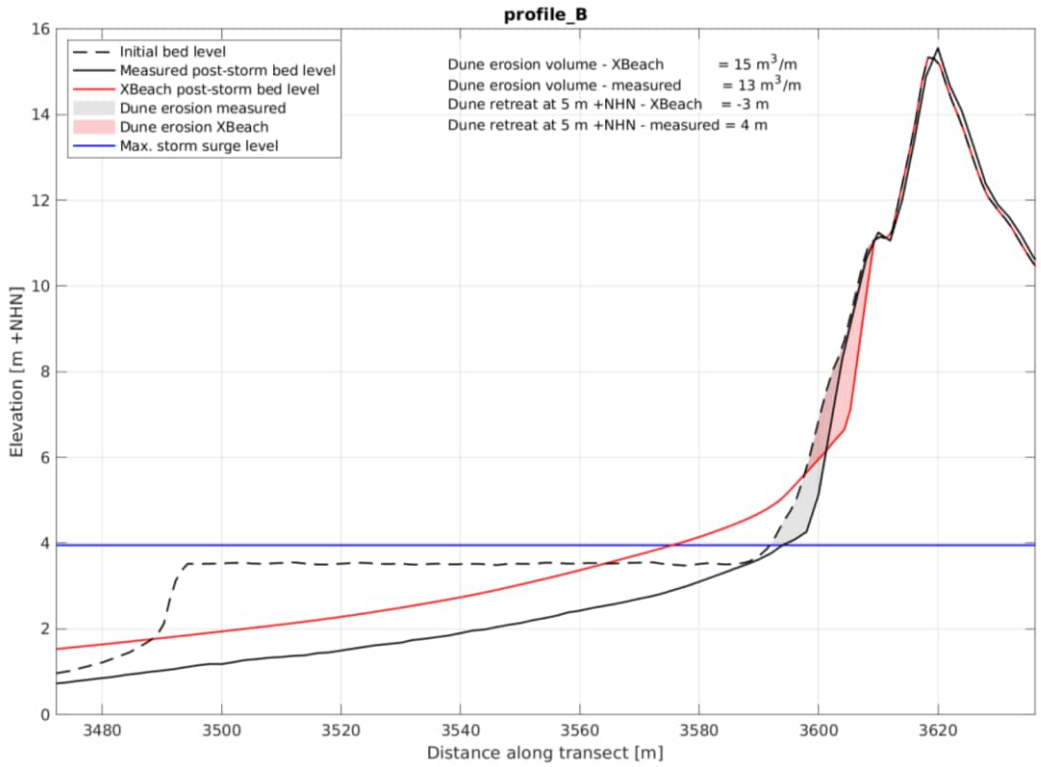

Figure C-80 XBeach results for cross-shore transect B at Langeoog. Initial bed levels are depicted by the black dotted line, observed post-storm bed levels by the black solid line and XBeach model results are presented in red. The modelled dune erosion is shown by the red shaded area.

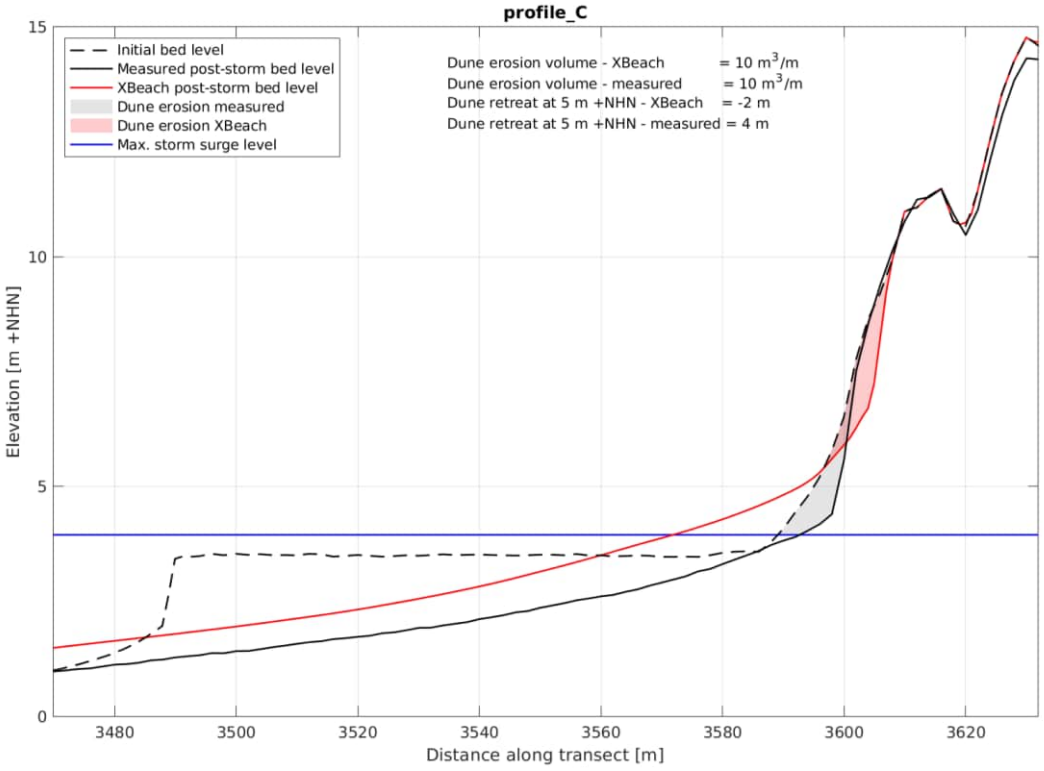

Figure C-81 XBeach results for cross-shore transect C at Langeoog. Initial bed levels are depicted by the black dotted line, observed post-storm bed levels by the black solid line and XBeach model results are presented in red. The modelled dune erosion is shown by the red shaded area.

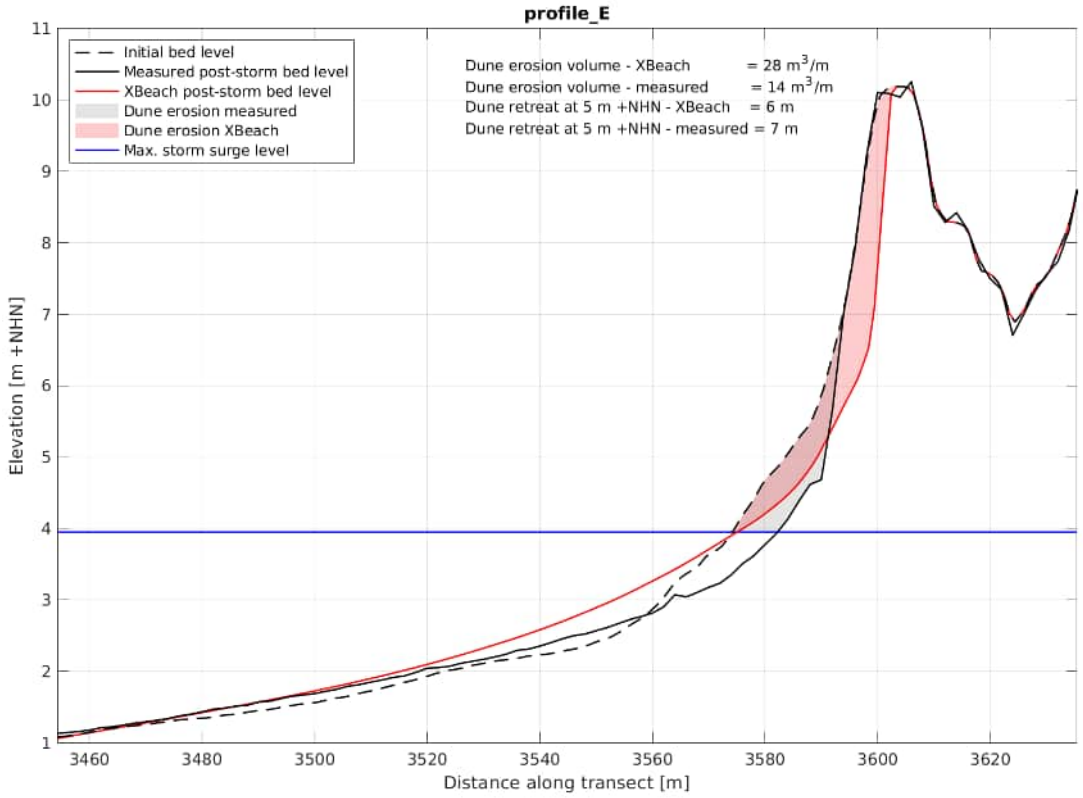

Figure C-82 XBeach results for cross-shore transect E at Langeoog. Initial bed levels are depicted by the black dotted line, observed post-storm bed levels by the black solid line and XBeach model results are presented in red. The modelled dune erosion is shown by the red shaded area.

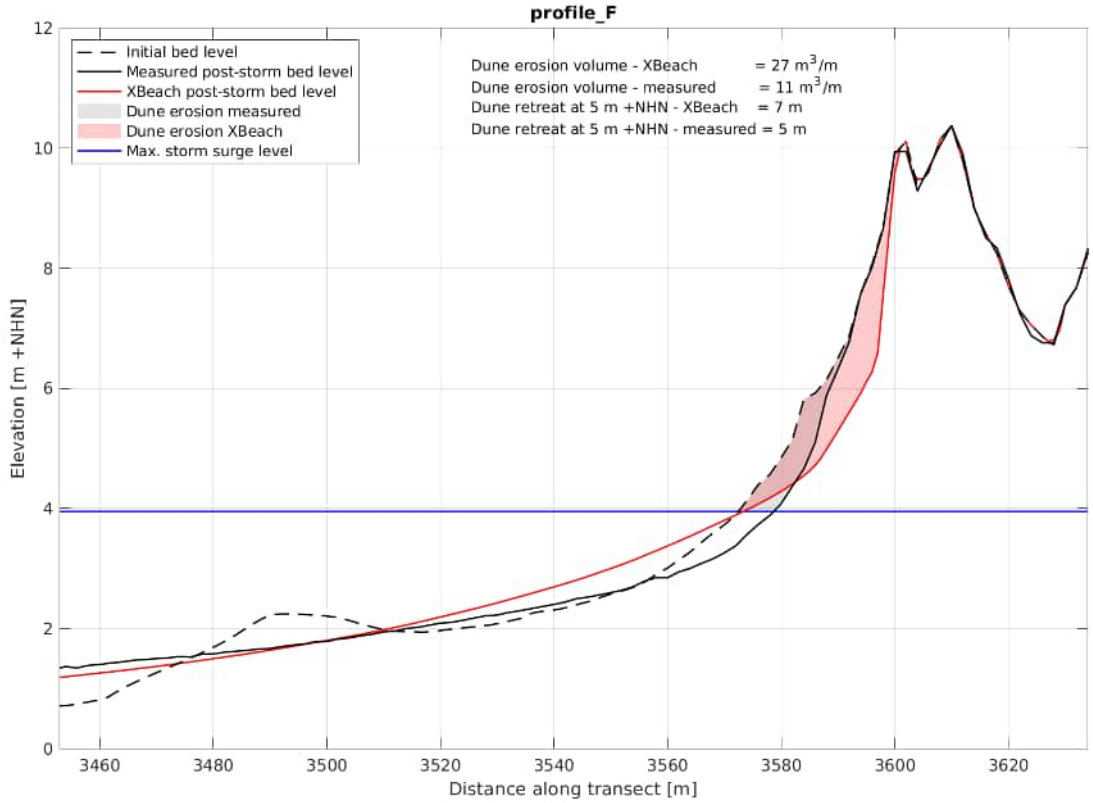

Figure C-83 XBeach results for cross-shore transect F at Langeoog. Initial bed levels are depicted by the black dotted line, observed post-storm bed levels by the black solid line and XBeach model results are presented in red. The modelled dune erosion is shown by the red shaded area.

APPENDIX 7 - FIELD CASE 7: HOLLAND COAST, 1976 (NL) [MORPHO]

Case description

The storm that hit the Dutch coast in the night between the 3rd and 4th of January 1976 is classified as a violent storm ('zeer zware storm'); 11 on the Beaufort scale. A storm event severity that is very rarely experienced in the Netherlands. While the storm surge and high waves impacted the entire Dutch coast, the Delta coast (Zeeland) was hit the hardest with a peak storm surge level of NAP + 4.1 m at Vlissingen: the highest water level since the 1953 storm surge (NAP + 4.5 m). The Belgian coast was also impacted heavily, including major flooding in the province of Antwerp. This led to the initiation of the Sigmaplan, designed to better protect the Scheldt basin from flooding during storm surges.

For this validation case the impact of the 1976 storm surge on the northern part of the Holland coast (the coastal section between Noordwijk and Den Helder) is compared to observations. For the hydraulic boundary conditions, the (Van der Werf & Van Santen, 2010) study is used as a starting point, briefly explained in the section below. This validation case then focusses on the morphodynamic comparison between simulated and observed dune erosion and dune retreat, which is available for a set of 30 profiles in the considered coastal section (between profile 568 in the north and profile 7100 in the south, as shown in Figure C-84). Most profiles have a profile with high dunes, multiple bars up above NAP - 9 m and slopes similar to the representative Holland coast profile.

The typical observed offshore peak conditions, also explained in more detail below, are as follows:

- The peak surge level consisting of tide and storm surge is NAP + 2.99 m.
- The peak significant wave height H_s during the storm is 6.1 meters.
- The maximum wave peak period T_p is 10.8 seconds.

Figure C-84 Location of all coastal profiles of the Holland coast 1976 validation case in red, from 568 in the north to 7100 in the south.

Model setup

A morphodynamics 1D XBeach simulation (with sediment transport and morphology) is set up for each of the 30 profiles where pre and post storm observations are available (568 up to 7100). Hydraulic forcing is adopted from the measurement and model data from the (Van der Werf & Van Santen, 2010) study. This model schematization process is outlined in the sections below.

Grid and bathymetry

In the period between October 1975 and February 1976 multiple series of cross-shore profile measurements were performed at locations in North Holland; from North to South: Julianadorp, Groote Keeten, Bergen aan Zee, Egmond, Castricum, Wijk aan Zee, Bloemendaal and Zandvoort. These measurements took place nearby abovementioned 30 different JarKus profile locations. The observations closest to the arrival of the storm are selected as the pre-storm observations and the series recorded closest after the storm are considered the post-storm observations.

In general, for all cross-shore profiles the JarKus 1975 data were used, corrected slightly for the pre-storm measurement data points and extended offshore using bathymetric data from the Dutch coastal model. This is shown in Figure C-85 for profile 3700; note that the profile continues farther offshore, beyond the figure limits. The offshore end of the profile is extended manually to deep water (NAP + ≥20.0 m for all profiles) with an artificial slope of 1:10 according to the BOI guidelines. The cross-shore grid was set-up using the standard BOI procedure, generally resulting in 2000 to 3000 grid points and a spatial resolution that varies from ~6 m offshore to a minimum of 1 m towards NAP + 3 m and above. Especially the higher offshore detail of the grid is the result of the 'points per wavelength' option that is set to 40, generating 40 grid cells over the (offshore) wavelength.

Figure C-86 gives an overview of all the 30 profiles, with their respective dune foot location (NAP + 3 m) defined at a cross shore distance of 0 m. The northern profiles close to Den Helder (blueish colours) cross some channels and banks connected to the Marsdiep, resulting in a relatively steep and deep shoreface up to 2 km offshore after which it becomes shallower again. The more southern profiles (yellow through red colours) have a more gentle sloping shoreface (around 1:180 like the representative Holland coast profile) to about NAP - 15 to - 20 m (deep water) with some subtidal banks up to about NAP - 9 m.

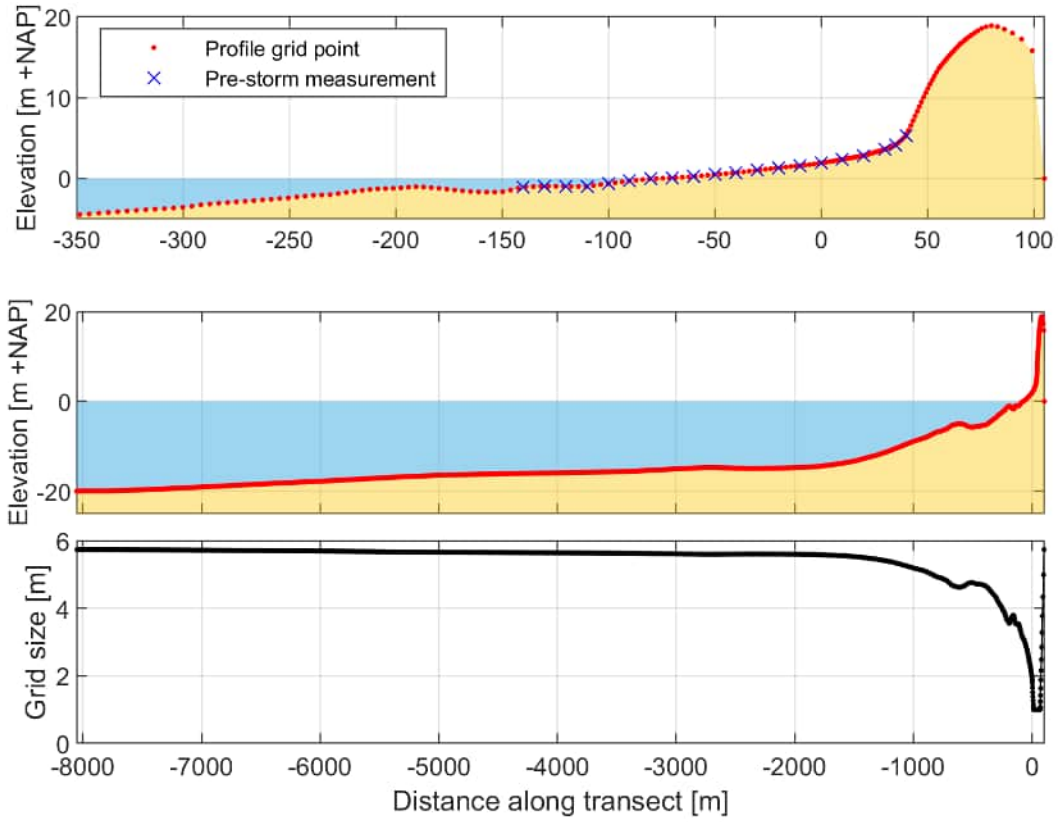

Figure C-85 Overview of the initial bed level based on the JarKus profile 3700 (upper panel and middle panel) and grid cell size (bottom panel) along the XBeach transect.

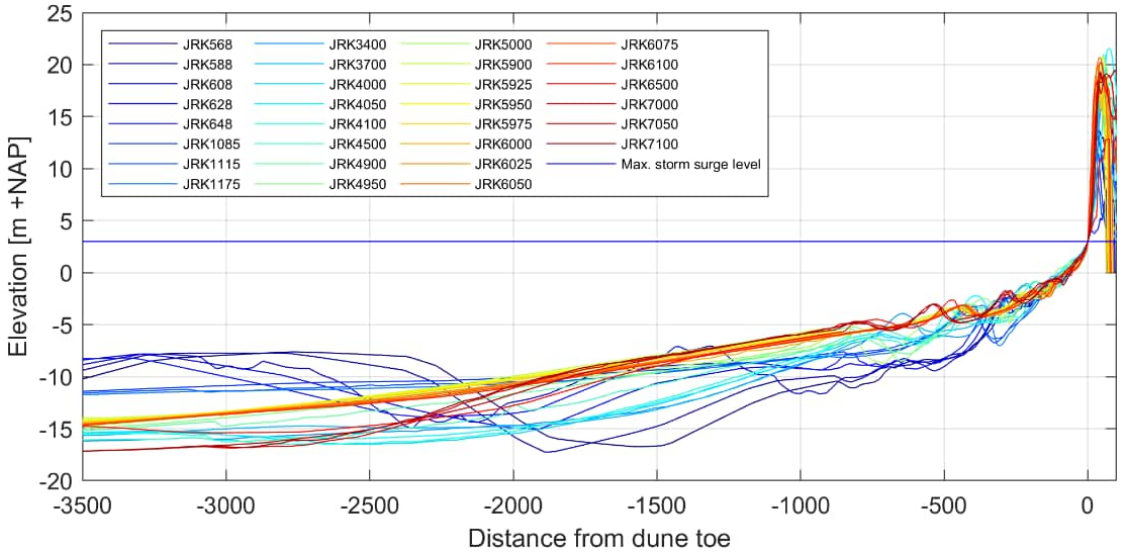

Figure C-86 Overview of the XBeach cross-shore profiles of all 30 selected profiles along the northern Holland coast. The profiles continue at the offshore side to deep water.

Grain size

There is a slight variation in grain size along the profiles that are assessed. The D_{50} in the dunes ranges from an average of 240 µm in the north, to an average of 210 µm in the south based on samples of 1982 that are used in the current WTI (WL, 2007). For each profile, the associated D_{50} is used in the simulation (Table C-9). The value ranges from a minimum of 174 µm, a maximum of 246 µm and an overall mean of 222 µm. The variation in grain size along the coast is visualized in Figure C-87. According to the BOI guidelines, a value of 1.5 times the D_{50} is used for the corresponding D_{90}.

Table C-9 Median grain size (D_{50}) for the XBeach 1D profiles along the Holland coast (case 7) based on the current WTI (WL, 2007). In bold: profiles that include the dune foot in the measured post-storm profile.

Profile nr.	568	588	608	628	648	1085	1115	1175	3400	3700	4000	4050	4100	4500	4900	…
D_{50} [µm]	214	212	210	214	**217**	237	233	224	**237**	245	**240**	**237**	**234**	**227**	218	

…	4950	5000	5900	5925	5950	5975	6000	6025	6050	6075	6100	6500	7000	7050	7100
continued	216	**215**	**246**	**242**	**238**	**234**	**230**	**225**	**221**	**217**	**213**	**174**	**192**	**193**	**193**

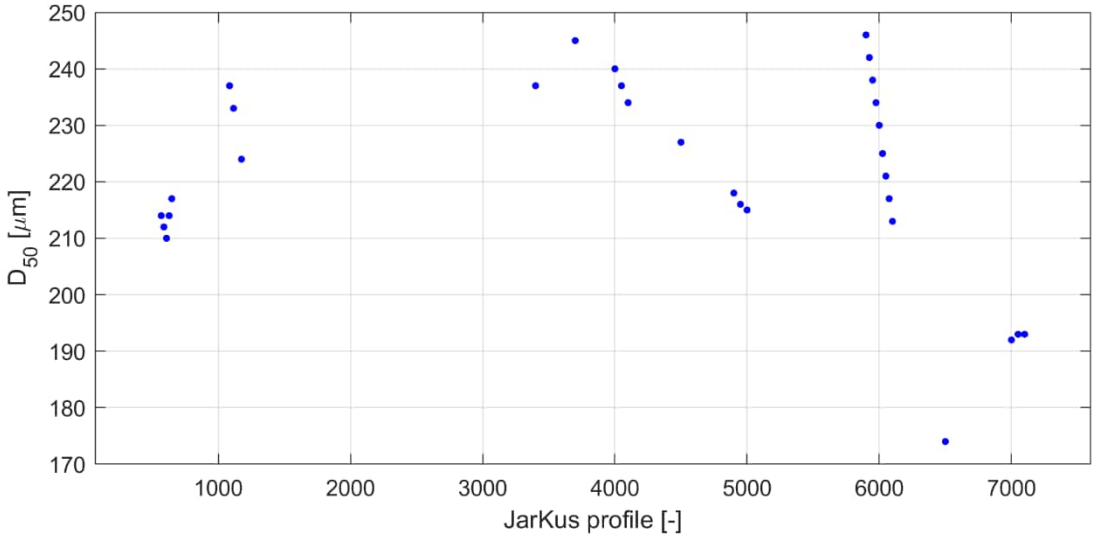

Figure C-87 Visualization of the variation in median grain size D_{50} along the coastal stretch.

Hydraulic conditions

For the schematization of the hydraulic boundary conditions, the measurements and model data available from (Van der Werf & Van Santen, 2010) is used as a starting point.

For the water level, observed time series are available at multiple locations from Hoek van Holland to Den Helder (Figure C-88). There exists only a minor difference in observed water level and phase at the southern 3 locations. The time series at Den Helder is slightly different with a somewhat more damped signal and roughly 3 hours delay in peak values. As was opted for in (Van der Werf & Van Santen, 2010), the water level time series at IJmuiden was used for the offshore water level forcing for all profiles considered. A note should be made that this might lead to a slight mistiming between (peak) water levels and (peak) wave conditions for the northern profiles (585 through 1175).

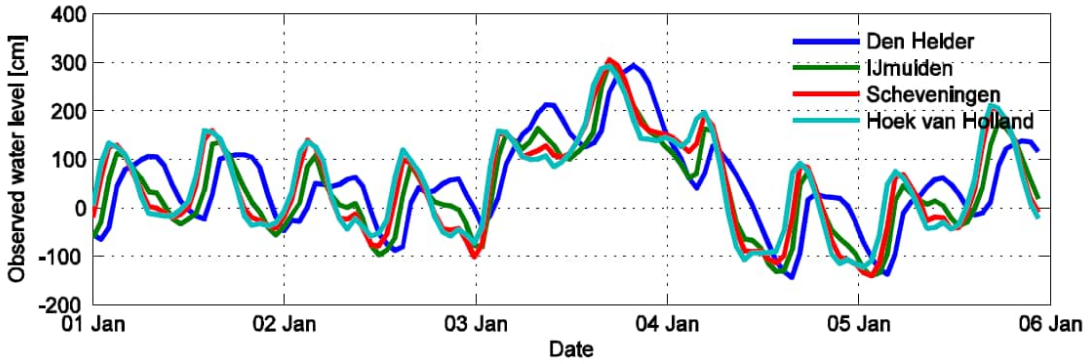

Figure C-88 Observed water levels at Den Helder, IJmuiden, Scheveningen and Hoek van Holland during the 1976 storm event, from (Van der Werf & Van Santen, 2010).

For the wave parameters H_s and T_{mean} data are available from the wave rider buoy just offshore at IJmuiden at a depth of 16 m from (Vellinga, 1978) and wave hindcast simulation data at MP1, located some 10 km offshore at Callantsoog at a depth of 20 m from (Caires, Groeneweg, & Sterl, 2008)[12]. Figure C-89 shows the observed significant wave height and wave peak period for the 1976 storm surge event, where the peak period was obtained by multiplying the observed mean period with a factor 1.2. Peak values of 6.1 m and 10.8 s were registered for the wave height and wave period, respectively. What can also be observed, is that there is no significant difference in wave height, wave period and/or phasing at both locations, while they are located roughly 38 km apart in longshore direction. It is therefore assumed that that the wave forcing during the 1976 storm surge event was generally constant in space over the entire coastal section that is considered for this case. In addition, both measurement locations are located in deep water, this means that the data can be directly used as wave boundary forcing input for the XBeach evaluation of the local profiles. The MP1 data are adopted for the wave boundary forcing. For the wave spreading the BOI default value of s = 6 was used (roughly equal to 30°).

In summary, Figure C-90 shows the time series of all time-varying XBeach offshore hydraulic boundary conditions for the 1976 storm surge forced at profile 3700 over the length of the model simulation time: January 3rd 0:00 – January 4th 18:00 for a total simulation time of 42 hours.

[12] *Note that the 2D wave spectrum files (.sp2 SWAN files) resulting from the hindcast model from the (Van der Werf & Van Santen, 2010) study were also available for the schematization of the 1D XBeach simulation. However, in the study conclusions it is recommended to not use this data for wave boundary forcing as it shows too little agreement with observed data. Upon inspection, the significant wave height associated with these spectrum files peaked no higher than roughly 4 m, significantly lower than the registered peak value of approximately 6 m at IJmuiden and MP1. In addition, when applying the energy density spectrum as XBeach boundary condition, the resulting T_{rep} is also significantly lower than the observed T_{mean}.*

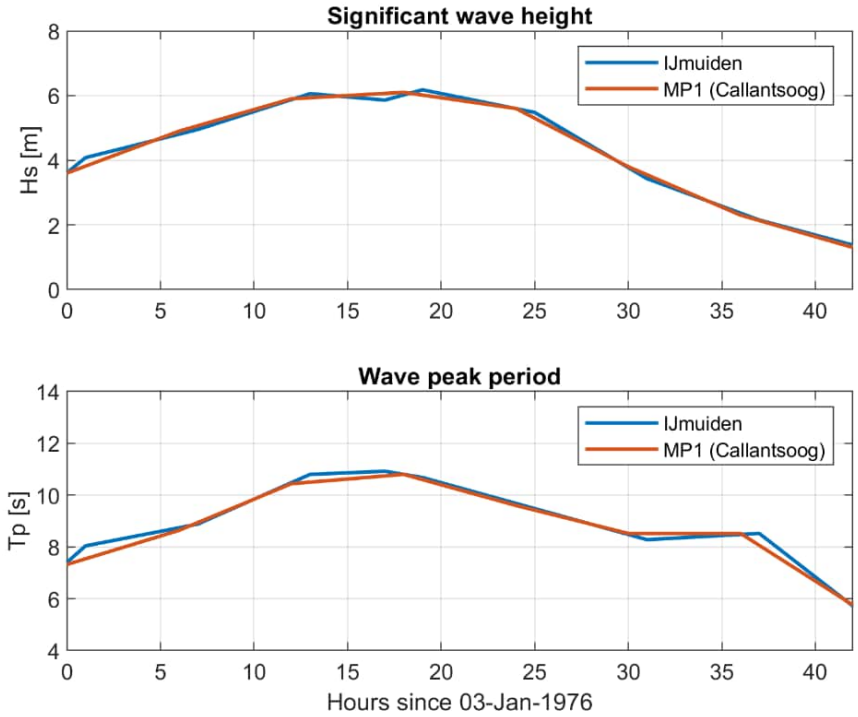

Figure C-89 Observed significant wave height and mean wave period during the 1976 storm event, at IJmuiden (Vellinga, 1978) and at MP1 (Van der Werf & Van Santen, 2010).

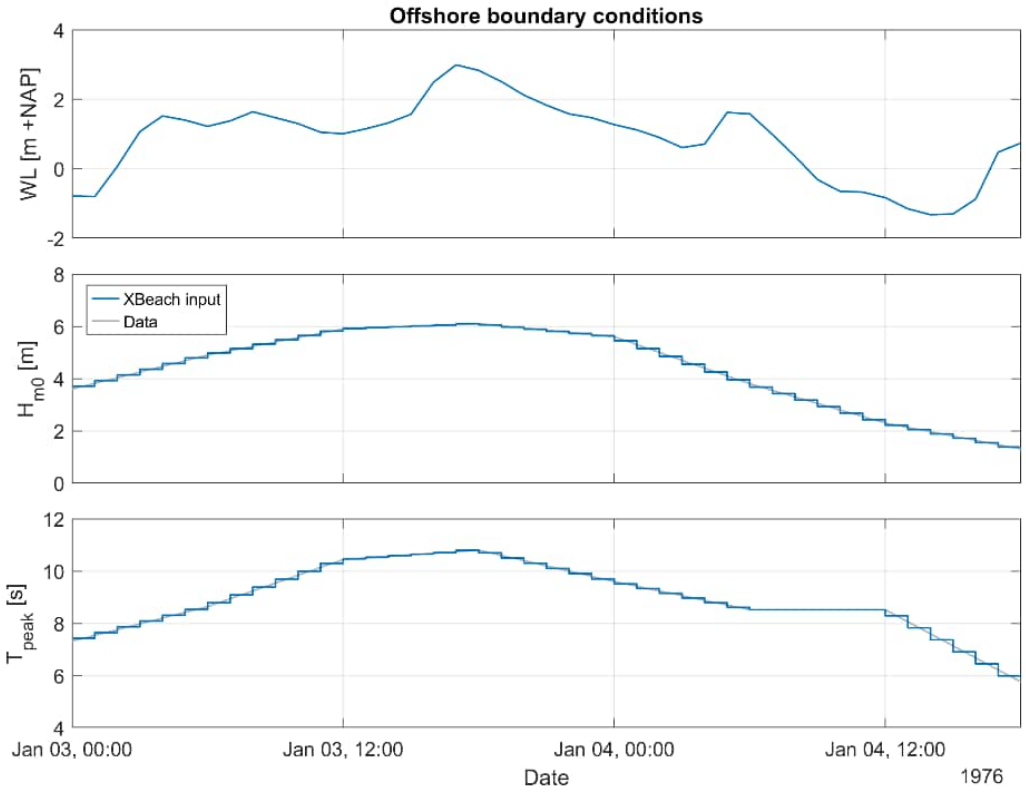

Figure C-90 Time series of all time-varying XBeach offshore hydraulic boundary conditions for the 1976 storm surge, forced on all 30 profiles.

Results

For this validation case, the simulated XBeach post-storm profiles are compared with post-storm profile measurements. Just like was the case for the pre-storm measurements, the post-storm measurements only cover the cross-shore distance from roughly the ebb waterline towards the dune foot with roughly 20 data points per profile. This results in the coverage of roughly NAP - 2 m towards NAP + 2 to 6 m over the vertical. For most profiles, the top extent of the measurement is not sufficient to assess the full erosion profile. In these cases, it is assumed that the measured profile reached the post storm dune foot and thus the measured post-storm profile is extended with a 1:1 slope towards the 1975 JarKus profile to obtain the full erosion profile. The measured dune erosion volume above storm surge level as well as the dune retreat at NAP + 4 m can then be computed.

Changes in morphology in the cross-shore profiles
From the 30 profiles that are available for comparison, Figure C-91 shows four profiles (nr. 648, 5925, 5000 and 628) that represent the different trends that are observed in all comparisons: a good fit between measured and modelled dune erosion, overestimation of the measured erosion by XBeach, underestimation and cases with incomplete data. The figures for the other profiles are included in the Additional Figures section.

- Overestimation: For among others profile 5925, the location where dune erosion starts is similar in the XBeach simulation and the measured profiles, but the XBeach dune front eroded further landward than in the measurements and the dune foot is located higher in the profile. As a result, both the simulated dune erosion volume and the maximum dune retreat distance is larger than observed.
- Underestimation: For among others profile 5000, both the simulated dune erosion volume and retreat distance is smaller than observed since the dune front displacement is smaller in the simulation. However, the dune foot in the simulated post-storm profile is still located higher in the vertical.
- Incomplete data: For among others profile 628, the post-storm profile does not clearly pass the break in profile slope representing the dune foot. The 1:1 slope to calculate dune erosion starts at the end of the available profile, which might result an underestimation of the measured dune erosion. Hence, in these cases, only a visual comparison of the measured and modelled post-storm profiles is reliable. In case of profile 628, these profiles fit quite well.

The post-storm measurements do not run far enough offshore to be able to fully compare measured and simulated sedimentation profiles. Looking at the simulated sedimentation profiles in Figure C-86 and in the Additional Figures section, it can be observed that the sedimentation behaves as expected. Eroded material is deposited offshore from the erosion profile, spread out over a large cross-shore distance, in the order of 100 meters. The deposited volume seems to be comparable to the eroded volume, indicating little to none onshore directed sediment transport in this section of the profile. Generally, where measurements are available, they show sedimentation where the simulation does, however not always in the same amount (i.e. sedimentation thickness can be slightly different).

Dune erosion volumes and dune toe retreat distances
Table C-10 shows a quantitative comparison of the measured and modelled dune erosion for 20 profiles: all profiles with apparent incomplete post-storm erosion profile measurements are excluded (10 profiles north of IJmuiden: 568, 588, 608, 628, 1085, 1115, 1175, 3700, 4900 and 4950). A scatter plot with the modelled versus measured dune erosion is shown in Figure C-92. This scatter plot shows no clear relation between the D_{50} and the difference between measured and modelled.

The dune erosion volumes range between about 20 and 70 m^3/m. The range in calculated differences between simulation and measurement for the dune erosion volume is -29% to +147% relative to the measured volumes and -19.8 to +29.8 m^3/m in absolute numbers, with an average of 13% and +1.3 m^3/m. Profile 6025 defines the maximum and is an outlier due to its profile shape (a relatively small overestimation of the retreat of the dune front resulted in a large increase in dune erosion volume since the original dune strongly increased in height over this distance, see Figure C-116). The standard deviation in the dune erosion volume difference is 12 m^3/m. In total, 11 profiles have a larger modelled dune erosion volume, and 9 profiles a smaller volume.

The dune retreat distances range between 4 and 24 m. The range in difference in dune retreat distance is somewhat smaller than that of the dune erosion volume: -46% to +11% relative to the measured distances and -4.3 to +1.7 m in absolute numbers, with an average of -19% and -1.5 m (i.e. a slight underestimation).

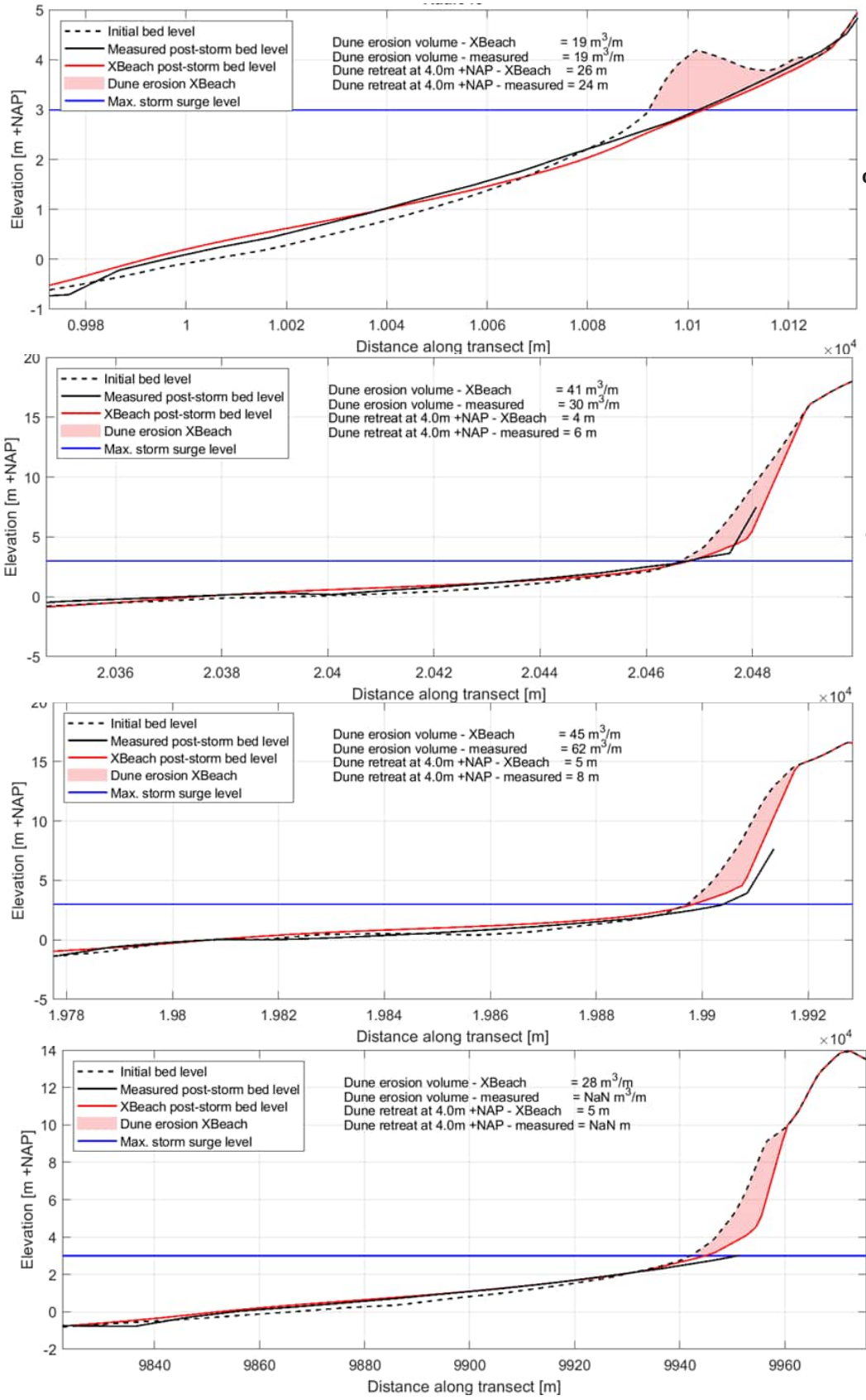

Figure C-91 Cross-section for JarKus profiles 648 (top frame), 5925 (second frame), 5000 (third frame) and 628 (bottom frame) before and after the 1976 storm based on the measurements and XBeach, including dune erosion volumes and retreat distances. Zoomed in on erosion profile.

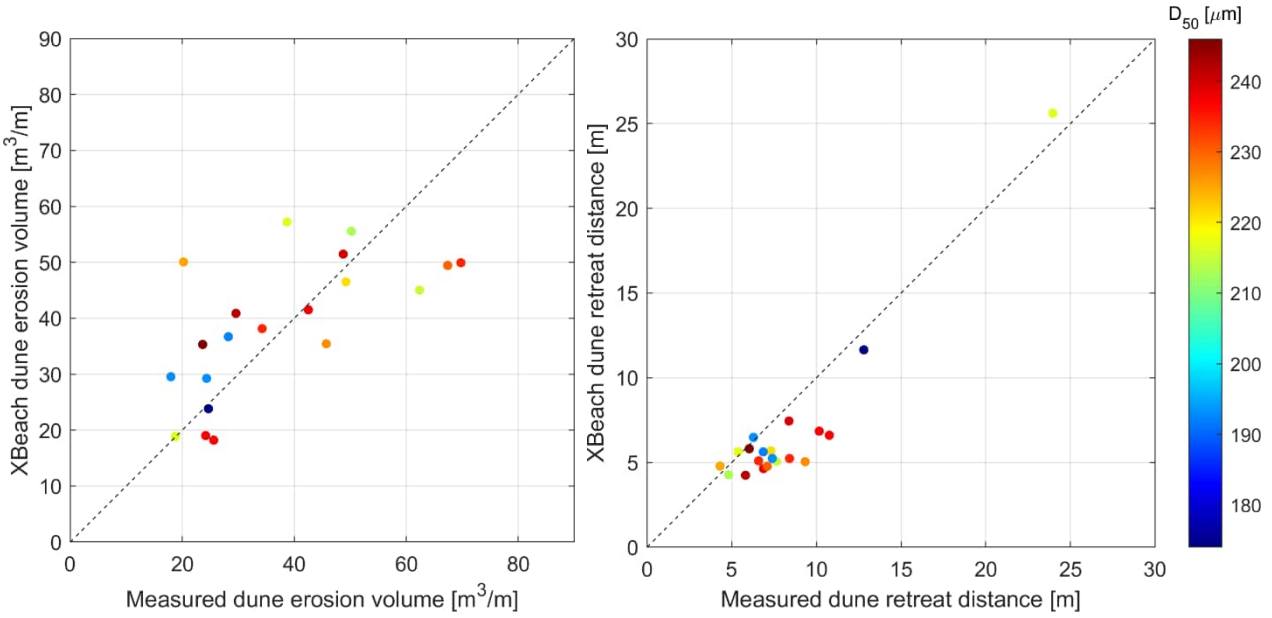

Figure C-92 Modelled versus measured dune erosion volumes and dune retreat distances for the 1976 storm along the Holland coast. The dashed line indicates a perfect fit; colours indicate the grain size used for each profile.

Table C-10 Dune erosion volume and retreat distance for the 1976 storm in the XBeach simulation and the measured profiles for the 20 profiles along the northern Holland coast with a visibly complete post-storm profile measurement. Negative differences mean underestimation of the measured values in the XBeach simulation. Colours per column indicate the degree of similarity between the simulations and observations based on all morphological cases (greener = better fit).

Profile nr.	Erosion volume				Retreat distance at NAP + 4 m			
	XBeach [m³/m]	Measured [m³/m]	Difference [m³/m]	Difference [%]	XBeach [m]	Measured [m]	Difference [m]	Difference [%]
648	19	19	0.1	0%	25.6	24.0	1.7	7%
3400	19	24	-5.2	-21%	6.8	10.2	-3.3	-33%
4000	51	49	2.7	6%	7.4	8.4	-0.9	-11%
4050	18	26	-7.4	-29%	6.6	10.8	-4.2	-39%
4100	38	34	3.9	11%	5.1	6.6	-1.5	-23%
4500	35	46	-10.3	-23%	5.0	9.3	-4.3	-46%
5000	45	62	-17.4	-28%	5.1	7.6	-2.6	-34%
5900	35	24	11.7	48%	5.8	6.0	-0.2	-4%
5925	41	30	11.3	39%	4.2	5.8	-1.6	-27%
5950	41	43	-1.0	-3%	4.6	6.9	-2.2	-33%
5975	50	70	-19.8	-28%	5.2	8.4	-3.2	-38%
6000	49	67	-18.0	-27%	4.8	7.1	-2.3	-33%
6025	50	20	29.8	147%	4.8	4.3	0.5	11%
6050	46	49	-2.7	-6%	5.7	7.3	-1.6	-22%
6075	57	39	18.5	47%	5.6	5.4	0.3	5%
6100	56	50	5.3	11%	4.3	4.8	-0.5	-11%
6500	24	25	-0.8	-3%	11.6	12.8	-1.2	-9%
7000	37	28	8.5	31%	5.6	6.9	-1.2	-18%
7050	29	24	4.9	21%	5.2	7.4	-2.2	-29%
7100	30	18	11.6	65%	6.5	6.3	0.2	3%
Average	**39**	**37**	**1.3**	**13%**	**6.8**	**8.3**	**-1.5**	**-19%**

Discussion

The modelled dune retreat distance – on average – is somewhat smaller than the measured values (bias = -1.5 m). In relation to that it is found (visually) that the shape of the simulated dune front in some cases deviates from the measured profile shape: the simulated dune erosion volume is located 'higher' in the profile compared to the observed dune erosion. The estimates of the total dune erosion volume is not negatively affected by this difference in profile shape, because the largest erosion volumes are found well above maximum storm surge level. Nevertheless, the modelled shape of the cross-shore profile close to the dune foot is a point of attention in some cases. But, for the purpose of dune safety assessment (in BOI framework) the dune erosion volume is the primary indicator, and this aspect is captured sufficiently well by XBeach. The bias in calculated volumes is limited (1.3 m^3/m, on average); with deviations up to ± ~20 m^3/m for individual cases.

Below, an overview is given of the main assumptions that were made for this validation, in order to best be able to set up the XBeach model schematizations for this case and apply measured data for comparison with simulation results. Aside from the assumptions, the grain size sensitivity in relation to the BOI parameter αD50 is discussed.

Assumptions in hydraulic boundary conditions
Some assumptions in the hydraulic boundary conditions might have resulted in an error in the XBeach dune erosion results. A water level time series that is constant in space is applied for all profiles. While water level observations along the coast show a fairly constant storm surge gradient in space for the most part, the Den Helder observation is slightly different. Especially the peak is somewhat lower, but lasts longer and occurs slightly later in comparison. This is not accounted for in the simulations and might lead to (minor) errors in the simulations of the northern profiles.

A wave forcing time series that is uniform along the coast is applied for all profiles. The two wave measurement time series that are available cover most of the study area and show that this is a reasonable assumption. However, the wave field closer to Den Helder might be increasingly different because of the shape of the coastline. In addition, an assumption was made for the peak period being 1.2 times larger than the observed mean period. Lastly, as no data were available on the wave spreading, the BOI default of 6 was applied, constant in space and time.

Extrapolation of post-storm profiles
The available measurements for the pre- and post-storm profile cover a cross-shore section generally limited to NAP - 2 m and NAP + 6 m, but sometimes less. While this is not much of an issue for the pre-storm profile, as the measurement is much in agreement with the JarKus profile data of 1975, it can provide an issue to deduce the full post-storm profile and corresponding dune erosion volumes and retreat distances. To complete the post-storm profile, it is extended upwards with a 1:1 slope. However, this introduced an uncertainty in the measured dune erosion volumes and distances. In the quantitative comparison, many (10) northern profiles are excluded since it is uncertain where the post-storm dune foot is located and hence no realistic 1:1 slope could be fitted.

Grain size sensitivity
Figure C-93 shows the grain size dependency of the measured and modelled dune erosion for the 20 profiles. Surprisingly, the 'measured' dune erosion volumes seem to increase on average with the D_{50}, although the scatter is large. On the other hand, the measured dune retreat distances decrease on average with increasing D_{50}, as expected. In the XBeach simulations , both the dune erosion volumes and retreat distances show a similar trend as the measured values. Overall, this indicates that the current grain size dependence (with $\alpha D_{50} = 0.4$) is fine for this field case.

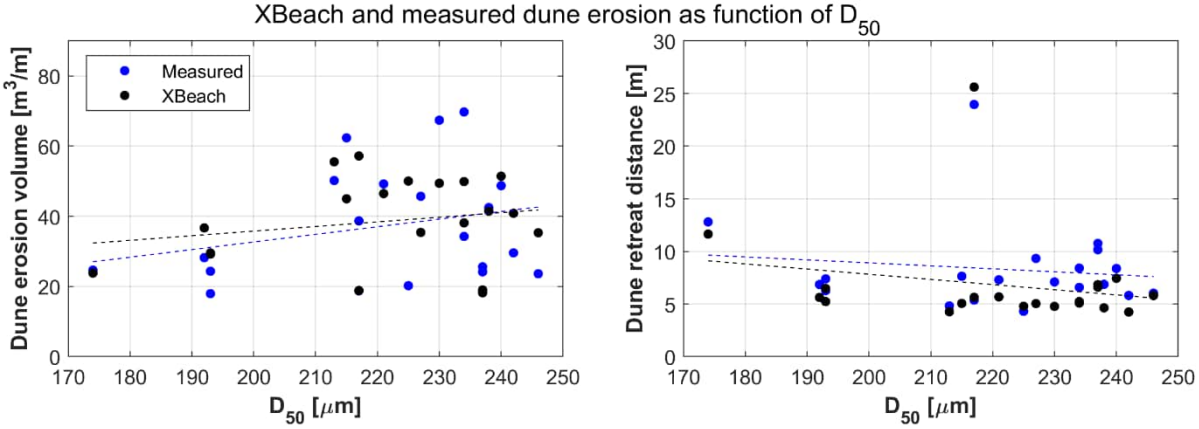

Figure C-93 Modelled (black dots) and measured (blue dots) dune erosion volumes (left) and dune retreat distances (right) as function of the median grainsize of each profile in the Holland 1976 storm case. Only the 20 profiles with a measured post-storm profile that includes the dune foot are included. The dashed lines are linear trendlines through the data.

General findings
Overall, some general findings of this case study are:

- The model performs well regarding the dune erosion volumes: the average dune erosion volumes are not biased if compared to the measured profiles (difference of 1 m^3/m or 3%), although the individual profiles show deviations up to ± ~20 m^3/m (std.dev.=12 m^3/m).
- The measured dune retreat is underestimated by the simulations by 1.5 m or 18% on average.
- The distribution of the simulated dune erosion volume seems to be located higher in the vertical than measured, contributing to the difference in dune retreat when compared at a fixed level of 1 meter above maximum storm surge level.
- Where the post-storm measurement includes (part of) the dune front, it often appears a little less steep than the simulated post storm dune front, which is 1:1 as a result of the BOI dry slope setting.
- Based on the similar trend in dune erosion volume and retreat distances with the D_{50} for the XBeach simulations and the measured profiles, the sensitivity to grain size diameter (αD_{50} parameter) is set correctly for this field case.

Conclusion

The goal of this validation case was a morphodynamic comparison of the observed and simulated impact of the 1976 storm surge event that resulted in about 20 to 70 m^3/m dune erosion. Due to availability of measurements for both hydrodynamics and pre and post storm coastal profiles, it was possible to schematize the input files for 30 XBeach simulations and compare the outcome with observations. Of those 30 profiles, 20 seemed to be eligible for the assessment of the morphodynamic performance of XBeach. On average, the model performed well as the modelled dune erosion volumes did not show a substantial bias with the measurements, although the variation between the individual profiles is relatively large (std.dev. of 12 m^3/m).

The post-storm profile shape was produced less well, as the dune erosion appeared higher in the vertical than in the measurements and the post-storm dune front seemed slightly steeper than in the measurements. This resulted in the underestimation of the dune retreat distances by the model that are measured at a fixed height of 1 m above the maximum storm surge level. Lastly, the sensitivity to the grainsize (αD_{50} setting) seems to be correct for this field case.

Overall, it is concluded that XBeach, with the current BOI settings, generally is well capable of reproducing observed dune erosion along the Holland Coast for the 1976 storm event.

Additional figures

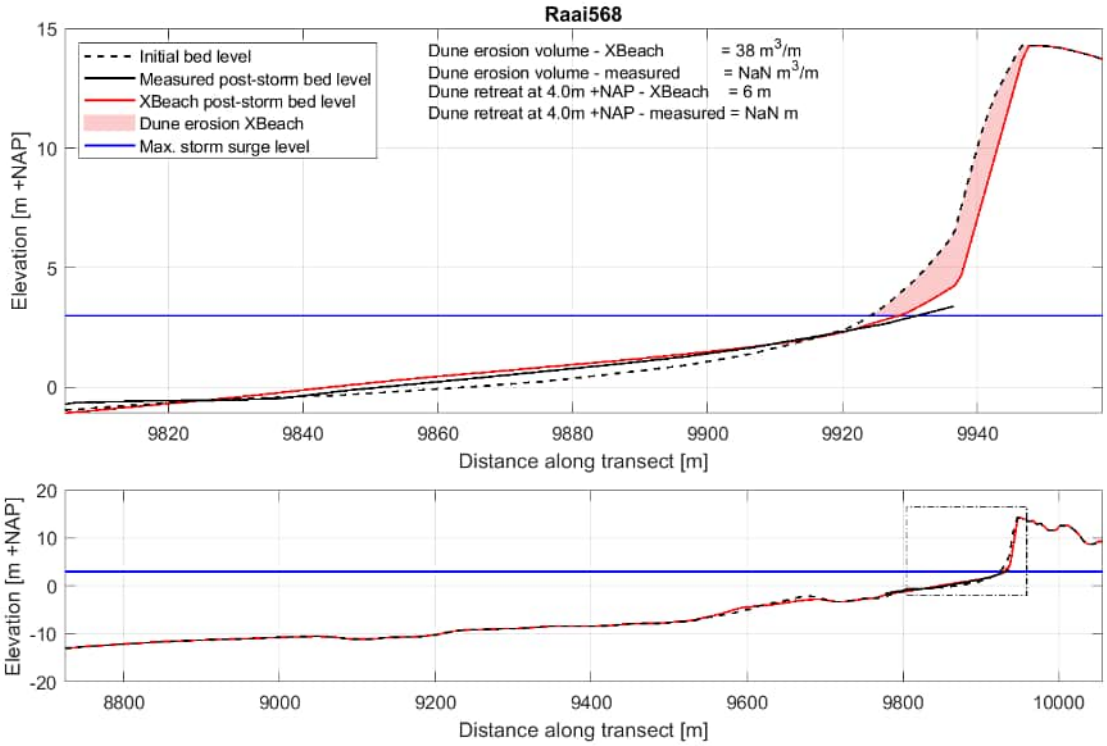

Figure C-94 Cross-section profile 568 before and after the 1976 storm based on the measurements and XBeach, including dune erosion volumes and retreat distances. Bottom: entire XBeach profile, top: zoom of beach and dune profile.

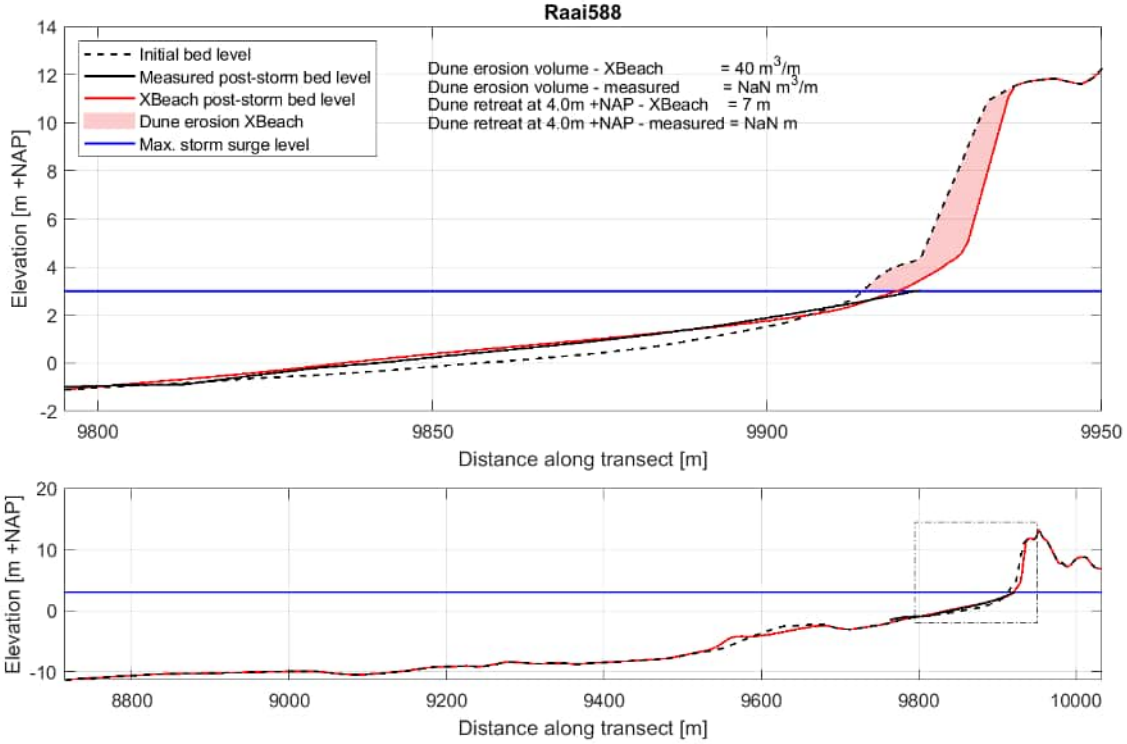

Figure C-95 Cross-section profile 588 before and after the 1976 storm based on the measurements and XBeach, including dune erosion volumes and retreat distances. Bottom: entire XBeach profile, top: zoom of beach and dune profile.

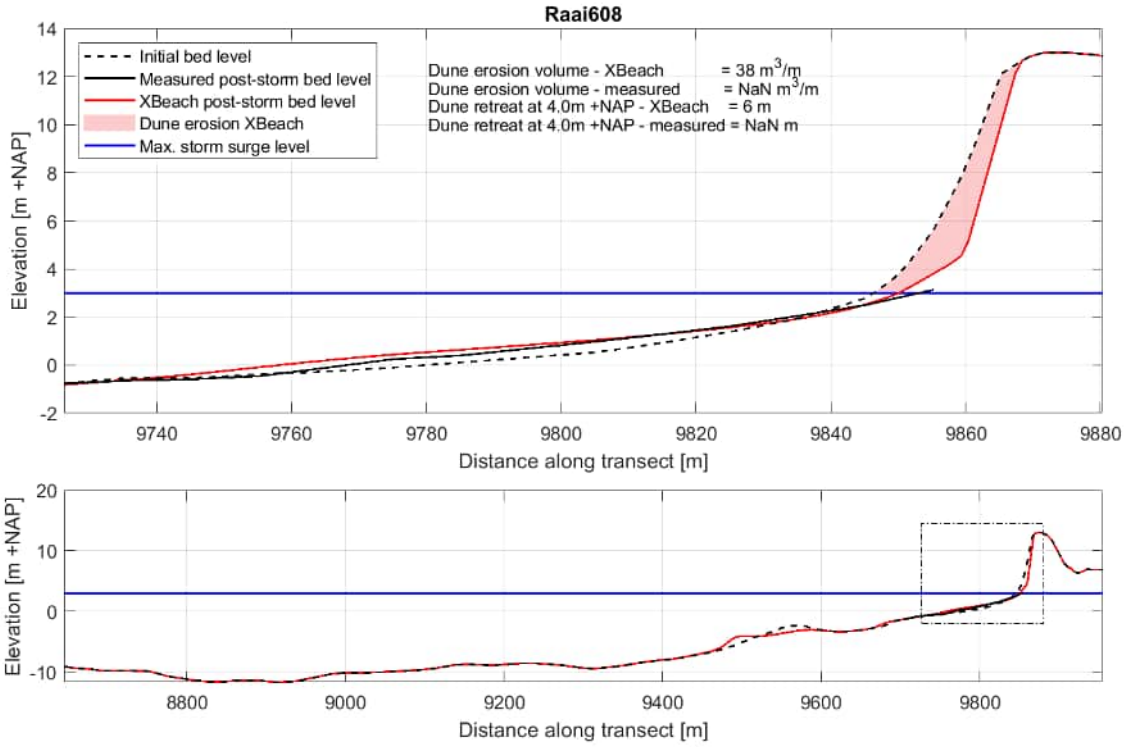

Figure C-96 Cross-section profile 608 before and after the 1976 storm based on the measurements and XBeach, including dune erosion volumes and retreat distances. Bottom: entire XBeach profile, top: zoom of beach and dune profile.

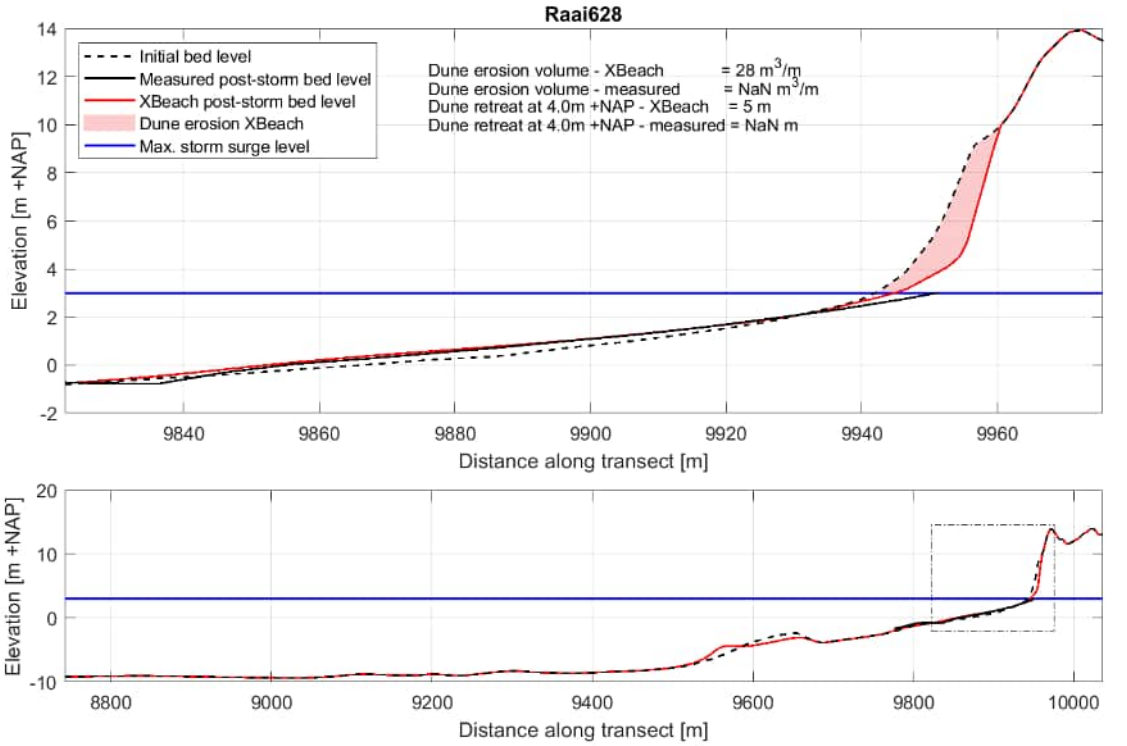

Figure C-97 Cross-section profile 628 before and after the 1976 storm based on the measurements and XBeach, including dune erosion volumes and retreat distances. Bottom: entire XBeach profile, top: zoom of beach and dune profile.

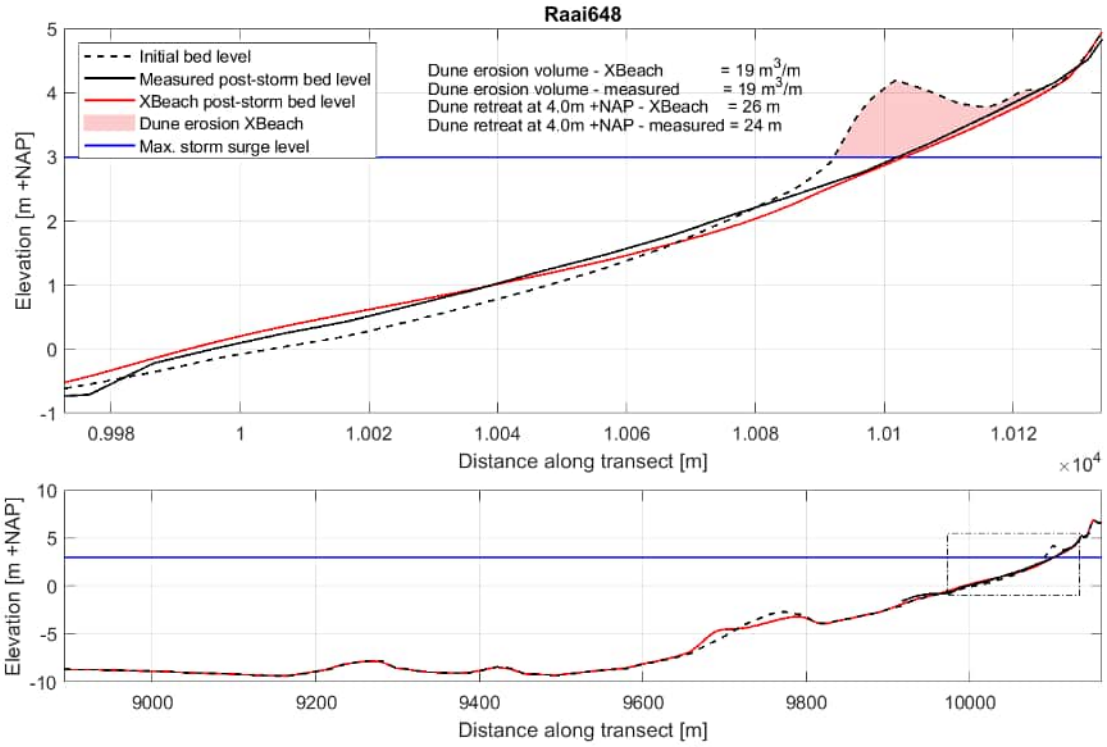

Figure C-98 Cross-section profile 648 before and after the 1976 storm based on the measurements and XBeach, including dune erosion volumes and retreat distances. Bottom: entire XBeach profile, top: zoom of beach and dune profile.

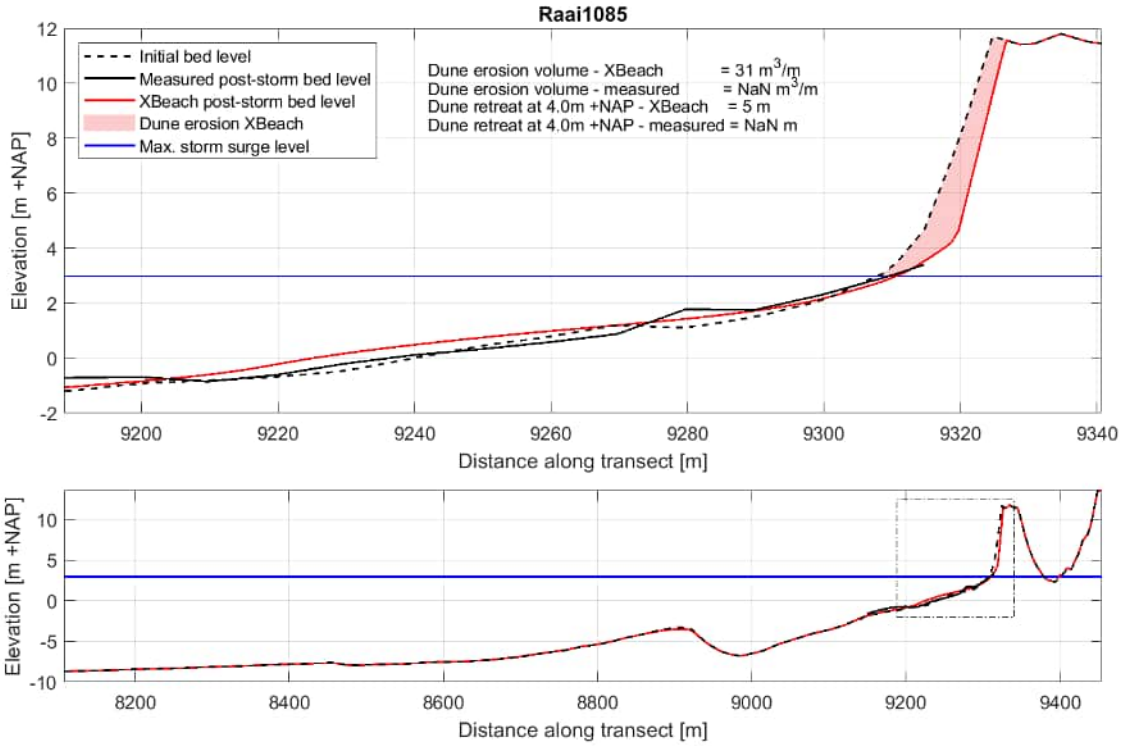

Figure C-99 Cross-section profile 1085 before and after the 1976 storm based on the measurements and XBeach, including dune erosion volumes and retreat distances. Bottom: entire XBeach profile, top: zoom of beach and dune profile.

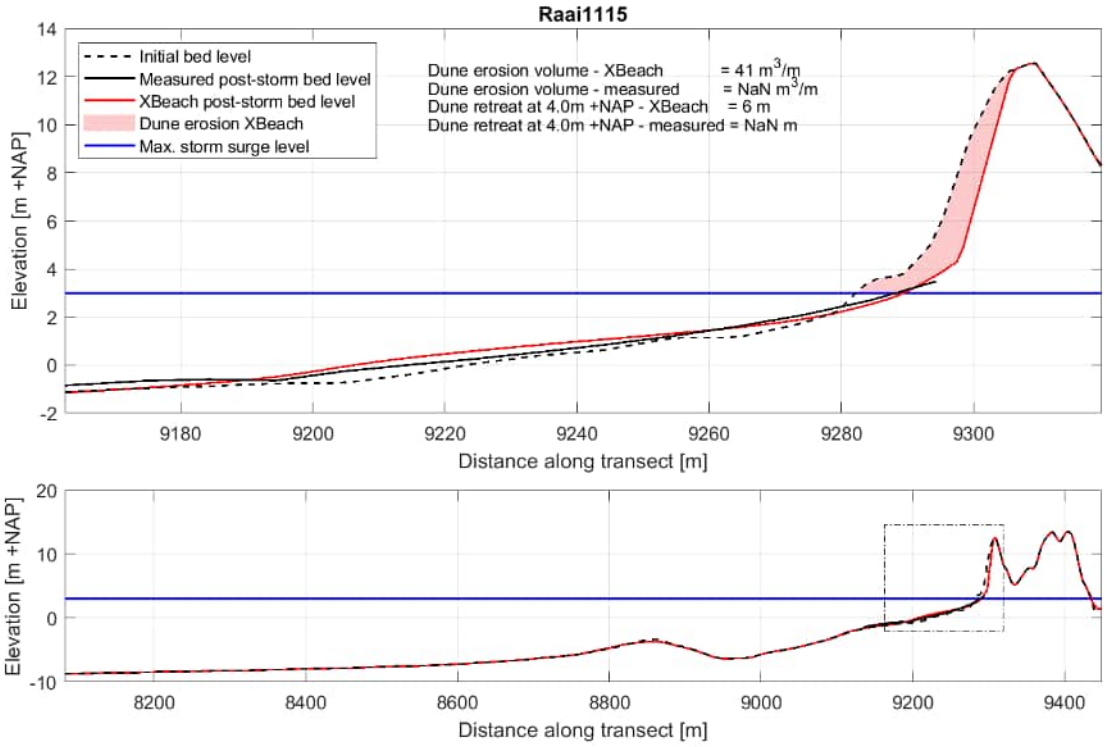

Figure C-100 Cross-section profile 1115 before and after the 1976 storm based on the measurements and XBeach, including dune erosion volumes and retreat distances. Bottom: entire XBeach profile, top: zoom of beach and dune profile.

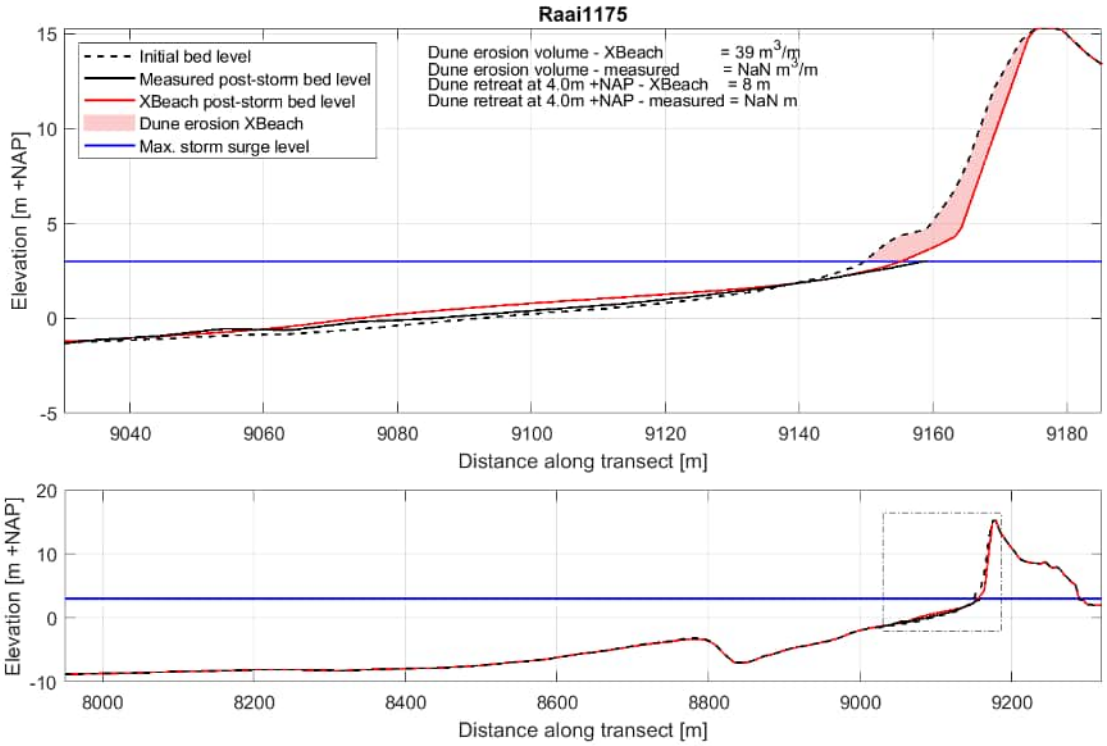

Figure C-101 Cross-section profile 1175 before and after the 1976 storm based on the measurements and XBeach, including dune erosion volumes and retreat distances. Bottom: entire XBeach profile, top: zoom of beach and dune profile.

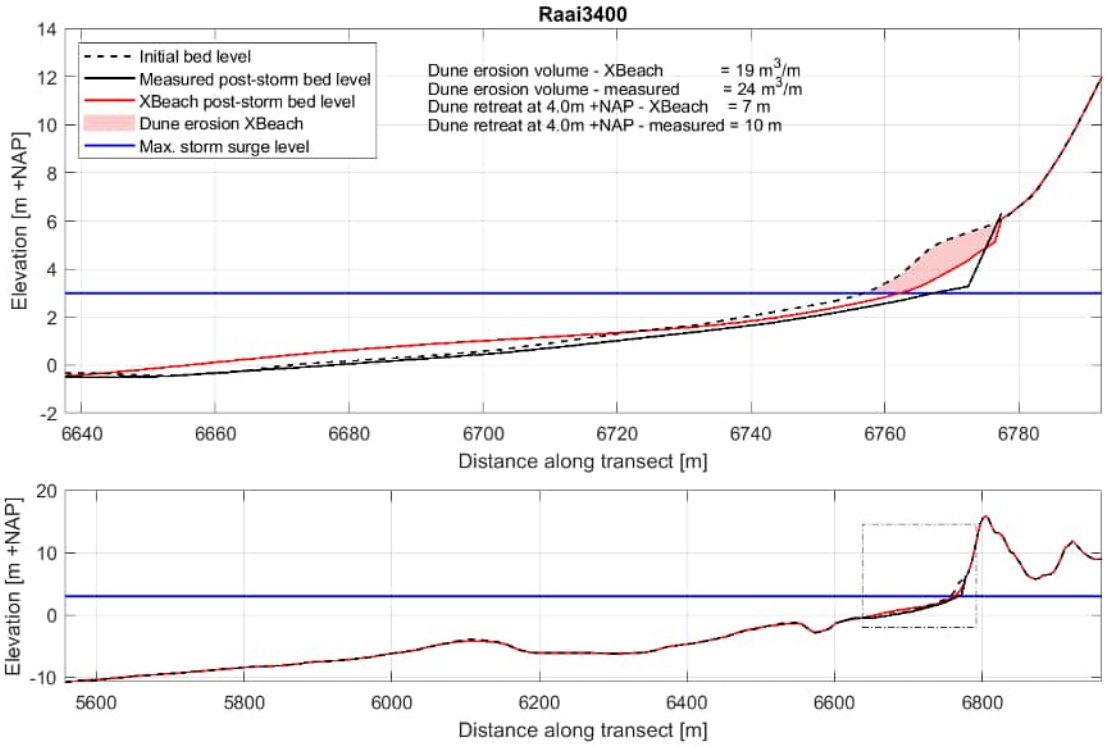

Figure C-102 Cross-section profile 3400 before and after the 1976 storm based on the measurements and XBeach, including dune erosion volumes and retreat distances. Bottom: entire XBeach profile, top: zoom of beach and dune profile.

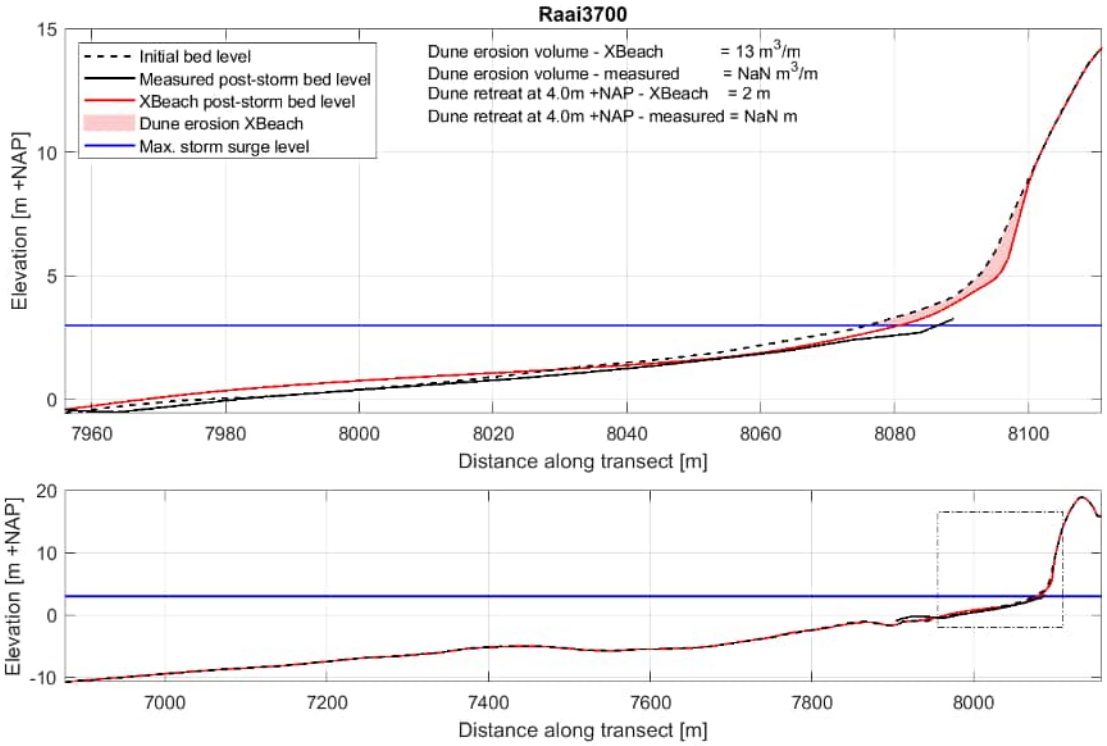

Figure C-103 Cross-section profile 3700 before and after the 1976 storm based on the measurements and XBeach, including dune erosion volumes and retreat distances. Bottom: entire XBeach profile, top: zoom of beach and dune profile.

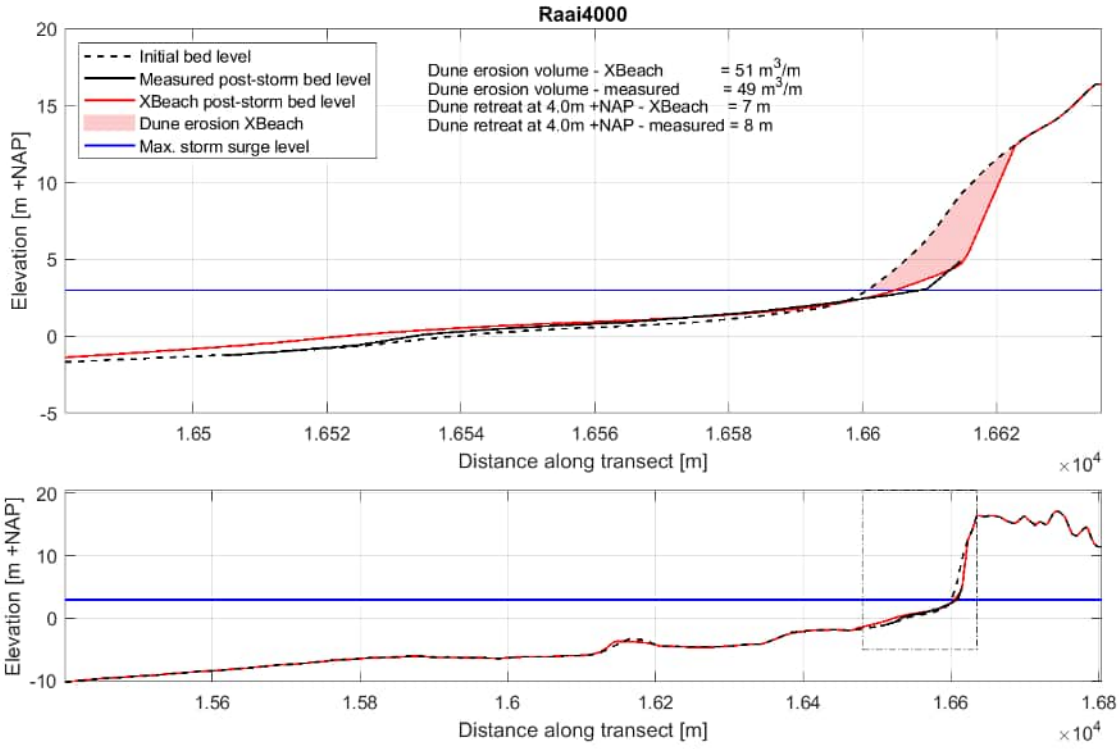

Figure C-104 Cross-section profile 4000 before and after the 1976 storm based on the measurements and XBeach, including dune erosion volumes and retreat distances. Bottom: entire XBeach profile, top: zoom of beach and dune profile.

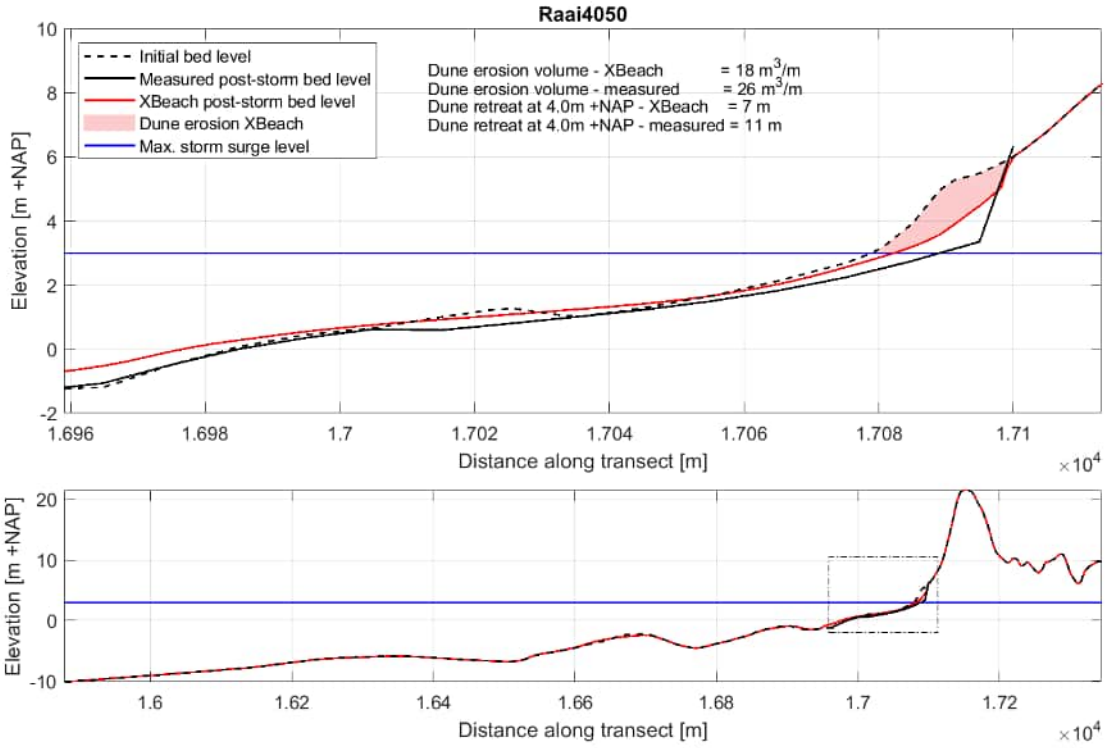

Figure C-105 Cross-section profile 4050 before and after the 1976 storm based on the measurements and XBeach, including dune erosion volumes and retreat distances. Bottom: entire XBeach profile, top: zoom of beach and dune profile.

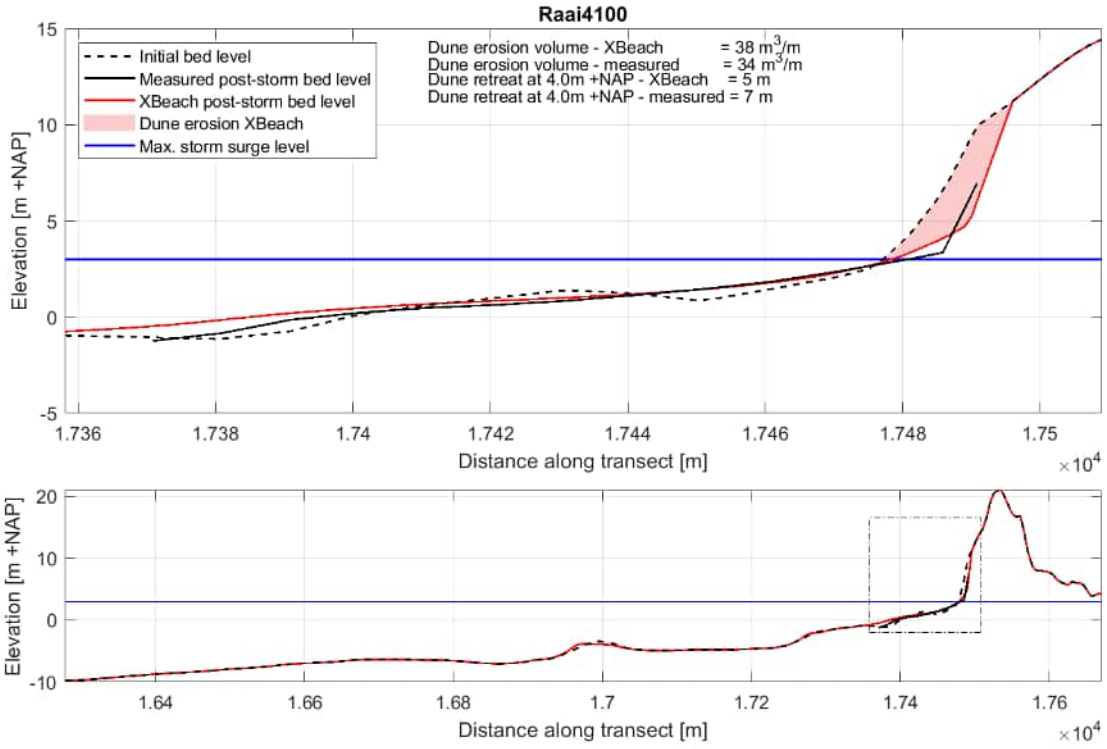

Figure C-106 Cross-section profile 4100 before and after the 1976 storm based on the measurements and XBeach, including dune erosion volumes and retreat distances. Bottom: entire XBeach profile, top: zoom of beach and dune profile.

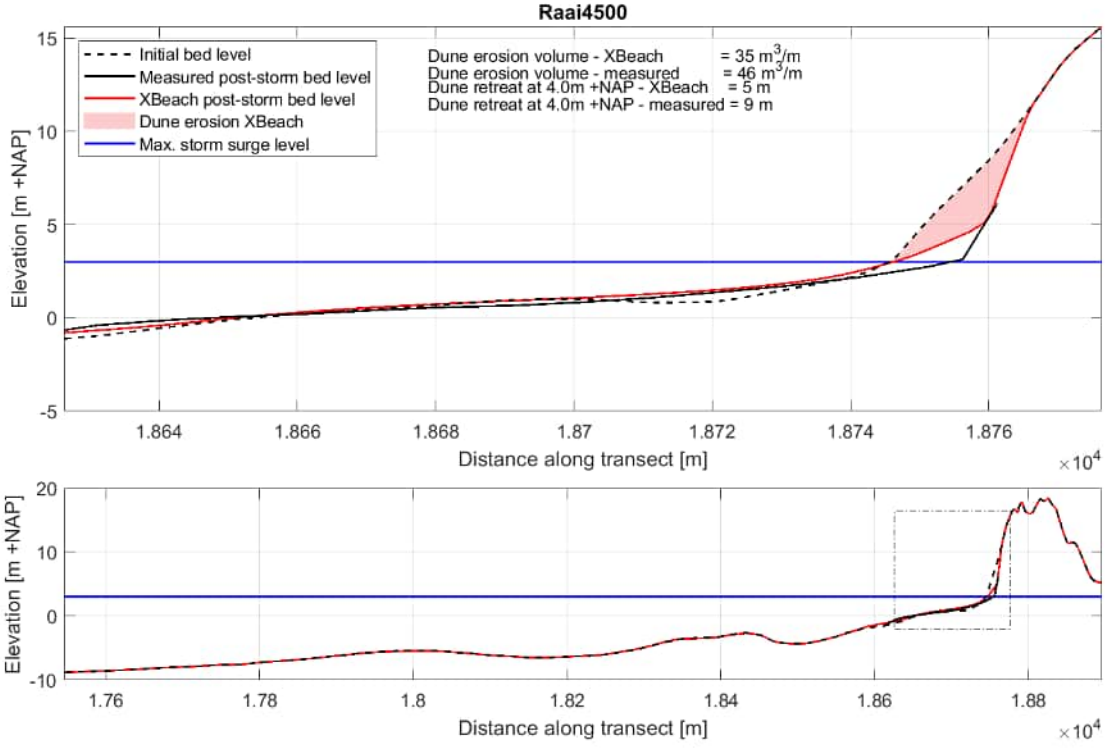

Figure C-107 Cross-section profile 4500 before and after the 1976 storm based on the measurements and XBeach, including dune erosion volumes and retreat distances. Bottom: entire XBeach profile, top: zoom of beach and dune profile.

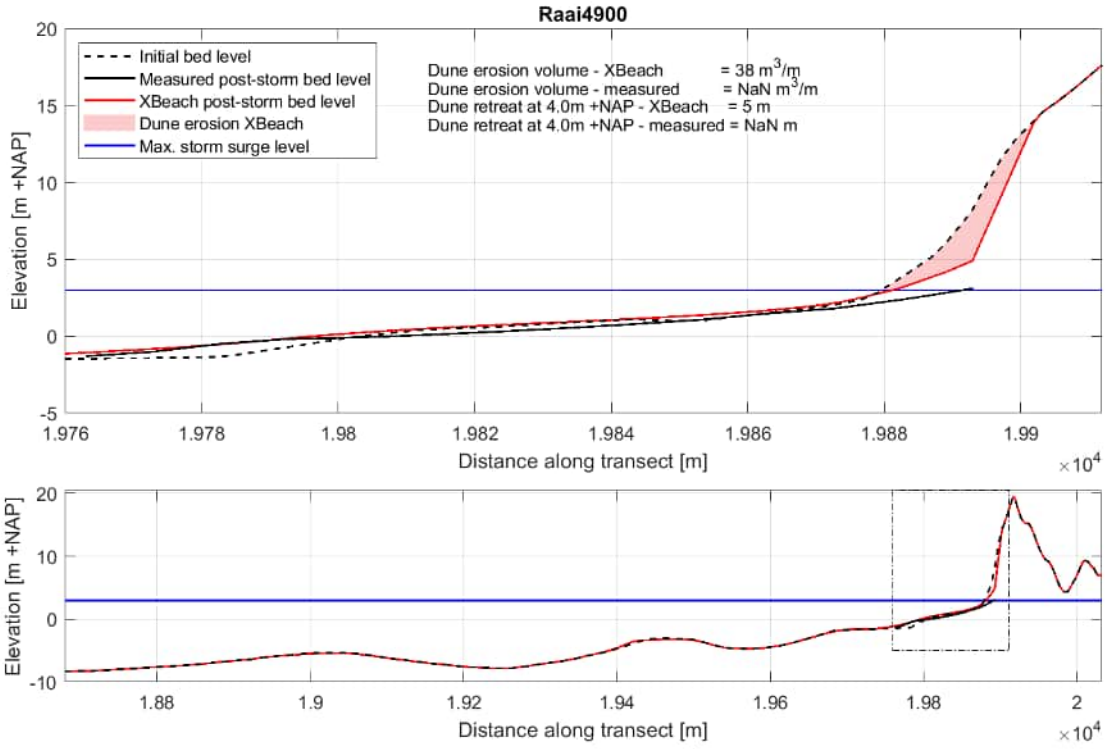

Figure C-108 Cross-section profile 4900 before and after the 1976 storm based on the measurements and XBeach, including dune erosion volumes and retreat distances. Bottom: entire XBeach profile, top: zoom of beach and dune profile.

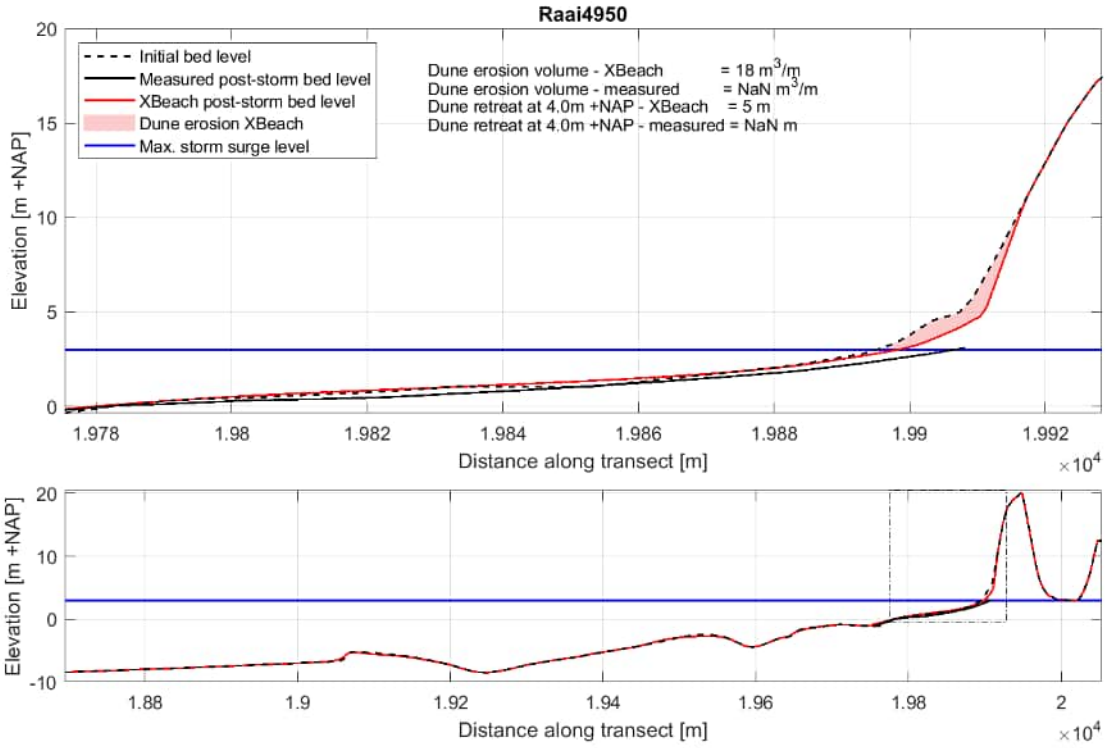

Figure C-109 Cross-section profile 4950 before and after the 1976 storm based on the measurements and XBeach, including dune erosion volumes and retreat distances. Bottom: entire XBeach profile, top: zoom of beach and dune profile.

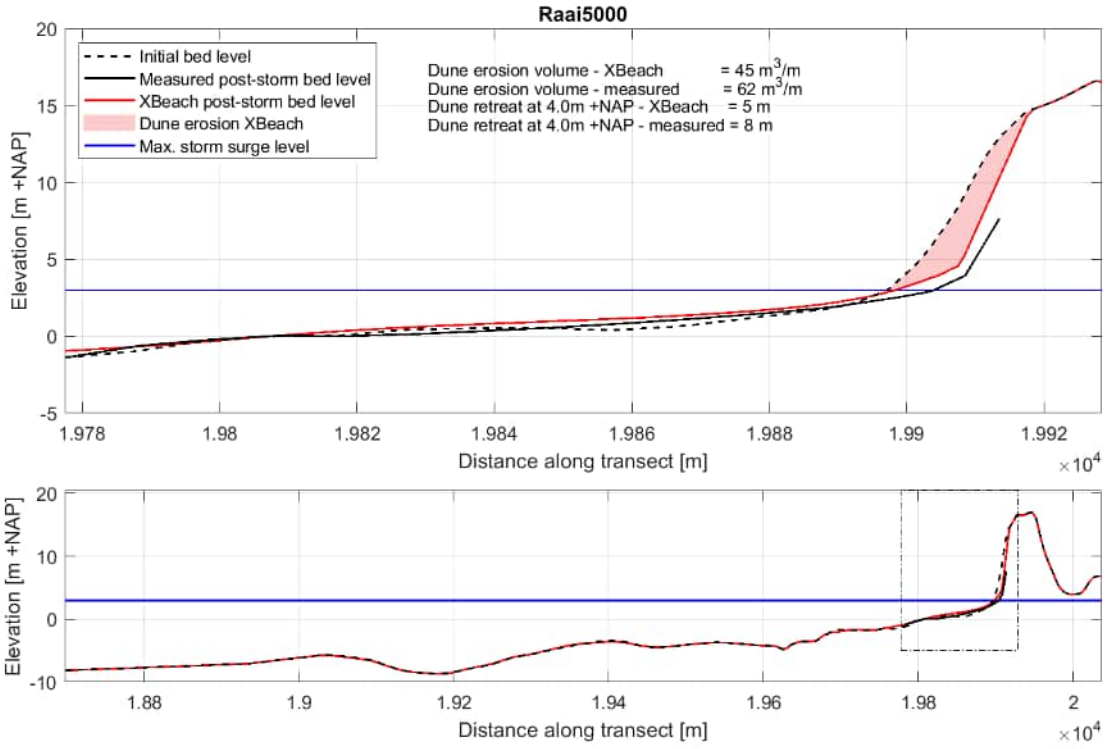

Figure C-110 Cross-section profile 5000 before and after the 1976 storm based on the measurements and XBeach, including dune erosion volumes and retreat distances. Bottom: entire XBeach profile, top: zoom of beach and dune profile.

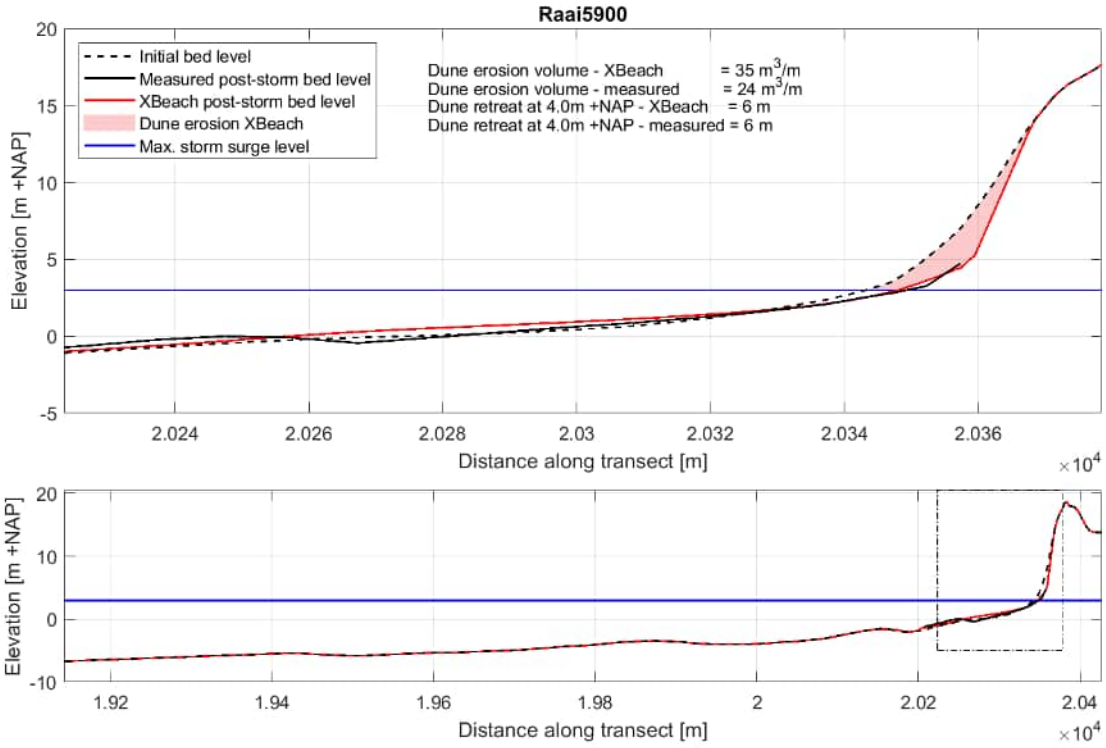

Figure C-111 Cross-section profile 5900 before and after the 1976 storm based on the measurements and XBeach, including dune erosion volumes and retreat distances. Bottom: entire XBeach profile, top: zoom of beach and dune profile.

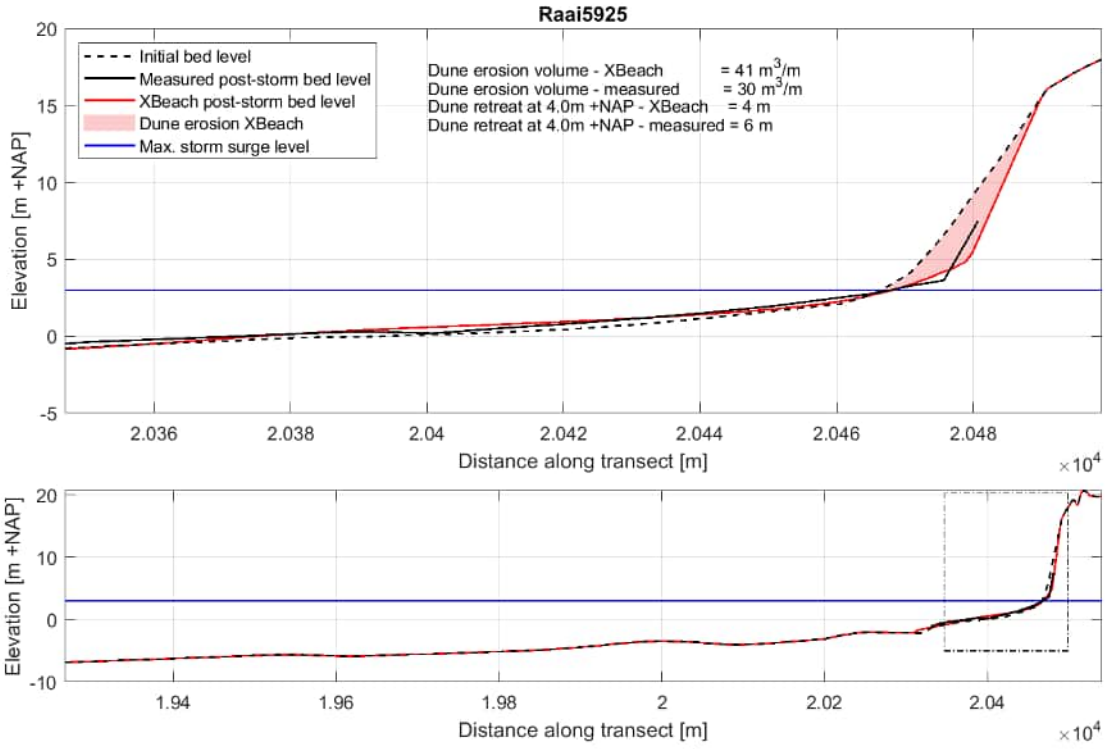

Figure C-112 Cross-section profile 5925 before and after the 1976 storm based on the measurements and XBeach, including dune erosion volumes and retreat distances. Bottom: entire XBeach profile, top: zoom of beach and dune profile.

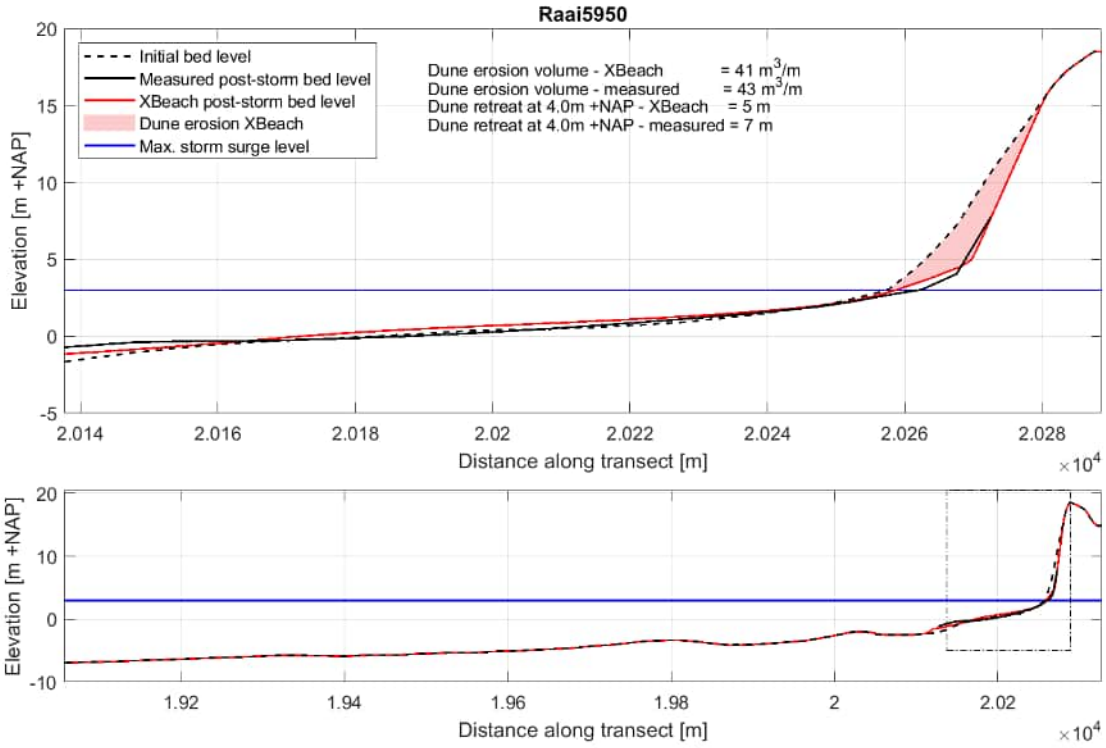

Figure C-113 Cross-section profile 5950 before and after the 1976 storm based on the measurements and XBeach, including dune erosion volumes and retreat distances. Bottom: entire XBeach profile, top: zoom of beach and dune profile.

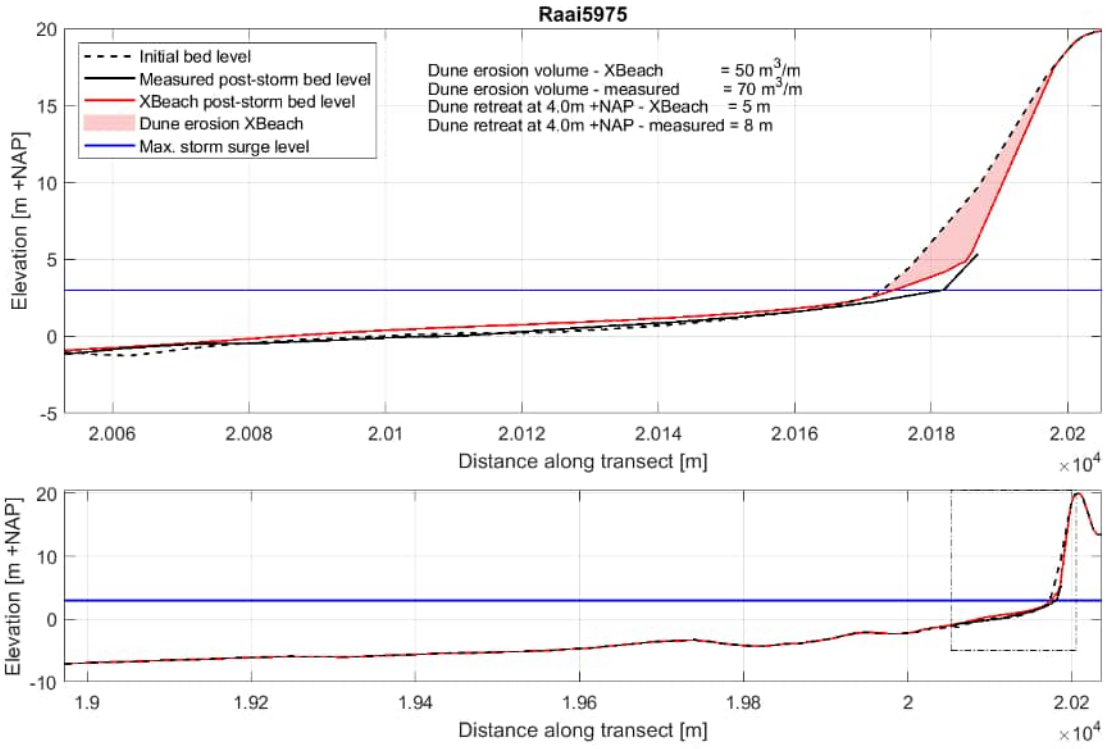

Figure C-114 Cross-section profile 5975 before and after the 1976 storm based on the measurements and XBeach, including dune erosion volumes and retreat distances. Bottom: entire XBeach profile, top: zoom of beach and dune profile.

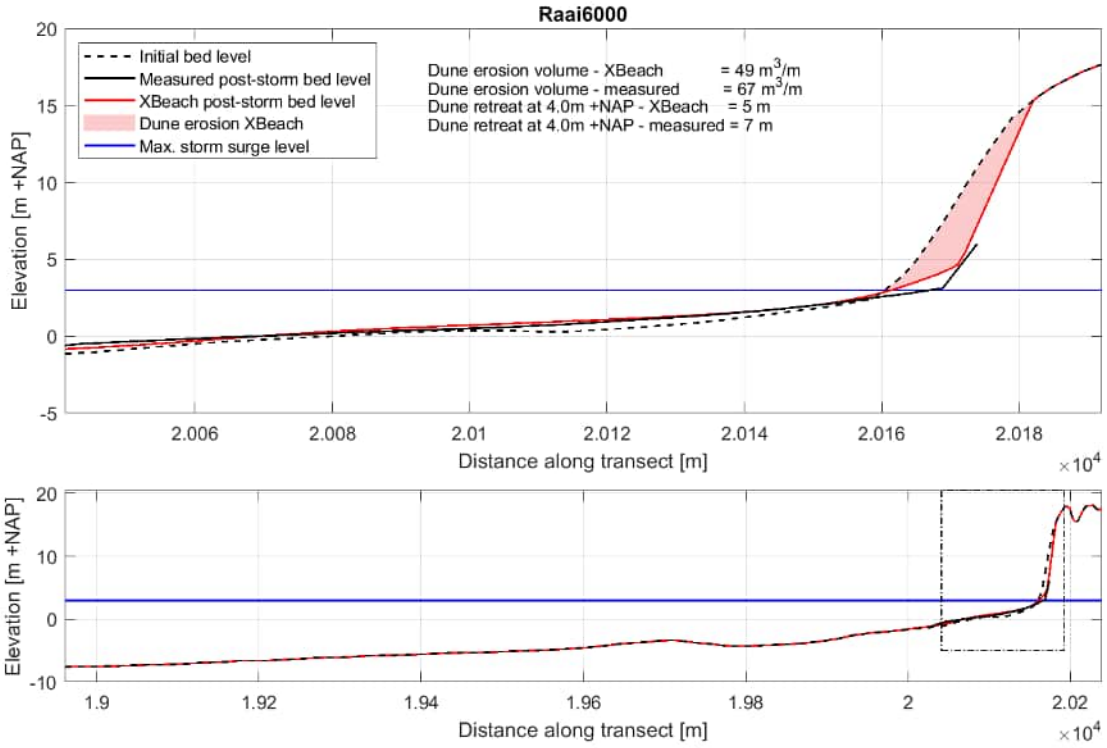

Figure C-115 Cross-section profile 6000 before and after the 1976 storm based on the measurements and XBeach, including dune erosion volumes and retreat distances. Bottom: entire XBeach profile, top: zoom of beach and dune profile.

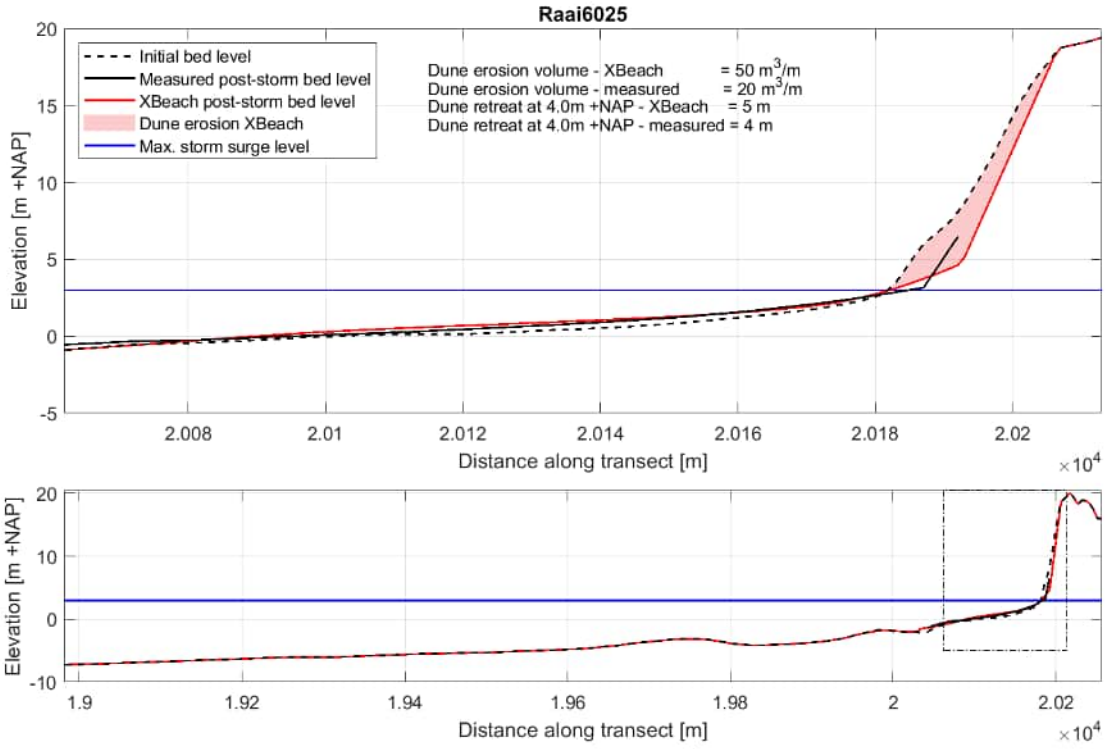

Figure C-116 Cross-section profile 6025 before and after the 1976 storm based on the measurements and XBeach, including dune erosion volumes and retreat distances. Bottom: entire XBeach profile, top: zoom of beach and dune profile.

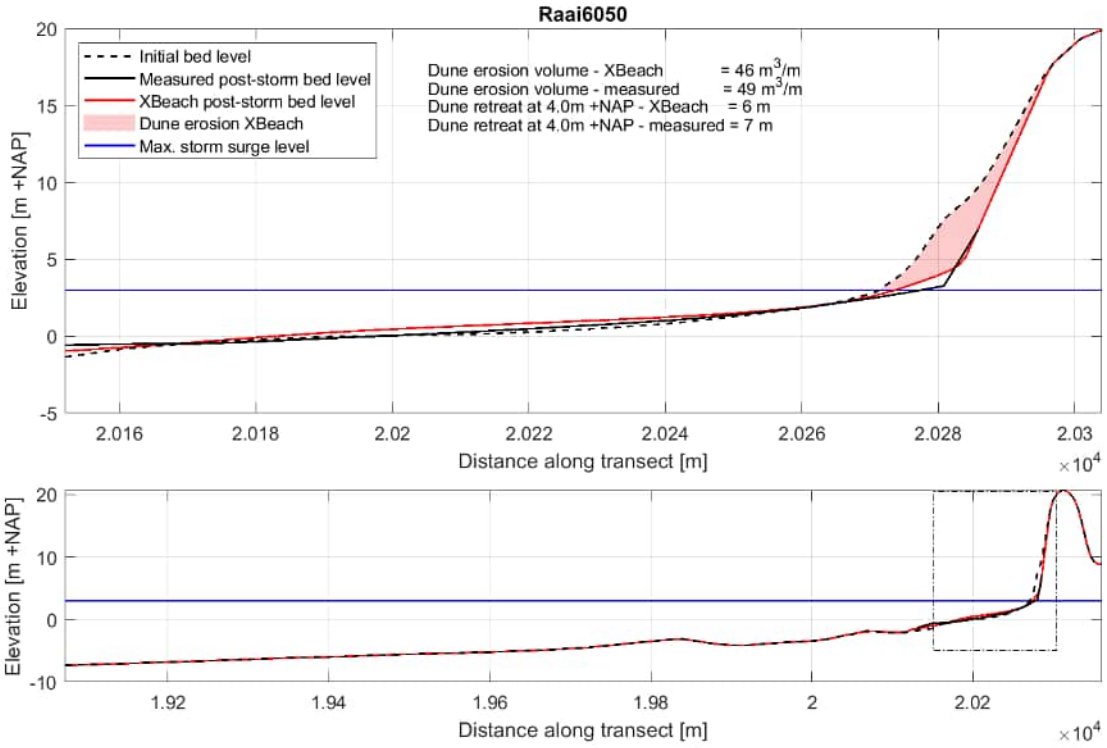

Figure C-117 Cross-section profile 6050 before and after the 1976 storm based on the measurements and XBeach, including dune erosion volumes and retreat distances. Bottom: entire XBeach profile, top: zoom of beach and dune profile.

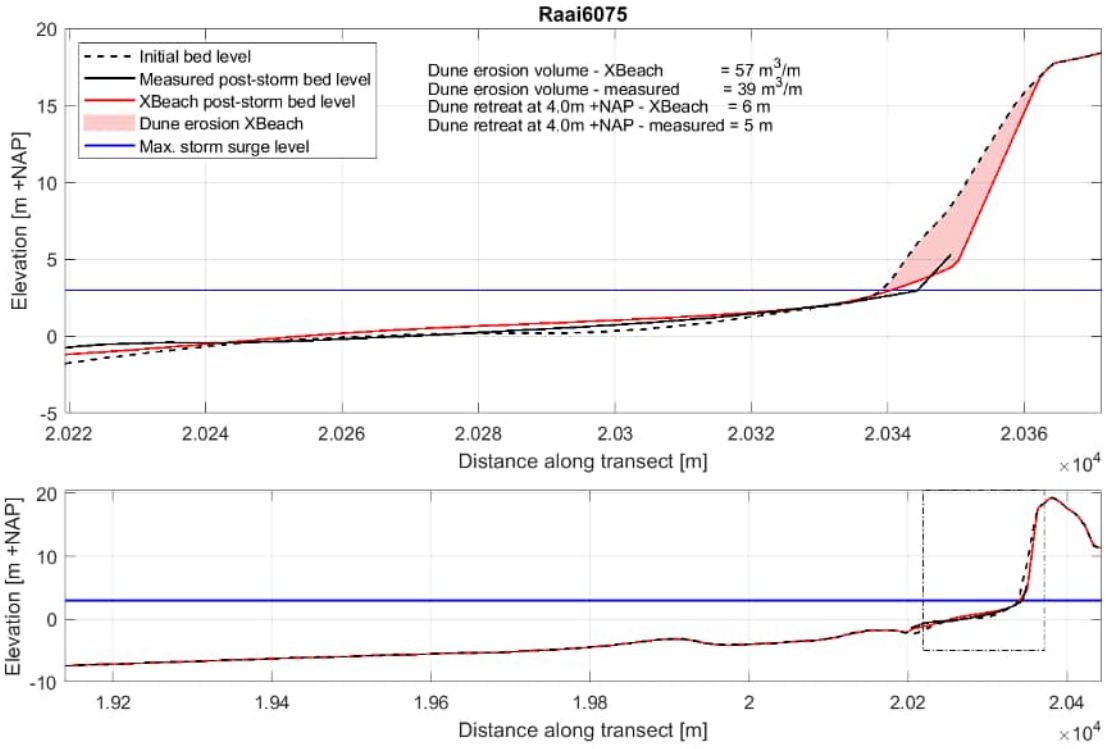

Figure C-118 Cross-section profile 6075 before and after the 1976 storm based on the measurements and XBeach, including dune erosion volumes and retreat distances. Bottom: entire XBeach profile, top: zoom of beach and dune profile.

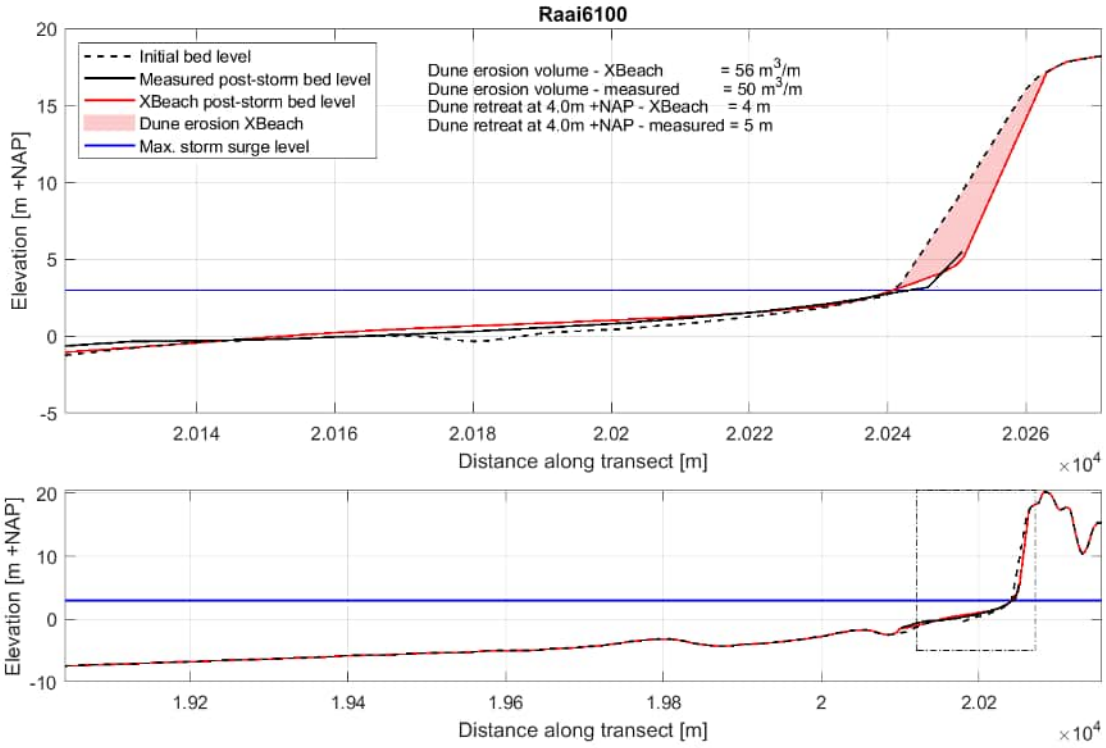

Figure C-119 Cross-section profile 6100 before and after the 1976 storm based on the measurements and XBeach, including dune erosion volumes and retreat distances. Bottom: entire XBeach profile, top: zoom of beach and dune profile.

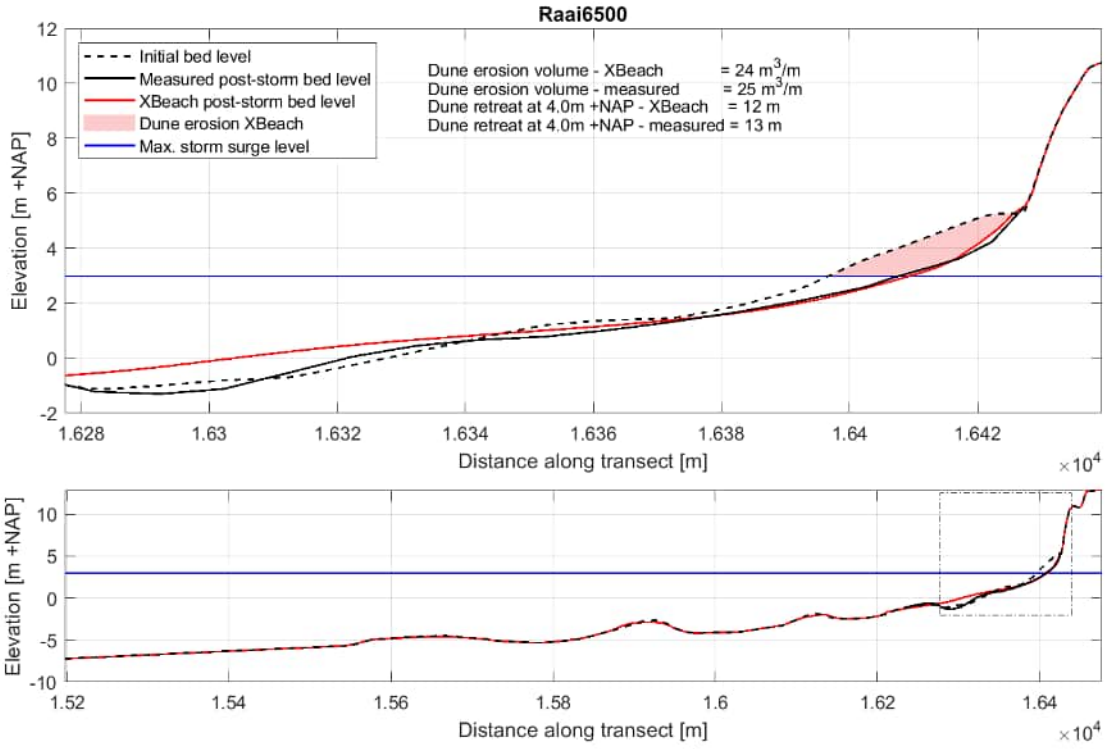

Figure C-120 Cross-section profile 6500 before and after the 1976 storm based on the measurements and XBeach, including dune erosion volumes and retreat distances. Bottom: entire XBeach profile, top: zoom of beach and dune profile.

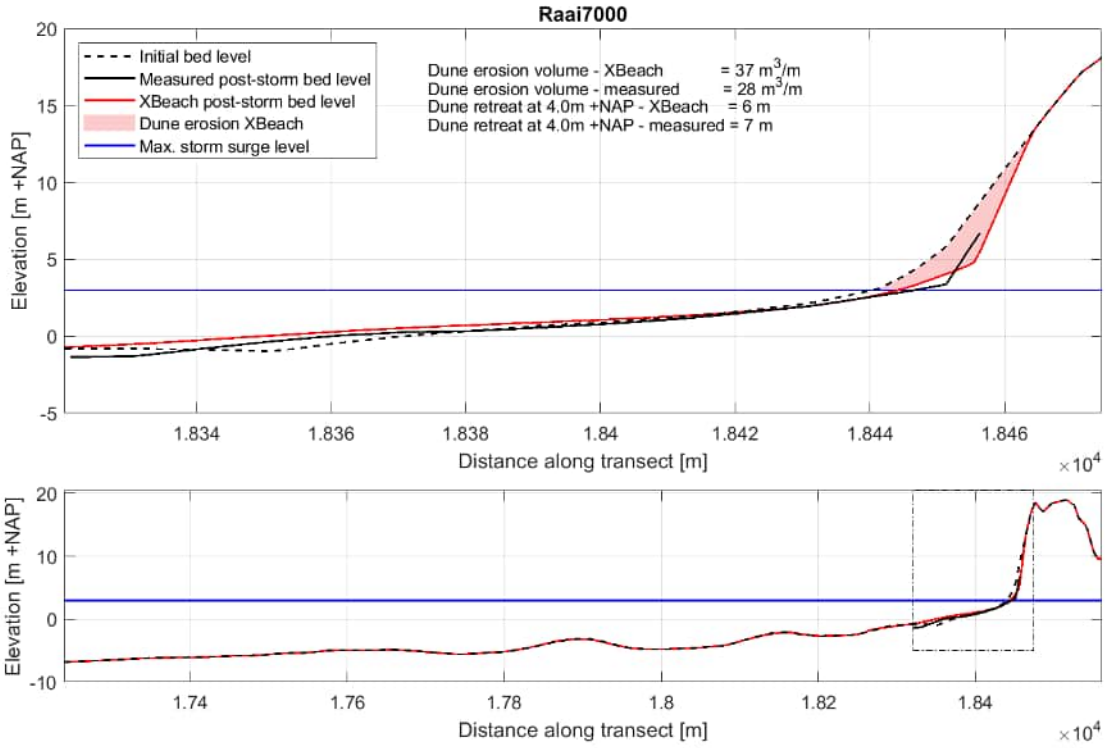

Figure C-121 Cross-section profile 7000 before and after the 1976 storm based on the measurements and XBeach, including dune erosion volumes and retreat distances. Bottom: entire XBeach profile, top: zoom of beach and dune profile.

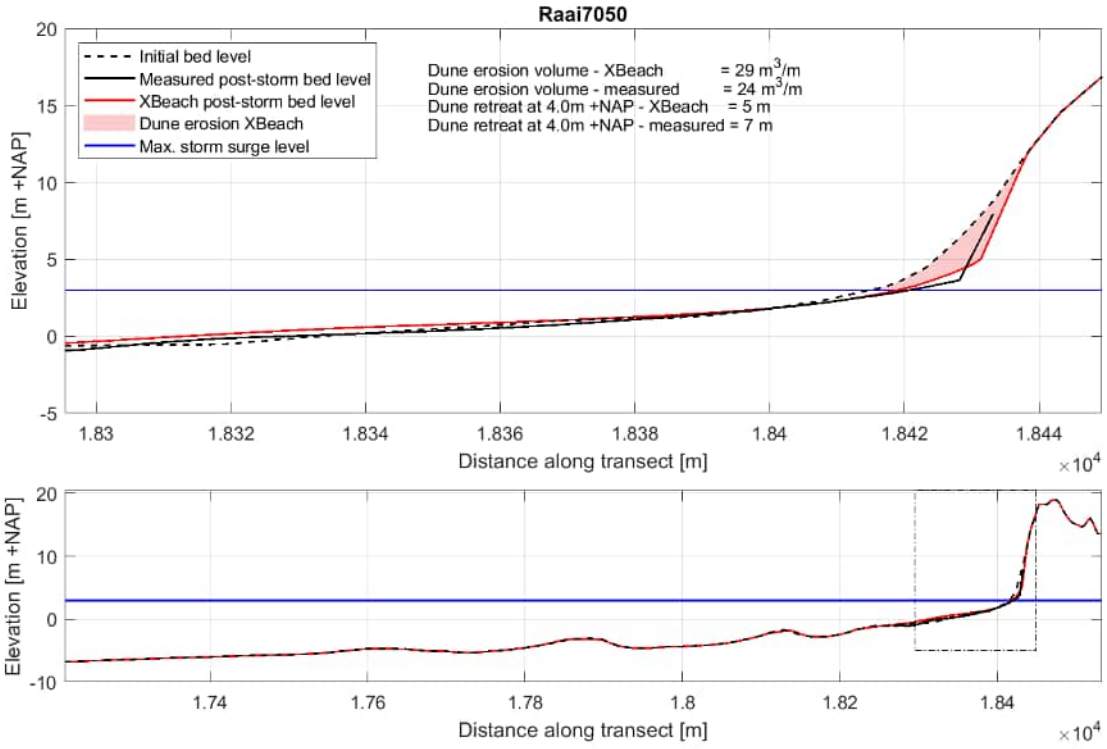

Figure C-122 Cross-section profile 7050 before and after the 1976 storm based on the measurements and XBeach, including dune erosion volumes and retreat distances. Bottom: entire XBeach profile, top: zoom of beach and dune profile.

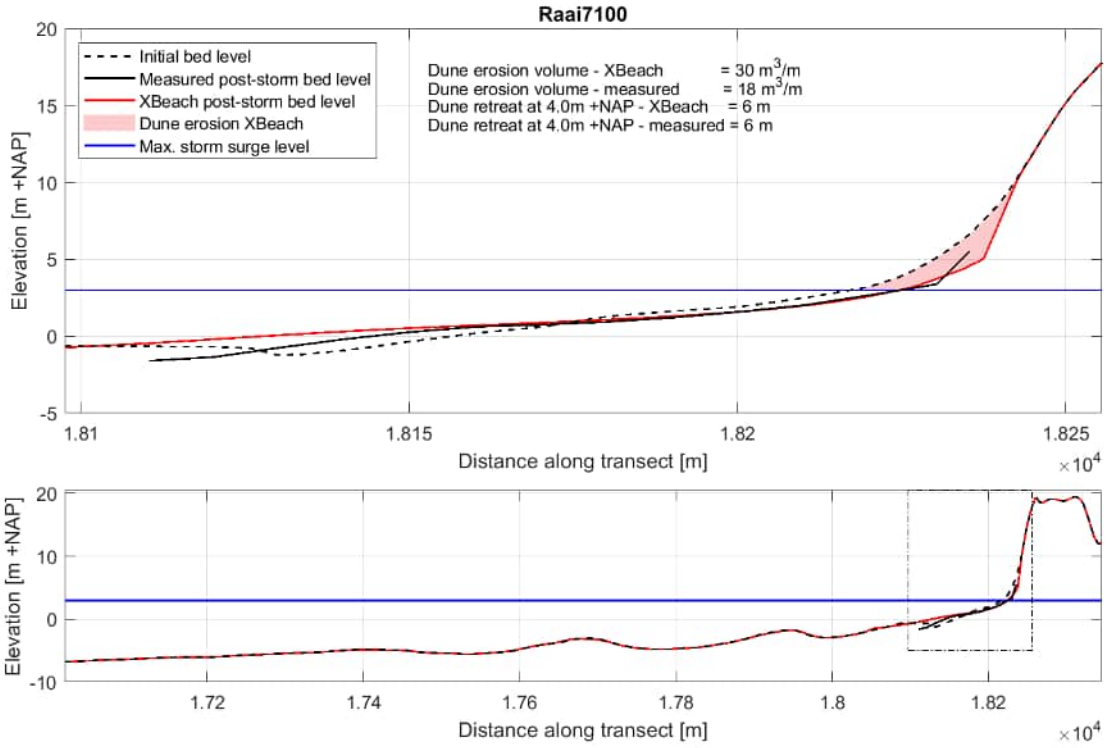

Figure C-123 Cross-section profile 7100 before and after the 1976 storm based on the measurements and XBeach, including dune erosion volumes and retreat distances. Bottom: entire XBeach profile, top: zoom of beach and dune profile.

APPENDIX 8 - FIELD CASE 8: HOLLAND COAST, 1953 (NL) [MORPHO]

Case description

One of the most memorable storm surges in recent history is the storm surge in early February of 1953, leading up to the flooding of large areas in the southwest of the Netherlands and resulting in hundreds of casualties. The storm surge was especially disastrous because of the occurrence of the worst case scenario where a storm surge coincides with spring tide. A very strong north-westerly storm and spring tide led to one of the largest natural disasters (called the 'Watersnoodramp'). It was one of the main causes for the initiation of the Dutch Delta plan, with the primary goal to increase and regulate the flood safety levels of the Dutch coast.

A BOI XBeach simulation is setup for the Holland coast for the 1953 storm as morphological validation case for dune erosion. Because the event occurred in 1953, the amount of available data is limited and as such, the results of this study should be regarded as being indicative of the true conditions. As such, a generalized coastal profile representative for the Holland coast is applied as pre-storm profile. For the hydrodynamic conditions representative for the coastal section between Hoek van Holland – Scheveningen (Figure C-124), a combination of satellite derived reanalysis data (ERA5-data) (Bell et al., 2021) and literature (Gerritsen, 2005) is used. Finally, the properties of the simulated post-storm profile will be compared to reported dune erosion volume of around 90 m^3/m (Van Thiel and De Vries, 2009) and reported changes in dune foot location ranging from 8 to 16 m along the Holland coast (Ruessink & Jeuken, 2002).

The typical observed offshore peak conditions, also explained in more detail below, are as follows:

- The peak surge level consisting of high (spring) tide and storm surge is NAP + 4.0 m.
- The peak significant wave height H_s during the storm is 7.3 meters.
- The maximum wave peak period T_p is 14 seconds.

Figure C-124 Overview of the extent of the southern part of the Holland coast (Hoek van Holland to IJmuiden) and the location of the ERA5 data (Google Earth).

Model setup

A hydrodynamic XBeach 1D simulation (with sediment transport and morphology) for the 1953 storm for the coastal section between Hoek van Holland – Scheveningen is set up using a representative cross-shore profile and a hydraulic forcing on the offshore boundary compiled from multiple sources. This schematization process is outlined in the sections below. As the profile is representative for a stretch of the Holland coast, no specific grain size can be selected, instead an average is used for the southern part of the Holland coast: 225 µm.

Grid and bathymetry

A cross-shore profile representative for the Holland coast was used for this validation case, shown in Figure C-125. The representative profile is adopted from Tilmans (1982). The offshore end of the profile is extended manually to deep water (NAP - 23.8 m) with an artificial slope of 1:10 according to the BOI guidelines. The cross-shore grid was set-up using the standard BOI procedure, resulting in 858 grid points and a spatial resolution that varies from 7.4 m offshore to a minimum of 1.0 m towards NAP + 3 m and above.

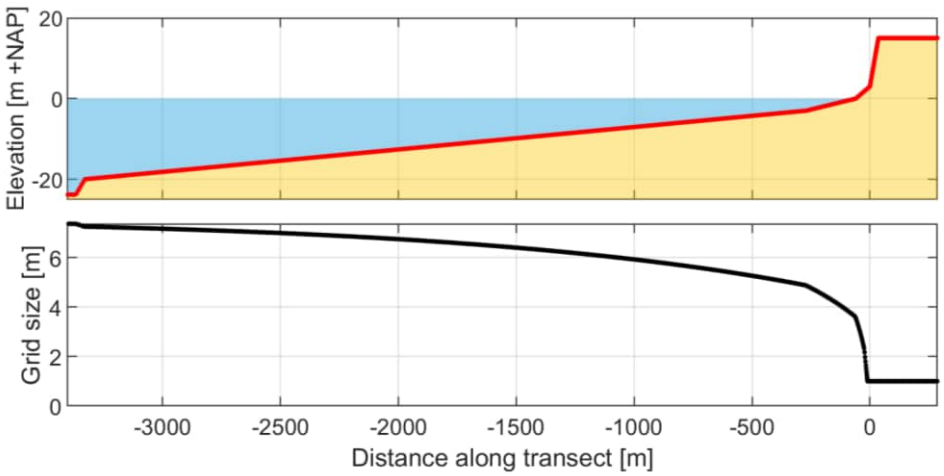

Figure C-125 Overview of the initial bed level based on the representative cross-shore profile (upper panel) and grid cell size (bottom panel) along the XBeach transect.

Hydraulic boundary conditions

Figure C-126 shows the time series of all time-varying XBeach offshore hydraulic boundary conditions for the 1953 storm surge over the length of the model simulation time; January 31st 9:00 – February 2nd 9:00 for a total simulation time of 48 hours. The hydraulic boundary conditions for the 1953 case were compiled from different sources. First, Gerritsen (2005) is used to deduce the exact shape of the water level time series as was observed at Hoek van Holland (the temporal component). Subsequently, data from Wemelsfelder (1953) is used to analyse the behaviour of the storm along the Holland coast (the spatial component). By combining the data, a water level time series representative for the Holland coast is reconstructed. Finally, for the schematization of the waves, ERA5 data are used, as further explained below.

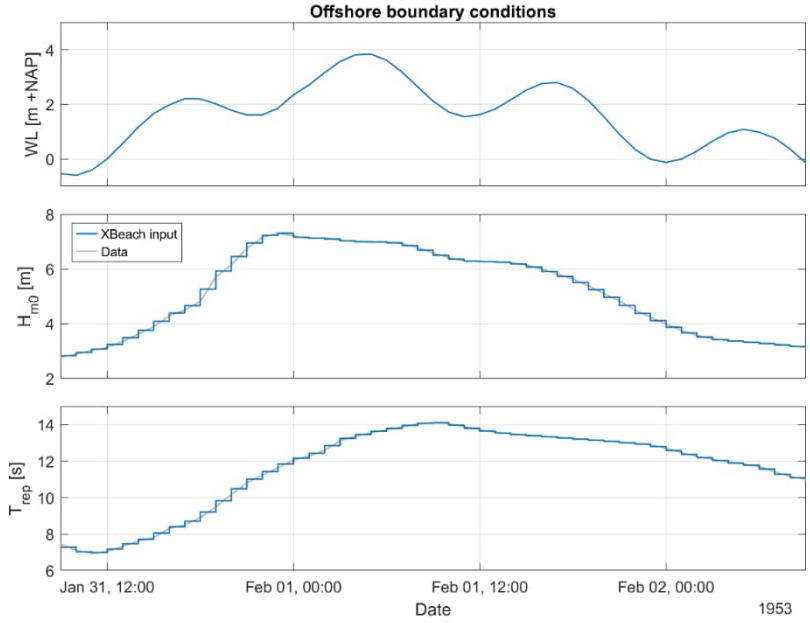

Figure C-126 Time series of all time varying XBeach offshore hydraulic boundary conditions for the 1953 case for the Holland coast. Water level based on Gerritsen (2005) and Wemelsfelder (1953), wave height and wave peak period based on ERA5 data.

The water level time series follow from observed model hindcast time series of the total water level and the storm setup for Hoek van Holland for the 1953 storm as presented in Gerritsen (2005), shown in the top frames in Figure C-127. The time series consists of a tidal signal with an amplitude of approximately 1 m (i.e. a tidal range of 2 m) and an additional surge with a peak at approximately 3.3 m.

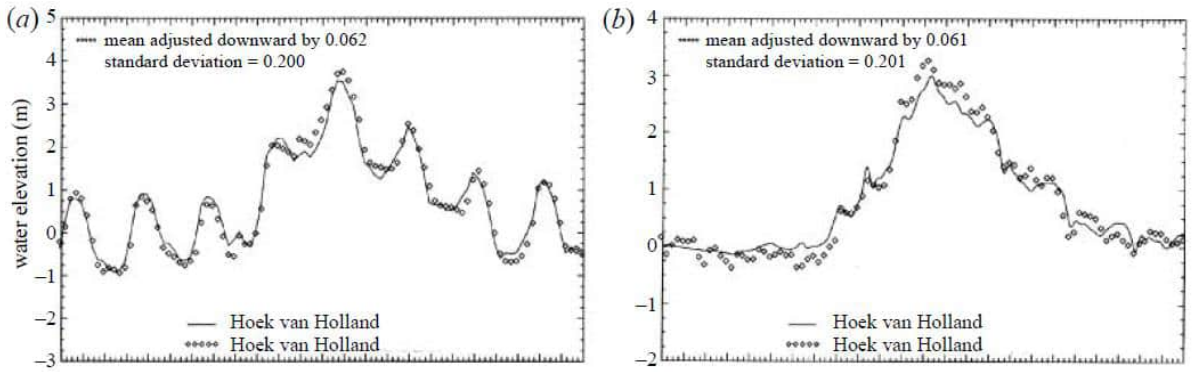

Figure C-127 Observed model hindcast time series of the total water level (a) and just the storm setup (b) for Hoek van Holland for the 1953 storm (Gerritsen, 2005).

As was reported in a number of sources and documented in detail in Wemelsfelder (1953), there existed a phase difference between high-tide and the occurrence of the exact peak of the storm surge. For the entire Dutch coast, this phase difference is fairly constant at approximately 3 hours, where the peak surge occurs 3 hours before high (spring) tide. This is illustrated for Hoek van Holland in Figure C-128 (indicated with the blue line), where the cross section with the left red line is the occurrence of the storm surge peak on February 1st at 1:00 AM and the cross section with the red line on the left indicated the moment of local high tide at 4:00 AM. It can be observed that the phase difference remains fairly constant along the Holland coast, between Hoek van Holland and Den Helder.

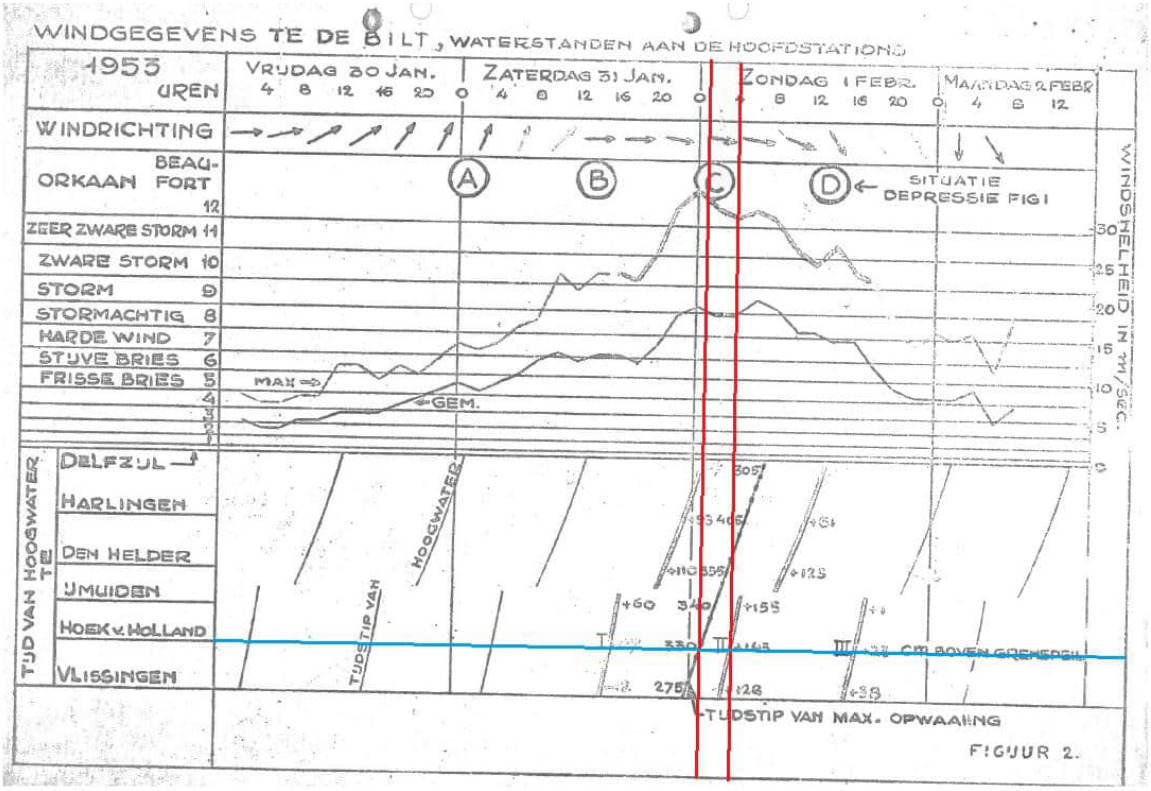

Figure C-128 Wind time series at De Bilt, water level at the main station along the coast (Wemelsfelder, 1953). Timing of peak storm surge (indicated at the bottom with 'tijdstip van max. opwaaiing') and high tide (red vertical lines) indicated for the Hoek van Holland station (blue horizontal line).

Following the above, the total water level can be reconstructed as a summation of the tide and the storm surge, while accounting for the phase difference. This is shown in Figure C-129, note the high level of agreement with the observed and hindcasted water level time series as presented in Figure C-127a from Gerritsen (2005). The resulting total water level time series can be seen as representative for the Holland coast. While forcing does not occur simultaneous at the entire coastal section as it moves from south to north, the forcing itself is approximately constant, with only a minor change in the surge component from 3.30 m at Hoek van Holland to 3.40 m at IJmuiden (see Figure C-128). Hence, the reconstructed water level time series for Hoek van Holland could be used as representative for the Holland coast in this case study.

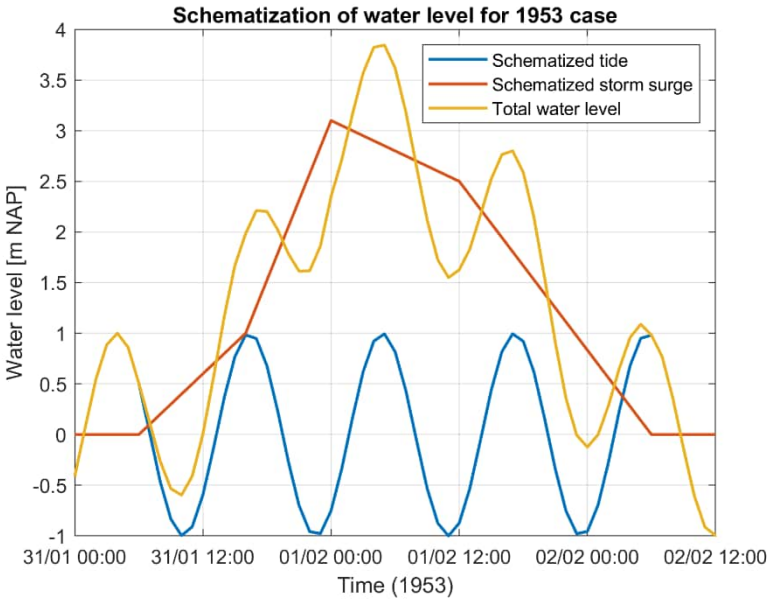

Figure C-129 Schematization of water level for the 1953 case.

For the wave parameters, data from the Copernicus Climate Change Service (C3S) Climate Data Store (CDS) was used. This database can provide all relevant wave parameters on an hourly interval, based on a model reanalysis that was calibrated with satellite data (ERA5). From this dataset, time series for the significant wave height and wave peak period were extracted at a central location offshore from the Dutch coast. For the wave spreading the BOI default value of s = 6 was used (roughly equal to 30 degrees), as the ERA5 data did not provide reliable results for this parameter. Please note that, while using the closest data point where data was available, this data point is still located roughly 100 km offshore at a depth of about 50 m. However, it is assumed that the conditions can still be viewed as representative for the offshore end of the XBeach profile at roughly half that depth, as both can be considered deep water.

The peak wave height occurs around midnight February 1st which (with the higher peak wave periods trailing further behind in time) roughly coincides with the occurrence of peak storm surge at the southern section of the Holland coast. While we do know that the storm depression moved roughly from north to south, no real data is available for the spatial behaviour of the wave field during the storm peak. Therefore, it is assumed that the wave time series is representative for the entire Holland coast (i.e. negligible spatial difference during the storm peak). This also means that there exists a growing temporal discrepancy between the highest waves and the highest water level going from south to north, with the peak waves occurring before the peak surge going further north. This might impact the total dune erosion as there exist a relatively large sensitivity to the water level during peak wave conditions. This variation is not accounted for in the single representative XBeach simulation for this validation case. Thus, based on the forced boundary conditions, one can argue that the simulation is mostly representative for the section Hoek van Holland – Scheveningen.

Results

Available data

Just like the pre-storm profile data, the post-storm data for the 1953 storm event is fairly limited. From (Van Thiel de Vries, 2009) a representative range for the dune erosion above storm surge level along the Holland coast is available: 90 ± 26 m^3/m (with 90 m^3/m being the mean of all observations and 26 m^3/m being equal to 1 standard deviation).

From (Reussink & Jeuken, 2002) the cross-shore displacement of the dune foot along the Dutch coast through the years is available, shown in Figure C-130. Looking at the 1953 timeframe specifically, a noticeable negative displacement (i.e. erosion) can be observed for all locations along the Delta coast (Walcheren and Schouwen) and the Holland coast (Hoek van Holland to Den Helder). The displacement at Vlieland and Terschelling is less pronounced. Assuming that the entire displacement within this specific measurement interval is the result of the 1953 storm surge, the resulting dune foot erosion can be deduced. The result was quantified and collected in Table C-11. An uncertainty range of ± 1.5 m is added due to the visual deduction method. It can be observed that the southern-most coastal sections show the largest dune foot erosion of up to 16.5 ± 1.5 m. Towards the north, the dune foot erosion gradually reduces, down to 8.5 ± 1.5 m at Den Helder, possibly due to the increasing time difference between the peak waves and the peak water level, as was previously discussed. The source does not specifically mention the height at which the retreat is measured, hence a height of 1 meter above maximum storm surge level (i.e. NAP + 5 m) is assumed.

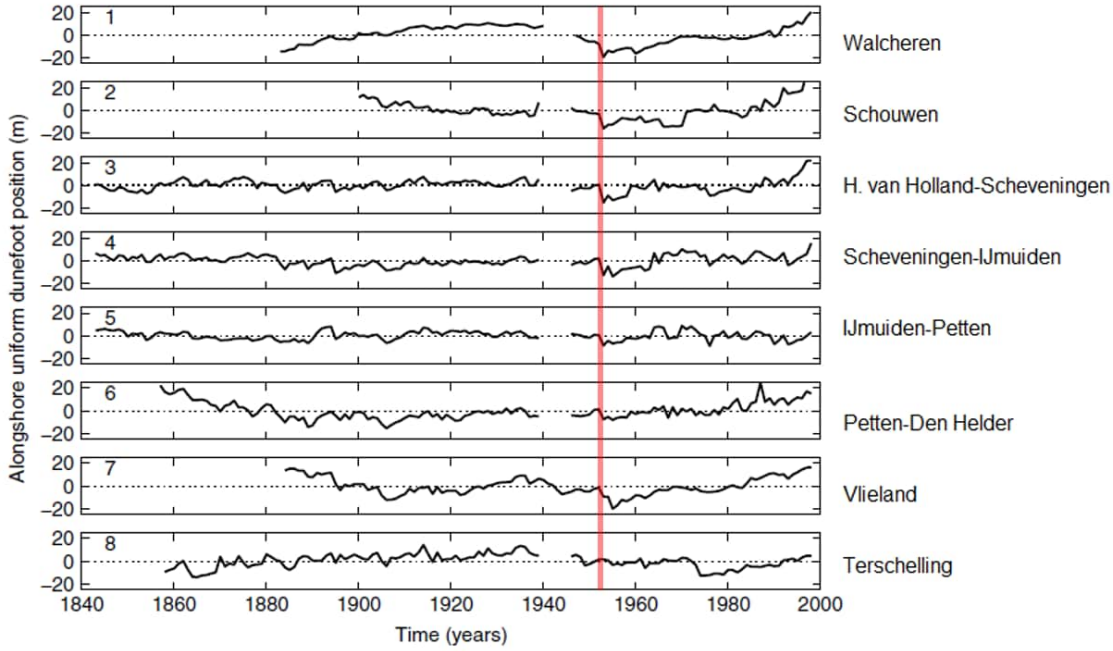

Figure C-130 Cross-shore dune foot displacement in meter over the years along Dutch coast from (Reussink & Jeuken, 2002). Displacement due to 1953 storm surge indicated in red.

Table C-11 Summary of dune foot displacement in early 1953, based on Figure C-130.

Location or coastal section	Dunefoot displacement [m]
Walcheren	15.0 ± 1.5
Schouwen	15.0 ± 1.5
Hoek van Holland-Scheveningen	16.5 ± 1.5
Scheveningen-IJmuiden	14.0 ± 1.5
IJmuiden-Petten	10.0 ± 1.5
Petten-Den Helder	8.5 ± 1.5

Comparison

Figure C-131 shows the (representative) pre storm profile (dashed) and the simulated post storm profile (red). The computed dune erosion volume above maximum storm surge level is 111 m^3/m. This is within the reported range of the erosion volumes of 90± 26 m^3/m in (Van Thiel de Vries, 2009).

The dune foot displacement at 1 meter above maximum storm surge level (approximately NAP + 4 m + 1 m = NAP + 5 m) is 16 m. Based on the relative timing of the surge and wave time series, as well as the peak surge level for the hydraulic boundary conditions of the XBeach simulation, it was argued that the case is mostly representative for the coastal section between Hoek van Holland and Scheveningen. At this location, the displacement of the dune foot during the interval between the measurement before and after the 1953 storm event was observed to be 16.5 ± 1.5 m (Reussink & Jeuken, 2002). This is in agreement with the simulated displacement of 16 m. However, it is not documented at what elevation this displacement is measured. For reference, the largest simulated dune foot displacement occurs at 1.5 m above maximum storm surge level and is 17 m. This is also within the range derived from (Reussink & Jeuken, 2002). At maximum storm surge level, the displacement is 12 m, which is somewhat lower than based on (Reussink & Jeuken, 2002).

In Table C-12 the complete quantitative comparison is summarized.

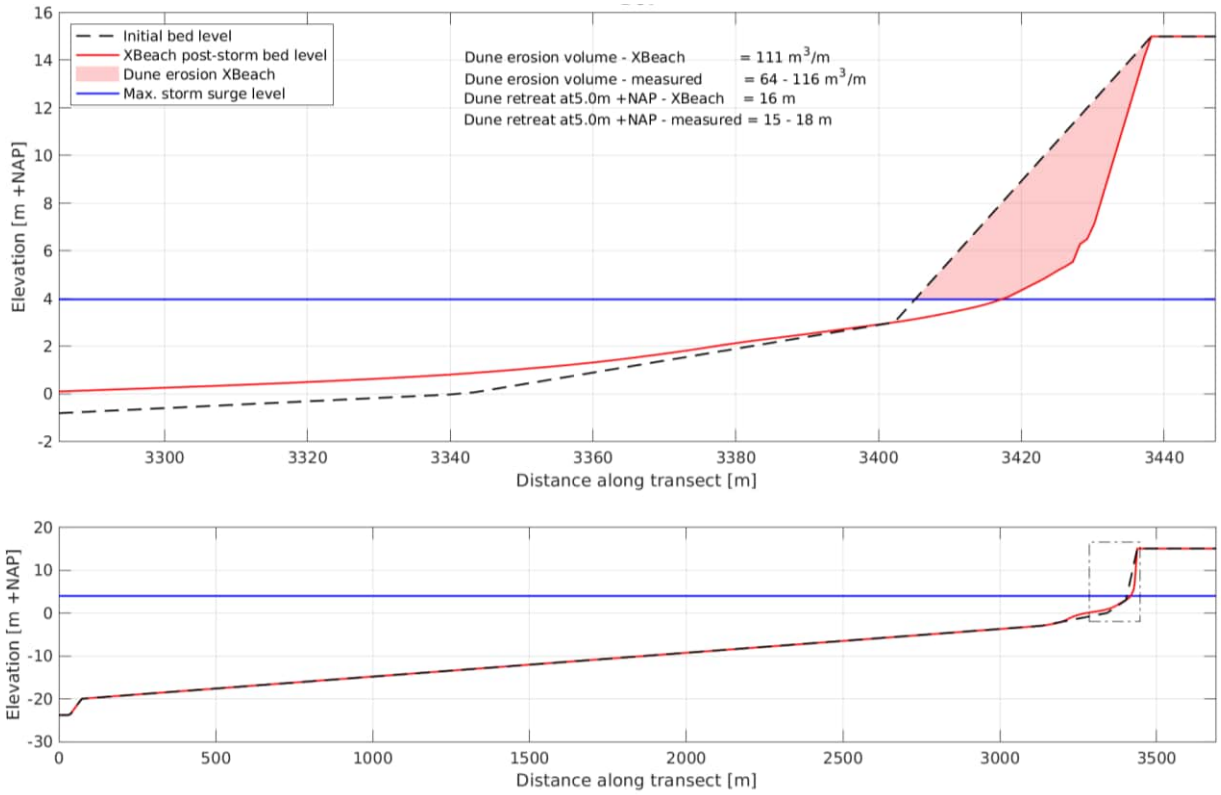

Figure C-131 Pre and post storm surge profile as computed by XBeach. Upper frame shows the dune erosion section, the lower frame shows the entire XBeach profile.

Table C-12 Quantitative comparison between observed mean value and simulated dune erosion and dunefoot displacement during the 1953 surge event at the Hoek van Holland - Scheveningen coastal section. The retreat distance is compared at maximum storm surge level, 1 meter higher and at maximum simulated retreat (from top row to bottom).

Erosion volume		Retreat distance	
XBeach [m^3/m]	Measured [m^3/m]	XBeach [m]	Measured [m]
111	64 - 116	12.1	15 - 18
		15.8	
		17.4	

Discussion

For this validation case several assumptions were made, mostly to circumvent lack of, or incomplete data. In addition, the data that were available, are very different in nature (literature, observations, hindcast, reanalysis) resulting in a model schematization consisting of a compilation of a range of sources. An overview of the assumptions with brief explanation is given below.

One representative profile and grain size
For both the coastal profile as well as the grain diameter representative data was used; the representative cross-shore profile from (Tilmans, 1982) and a 225 µm grain diameter (Holland coast average, with most profiles consisting of 195 to 250 µm). While representative for the Holland coast, the impact of (small) longshore variations in profile shape and grain diameter on (dune) erosion is not accounted for.

Assumptions in hydraulic boundary conditions
Although the time lag between high (spring) tide and peak storm surge was fairly constant along the Holland coast at 3 hours, it does reduce somewhat going northward, following from (Wemelsfelder, 1953). In addition, the maximum storm surge component also increased somewhat going northward. While this variation is obviously not included in the single XBeach simulation, it does impact the shape of the resulting total surge level time series along the coast, possibly resulting in more erosion. This means that the schematized water level time series is mostly representative for the southern section of the Holland coast.

Much like the timing of the high tide and storm surge, the relative timing of the water level time series and wave time series is not constant along the coast. As the storm depression moved from north to south and the peak surge moved from south to north, it can be expected that the relative timing is not constant, with the peak waves occurring in increasing advance before the peak water level going northwards, likely resulting in relatively lower dune erosion along the northern coastal section. The current schematization adopted for this validation case is, again, mostly representative for the southern section of the Holland coast.

Uncertainty in observed dune foot displacement
Finally, some uncertainties follow from the use of the observed validation data used for the dune foot displacement. It is assumed that the full displacement between the measurements before and after the 1953 storm event is due to the 1953 storm surge event. In addition, the exact elevation where the dune foot displacement is measured was not documented. The uncertainty introduced by the latter item is slightly reduced by comparing the simulated dune foot displacement at different heights above the maximum storm surge water level.

Conclusion

The goal of this validation case was a morphological comparison of the observed and simulated dune erosion of the 1953 storm surge event: an event with relatively large observed dune erosion volumes. Due to limited data that could be used as model input, several assumptions had to be made when schematizing the input files for the XBeach simulation. In addition, the model results could only be compared to indicative dune erosion volumes and dune toe retreat distances, since no pre- and post-storm profiles were available. The simulated values for the dune erosion and dune foot displacement are within of the range of the observed values. Hence, as far as can be concluded based on this indicative comparison, the XBeach model with BOI settings performed well for this case.

APPENDIX 9 - FIELD CASE 9: EGMOND AAN ZEE (NL) [HYDRO + MORPHO]

Case description

A dataset with field measurement for seven (7) cross-shore profiles near Egmond aan Zee (Figure C-132) is used for both a hydrodynamic and a morphodynamic validation of the BOI-version of XBeach.

Egmond aan Zee is located along the Dutch Holland coast (Figure C-132), where tides are semi-diurnal, with a neap and spring tidal range of ~1.4 and 1.8 m. The annual mean offshore wave height is H_{m0} = 1.3 m and the wave period T_{m02} = 4.5 s (Wijnberg, 2002). During north-westerly storms, significant wave heights can reach up to 7 m and storm surges can raise the water level by more than 1 m (Ruessink et al., 2019). The coastal zone of the field site is characterized by 2-3 subtidal bars and an intertidal bar on a gently sloping intertidal (1:40) beach. The shoreface near Egmond has a 1:200 slope, resembling a typical profile of the Holland coast. The dune toe is located at MSL (or NAP) + 3 m and changes into a steep foredune with a 1:2.5 slope. Around MSL + 14 to 17 m, the profile abruptly changes in slope and continues gently to the foredune crest at a height of MSL + 20 to 25 m. Alongshore variability in foredune shape and height is small. During multiple years without dune erosion, embryo dunes can develop at the toe of the foredune (De Winter et al., 2015). The well-sorted quartz sand at the study site has a medium grain size of 250–300 µm, with a tendency to decrease in the landward direction.

The field data for this validation study was collected and shared by the department of Physical Geography of Utrecht University, where a 'quick reaction force' was set up to collect field data directly preceding, during and following storms, as outlined in Ruessink et al. (2019). For this study, the dune erosion event on 8-9 January 2019 is selected for validation. The 7 locations were spaced 250 – 750 m apart, distributed over 3 km alongshore. At each of these alongshore locations, one pressure sensor was located above the high tide water level, each at different elevations with a maximum difference of 1 m (Price et al, 2021). A second pressure was deployed within each cross-shore profile 40 m seaward of the first sensor the day before the arrival of the storm. Elevation of the pressure sensors above the bed were interpolated linearly in time, based on the measured pre- and post-storm bed levels.

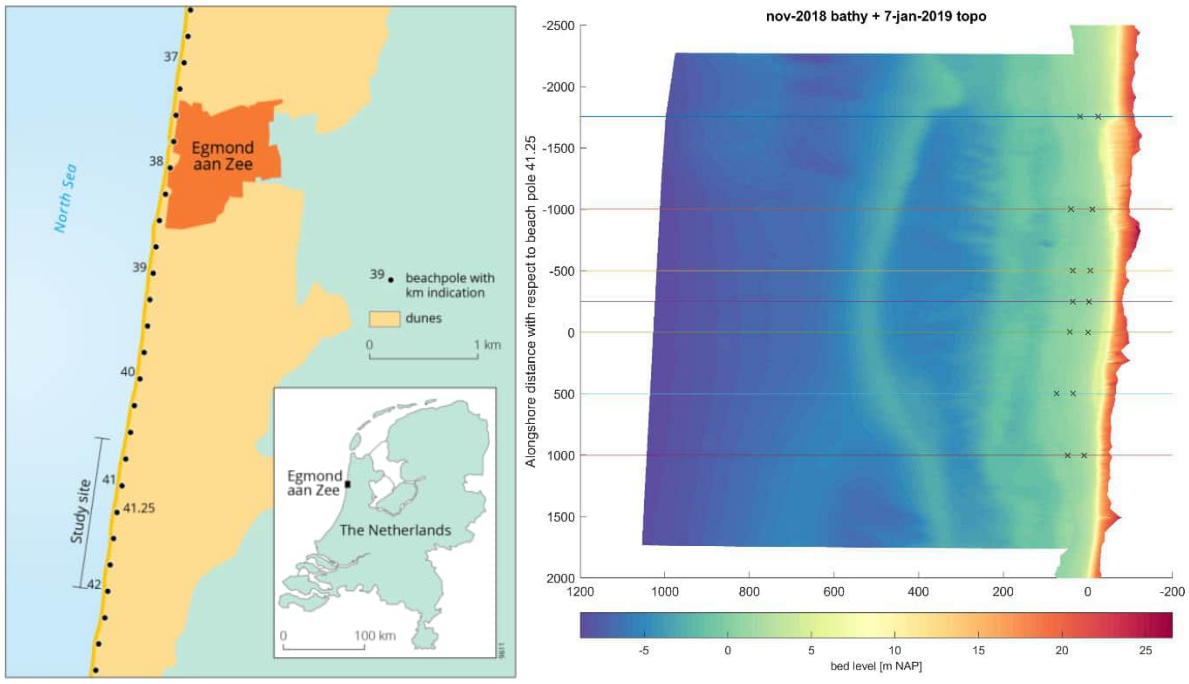

Figure C-132 Location of study site (left panel). The beach poles form an alongshore reference line, with the km number referring to the distance to the zero point at the northern end of the Holland coast. The origin of the local coordinate system used (right panel) is at beach pole 41.25, with positive x and y in the seaward and southern direction, respectively. The crosses ('x') indicate the location of the pressure sensors and the different cross-sections are referred to by their y-coordinate in this local coordinate system. Left panel adopted from Ruessink et al. (2019).

Water surface elevations were collected at a frequency of 5 Hz and post-processed into consecutive bursts of 30 min. Only the bursts in which the sensor was continuously submerged were considered to calculate mean water levels and significant wave heights in the sea-swell ($H_{S,SS}$) and infragravity ($H_{s,IG}$) frequency band (0.005 - 0.05 Hz) .

During the considered measurement campaign, the offshore water level near the study site (tidal station near IJmuiden) reached NAP + 2.1 m. The maximum significant wave height (H_s), measured with a wave buoy at 20 m water depth, was 5.2 m and maximum peak period (T_p) was 15 s. The waves arrived obliquely incident, from west-southwest during the beginning of the storm and the direction changed to the northwest for the remainder of the storm.

Full bathymetric (sonar-equipped jetski) and topographic (mobile laser scanner) surveys provided pre- and post-storm observations. Bathymetric data was collected on 23 November 2018 and 22 January 2019, while topographic data was collected directly before (7 January 2019) and after (10 January 2019) the storm event. The bed level measurements show that the storm did not result in large erosion volumes, but erosion of the lower dune face did occur along the entire field site. In the period between the bathymetrical surveys, the outer crescentic bar mostly rotated clockwise, leading to an alternation of onshore and offshore migration of the bar alongshore.

Model setup

First, a hydrodynamic XBeach 1D simulation (without sediment transport and morphology) has been set-up and run for 7 transects for the hydrodynamic validation. Subsequently, the model has been run again for the 7 transects, but this time including sediment transport and morphology for the morphodynamic validation with the same boundary conditions. For these runs, a D_{50} of 250 µm is applied, based on the observed mean grain size that was found closest to the dune front.

Grid and bathymetry

The topographic data obtained on January 7th, 2019 was merged with the bathymetric data collected on November 2018, and interpolated on a 2D grid using a local coordinate system (see right panel of Figure C-132). Within this local coordinate system, 7 transects were defined along the 7 pressure sensors pairs. The 7 profiles are referred to by their y-coordinate from the local coordinate system, e.g. ‘profile -1755’.

While considering the offshore conditions presented in Figure C-135 as the governing maximum conditions (H_{m0} ~ 6m, T_p ~ 15s), each profile has been extended seaward according to BOI guidelines with a 1:50 slope to a depth of ~20 m. Cross-shore grids were set-up following standard BOI procedure resulting in approximately 350 ± 50 grid cells per profile and spatial resolution that varies from 7.5 m (offshore) to 1 m at the dune. The initial bed level across the 1D transects of profile -1755 as well as the cross-shore distribution of grid sizes are presented in Figure C-133. In addition, the initial bed levels of all seven profiles are depicted together in Figure C-134. Note that the main difference between the different profiles is the cross-shore position of the breaker bars.

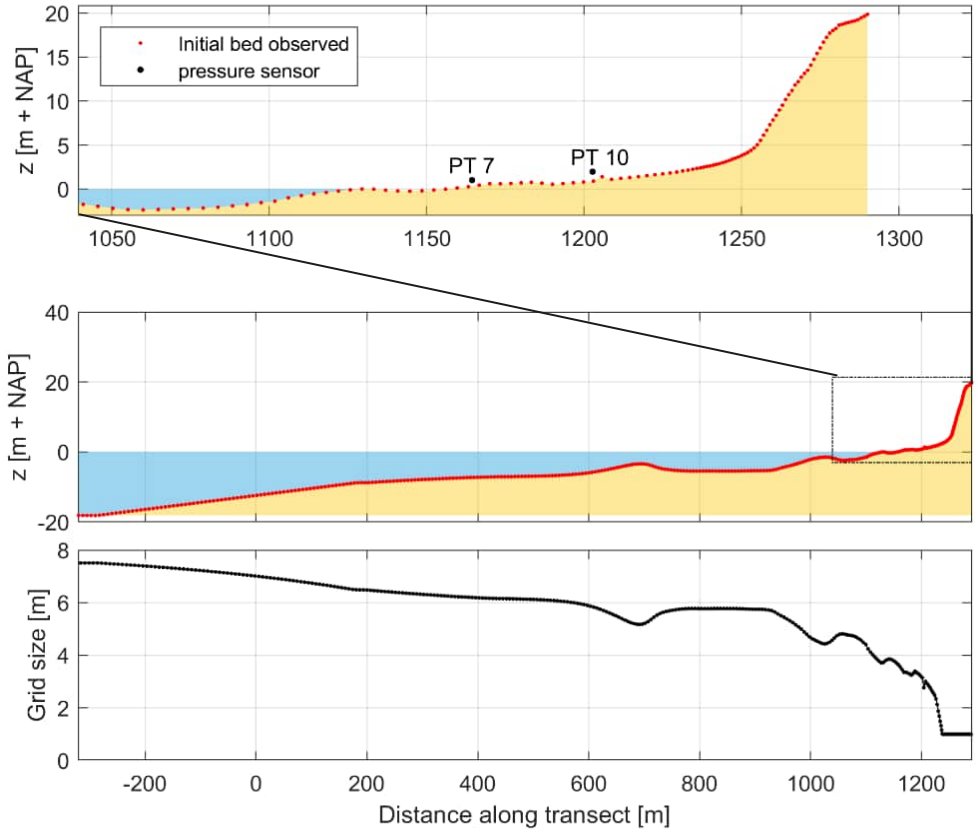

Figure C-133 Overview of the initial bed level along the 1D XBeach profile 0 near Egmond aan Zee (middle panel, in which the red dots represent the bed level per grid point), and cross-shore distribution of the grid size (lower plot). Besides that, the upper plot presents a zoom on the last part of the profile.

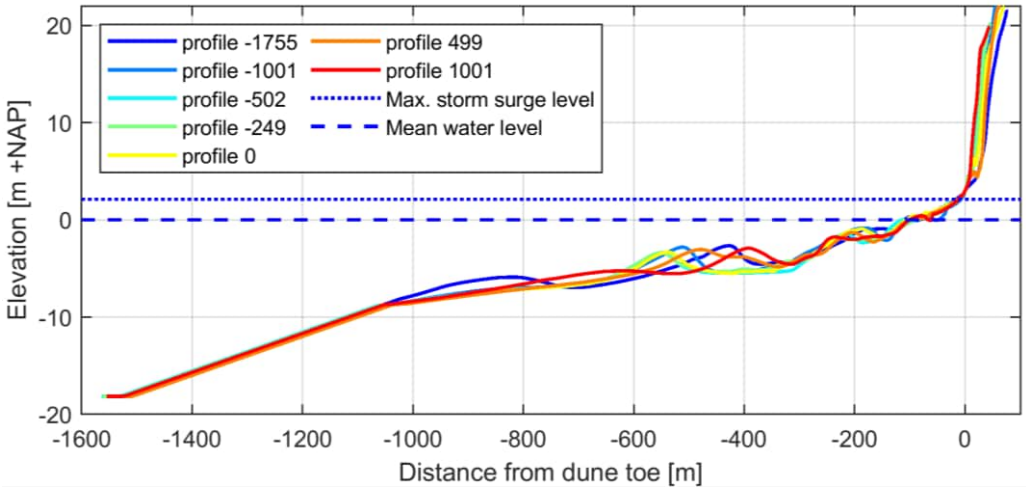

Figure C-134 Overview of the initial bed levels for the seven different transects. Dune toe for this specific case is defined at NAP + 3 m.

Hydraulic boundary conditions

The hydraulic boundary conditions are collected from a tidal station near IJmuiden located 20 km west-southwest of Egmond. A wave buoy located 40 km of the study site at 20 m water depth provides the wave forcing conditions. The model is forced with a sequence of hourly-varying JONSWAP spectra based on the wave characteristics. Instead of using the time-varying mean wave directions, the mean wave direction of the JONSWAP wave spectra is defined perpendicular to the coast, and a directional spreading of approximately 30° (s = 6) is used (in analogy with the BOI procedure). An overview of the hydrodynamic forcing conditions is presented in Figure C-135. The models are run for a total simulation period of 38 h, which captures the entire period where elevated water levels and increased wave heights were observed during the January 2019 storm.

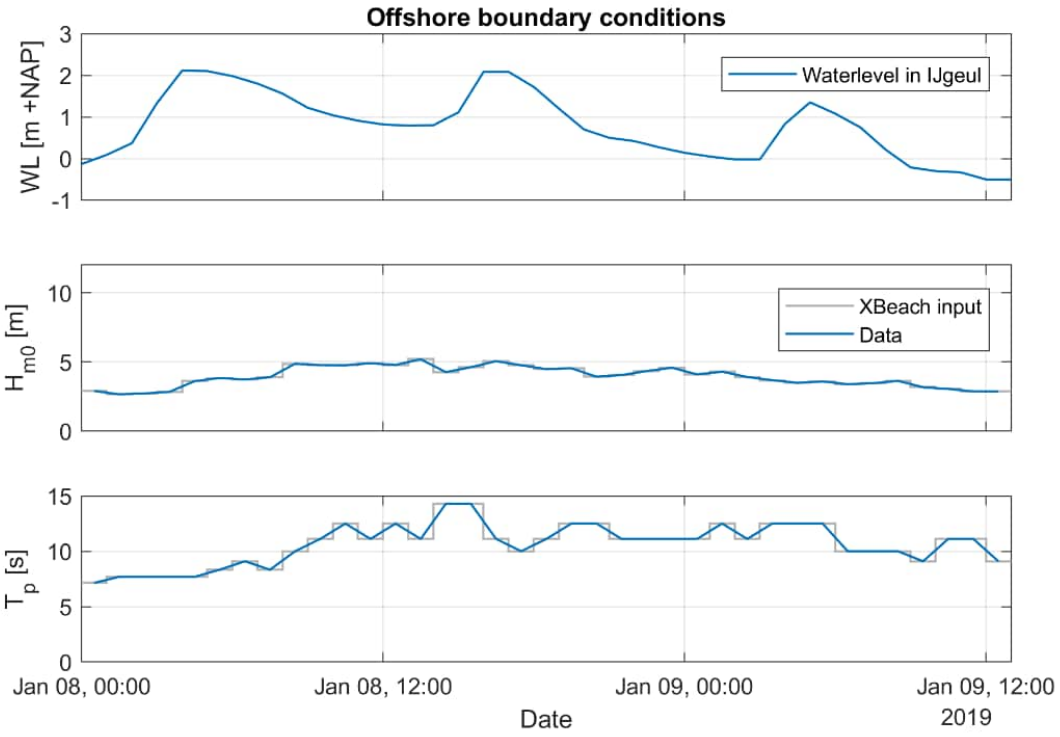

Figure C-135 Time series of the XBeach offshore hydraulic boundary conditions for the Egmond aan Zee case.

Model output settings and post-processing

For the hydrodynamic validation runs, the modelled water level (zs) and rms-wave height (H_{rms}) are saved with a frequency of 10 Hz (compared to 5 Hz for the measured data) at the location of the pressure transducers. The spectral significant wave height (H_{m0}) of the short waves (0.05-1 Hz, referred to with 'ss': sea-swell or 'hf': high frequency) is calculated as $\sqrt{2} * H_{rms}$ and root-mean-square-averaged over the same 30-min blocks as the measured data. The H_{m0} of the infragravity waves (0.005-0.05 Hz, referred to with 'ig') is determined from the spectral integration (using Hann filter and Welch method) of the detrended water level signal in the 0.005-0.05 Hz domain (based on fast Fourier transformation) for the same 30-min blocks. These wave characteristics and the water level are compared with the measured data.

For the morphodynamics validation runs, the XBeach profile at the last timestep is compared with the first time step. The XBeach dune erosion volume is calculated as the negative volume difference between these profiles above the highest storm surge level (NAP + 2.1 m). The measured dune erosion volume is calculated in the same way using the initial and post-storm profile. The dune retreat distance is measured at NAP + 3.0 m (dune toe), where generally most erosion occurred in the measurements.

Results hydrodynamics

In this section, the hydrodynamic XBeach validation results are presented and compared to the measured data for all pressure sensors along the 7 profiles. First, the water levels are analysed using the time series of observed and modelled water levels in Figure C-136, followed by the high frequency and infragravity wave heights in Figure C-137 and Figure C-138 respectively. In both sections, the degree of the goodness of fit (GoF) between the model and measured data is supported by the indicators presented in Table C-13. Lastly, the overall trends in the data are visualized and discussed using an aggregated scatter plot (Figure C-139). Discussion on the causes of differences between modelled and measured values and the link between the water depth and wave heights follows in the Discussion section.

Water levels

Observations show that water levels are tidally-modulated and reach up to NAP + 3.0 m during the peak of the storm (Figure C-136). Some of the sensors run dry during lower water elevations, especially the sensors closer to the beach (right column in the figures). Since only 30-min bursts for which the sensor was continuously submerged are included in the measurements, this results in some gaps in the observations. Comparing the observed water levels between the sensors reveals an alongshore variation in the water levels in the order of 0.2-0.5 m (e.g. compare sensor 5 and 3 in Figure C-136). The modelled water levels do not show a strong alongshore variation in the water levels: they are similar for each transect. Modelled water levels compare well with observations for sensors 4, 3 and 7, but for the other sensors XBeach underestimates the water levels (Figure C-136). The average bias for all sensors is -0.45 m for the modelled water levels, corresponding to an underestimation by the model of 20% (Table C-13).

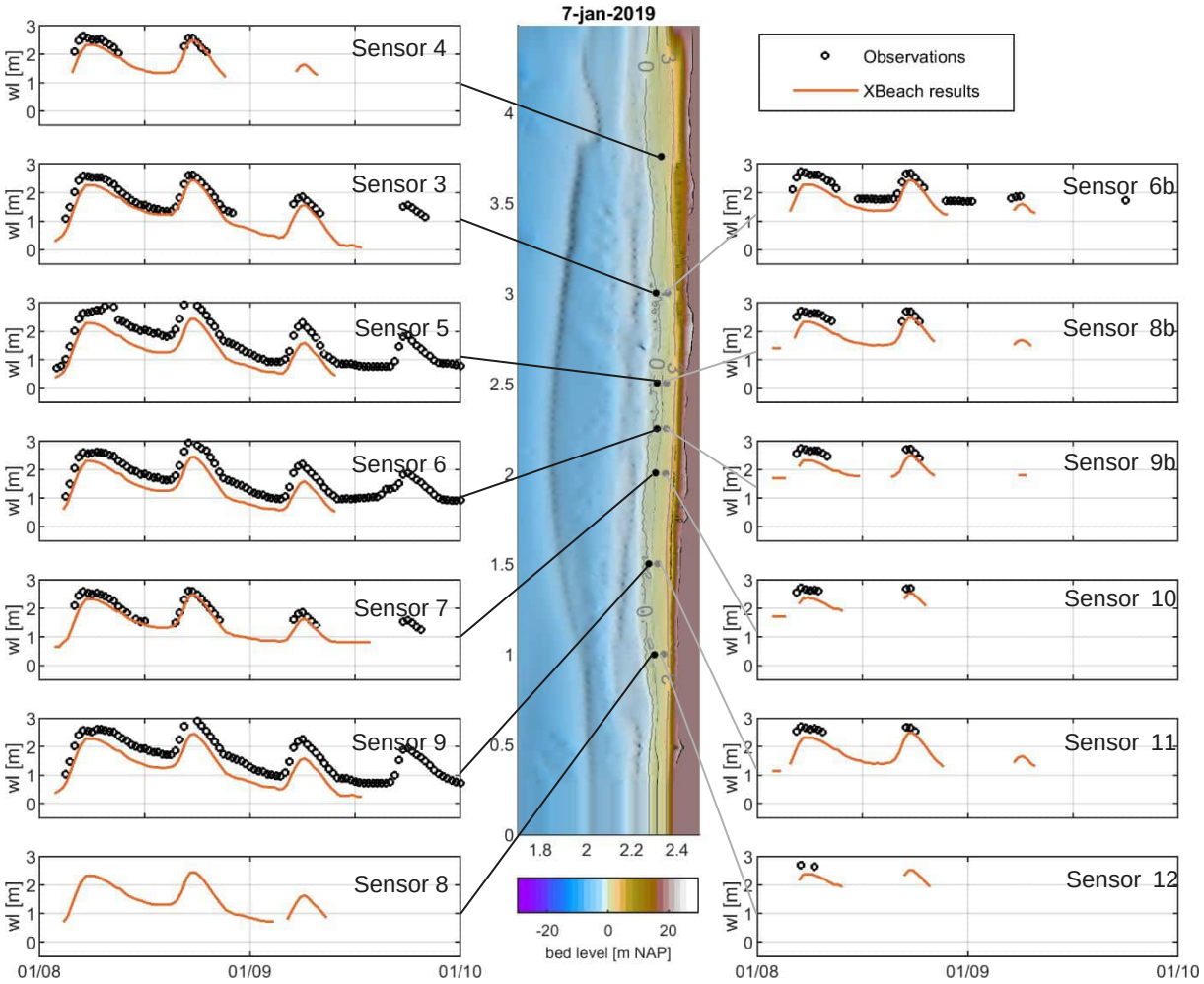

Figure C-136 Observed water levels (black circles) against the modelled water levels (orange) for all pressure sensors. The panel in the middle shows the location of the pressure sensors, and the surrounding subpanels follow the order from North to South (top to bottom) and from sea (left) to the beach (right).

Short- and infragravity wave heights

The modelled short- and infragravity wave heights correspond well with observations (Figure C-137 and Figure C-138), despite the underestimated water levels.

The seaward located pressure sensors show short-wave heights up to 1.5 m during peak of the storm (disregarding two sensors with large irregularities in the observations that are not observed at the landward sensor, caused by measurement inaccuracies), whereas the wave-heights at the landward located pressure sensors do not exceed 1 m. This cross-shore wave dissipation is both found in observations as well as in the model results. For most of the pressure sensors, there is a good resemblance between modelled and observed short-wave heights with relative biases < 15% (Table C-13). A large bias of 0.45 m is found for the landward pressure sensor 6b (second from the North). However, since the spatial and temporal variation is captured well for the other pressure sensors, this bias might be related to uncertainties in the initial bed level governing wave breaking.

During the storm in January 2019, infragravity waves are found in the order of 0.5 – 1 m. In general, there is a good correspondence between modelled and observed infragravity wave heights (Figure C-138). The modelled infragravity waves are somewhat lower right after start of the simulation, but the magnitude is right throughout the rest of the simulation (relative bias < 10 %, Table C-13).

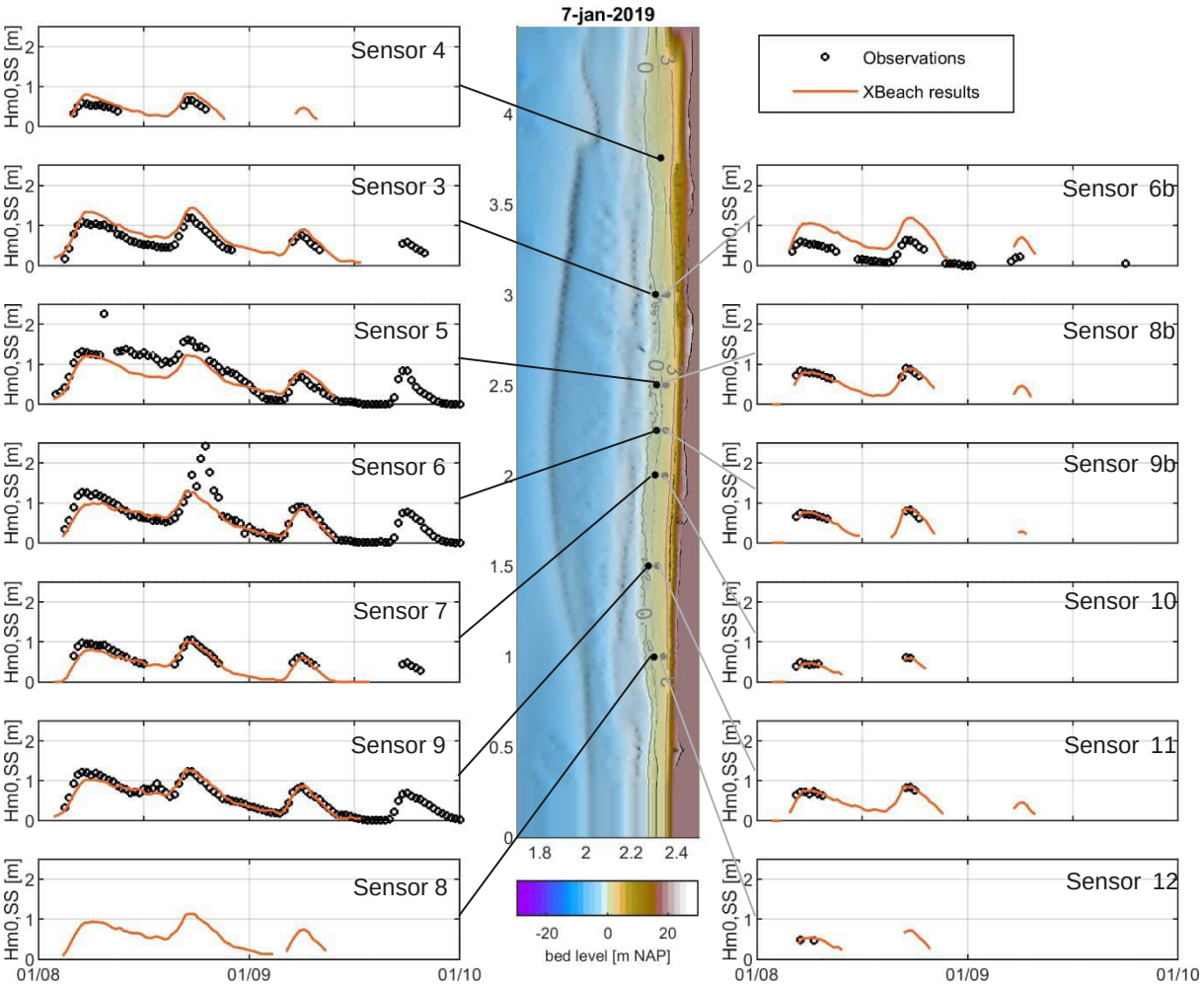

Figure C-137 Observed short-wave heights (black circles) against the modelled short-wave heights (orange) for all pressure sensors. The panel in the middle shows the location of the pressure sensors, and the surrounding subpanels follow the order from North to South (top to bottom) and from sea (left) to the beach (right).

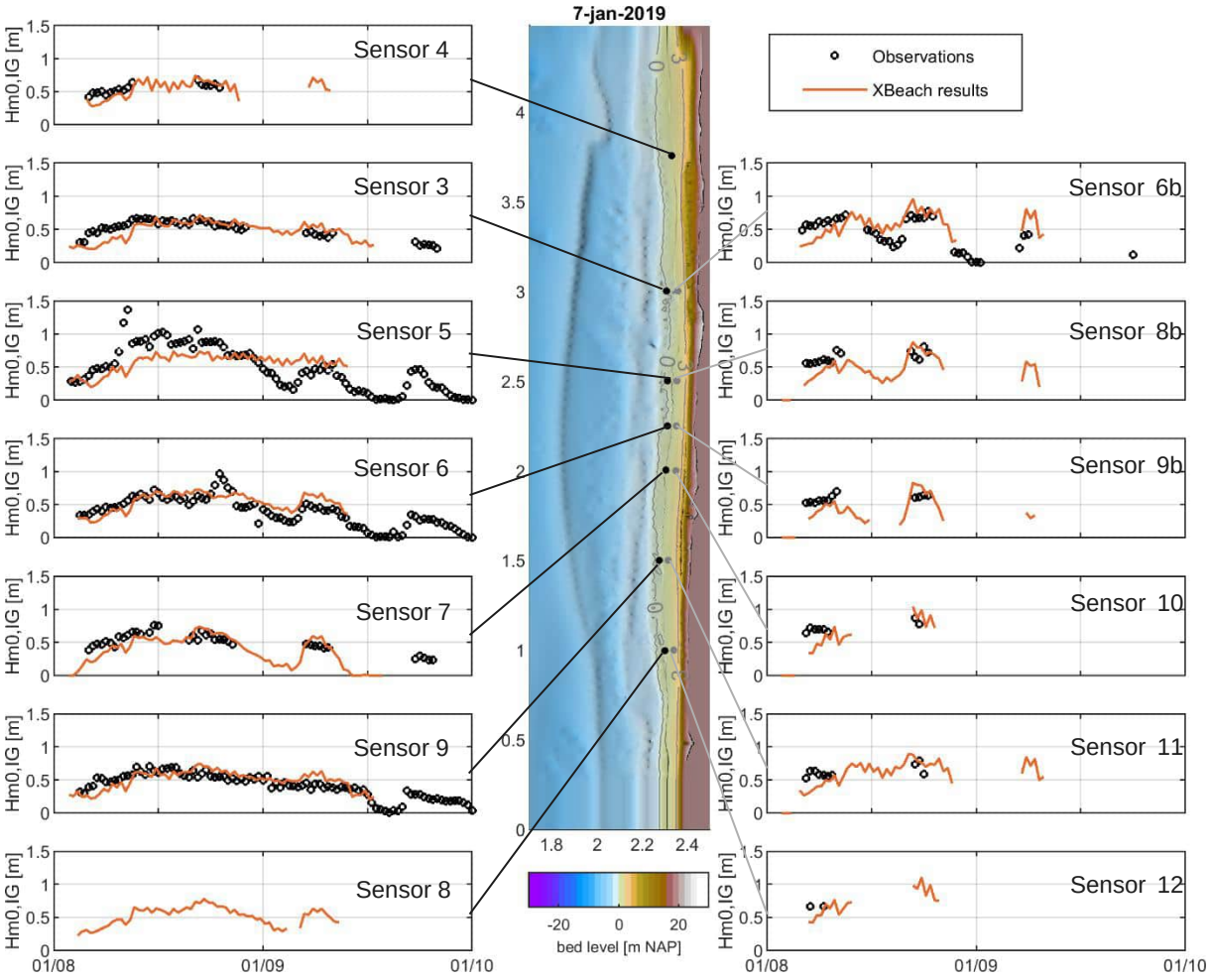

Figure C-138 Observed infragravity wave heights (black circles) against the modelled infragravity wave heights (orange) for all pressure sensors. The panel in the middle shows the location of the pressure sensors, and the surrounding subpanels follow the order from North to South (top to bottom) and from sea (left) to the beach (right).

Table C-13 Goodness-of-fit (GoF) indicators for the modelled water level and the spectral significant wave height for high frequency (HF) and infragravity (IG) waves compared to the measurements at each pressure sensor from North to South for the entire modelled storm period. Colours per indicator indicate relative GoF between the locations of all hydrodynamic cases (greener = better fit). Note that the GoF indicators for some of the pressure sensors (e.g. sensor 12) are based on very limited data points. Overall values are based on all data points of all sensors together.

Pressure sensor nr.	Water level [m +NAP]				$H_{m0\ HF}$ [m]				$H_{m0\ IG}$ [m]			
	RMSE	sci	bias	rel. bias	RMSE	sci	bias	rel. bias	RMSE	sci	bias	rel. bias
4	0.39	0.16	-0.32	-0.13	0.17	0.32	0.11	0.20	0.08	0.15	-0.03	-0.05
6b	0.47	0.21	-0.36	-0.16	0.49	1.21	0.45	1.12	0.23	0.42	0.08	0.15
3	0.50	0.26	-0.32	-0.16	0.30	0.39	0.18	0.24	0.09	0.16	-0.03	-0.05
5	0.71	0.35	-0.56	-0.27	0.58	0.48	-0.28	-0.23	0.24	0.35	-0.06	-0.09
8b	0.48	0.19	-0.44	-0.17	0.12	0.16	-0.07	-0.09	0.11	0.17	-0.07	-0.11
9b	0.49	0.19	-0.48	-0.18	0.13	0.18	-0.08	-0.12	0.14	0.24	-0.10	-0.16
6	0.66	0.33	-0.51	-0.26	0.42	0.45	-0.13	-0.14	0.14	0.26	0.04	0.09
7	0.44	0.21	-0.30	-0.14	0.23	0.31	-0.12	-0.16	0.11	0.20	-0.04	-0.07
10	0.40	0.15	-0.39	-0.15	0.10	0.21	-0.07	-0.14	0.16	0.22	-0.10	-0.14
11	0.46	0.18	-0.45	-0.17	0.10	0.14	-0.05	-0.07	0.12	0.20	-0.07	-0.11
9	0.69	0.36	-0.56	-0.29	0.21	0.28	-0.04	-0.05	0.10	0.20	0.01	0.02
12	0.40	0.15	-0.39	-0.15	0.05	0.10	0.02	0.05	0.12	0.18	-0.02	-0.03
Overall	0.59	0.28	-0.45	-0.21	0.36	0.42	-0.04	-0.05	0.15	0.27	-0.01	-0.02

Hydrodynamic scatter plots

An aggregated scatter plot of observed versus modelled water levels and wave heights is presented in Figure C-139. In line with the above presented analyses, the linear fit shows that the trend with an increase in water level is correctly modelled, but the modelled water level tends to be lower than in the measurements and the results are scattered. Furthermore, the trend of the short- and infragravity wave height is generally represented correctly by the model, but the scatter is large and the signal of a few pressure sensors with outliers and offsets in the measurements (outliers for sensor 5 and 6, offsets especially in case of the short waves for 6b and 3) result in a linear fit that is suggests that XBeach tends to underestimate the larger wave heights and overestimate the smaller wave heights. Without these measurements, the linear fit is closer to the 1:1-line.

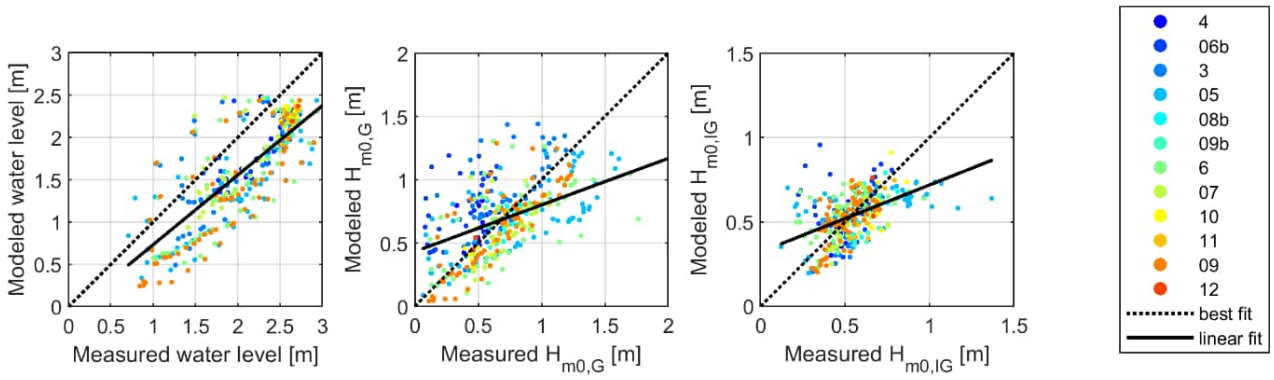

Figure C-139 Scatter plot of the modelled versus measured water level (left), spectral significant wave height (Hm0) of short waves (G) (middle) and infragravity waves (IG) (right) for all pressure transducers near Egmond aan Zee. The dashed line indicates a perfect fit, the continuous line represents a linear fit through the point cloud.

Results morphodynamics

In this section, the morphodynamic XBeach validation results are presented and compared to the measured data for all 7 profiles. The model results are validated using the topography measurements of the beach and dunes, collected on January 10th. A quantitative comparison between observed and modelled erosion volumes and dune retreat is presented in Table C-14. Figure C-140 and Figure C-141 show the cross-sections along two transects as an example; the other cross-sections are included in the Additional figures section.

For all transects except profile -1001, the observed and the modelled dune erosion volumes are well below 10 m^3/m (Table C-14): only some erosion occurred at the dune toe. In general, the modelled dune erosion is in line with the observed dune erosion. However, small absolute differences may result in large relative differences due to the limited amount of dune erosion. This is especially the case for the two northern transects, where hardly any dune erosion (≤ 1 m^3/m) was observed, whereas XBeach still predicts dune erosion volumes up to 13 m^3/m. This is visible in Figure C-140 (and Figure C-142 in the Additional figures). These profiles strongly affect overall average percentual difference of the profiles.

For the other transects, the absolute difference in dune erosion is small (max. 3 m^3/m and 1.7 m; Table C-14) and the relative difference is quite large due to the small measured amount of dune erosion: on average ~30%. The dune erosion volumes are generally slightly overestimated. This slight overestimation is visible in Figure C-141 (and in the Additional figures). This figure also shows that the post-storm measured and XBeach dune erosion profiles are similar. Hence, for most profiles, both the shape of the profile as well as the absolute dune erosion volumes and dune retreat distances are well reproduced, though relative differences are quite large.

Table C-14 Dune erosion volume and retreat distance in the XBeach simulations and measured profiles for 7 profiles near Egmond aan Zee. Negative difference = underestimation of the measured values in the XBeach simulation. Colours per column indicate the degree of similarity between the simulations and observations based on all morphological cases (greener = better fit).

Profile nr.	Erosion volume				Retreat distance [m] at NAP + 3 m			
	XBeach [m^3/m]	Measured [m^3/m]	Difference [m^3/m]	Difference [%]	XBeach [m]	Measured [m]	Difference [m]	Difference [%]
-1755	7	0	6.9	27233%	4.9	0.6	4.3	749%
-1001	13	1	11.6	836%	5.6	1.7	3.9	227%
-502	8	6	1.3	22%	3.1	4.2	-1.1	-26%
-249	8	8	-0.1	-1%	2.1	3.7	-1.7	-44%
0	5	4	0.9	24%	1.5	2.8	-1.3	-46%
499	7	4	3.1	79%	3.0	2.6	0.4	16%
1001	8	6	2.5	43%	2.6	4.0	-1.5	-36%
Average	**8**	**4**	**3.8**	**4034%**	**3.2**	**2.8**	**0.4**	**120%**

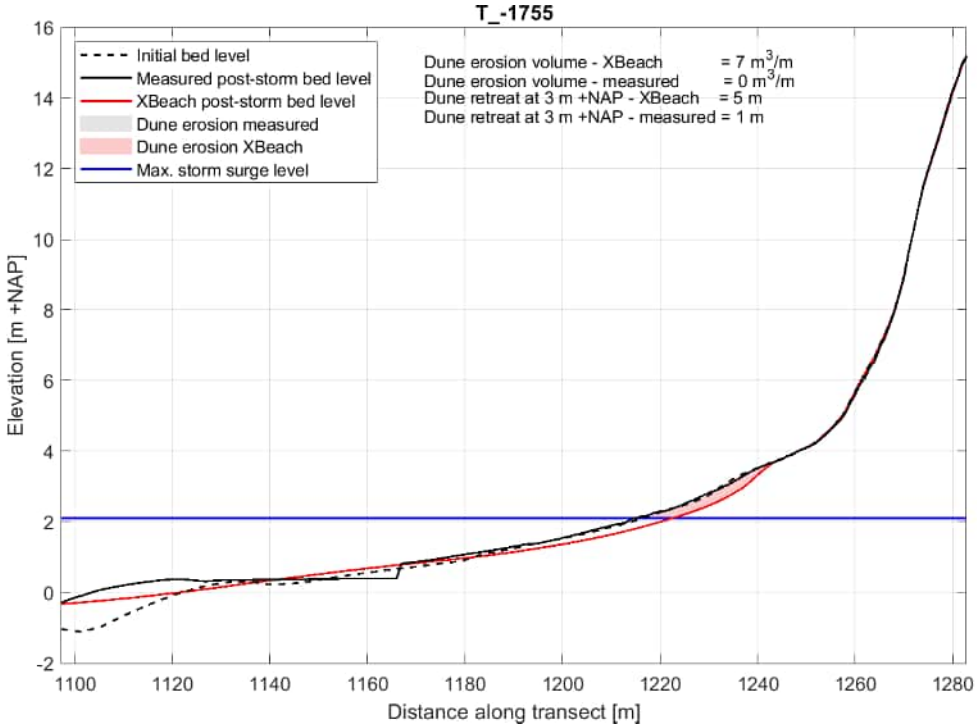

Figure C-140 XBeach results for cross-shore transect -1755 at Egmond aan Zee. Initial bed levels are depicted by the black dotted line, observed post-storm bed levels by the black solid line and XBeach model results are presented in red. The modelled dune erosion is shown by the red shaded area. Note that the kink in the measured post-storm profile (around x = 1165 m) is due to merging of post storm bathymetry and topography measurements.

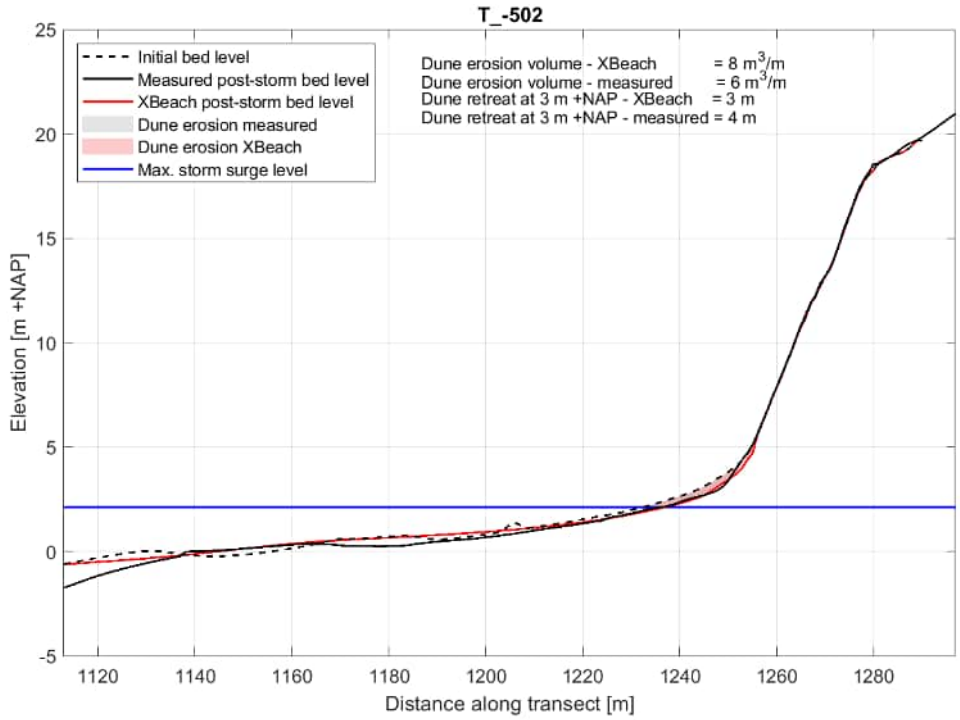

Figure C-141 XBeach results for cross-shore transect -502 at Egmond aan Zee. Initial bed levels are depicted by the black dotted line, observed post-storm bed levels by the black solid line and XBeach model results are presented in red. The modelled dune erosion is shown by the red shaded area.

Discussion

Hydrodynamics

Regarding the modelled hydrodynamics near Egmond aan Zee, the general temporal and spatial patterns are captured and the wave heights are predicted with on average a minor underprediction of a few centimetre. However, there seems to be an offset between the observed and modelled water levels and the observed alongshore variation in the water levels are not reflected by the modelled water levels. This offset is at least partly caused by uncertainties in the measurements (or measurement processing). The water levels show large alongshore water levels gradients between the observation points that seem unrealistic as it would most likely cause unrealistic large alongshore currents. The observed wave heights are well captured by the model, which would probably not have been the case when modelled water depths were incorrect (as wave heights are determined by depth-induced breaking). Next to these aberrant alongshore variations, the observed water level also shows an atypical decrease towards the beach between for example sensor 5 and 8b. Other potential reasons than measurement errors for the water level offset are (1) the model approach, i.e. 1D transect models will not be able to calculate longshore-driven processes, (2) uncertainties in the forcing conditions used in this study, more specifically the water levels (tide + surge) and (3) interference of incoming and reflecting infragravity waves causing locally deviating measured water levels (and wave characteristics).

The hydrodynamic results do not give a direct cause for adjustments in the 1D BOI XBeach approach or settings. The minimal overall bias of the infragravity wave height of -0.01 m and relative bias of -0.02 indicates that the correction factor αE of 0.3 - to mimic the directional wave spreading effect in the 1D approach and prevent overproportioned IG waves - is appropriate for this case. Moreover, the small overall bias of -0.04 m for the short wave height indicates that for this case, short wave breaking seems to be simulated correctly and hence no adjustments in for example the wave breaking parameter *gamma* is required for this case.

Morphology

Given the uncertainty in the hydrodynamics as presented above, the measured absolute erosion volumes and the dune erosion-deposition profile are well captured. Except one profile, all absolute differences are less than 7 m^3/m. This results in large relative differences because of the small absolute measured erosion volumes. Differences related to the quality of the input data and/or measurement data probably cause a large part of this difference. For example, the initial bathymetry was measured two months prior to the storm. When considering small erosion volumes, the initial configuration of the bathymetry and topography becomes more important. Hence, (small) bed level changes in those two months could have contributed to the large relative differences between model and measured. In addition to that, alongshore sediment transport processes and spatial variation in dune strength due to differences in rooting of vegetation and grain sizes that are not captured within the 1D XBeach model could be an explanation for spatial variation in dune erosion that is not visible in the model results (e.g. no dune erosion in profile -1755). Finally, it should be noted that the erosion retreat distances are in the order of meters, which is close to the model resolution of 1.0 m in the dunes.

Conclusion

A mild storm at Egmond aan Zee in the Netherlands resulted in erosion along the lower dune face (< ~10 m^3/m) on January 8th, 2019. Observations on nearshore water levels, wave heights and post-storm topography were collected and are used in this case study for both hydrodynamic and morphodynamic validation of the XBeach model.

Hydrodynamic validation shows that the short and infragravity wave heights are predicted well by the model for 12 pressure sensors, but water levels are underestimated with on average a bias of -0.45 m. Morphodynamic validation shows that for the 7 transects the modelled erosion is in line with the observed erosion, but small absolute differences may result in large relative differences due to the limited amount of erosion.

Additional figures

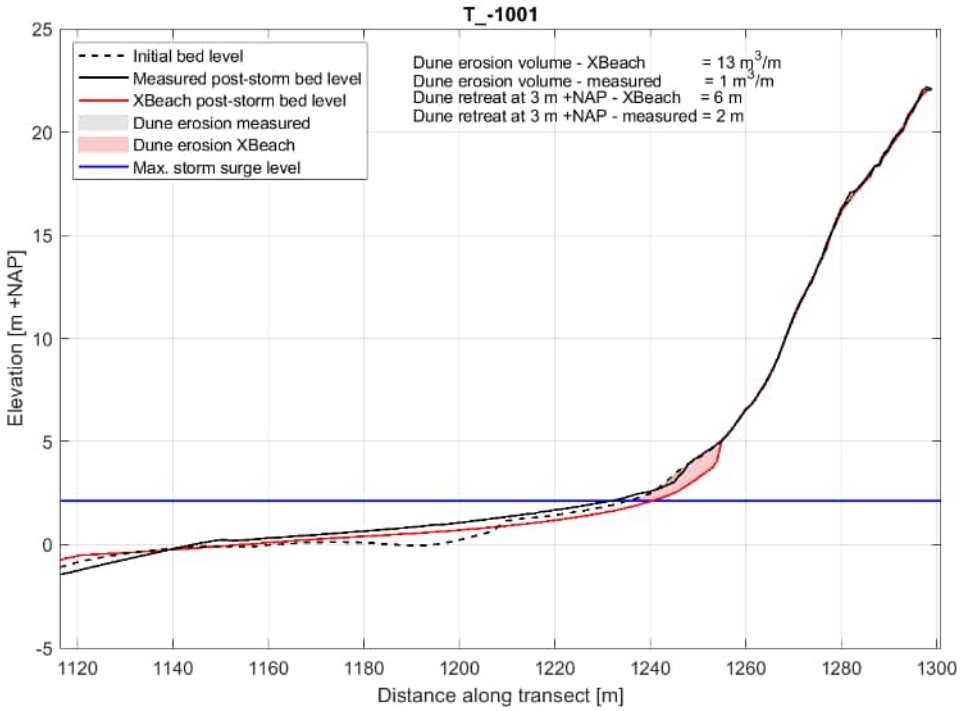

Figure C-142 XBeach results for cross-shore transect -1001 at Egmond aan Zee. Initial bed levels are depicted by the black dotted line, observed post-storm bed levels by the black solid line and XBeach model results are presented in red. The modelled dune erosion is shown by the red shaded area.

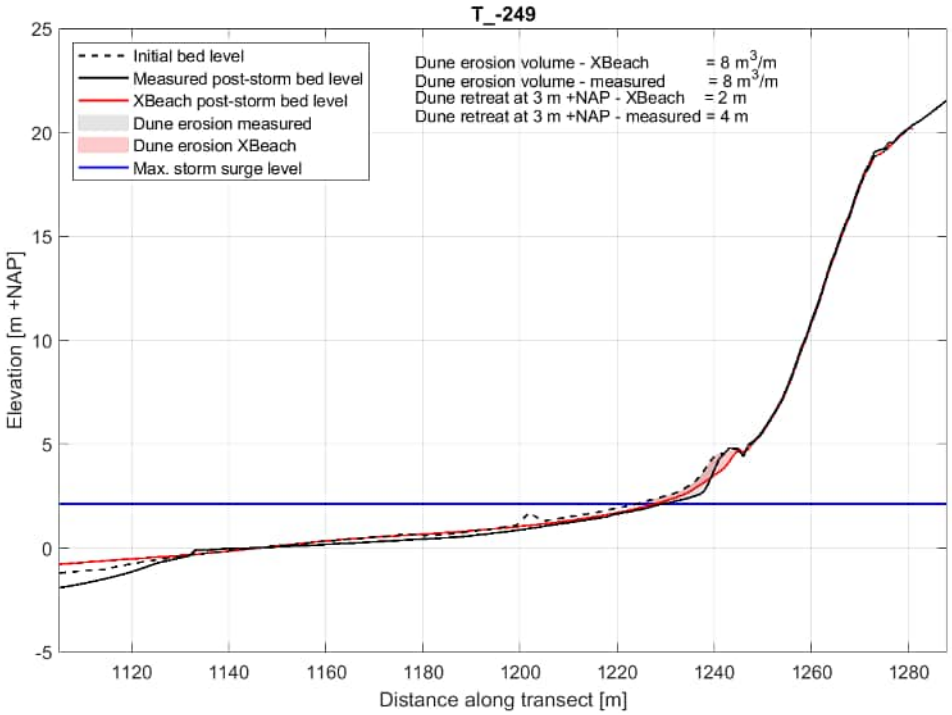

Figure C-143 XBeach results for cross-shore transect -249 at Egmond aan Zee. Initial bed levels are depicted by the black dotted line, observed post-storm bed levels by the black solid line and XBeach model results are presented in red. The modelled dune erosion is shown by the red shaded area.

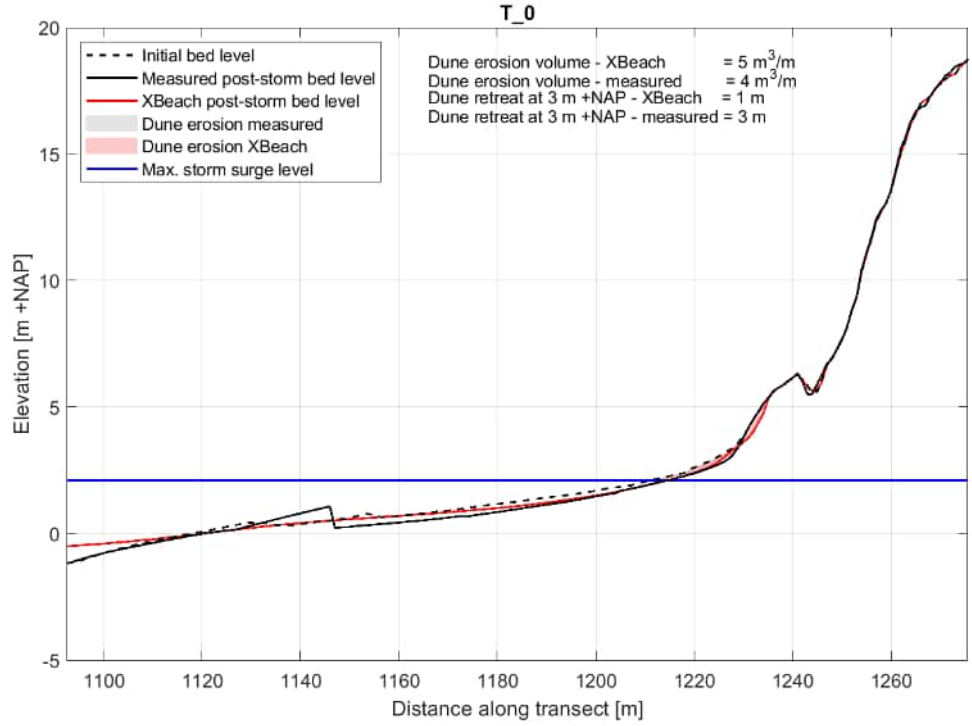

Figure C-144 XBeach results for cross-shore transect 0 at Egmond aan Zee. Initial bed levels are depicted by the black dotted line, observed post-storm bed levels by the black solid line and XBeach model results are presented in red. The modelled dune erosion is shown by the red shaded area. Note that the kink in the measured post-storm profile (around x = 1145 m) is due to merging of post storm bathymetry and topography measurements.

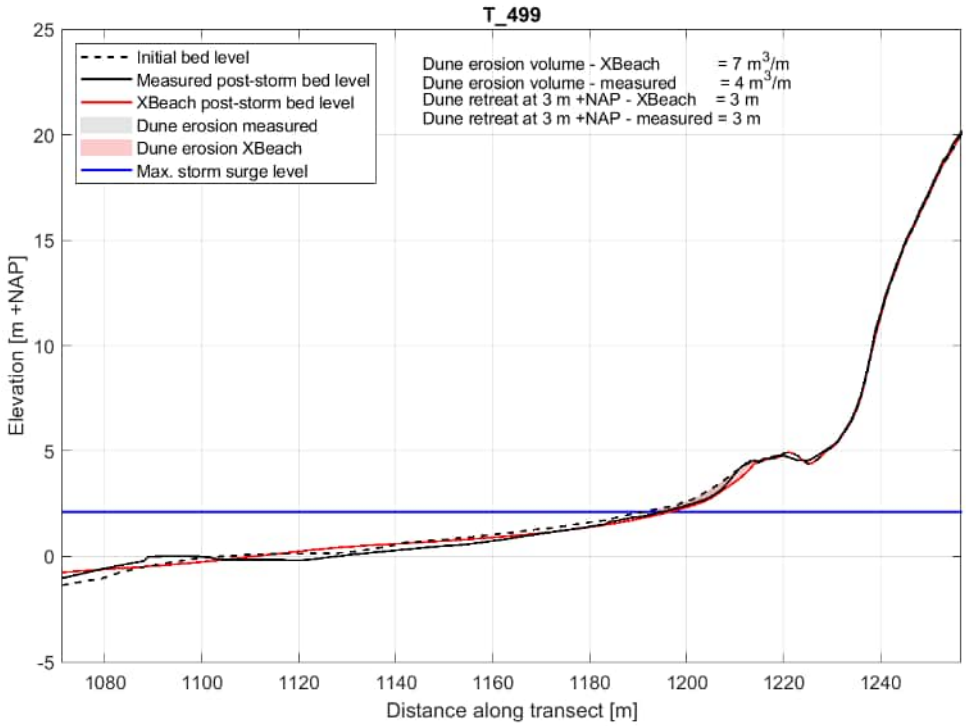

Figure C-145 XBeach results for cross-shore transect 499 at Egmond aan Zee. Initial bed levels are depicted by the black dotted line, observed post-storm bed levels by the black solid line and XBeach model results are presented in red. The modelled dune erosion is shown by the red shaded area.

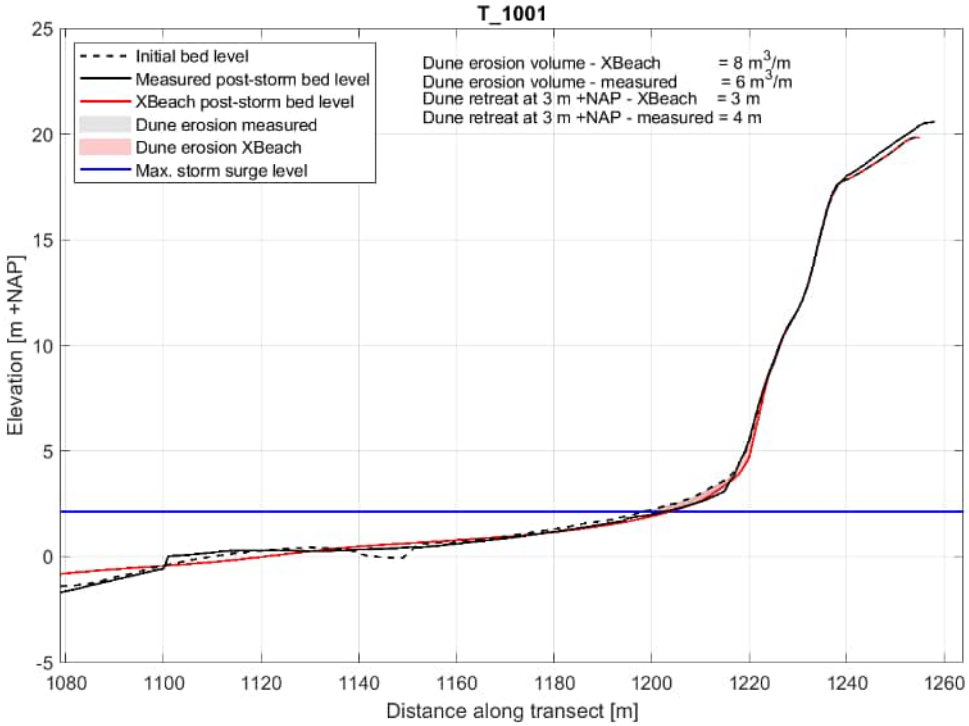

Figure C-146 XBeach results for cross-shore transect 1001 at Egmond aan Zee. Initial bed levels are depicted by the black dotted line, observed post-storm bed levels by the black solid line and XBeach model results are presented in red. The modelled dune erosion is shown by the red shaded area. Note that the kink in the measured post-storm profile (around x = 1100 m) is due to merging of post storm bathymetry and topography measurements.

COLOPHON

VALIDATION OF DUNE EROSION MODEL XBEACH
DEVELOPMENT OF 'BOI SANDY COASTS'

CLIENT
Rijkswaterstaat

LEAD AUTHOR
Laura Coumou

PROJECT NUMBER
C06041.000018.0100

DOCUMENT REF.
D10029117:3.0

DATE
March 21, 2022

STATUS
Final

CHECKED BY

Henk Steetzel
Senior expert

RELEASED BY

Robbin van Santen
Project manager

Arcadis Nederland B.V.
P.O. Box 137
8000 AC Zwolle
The Netherlands
+31 (0)88 4261 261

www.arcadis.com